Four-dimensional imaging for radiotherapy planning in children and teenagers

Dr Naomi Lavan

Institute of Cancer Research

and

The Royal Marsden NHS Foundation Trust

A thesis submitted to the University of London for the degree of Doctor of Medicine, MD (res)

Volume 1 of 1

July 2020

Author's declaration

I declare, as sole author of this thesis, that the work presented here represents my personal research conducted as a research fellow at the Institute of Cancer Research and the Royal Marsden NHS Foundation Trust between 2016 and 2018. Tables and figures herein are my own work unless credited otherwise.

Naomi Lavan

June 2020

Abstract

Respiratory-related organ motion (RROM) is a potential source of geometric uncertainty in RT planning and delivery. Approaches to mitigate its effects are well described in adults. For example, four-dimensional computed tomography (4DCT) mitigates the effects of RROM on image quality and motion-encompassing approaches to target volume delineation can incorporate individualised motion information from 4DCT into RT planning. This thesis explores the feasibility of adopting 4D imaging in children and teenagers for individualised motion assessment for radiotherapy planning.

The feasibility of using 4DCT for upper abdominal motion assessment in children is assessed. Kidney motion is determined by extracting deformation vector field and centre of mass displacements from 4DCT datasets in 25 children. The effect of general anaesthetic on organ motion is examined as are potential associations between motion and patient related variables; age, height, weight and body surface area.

Consideration of additional ionising radiation dose in children is important as children are inherently more sensitive to the deleterious effects of radiation exposure, in particular second malignancy induction. The feasibility of using 4DMR and ultrasound as alternative non-ionising imaging modalities for individualised motion assessment in children is explored. Feasibility and respiratory related organ displacements are presented per imaging modality

and compared to 4DCT; the current gold standard for adult RT planning in tumour sites susceptible to RROM.

The application of a respiratory motion encompassing RT planning technique is applied to upper abdominal neuroblastoma RT planning in children. The potential dosimetric benefits of using an internal target volume approach is described and compared to a conventional approach to RT planning.

The introduction of advanced radiotherapy techniques in children often lags behind their adult counterparts. This thesis describes the feasibility of adopting individualised motion assessment in children and contributes to the understanding of RROM in children.

Table of Contents

Table of Figures

Table of Tables

Abbreviations

2D US	Two-dimensional ultrasound
3D US	Three-dimensional ultrasound
3DCRT	Three-dimensional conformal RT
3DCT	Three-dimensional computed tomography
4DCT	Four-dimensional computed tomography
4DMR	Four-dimensional magnetic resonance
AAPM	American Association of Physicists in Medicine
AP	Anterior-posterior
BSA	Body surface area
CBCT	Cone beam computed tomography
CECT	Contrast-enhanced computed tomography
COM	Centre of mass
CR	Complete response
CTDI	Computed tomography dose index
CTV	Clinical target volume
DIBH	Deep inspiration breath hold
DIR	Deformable image registration
DVF	Deformation vector field
GA	General anaesthetic
GTR	Gross total resection
HR-NBL	High risk neuroblastoma
ICRU	International Commission on Radiation Units and Measurements
IGRT	Image guided radiotherapy
IM	Internal margin
IMAT	Intensity modulated arc therapy
IMPT	Intensity modulated proton therapy
IMRT	Intensity modulated radiotherapy
ITV	Internal target volume
MidV	Midventilation
MRGRT	Magnetic resonance guided radiotherapy
MRI	Magnetic resonance imaging
OAR	Organs at risk
POI	Point of interest
POP	Parallel opposed pair
PROS	Paediatric Radiation Oncology Society
PT	Proton therapy
PTV	Planning target volume
QUANTEC	Quantitative Analyses of Normal Tissue Effects in the Clinic
QUARTET	Quality and excellence in radiotherapy and imaging for children and adolescents across Europe in clinical trials.
RL	Right-left
RROM	Respiratory-related organ motion
RT	Radiotherapy

SD	Standard deviation
SI	Superior- inferior
SIOPEN	International Society of Paediatric Oncology, European Neuroblastoma
SM	Set-up margin
US	Ultrasound
VMAT	Volumetric modulated arc therapy
WT	Wilms' tumour

Acknowledgements

I would like to thank all the brave children, and their parents or guardians, who agreed to take part in the APAChe study and make the work contained in this thesis possible.

I would like to thank my supervisors Henry Mandeville and Uwe Oelfke for their expertise, insight and encouragement but mostly for their patience – 'it always seems impossible until it's done'.

Thank you to the nurses and play therapists in the Oak Centre and to the physicists and radiation therapists at RMH/ICR. I would like to give a special mention to Gregory Smith, Sarah Mason, Emma Harris, Andreas Wetscherek, Dualta McQuaid, Helen McNair, and Erica Scurr who were crucial in elements of this work coming to fruition.

Research is hugely rewarding but can also be immensely challenging at times. My fellow fellows, Ingrid, Angela, Hannah and Ali, made research fun and helped me maintain momentum to the not so bitter end.

Family is at the heart of all things. I would like to thank my mum, sister, brothers and aunt for their words of encouragement during my write up. I know my Dad would be proud to see me complete this. To my husband Aonghus,

you bore the brunt of the temper tantrums in recent months (some were mine); I could not have started, or finished this, without you. To Aifric and Niamh, my girls; the story is finally finished – let's go and play now.

Chapter 1 - Introduction

1.1 Publications

Sections of this work have been published in:

Radiation Treatment Planning in Pediatric Radiation Oncology. In Voss McHugh (Eds). *Imaging in Paediatric Oncology*, Springer 2019

Adopting Advanced Radiotherapy Techniques in the Treatment of Paediatric Extracranial Malignancies: Challenges and Future Directions. *Clin Oncol (R Coll Radiol)*. 2019; 31(1):50-57.

1.2 Background

1.2.1 Cancer in childhood

A diagnosis of cancer in infants and children under 18 years of age is rare. Despite a reported overall increase of 13% in the incidence of childhood cancers since the early 1990's such a diagnosis represented less than 1% of all cancer cases in the UK from 2013 – 2015 [1].

Childhood cancers are notably different to adult cancers; ~~–~~the most common solid tumours in children occur in different anatomical sites compared to common tumours occurring in adults ~~they arise in different parts of the body~~, comprise unique pathologies not often seen in adults, and respond differently to anticancer treatments [2]. Children between the ages of

0 and 4 years of age have the highest incidence of cancer [1]. Neuroblastoma and Wilms' tumour represent the most common extra-cranial solid tumours in children. These two tumour types typically arise in upper abdominal locations. Cancer incidence then falls amongst 5 – 14 year olds but rises again in adolescents and young adults (AYA) over the age of 15. The bimodal peak in incidence reflects the two periods of rapid growth; early childhood and adolescence/ puberty.

The oncological management of the majority of extra-cranial malignancies in children is multi-modal including intensive chemotherapy regimens, surgery and radiotherapy with treatment protocols lasting many months. Approximately 40 - 50% of children diagnosed with cancer will receive radiotherapy (RT) as part of their first line treatment [3].

1.2.2 What makes paediatric radiotherapy different to adult radiotherapy?

1.2.2.1 The use of general anaesthetic for immobilisation

Very young children having RT often require general anaesthesia (GA) to remain adequately still for simulation and treatment delivery. This applies to the majority of children under the age of 5 years. Some older children for a variety of reasons may also require GA to attain the necessary level of immobilisation for safe and reproducible RT. Most RT departments use intravenous anaesthetic agents as opposed to full intubation with respiratory muscle paralysis. Children anaesthetised in this way remain free-breathing. A scenario requiring muscle paralysis would be treatment for retinoblastoma when the globe needs to be immobilized achieved by paralysis of the extra-ocular muscles.

Though repeated GA for RT is safe, the time to deliver a RT plan and hence the time a child is required to remain under GA is always a consideration for paediatric radiation oncologists. Advanced RT delivery techniques that require longer times for imaging or treatment could reduce the threshold age for a child to require GA for immobilisation. This could have a significant impact on RT department resources as anaesthetic services are often delivered by anaesthetists servicing already busy surgical and diagnostic radiology lists. It is common that RT departments are limited in the number of children that can be treated under GA at any one time. If that number of children is exceeded a child requiring RT would have to be treated at a different institution that may be a significant distance from their home.

Formatted: Right: 0.08 cm, Space Before: 0 pt, Line spacing: Multiple 2 li

1.2.2.2 Organs at risk (OAR)

All tissue in the irradiated volume of a child is potentially at risk for toxicity. Developing tissues in children have a lower tolerance to RT than in adults [4]. Paediatric tumours are, in general, more sensitive to radiation than adult-type tumours.

~~This~~ These factors ~~is~~are reflected in the use of lower doses per fraction, and lower overall total doses, compared to fractionated schedules used in adults [4]. Organs and normal tissues largely ignored in adults are of prime concern in children.

For example, RT dose in the range of 18 - 20 Gy will significantly impair future bone growth in pre-pubertal children. As a result, current practice dictates that we deliberately increase dose outside of the target volume to symmetrically irradiate adjacent vertebrae in order to avoid the late effects produced by asymmetrical bone growth arrest in the spine such as kyphosis or scoliosis [6]. Highly conformal RT techniques with steep dose gradients can result in asymmetrical dose to musculoskeletal structures compared to a parallel opposed pair (POP) beam arrangement. Such asymmetrical dose could adversely impact future growth and cause deformity or suboptimal cosmetic results in the treated field.

The kidneys are the main dose-limiting OAR in upper abdominal RT given their inherent radiation sensitivity~~, a TD 5/5 (normal tissue complication probability of 5% at 5 years) of 23 Gy and TD 50/5 of 28 Gy.~~. Adult organ tolerance data derived from Quantitative Analyses of Normal Tissue Effects in the Clinic (QUANTEC) inform paediatric practice [7]. However, limitations exist in applying this data to children who often receive intensive multi-modal therapies in addition to their inherently more radiosensitive tissues. The use of intensive multi-modality therapy, including high dose myeloablative chemotherapy and nephrotoxic agents, in children with high-risk neuroblastoma (HR-NBL) may have additional negative impact on renal radiation tolerance. Reducing the volume of high dose delivered to the liver is also an important consideration for

children with veno-occlusive disease, a recognised complication of myeloablative therapy.

1.2.2.3 Risk of secondary malignancy

The induction of an incurable second malignancy is a dreaded consequence of RT in childhood. Secondary malignancy is of greater concern in children compared to adults given their long life expectancy and the increased radiation sensitivity of their developing tissues. Conventionally there has been reluctance to adopt highly conformal RT planning techniques in children due to evidence from modelling studies that the increased integral dose associated with IMRT techniques may increase the risk of second malignancy by almost a factor of 2 [8]. However, it is increasingly acknowledged that second cancers often arise in the high dose region outside the target, thereby challenging original estimates [5, 9, 10]. Highly conformal RT techniques reduce high to moderate dose compared to parallel opposed or 3DCRT but the contribution of low dose to the risk of secondary malignancy requires prospective attention when highly conformal RT techniques are used in children [4].

1.2.2.4 Treatment planning complexity

RT treatment volumes in children are often significantly larger than those seen in adults; for example in advanced stage Hodgkin lymphoma, RT fields can span above and below the diaphragm, irradiation of multiple metastatic sites is sometimes indicated in metastatic rhabdomyosarcoma and Ewing's tumours. Delivering RT above and below the diaphragm in two sequential treatments due to resultant myelosuppression is not unusual, for example in Hodgkin

lymphoma or extensive metastatic rhabdomyosarcoma, (Figure 1.1). All of these factors result in significantly increased RT treatment planning complexity compared to common adult tumour sites such as breast and

prostate where treatment planning templates can often be used to improve planning efficiency [11].

1.2.2.5 Late effects of radiotherapy in children

Survival for children with childhood cancers in the UK has doubled over the last 40 years. Today, 5 and 10 year survival is 80% and 76% respectively [1]. Unfortunately, an estimated 73% of childhood cancer survivors develop treatment-related complications [12]. This means that all survivors of childhood cancer live with the very real risk of treatment-related morbidity and mortality.

Thoracic and abdominal RT increases a child's risk of cardiac, pulmonary, musculoskeletal (including cosmetic), renal, metabolic, endocrine, hepatic, and vascular late effects [13-18] as well as an increased risk of second malignancies [19, 20]. Given the heavy burden of post RT morbidity, attempts to reduce childhood exposure to RT have included the omission of RT entirely from the treatment paradigm, RT dose reductions and/ or, RT target volume reductions [21]. The use of RT in children has, as a result, declined over recent decades in some tumour sites, one notable example being the use of cranial RT in acute lymphoblastic leukaemia [22]. However, the systematic use of RT and the influence of local control on progression-free and overall survival have been demonstrated in a number of extra-cranial paediatric tumour sites [23, 24]. It is therefore clear that RT will continue to play an important role in the management of paediatric tumours [21, 25]. Where RT cannot be avoided, or the RT dose reduced, rationalising the planning target volume (PTV) and thereby reducing the irradiated volume of normal tissue is ~~an~~ one attractive strategy to reduce RT-related morbidity in children.

1.3 Optimising upper abdominal paediatric radiotherapy

Conventionally parallel opposed pair (POP) beam arrangements have been favoured for paediatric RT planning. This beam arrangement optimally spares normal tissue at a distance from the target and minimises the risk of secondary malignancy induction in these peripheral tissues. However, with this beam arrangement the moderate to high doses are not well conformed to the target, (Figure 1.2). High to moderate RT dose regions are implicated in the development of many late normal tissue toxicities in children [21]. The clinical benefits of the reduction in the volume of normal tissue receiving high to moderate dose achieved with advanced photon RT techniques have been demonstrated in children with tumours in the brain, and the head and neck regions. These studies have demonstrated reduced grade 3 and 4 ototoxicity in medulloblastoma survivors and reduced mucositis in the treatment of childhood nasopharyngeal carcinoma [26, 27]. Advanced photon RT techniques in clinical use include intensity modulated RT (IMRT), volumetric modulated arc therapy (VMAT) and tomotherapy; hereafter collectively referred to as highly conformal photon techniques.

A 2013 report from International Society of Paediatric Oncology, European Neuroblastoma (SIOPEN) revealed that in a sample of ~~99~~ 100 patients treated within the SIOPEN high risk neuroblastoma (HR-NBL 1) study ~~[29]~~; ~~the majority of children (N = 67) were treated with POP beam arrangements (anterior/ posterior or oblique pairs) and only 11 patients received 3D conformal~~

~~techniques with 3 – 5 fields~~ 99 patients were treated conventionally and 1 patient was treated using intensity modulated arc therapy. Of the 99 patients treated conventionally, 87 were treated with POP beam arrangements (anterior/ posterior or oblique pairs) [30]. This reports highlights that contemporary paediatric radiation oncology lags behind adults in terms of the adoption of highly conformal photon RT techniques.

The same group reported on RT quality assurance in 100 patients treated on the same HR-NBL1 study and revealed that only 48% of RT plans complied with protocol recommendations. One major factor influencing the rates of non-compliance to the study protocol was that the maximum deliverable prescribed dose was limited by the proximity of kidneys and liver to the target [5].

Compared to POP beam arrangements, and 3DCRT, highly conformal photon RT techniques have been shown to dosimetrically improve kidneys sparing, particularly in the treatment of midline abdominal targets, (Figure 1.3), [28, 31]. Schaffer et al compared POP, 3DCRT, rotational IMRT and step and shoot IMRT techniques in eight retroperitoneal tumour sites (five children with neuroblastoma were included). Various dose prescriptions were used according to diagnosis. Compared to POP, conformity was improved by 3D-CRT and both types of IMRT. The shortest treatment times were achieved with rotational IMRT delivery; relevant when treating young children both for time under GA and for those not under GA who may not tolerate longer treatment times; as discussed in section 1.2.2.1 [32]. For lateralised targets, the contralateral mean kidney doses were lowest with a POP technique although all techniques met the constraint of mean kidney dose <12 Gy. Paulino et al compared conventional RT plans with fixed field IMRT in six children with neuroblastoma and concluded that IMRT was advantageous in midline

Formatted: Right: 0.08 cm, Space Before: 0 pt

tumours but increased the contralateral mean kidney dose in the setting of lateralised targets [28]. Gains et al, however, demonstrated a benefit from

rotational IMRT in patients with lateralised tumours who were protocol non-compliant using conventional POP (reduced total dose or reduced coverage of PTV to respect normal tissue tolerance) [31]. So, the dosimetric advantages of highly conformal photon RT techniques in upper abdominal and retroperitoneal tumour sites in children have been described [28, 31-34]. Institutional series have described no detriment in local control in HR-NBL with the use of IMRT [35, 26]. A UK national randomised phase II study is currently investigating rotational IMRT (the IMAT study), and dose escalation, in HR-NBL [37].

Optimising photon RT delivery techniques and planning target volumes (PTV) could translate into real benefits for our young patients who still require RT and even minor improvements could have major impact on the risk of late effects [38]. Acknowledgement of the potential benefits of advanced RT techniques in children was reflected in the recent Paediatric Radiation Oncology Society (PROS) position paper and the group have strongly recommended that advanced RT delivery techniques be made available to children [39].

The challenge in adopting advanced photon RT techniques is ensuring geometric accuracy and precision in treatment delivery so that the excellent local control rates achieved with conventional beam arrangements can be maintained or improved. POP and 3DCT beam arrangements offer a buffer to changes in internal organ position during treatment. That buffer is lost when techniques with highly conformal, complex dose distributions and steep dose gradients are introduced. In this setting inadequate CTV to PTV margins could result in relapse due to geographical misses. Conversely, overly generous margins could negate the potential benefits of enhanced normal tissue sparing when highly conformal techniques are used. It is not unsurprising that the

clinical evidence for, and general use of, advanced photon RT techniques in paediatric RT, are predominantly in intracranial and head and neck tumour sites where the target volume is not subject to significant motion [21].

1.3.1 Geometric uncertainty in treatment delivery

The known sources of geometrical uncertainty in RT are defined as systematic and/ or random in their occurrence and have different effects on the delivered dose distribution. Examples of geometric uncertainties include: delineation (systematic), organ motion (systematic and random), and patient set-up (systematic and random). Organ motion and patient set-up errors can occur between one treatment session and another (interfraction) but also during a single treatment session (intrafraction).

Geometric uncertainties, if not accounted for, result in a difference between a planned and delivered dose distribution to the clinical target volume (CTV) [40]. Systematic errors result in the planned dose distribution being consistently shifted with respect to the target. Random errors typically result in a blurring of the planned dose distribution with respect to the target as the deviation is not consistently in one direction for the entire course of treatment [41].

Applying a geometric planning target volume (PTV) around a target increases the probability of desired target coverage, (Figure 1.4). Population-based margin recipes give a defined level of confidence of delivering a given minimum dose to CTV such as 95% of prescription dose delivered to 90% of the population [42].

The systematic and random uncertainties in a child's set-up relative to the treatment beam geometry [set-up margin (SM)] and in target position relative to

the child's bony anatomy [internal margin (IM)] are accounted for in a PTV expansion [43]. Systematic uncertainties are weighted more heavily than random uncertainties in population-based margin (M) recipes as given by the equation:

$$M = 2.5 \sum + 0.7\,\delta \quad (42)$$

Where the systematic error (∑) is the square root of the quadratic sum of standard deviations (SD) of the individual means of the errors and the random error (δ) is the square root of the quadratic sum of the root mean squares of the individual errors. Reducing systematic errors will have the greatest impact on margin reduction strategies.

Systematic and random set-up errors will vary between RT departments according to immobilisation, imaging frequency, imaging modality and correction strategy used. Applying a daily online IGRT strategy (with all couch translations corrected on a daily basis) the interfraction set-up error could be considered to be zero (although in reality there would be residual error, for example, from uncorrected rotations). The calculated M would then comprise of the intrafraction set-up error. As patient set-up errors reduce with the implementation of daily IGRT, uncertainties relating to organ and target motion relative to the planned isocentre dominate the CTV to PTV margins.

Many departments apply CTV to PTV margins that vary according to anatomical site (reflecting the differences in immobilisation and internal motion between anatomical sites) but not according to the age or size of the patient; they apply the same CTV to PTV margin in both children and adults [44]. A statistically significant difference in set-up error in the SI direction between 48 adult and 39 paediatric (< 7 years of age) abdominal tumour sites of 8.0 mm

compared to 5.0 mm highlights the potential differences in setup error between adults and children [45].

It has been demonstrated that small numerical reductions in applied PTV margins translate into a significant reduction in the volume of normal tissue irradiated to moderate to high doses [46]. The current practice of extrapolating CTV to PTV margins from adults to children is questionable. It is also likely that using the same population-based CTV to PTV margins for a 3 year old and a 13 year old is not optimal. Therefore, it is important to fully characterise organ motion, particular to children across the age spectrum, as an initial step to delivering optimal RT dose distributions in anatomical sites susceptible to RROM.

1.3.2 Respiratory - related organ motion (RROM)

Breathing is the primary source of organ and target motion in the upper abdomen and will hereafter be referred to as respiratory-related organ motion (RROM). Cardiac pulsation, peristalsis and gastrointestinal filling or emptying can also contribute to internal motion depending on the anatomical location of the target [47-49].

The knowledge that RROM is patient-specific in adults has resulted in the widespread adoption of individualised approaches to motion assessment and motion management in adult thoracic, and increasingly, upper abdominal RT planning and treatment [41, 50].

The AAPM report on the management of RROM in photon RT recommends that motion management techniques are not required below a threshold of 5 mm [51]. A recent study reported statistically significantly smaller right and left

kidney displacements in 35 children (2.8 mm, 2.9 mm) compared to 35 adults (5.6 mm, 5.2 mm) [41]. The AAPM report pertains to photon RT in adults and it is acknowledged in the body of the text that data in relation to children is lacking. Furthemore, young children have significantly higher metabolic rates than adults, and therefore have a higher oxygen demand which in turn resuts in higher respiratory rates compared to adults. The diaphragm is the principle muscle of respiration in infants and young children, and so abdominal breathing patterns are more common in children than in adults. It is not known whether it is correct to apply the same magnitude of motion for motion management techniques to both a 170 cm 60 year-old adult and a 90 cm 4 year old.

1.3.3 Quantifying intrafraction organ motion

1.3.3.1 Intrafraction RROM in adults

In adults, publications have focused on quantifying organ motion in order to define accurate population-based margins for specific tumour sites [47]. Published adult studies have used a variety of metrics to quantify organ motion; centre of mass (COM) displacement, organ edge (or bounding box) displacement, and points of interest (POI) displacement. POI metrics in adults have involved, for the most part, measurement of fiducial motion. There has been variations in the reported imaging modality used for motion estimation [fluoroscopy, four-dimensional computed tomography (4DCT), four-dimensional magnetic resonance (4DMR) and ultrasound (US)] as well as in the breathing conditions under which motion has been quantified (free-breathing, breath-hold). The number of breathing cycles from which data is obtained also differs depending on the duration of scan acquisition; generally shorter for 4DCT compared to longer cine magnetic resonance (MR) or 4DMR

acquisitions.

The variation in approaches affects the motion values derived and the interpretation of comparisons. An illustrative selection of reported adult upper

abdominal organ motion in free-breathing is presented in Table 1.1. To summarise, studies of organ motion in adults have demonstrated that abdominal organs appear to move synchronously according to 4DCT phase but to different amplitudes depending on their proximity to the diaphragm; the principal muscle of respiration [53]. Organs at a greater distance from the diaphragm still display RROM but also have the potential to move variably due to other deformable structures that are in close proximity to them e.g. stomach, small and large bowel [53].

Studies of adult kidney motion, in free-breathing, have demonstrated that motion is greatest in the superior/ inferior (SI) direction and smallest in the right/ left (RL) direction [53-57]. The superior pole of the kidney has been shown to move more than the lower pole [58, 59]. It has been demonstrated that the magnitude of motion in one kidney does not correlate with the contralateral kidney. There is substantial interpatient variation in RROM, particularly in the SI direction [53-55, 57, 59, 60]. Poor correlation between diaphragm motion and right and left kidney motion has been demonstrated. This limits the ability to consider the diaphragm as a potential surrogate of kidney motion for real-time tracking [55]. A study of 20 adult patients failed to demonstrate statistically significant associations between motion and patient-related variables (age, sex, height or weight) [54]. Liver COM displacements measured on 4DCT are greatest in the SI direction with a reported range of 5 – 50 mm. In a study of 18 adult patients with liver or pancreatic cancers, liver motion (measured using a bounding box metric) demonstrated that superior edge liver motion was 1.5 times greater than motion of the inferior liver edge in 80% of patients [53]. These findings suggest non-rigid motion (deformation) of

the liver. In the presence of deformation, COM may underestimate organ motion and shape changes as it is less sensitive to these effects. Estimations of intrafraction motion of lung, liver, pancreas, lower oesophageal tumours also demonstrate interpatient variation and that the magnitude of motion varies relative to the proximity of the tumour to the diaphragm. Tumour motion in the upper abdomen is often estimated using implanted fiducials as surrogates given the relative reduced soft tissue contrast in this region of the body in comparison to the lung where tumours are high density relative to the low density lung parenchyma. In reality, for adult tumours in anatomical sites susceptible to breathing motion individualised motion assessment is now accepted to be standard of care.

1.3.3.2 Intrafraction RROM in children

Estimates of a population-based paediatric-specific margin would aid RT departments without access to 4D imaging, noting that a significant proportion of childhood cancers occur in low to middle income countries [39]. However, cancer in childhood is so rare that the small number of patients will make the derivation of population-based margins in children a significant challenge. Another challenge is that RT in children is often delivered after surgery unlike in adults where in general RT is delivered with definitive intent with the gross tumour volume (GTV) present at the time of RT delivery. Alternatively, surgical clips in the operative bed can be measured although the placement of fiducials to delineate the tumour bed by surgeons is not standardised in paediatric RT. In the absence of GTV, or surgical clips, motion of adjacent organs at risk could be measured as surrogates for tumour bed motion.

In a report of 20 children with 4DCT, SI kidney motion was shown to increase with every yearly increase in age; right kidney 0.148 ± 0.064 mm, left kidney 0.121 ± 0.047 mm [61]. Intrafraction RROM in the children was quantified using 4DCT and 4DMRI in median 20 patients (range 15 – 35) [61-63]. Mean SI displacements of the right and left kidney, liver, spleen and diaphragm were 1.9 – 4.7mm, 1.4 - 4.8mm, 3.2 – 6.8mm, 3.0 – 6.9mm, and 3.6 – 9.6mm respectively. Organ displacements were no more than 2- 3 mm AP and RL. Anisotropic CTV to PTV margin expansions would be indicated where there is evidence of differential motion in the three cardinal axes.

In this study by Panandiker et al. the use of GA and patient age was found to be highly correlated ($p = 0.0075$). This means that age and height cannot be considered independent variables and limits the statistical inferences that can be made from the described associations between motion, age and height. Huijsken et al demonstrated that the median motion vectors of intrafraction variation in diaphragm displacement were statistically significantly smaller for a subset of children under GA compared to non-anaesthetised children of similar ages (n= 7; 2-11 years, n=12; 3-10 years); 1.6mm vs 2.4 mm respectively ($p<0.05$). However, mean amplitude and interfraction variation of diaphragm motion did not differ between the groups [64].

Younger children are more likely to be shorter and lighter and have a lower body surface area (BSA). Younger children are also more likely to require GA. The use of GA in paediatric RT is highly variable. Some institutions routinely anaesthetise children under the age of 7 [61]. Other institutions report treating young children during their routine nap time obviating the requirement for GA [51]. In other institutions children may be simulated under GA but then receive

daily treatment awake [65]. In the UK, the majority of children under the age of 5 years will require GA with use of play therapy and the wider multi-disciplinary team enabling older children to manage RT without GA [2]. Though the focus of this thesis is highly conformal photon RT, the use of intensity modulated proton RT (IMPT) is increasing. The longer treatment times required for proton RT will increase the threshold for using GA in children who may not have required it for photon RT [66]. Contributing to the body of literature on RROM in children, as is the focus of this thesis, with different thresholds for the use GA, is valuable as the influence of GA on RROM is at present not well understood. It is possible that the use of GA should be considered in the derivation of CTV to PTV margins in children.

1.3.4 Individualised respiratory-motion assessment

1.3.4.1 Four-dimensional computed tomography (4DCT)

The use of 4DCT has evolved to minimise respiratory- related motion artefact in static 3D imaging (in the setting of a stable respiratory breathing pattern). Distortion of targets caused by breathing artefact can result in incorrect positional and volumetric information. This incorrect information would be propagated from the RT planning phase through to treatment delivery as a systematic error [50, 67, 68]. Methods for 4DCT image acquisition and sorting, using phase- or amplitude-based binning techniques, have been previously described in detail for adults [38-30]. Briefly; a 4DCT is created by binning oversampled CT data according to an external breathing surrogate. This process results in 8 – 10 three-dimensional computed tomography (3DCT) scans representing the patient's anatomy for each given phase of the

respiratory cycle, (Figure 1.5). Although images are acquired over several breathing cycles, a 4DCT dataset represents a single averaged breathing cycle. The process of 4DCT data acquisition and image sorting used in this thesis will be described in further detail in Chapter 2.

4DCT for individualised RROM assessment is the established standard of care in adult lung cancer and, increasingly, in adult upper abdominal tumours including liver, oesophagus, gastric, pancreas, renal and adrenal tumours [58, 70-72].

Reported 4DCT imaging protocols in adults deliver a volume CT dose index (CTDI), a general dose measure used in reported imaging-related dose, to the patient ranging from 2 -10 times the dose of a conventional 3DCT planning scan [56, 59]. In adult RT, the enhanced geometric certainty in treatment delivery afforded by the use of 4DCT justifies this additional dose exposure to the patient. However, the additional radiation dose exposure associated with 4DCT imaging is the principle disadvantage of the modality in children and is the single most significant factor limiting its use in paediatric RT planning [73, 75]. Dose exposure in children and young people is a prime consideration due to the risk of secondary malignancy induction [75]. Few institutions have reported on the clinical implementation of 4DCT for paediatric RT planning. A single institution report a 4DCT CTDI (measured in a phantom) of 33 mGy [61]. Another series reported a mean CTDI of 11.4 (SD 2.0) mGy in three paediatric patients imaged using an adult protocol [76]. A third publication reference the use of tube modulation for 4DCT acquisition that results in 1.6 times the dose of a conventional 3DCT [62].

4DCT has accepted limitations in terms of image quality and spatio-temporal accuracy and these limitations challenge its overall effectiveness in adults. Imaging artefacts can occur despite 4DCT image reconstruction techniques. As demonstrated in adults such artefacts occur due to intra-patient variation in the amplitude and frequency of breathing cycles during scan acquisition [77]. A 4DCT is an averaged representation of patient-specific RROM captured over a short number of breaths. Day-to-day variation in RROM is also described in adults. In the setting of irregular adult breathing patterns, the ability for a single 4DCT to fully characterise RROM in adults has been shown to be limited [78,79]. 4DCT images can be reconstructed in small increments e.g. 2.5 mm slice thickness. This is achieved by a process of binning and interpolation, but cannot compensate for under-sampling at couch positions if it occurs [80]. If images are not acquired at a sufficient sampling rate, and under-sampling occurs, the magnitude of RROM could be underestimated by 4DCT, which could in turn result in inappropriate motion encompassing or motion management being applied in treatment planning or delivery. A study comparing the amplitude of diaphragm motion between end-exhale and end-inhale projections of CBCT in 45 children and 45 adults found that overall variability was less in children than in adults [81]. This study suggests that 4DCT would be at least as effective in children as it is in adults. The finding of reduced intrafraction variation in diaphragm motion in children under GA compared to children not under GA suggests that 4DCT may be more representative of motion during RT treatment in children than it is in adults [64].

There is a clinical need to describe the dosimetric benefit of incorporating individualised motion information from 4DCT into paediatric RT planning and is the purpose of Chapter 5 of this thesis.

1.3.5 Addressing the limitations of (4D)CT

In adults, alternative imaging strategies are being developed in an attempt to overcome the inherent limitations of (4D)CT (and CT verification of target position on treatment). Magnetic resonance imaging (MRI) and ultrasound (US) provide time-resolved images, are non-ionising and acquire images over longer periods of time overcoming some of the described limitations of 4DCT. 4DCT effectiveness relies on constant and consistent concordance between internal organ motion and an external surrogate. Reconstruction of 4DMR images can be accomplished using an internal surrogate, whereas US imaging enables direct visualisation of the tissue in real-time.

1.3.5.1 Four-dimensional magnetic resonance (4DMR)

The role of MR in RT is rapidly evolving [82-84]. It is possible for MR to positively impact the RT delivery pathway from the target delineation stage and planning through to treatment delivery [82, 83, 85, 86]. Hybrid MR-guided RT (MRgRT) platforms that integrate clinical quality MR imaging with a modern linear accelerator are in both active development and clinical use [87-90]. The MRIdian system (ViewRay Inc., Oakwood Village, OH) has been clinically operational since 2014. Elekta Unity MR Linac (MRL) (Elekta AB, Stockholm, Sweden) machines, installed in two centres in the UK, are clinically operational since 2018 and a ‘first in man’ study in prostate cancer has been recently

reported [91]. MR images during the RT delivery stage enable soft tissue matching (as opposed to registration of planning CT to CBCT using bone match as is standard practice in paediatric RT) for patient verification and set-up prior to each RT fraction; reducing the SM component, and inter-fraction IM of the PTV. MR systems also have the ability to localise target and normal tissues during the delivery of each RT treatment to allow increasingly precise and accurate RT delivery by reducing CTV to PTV margins required for intra-fraction motion and plan adaptation if required.

4DMR sequences for assessment of organ motion in adults are evolving [92]. Daily on-line imaging and adaptive re-planning with MRgT are promising strategies for optimal IGRT in children without concerns related to additional radiation dose. MRI is increasingly advocated for diagnostic imaging of children due to the superior soft tissue contrast and absence of radiation dose [93]. The integration of diagnostic MR images in the RT treatment planning pathway to aid target delineation in paediatric RT planning is well described [94]. However, MR imaging of the abdomen in children represents unique challenges. Younger children have less abdominal fat to provide a natural contrast mechanism for MR imaging [95, 96]. In adults, breath-hold is essential for upper abdominal MR imaging as respiratory induced motion can result in imaging artefacts [96]. In contrast, paediatric diagnostic abdominal MR is often performed under quiet breathing conditions. Paediatric MR imaging with breath-hold is challenging at all ages; younger children are imaged under anaesthesia without intubation and older children may not comply reliably with breath-hold instructions [95, 97]. Furthermore, MR acquisitions take longer than CT acquisitions and as a result patient motion can significantly degrade

images in non-anaesthetised young children [92]. MR is also associated with increased sensory input for children including increased noise levels and body temperature. These conditions could be challenging for young children to tolerate awake. Children who may comply with immobilisation for a short CT scan without anaesthesia may not be able to comply for the duration of an MR scan. It is necessary to investigate the feasibility of integrating MR imaging for RT planning in children and is the purpose of Chapter 3 of this thesis.

1.3.5.2 Ultrasound

Ultrasound (US) is a non-ionising imaging modality that offers superior soft-tissue contrast compared to CT and high temporal imaging rates resulting in real-time motion assessment. Ultrasound can be integrated with a standard C-arm linear accelerator and can be used to verify interfraction and intrafraction organ/ target motion [98. 99]. Three trans-abdominal US devices are commercially available; BAT (B-mode Acquisition and Targeting device, Nomos, Cranberry Township, PA), SonArray (Varian, Palo Alto, USA) and Clarity (Elekta, Stockholm, Sweden). Inter-fraction target localisation using US has been described primarily in adult prostate cancer [98-100] and to a lesser extent in the adult upper abdomen [100-103]. The presence of stomach and bowel air/ gas can adversely affect US image acquisition in the upper abdomen [104].

Fuss et al used the BAT US system to aid IMRT target alignment in the upper abdomen using adjacent vascular structures as surrogates for target position in 62 patients, including 3 children with neuroblastoma [101]. 15 of the 62 patients had a control CBCT after US. In total, 1,337 BAT alignments were

attempted, with useful images obtained in 95.8% of patients. The evaluation of BAT accuracy by control CBCT scan showed that 14 of the 15 suggested BAT shifts reduced the initial setup error by 12 to 95% (mean 54%). 4.2 % of BAT images were not considered useful due to massive air content in colon and stomach that obscured visualisation of the defined guidance structures on a particular treatment day. Obesity compromised visualisation of structures in 7 patients; the authors found that the thickness of a patient's subcutaneous fat layer was inversely correlated with the quality of the US image. BAT US imaging also allowed real-time assessment of organ motion; target position variation during a breathing cycle ranged from < 5 mm to 2.5 cm; greatest for tumours in or adjacent to the liver. Daily localisation with US in this study also enabled intra-fraction assessment of the amplitude of breathing motion. 4 of 96 patients demonstrated, what the authors described as, major changes in breathing pattern that were largely related to tumour-related pain. This study suggests that US may be useful in the upper abdomen and warrants further investigation.

In paediatric diagnostic radiology, US is frequently used for the staging and surveillance of children with abdominal tumours. Children are often accustomed to ultrasound and are, in general, comfortable with the procedure. Children would, in general, have a more favourable body habitus with less subcutaneous fat compared to adults where obesity has been shown to compromise US localisation [101, 102]. US pre-treatment was explored in 4 patients out of a cohort of 10 children receiving RT for abdominal neuroblastoma using the SonArray system (Varian Medical Systems, Palo Alto, CA) [105]. US was used to localise the child's kidney and registered to the

kidney's position as contoured on the simulation CT. The offsets established by the US system were recorded. The authors reported no correlation between the recommended cone beam CT and US pre-treatment shifts and abandoned the investigation of US after 4 patients.

With both the SonArray, and BAT US devices localisation is performed using 2 different imaging modalities; simulation CT and US. Reference planning CT contours are registered to the US images acquired pre-treatment. With the Clarity system, freehand US reference images are acquired at CT-simulation and matched to pre-treatment US images enabling an intra-modality comparison of images; this has been shown to be more accurate than the inter-modality method of comparing US to CT [106]. The accuracy and precision of the Clarity US system has been shown to be < 1mm in all planes and has recently been confirmed to operate with millimetre precision in vivo for prostate intra-fraction verification which is comparable with other RT localisation techniques in clinical use [100, 107].

The potential role of US in motion assessment, as an alternative or adjunct to CBCT (with acquisition optimised for low dose and bone match) for interfraction soft tissue verification, in children is worth investigating. US is also comparatively inexpensive and this is an important consideration from a global perspective as the majority of childhood cancers occur in low/ middle income countries where RT departments are unlikely to be in the position to implement routine 4DCT or 4DMR for children [39].

1.3.6 Incorporating individualised motion assessment into paediatric RT planning

Approaches to control or minimise RROM motion in adult RT planning and treatment are outlined in Figure 1.6, [108]

1.3.6.1 Internal target volume (ITV) approach

In adults, 4DCT is used to determine the target position during the patient's entire breathing cycle. This in turn defines a volume, the ITV, which encompasses the full extent of a target's excursion [52]. The ITV concept has been described in adult upper abdominal tumour sites including oesophagus, liver, pancreas and stomach [109-115].

1.3.6.2 Mid-position/ mid-ventilation (MidV) approach

The ITV concept could be considered a conservative approach to motion management. The MidV concept extracts a target's time-averaged position and its standard deviation from 4DCT images. Target motion is then considered a random positioning error in a probabilistic safety margin calculation [116]. This approach has been described mostly in lung stereotactic ablative RT where reductions in PTV size up to 30% have been reported with 98% local control rates at median 21.9 months follow up [117]. The approach has recently been described in the upper abdomen despite the less favourable beam penumbra in this anatomical site compared to the wider penumbra in lung parenchyma [111, 118]. The MidV approach achieved adequate PTV coverage in a planning study of 18 patients with pancreatic tumours and a statistically significant reductions in PTV volume (mean 13.9%), and OAR doses were demonstrated

[111]. Significant advantages in a MidV approach are described in targets displaying large displacements where an ITV approach that encompasses the entire target excursion significantly increases the volume of normal tissue irradiated.

1.3.6.3 Breath - hold

Breath-hold in children has been described primarily for tumour sites in the thorax. A feasibility study in seven children aged 13 – 18 years, demonstrated that all seven children were capable of performing a deep inspiration breath-hold (DIBH) for 15 – 20 seconds at a time [119]. A median of 6 breath-holds (range 5 – 8) were required to perform the CT scan. In terms of OAR sparing, RT plans in DIBH resulted in a statistically significant 22% reduction in mean lung dose compared to free-breathing RT plans. Dose to thyroid, heart, and breast (in girls) were comparable between the two techniques. Demoor et al demonstrated that 10 children with a median age of 16.5 years (range 8.6 – 19 years) were able to perform 10 – 18 second breath holds. Imaging in DIBH prolonged simulation sessions by on average 10 minutes and patients required 2 – 4 training sessions [120]. These two studies demonstrate the feasibility of DIBH in older children and the latter study highlights the additional training required to implement such a technique successfully. Maraldo et al's pilot study recruited 27 volunteers, median age 8 years (range 5 – 15 years). Preparation included a 30 minute coaching session on a Linear Accelerator. 18 of the 27 volunteers recruited were capable of repeating 3 stable 20 second breath holds [121]. This pilot suggested that even young children could perform DIBH successfully. RT in DIBH, however, is not feasible in very young children under

GA. As previously described in section 1.2.2.1, GA for RT delivery does not routinely involve intubation and respiratory muscle paralysis. Children under GA are in a free-breathing state. The additional preparation and training required and prolonged imaging times could challenge the ability of younger children not under GA to comply. The reproducibility of breath holds and target position in children using this approach is not known. The pilot study performed by Maraldo et al [121] has informed the development of the prospective, non-randomised feasibility study, TEDDI (Radio**t**h**e**rapy **d**elivery in **d**eep-**i**nspiration; ClinicalTrials.gov Identifier: NCT03315546) in children aged 5 to 17 years. In addition to feasibility in this age group, this study will assess the dosimetric benefits of DIBH and determine the reproducibility of repeated breath holds and reproducibility of target position [122].

1.3.6.4 Other techniques

Other more technically challenging motion management approaches to RT planning and treatment, such as gating and tracking, have not yet been described in children.

1.4 Motivation for this thesis

Children cannot be considered ‘little’ adults for the purposes of RT planning and delivery. Children of different heights and weights will display significant physiological and developmental heterogeneity. This degree of heterogeneity between patients is not seen in adults as highlighted graphically in Figure 1.7.

Extrapolating knowledge of geometric uncertainties in adults, as has been done pragmatically in the past, and applying it collectively to all patients from infanthood to young adulthood is, for the reasons outlined, suboptimal. Highly conformal photon RT techniques are playing an increasing role in the treatment of children with cancer, and intensity modulated proton RT (IMPT) is being increasingly used in paediatric RT. The focus of this thesis is highly conformal photon RT. However, the effects of RROM are potentially greater on proton dose distributions than on photon dose distributions given the broader photon beam penumbra. The prospect of established intensity modulated proton beam therapy (IMPT) and magnetic resonance guided RT (MRgRT) services within the UK, also drives the need to quantify internal organ motion for extracranial tumour sites in children and young people, and evaluate its potential impact on RT delivery, to ensure delivery of the best possible dose distributions with the steepest dose gradients at normal tissue/ target interfaces.

1.5 Challenges

Multinational, cooperative clinical trials are necessary in paediatric oncology to have sufficient statistical power to detect clinically significant results from therapeutic strategies. Because childhood cancer is so rare these trials recruit over extended periods of time. These historically long timelines often mean that trial-related RT guidance is no longer deemed current by the time patient accrual is completed. This in turn challenges valid interpretation of results in light of rapidly changing RT practices. Inferences in relation to RT practices

must be made from other sources of data such as single institution studies, case series and retrospective data. It has been stated that research with special emphasis on the implementation of modern RT technologies in children is difficult and this is acknowledged as a challenge for the specialty internationally [39].

The results contained within this thesis were made possible through the development and implementation of a single institution RT study at the Royal Marsden NHS Foundation Trust. This study, APAChe (**A**daptive RT **p**lanning for upper **a**bdominal tumours in **ch**ildren and t**e**enagers), was set-up by me under the supervision and guidance of Dr. Henry Mandeville and with significant input from other members of the multidisciplinary team; physicists, radiographers, clinical nurse specialists, anaesthetists, play specialists, and administrative staff. The study protocol is included in Appendix 1.

1.6 Thesis structure

Chapter 2 describes the feasibility of introducing a paediatric specific-4DCT into clinical practice and presents a detailed description of renal motion in children as quantified by deformable image registration of 4DCT. **Chapter 3 and 4** investigate the feasibility of using 4DMR and the Clarity ultrasound system as platforms for individualised motion assessment in children. **Chapter 5** looks to incorporate individualised motion assessment into paediatric RT planning by demonstrating the dosimetric benefits of adopting an internal target

volume (ITV) approach in high-risk neuroblastoma (HR-NBL) planning; the most common extra-cranial solid malignancy of childhood.

1.7 References

1) CRUK. Cancer Research UK Children's cancer statistics [1/9/2017]. Available from: http://www.cancerresearchuk.org/health-professional/cancer-statistics/childrens-cancers#heading-Zero.
2) Gaze M. Good practice guide for paediatric radiotherapy. Clinical Oncology 2019; 31(3): 139-41.
3) Radiologists RCo. Radiotherapy dose fractionation – paediatric radiotherapy 2016 [2: [Available from: https://www.rcr.ac.uk/system/files/publication/field_publication_files/bfco163_9_paediatric.pdf.
4) Hess CB, Thompson HM, Benedict SH, Seibert JA, Wong K, Vaughan AT, et al. Exposure Risks Among Children Undergoing Radiation Therapy: Considerations in the Era of Image Guided Radiation Therapy. International Journal of Radiation Oncology*Biology*Physics 2016; 94(5): 978-992.
5) Hall EJ. Intensity-modulated radiation therapy, protons, and the risk of second cancers. International Journal of Radiation Oncology*Biology*Physics 2006; 65(1): 1-7.
6) Hoeben BA, Carrie C, Timmermann B, Mandeville HC, Gandola L, Dieckmann K, et al. Management of vertebral radiotherapy dose in paediatric patients with cancer: consensus recommendations from the SIOPE radiotherapy working group. Lancet Oncol 2019; 20(3):e 155-e66.
7) Dawson LA, Kavanagh BD, Paulino AC, Das SK, Miften M, Li XA, et al. Radiation-Associated Kidney Injury. International Journal of Radiation Oncology • Biology • Physics 76(3): S108-S15.
8) Hall EJ, Wuu C-S. Radiation-induced second cancers: the impact of 3D-CRT and IMRT. International Journal of Radiation Oncology*Biology*Physics 2003; 56(1): 83-88.
9) Radiologists RCo. Good Practice Guide Paediatric Radiotherapy 2012 [Available from: https://www.rcr.ac.uk/publication/good-practice-guide-paediatric-radiotherapy.
10) Merchant TE, Hua C-h, Shukla H, Ying X, Nill S, Oelfke U. Proton versus photon radiotherapy for common pediatric brain tumors: Comparison of models of dose characteristics and their relationship to cognitive function. Pediatric Blood & Cancer 2008; 51(1): 110-117.
11) Olch AJ. Pediatric Radiotherapy Planning and Treatment. London, UNITED STATES: CRC Press; 2013.
12) Newhauser WD, Durante M. Assessing the risk of second malignancies after modern radiotherapy. Nature Reviews Cancer 2011; 11: 438.
13) van Waas M, Neggers SJ, Raat H, van Rij CM, Pieters R, van den Heuvel-Eibrink MM. Abdominal radiotherapy: a major determinant of metabolic syndrome in nephroblastoma and

neuroblastoma survivors. PLoS One 2012; 7(12): e52237.
14) Bolling T, Willich N, Ernst I. Late effects of abdominal irradiation in children: a review of the literature. Anticancer Res 2010; 30(1): 227-231.
15) van Waas M, Neggers SJ, van Eck JP, van Noesel MM, van der Lely AJ, de Jong FH, et al. Adrenal function in adult long-term survivors of nephroblastoma and neuroblastoma. Eur J Cancer 2012; 48(8): 1159-1166.
16) Paulino AC, Wen BC, Brown CK, Tannous R, Mayr NA, Zhen WK, et al. Late effects in children treated with radiation therapy for Wilms' tumor. Int J Radiat Oncol Biol Phys 2000; 46(5): 1239-1246.
17) Bolling T, Konemann S, Ernst I, Willich N. Late effects of thoracic irradiation in children. Strahlenther Onkol 2008; 184(6): 289-295.
18) Dörr W, Kallfels S, Herrmann T. Late bone and soft tissue sequelae of childhood radiotherapy. Strahlentherapie und Onkologie 2013; 189(7): 529-534.
19) Paulino AC, Fowler BZ. Secondary neoplasms after radiotherapy for a childhood solid tumor. Pediatr Hematol Oncol 2005; 22.
20) Bhatia S, Sklar C. Second cancers in survivors of childhood cancer. Nat Rev Cancer 2002; 2(2): 124-132.
21) Paulino AC. The promise of intensity modulated radiation therapy. Pediatr Blood Cancer 2016; 63(9): 1513-1514.
22) Jairam V, Roberts KB, Yu JB. Historical trends in the use of radiation therapy for pediatric cancers: 1973-2008. Int J Radiat Oncol Biol Phys 2013; 85(3): e151-5.
23) Panandiker ASP, McGregor L, Krasin MJ, Wu SJ, Xiong XP, Merchant TE. Locoregional Tumor Progression after Radiation Therapy Influences Overall Survival in Pediatric Patients with Neuroblastoma. Int J Radiat Oncol 2010; 76(4): 1161-1165.
24) Mandeville HC. Radiotherapy in the Management of Childhood Rhabdomyosarcoma. Clinical oncology (Royal College of Radiologists {Great Britain}) 2019; 31(7): 462-70.
25) Gibbs IC, Tuamokumo N, Yock TI. Role of radiation therapy in pediatric cancer. Hematol Oncol Clin N 2006; 20(2): 455-+.
26) Paulino AC, Lobo M, Teh BS, Okcu MF, South M, Butler EB, et al. Ototoxicity after intensity-modulated radiation therapy and cisplatin-based chemotherapy in children with medulloblastoma. Int J Radiat Oncol Biol Phys 2010; 78(5): 1445-1450.
27) Laskar S, Bahl G, Muckaden M, Pai SK, Gupta T, Banavali S, et al. Nasopharyngeal Carcinoma in Children: Comparison of Conventional and Intensity-Modulated Radiotherapy. Int J Radiat Oncol Biol Phys 2008; 72.
28) Paulino AC, Ferenci MS, Chiang KY, Nowlan AW, Marcus RB, Jr. Comparison of conventional to intensity modulated radiation therapy for abdominal neuroblastoma. Pediatr Blood Cancer 2006; 46(7): 739-744.
29) Ladenstein R, Valteau-Couanet D, Brock P, Yaniv I, Castel V, Laureys G, et al. Randomized Trial of prophylactic granulocyte colony-stimulating factor during rapid COJEC induction in

pediatric patients with high-risk neuroblastoma: the European HR-NBL1/SIOPEN study. J Clin Oncol 2010; 28(21): 3516-3524.
30) Gaze MN, Boterberg T, Dieckmann K, Hormann M, Gains JE, Sullivan KP, et al. Results of a quality assurance review of external beam radiation therapy in the International Society of Paediatric Oncology (Europe) Neuroblastoma Group's High-risk Neuroblastoma Trial: a SIOPEN study. Int J Radiat Oncol Biol Phys 2013; 85(1): 170-174.
31) Gains JE, Stacey C, Rosenberg I, Mandeville HC, Chang YC, D'Souza D, et al. Intensity-modulated arc therapy to improve radiation dose delivery in the treatment of abdominal neuroblastoma. Future Oncol 2013; 9(3): 439-449.
32) Shaffer R, Vollans E, Vellani R, Welsh M, Moiseenko V, Goddard K. A radiotherapy planning study of RapidArc, intensity modulated radiotherapy, three-dimensional conformal radiotherapy, and parallel opposed beams in the treatment of pediatric retroperitoneal tumors. Pediatr Blood Cancer 2011; 56(1): 16-23.
33) Beneyton V, Niederst C, Vigneron C, Meyer P, Becmeur F, Marcellin L, et al. Comparison of the dosimetries of 3-dimensions Radiotherapy (3D-RT) with linear accelerator and intensity modulated radiotherapy (IMRT) with helical tomotherapy in children irradiated for neuroblastoma. BMC Med Phys 2012; 12:2.
34) Pai Panandiker AS, Beltran C, Gray J, Hua C. Methods for image guided and intensity modulated radiation therapy in high-risk abdominal neuroblastoma. Pract Radiat Oncol 2013; 3(2): 107-114.
35) Pai Panandiker AS, Beltran C, Billups CA, McGregor LM, Furman WL, Davidoff AM. Intensity modulated radiation therapy provides excellent local control in high-risk abdominal neuroblastoma.Pediatric Blood & Cancer 2013; 60(5): 761-765.
36) Nazmy MS, Khafaga Y. Clinical experience in pediatric neuroblastoma intensity modulated radiotherapy. J Egypt Natl Canc Inst 2012; 24(4): 185-189.
37) CRCTU B. IMAT Neuroblastoma [Available from: https://www.birmingham.ac.uk/research/activity/mds/trials/crctu/trials/ImAT-Neurobalstoma/index.aspx.
38) Merchant TE. Clinical Controversies: Proton Therapy for Pediatric Tumors. Seminars in Radiation Oncology 2013; 23(2): 97-108.
39) Kortmann R-D, Freeman C, Marcus K, Claude L, Dieckmann K, Halperin E, et al. Paediatric radiation oncology in the care of childhood cancer: A position paper by the International Paediatric Radiation Oncology Society (PROS). Radiotherapy and Oncology 2016; 119(2): 357-360.
40) T B. Effects of Motion on the Total Dose Distribution. Seminars in Radiation Oncology 2004; 14(1): 41-51.
41) Keall PJ, Mageras GS, Balter JM, Emery RS, Forster KM, Jiang SB, et al. The management of respiratory motion in radiation oncology report of AAPM Task Group 76a). Medical Physics

2006; 33(10): 3874-3900.
42) van Herk M, Remeijer P, Rasch C, Lebesque JV. The probability of correct target dosage: dose-population histograms for deriving treatment margins in radiotherapy. International Journal of Radiation Oncology*Biology*Physics 2000; 47(4): 1121-1135.
43) ICRU. Report 83. Journal of the International Commission on Radiation Units and Measurements 2010; 10(1): NP-NP.
44) ElBeltagi MN, Wall V, Marignol L. Planning target volume (PTV) margin practice patterns in adults and paediatrics among the Paediatric Radiation Oncology Society (PROS) members: an international survey. Journal of Radiotherapy in Practice 2018; 17(4): 368-372.
45) Nazmy M, O'Shea E, McCrickard E, O'Sullivan C. OC-0079: CTV-to-PTV margin for treatment setup errors: paediatric vs adult. Radiotherapy and Oncology 2015; 115: S40.
46) Verellen D, De Ridder M, Linthout N, Tournel K, Soete G, Storme G. Innovations in image-guided radiotherapy. Nat Rev Cancer 2007; 7(12): 949-960.
47) Langen KM, Jones DTL. Organ motion and its management. International Journal of Radiation Oncology*Biology*Physics 2001; 50(1): 265-278.
48) Suh Y, Dieterich S, Cho B, Keall PJ. An analysis of thoracic and abdominal tumour motion for stereotactic body radiotherapy patients. Physics in Medicine and Biology 2008; 53(13): 3623-3640.
49) van Herk M. Different styles of image-guided radiotherapy. Semin Radiat Oncol 2007; 17(4): 258-267.
50) Brandner ED, Chetty IJ, Giaddui TG, Xiao Y, Huq MS. Motion management strategies and technical issues associated with stereotactic body radiotherapy of thoracic and upper abdominal tumors: A review from NRG oncology. Medical physics 2017; 44(6): 2595-2612.
51) van Dijk I, Huijskens SC, de Jong R, Visser J, Fajardo RD, Rasch CRN, et al. Interfractional renal and diaphragmatic position variation during radiotherapy in children and adults: is there a difference? Acta oncologica (Stockholm, Sweden) 2017; 56(8): 1065-1071.
52) Landberg T, Chavaudra J, Dobbs J, Gerard JP, Hanks G, Horiot JC, et al. Report 62. Journal of the International Commission on Radiation Units and Measurements 1999; os32(1): NP-NP.
53) Hallman JL, Mori S, Sharp GC, Lu H-M, Hong TS, Chen GTY. A Four-Dimensional Computed Tomography Analysis of Multiorgan Abdominal Motion. International Journal of Radiation Oncology*Biology*Physics 2012; 83(1): 435-441.
54) Yamashita H, Yamashita M, Futaguchi M, Takenaka R, Shibata S, Yamamoto K, et al. Individually wide range of renal motion evaluated by four-dimensional computed tomography. Springerplus 2014; 3: 131.
55) Siva S, Pham D, Gill S, Bressel M, Dang K, Devereux T, et al. An analysis of respiratory induced kidney motion on four-dimensional

computed tomography and its implications for stereotactic kidney radiotherapy. Radiation oncology (London, England) 2013; 8: 248.
56) Brandner ED, Wu A, Chen H, Heron D, Kalnicki S, Komanduri K, et al. Abdominal organ motion measured using 4D CT. International Journal of Radiation Oncology*Biology*Physics 2006; 65(2): 554-560.
57) van Sörnsen de Koste JR, Senan S, Kleynen CE, Slotman BJ, Lagerwaard FJ. Renal mobility during uncoached quiet respiration: An analysis of 4DCT scans. International Journal of Radiation Oncology*Biology*Physics 2006; 64(3): 799-803.
58) Pham D, Kron T, Bressel M, Foroudi F, Hardcastle N, Schneider M, et al. Image guidance and stabilization for stereotactic ablative body radiation therapy (SABR) treatment of primary kidney cancer. Practical Radiation Oncology 2015; 5(6): e597-e605.
59) Gawthrop JB, Gill S. The use of respiratory-correlated four-dimensional CT where kidney motion has the potential to impact upon the radiotherapy planning process. Journal of medical imaging and radiation oncology 2012; 56(6): 689-695.
60) Sonier M, Chu W, Lalani N, Erler D, Cheung P, Korol R. Evaluation of kidney motion and target localization in abdominal SBRT patients. Journal of applied clinical medical physics 2016; 17(6): 6406.
61) Pai Panandiker AS, Sharma S, Naik MH, Wu S, Hua C, Beltran C, et al. Novel Assessment of Renal Motion in Children as Measured via Four-Dimensional Computed Tomography. International Journal of Radiation Oncology*Biology*Physics 2012; 82(5): 1771-1776.
62) Kannan S, Teo BK, Solberg T, Hill-Kayser C. Organ motion in pediatric high-risk neuroblastoma patients using four-dimensional computed tomography. Journal of applied clinical medical physics 2017; 18(1): 107-114.
63) Uh J, Krasin MJ, Li Y, Li X, Tinkle C, Lucas JT, Jr., et al. Quantification of Pediatric Abdominal Organ Motion With a 4-Dimensional Magnetic Resonance Imaging Method. Int J Radiat Oncol Biol Phys 2017; 99(1): 227-237.
64) Huijskens SC, van Dijk IW, Visser J, Rasch CR, Alderliesten T, Bel A. Magnitude and variability of respiratory-induced diaphragm motion in children during image-guided radiotherapy. Radiotherapy and oncology : journal of the European Society for Therapeutic Radiology and Oncology 2017; 123(2): 263-269.
65) Guerreiro F, Seravalli E, Janssens GO, van de Ven CP, van den Heuvel-Eibrink MM, Raaymakers BW. Intra- and inter-fraction uncertainties during IGRT for Wilms' tumor. Acta oncologica (Stockholm, Sweden) 2018; 57(7): 941-949.
66) Lim P, Pica A, Hrbacek J, Bachtiary B, Walser M, Lomax AJ, et al. Pencil Beam Scanning Proton Therapy for Paediatric Neuroblastoma with Motion Mitigation Strategy for Moving Target Volumes. Clinical Oncology 2020.
67) Vedam SS, Keall PJ, Kini VR, Mostafavi H, Shukla HP, Mohan R.

Acquiring a four-dimensional computed tomography dataset using an external respiratory signal. Phys Med Biol 2003; 48(1): 45-62.
68) Rietzel E, Pan T, Chen GT. Four-dimensional computed tomography: image formation and clinical protocol. Med Phys 2005; 32(4): 874-889.
69) Underberg RWM, Lagerwaard FJ, Cuijpers JP, Slotman BJ, van Sörnsen de Koste JR, Senan S. Four-dimensional CT scans for treatment planning in stereotactic radiotherapy for stage I lung cancer. International Journal of Radiation Oncology*Biology*Physics 2004; 60(4): 1283-1290.
70) <keall_review.pdf>.
71) Pham D, Kron T, Foroudi F, Siva S. Effect of different breathing patterns in the same patient on stereotactic ablative body radiotherapy dosimetry for primary renal cell carcinoma: a case study. Medical dosimetry : official journal of the American Association of Medical Dosimetrists 2013; 38(3): 304-308.
72) Gwynne S, Wills L, Joseph G, John G, Staffurth J, Hurt C, et al. Respiratory Movement of Upper Abdominal Organs and its Effect on Radiotherapy Planning in Pancreatic Cancer1. Clinical Oncology 2009; 21(9): 713-719.
73) Brody AS, Frush DP, Huda W, Brent RL, American Academy of Pediatrics Section on R. Radiation risk to children from computed tomography. Pediatrics 2007; 120(3): 677-682.
74) Slovis TL. Children, computed tomography radiation dose, and the As Low As Reasonably Achievable (ALARA) concept. Pediatrics 2003; 112(4): 971-972.
75) Goske MJ, Frush DP, Brink JA, Kaste SC, Butler PF, Pandharipande PV. Curbing potential radiation-induced cancer risks in oncologic imaging: perspectives from the 'image gently' and 'image wisely' campaigns. Oncology (Williston Park) 2014; 28(3): 232-238, 43.
76) Hubbard P, Callahan J, Cramb J, Budd R, Kron T. Audit of radiation dose delivered in time-resolved four-dimensional computed tomography in a radiotherapy department. Journal of medical imaging and radiation oncology 2015; 59(3): 346-352.
77) Korreman SS. Motion in radiotherapy: photon therapy. Phys Med Biol 2012; 57(23): R161-191.
78) Lens E, van der Horst A, Kroon PS, van Hooft JE, Davila Fajardo R, Fockens P, et al. Differences in respiratory-induced pancreatic tumor motion between 4D treatment planning CT and daily cone beam CT, measured using intratumoral fiducials. Acta oncologica (Stockholm, Sweden) 2014; 53(9): 1257-1264.
79) Minn AY, Schellenberg D, Maxim P, Suh Y, McKenna S, Cox B, et al. Pancreatic tumor motion on a single planning 4D-CT does not correlate with intrafraction tumor motion during treatment. Am J Clin Oncol 2009; 32(4): 364-368.
80) Molloy JA, Oldham SA. Benchmarking a novel ultrasound-CT fusion system for respiratory motion management in radiotherapy: assessment of spatio-temporal characteristics and

comparison to 4DCT. Med Phys 2008; 35(1): 291-300.
81) Huijskens SC, van Dijk I, Visser J, Balgobind BV, Rasch CRN, Alderliesten T, et al. The effectiveness of 4DCT in children and adults: A pooled analysis. Journal of applied clinical medical physics 2018.
82) Pathmanathan AU, van As NJ, Kerkmeijer LGW, Christodouleas J, Lawton CAF, Vesprini D, et al. Magnetic Resonance Imaging-Guided Adaptive Radiation Therapy: A "Game Changer" for Prostate Treatment? Int J Radiat Oncol Biol Phys 2018; 100(2): 361-3673.
83) Hunt A, Hansen VN, Oelfke U, Nill S, Hafeez S. Adaptive Radiotherapy Enabled by MRI Guidance. Clinical oncology (Royal College of Radiologists {Great Britain}) 2018; 30(11): 711-719.
84) White IM, Scurr E, Wetscherek A, Brown G, Sohaib A, Nill S, et al. Realizing the potential of magnetic resonance image guided radiotherapy in gynaecological and rectal cancer. The British journal of radiology 2019; 92(1098): 20180670.
85) Bainbridge HE, Menten MJ, Fast MF, Nill S, Oelfke U, McDonald F. Treating locally advanced lung cancer with a 1.5T MR-Linac - Effects of the magnetic field and irradiation geometry on conventionally fractionated and isotoxic dose-escalated radiotherapy. Radiotherapy and oncology : journal of the European Society for Therapeutic Radiology and Oncology 2017; 125(2): 280-285.
86) Guerreiro F, Seravalli E, Janssens GO, van den Heuvel-Eibrink MM, Lagendijk JJW, Raaymakers BW. Potential benefit of MRI-guided IMRT for flank irradiation in pediatric patients with Wilms' tumor. Acta oncologica (Stockholm, Sweden) 2019; 58(2): 243-250.
87) Mutic S, Dempsey JF. The ViewRay System: Magnetic Resonance–Guided and Controlled Radiotherapy. Seminars in Radiation Oncology 2014; 24(3): 196-199.
88) Lagendijk JJW, Raaymakers BW, van Vulpen M. The Magnetic Resonance Imaging–Linac System. Seminars in Radiation Oncology 2014; 24(3): 207-209.
89) Keall PJ, Barton M, Crozier S. The Australian Magnetic Resonance Imaging–Linac Program. Seminars in Radiation Oncology 2014; 24(3): 203-206.
90) Fallone BG. The Rotating Biplanar Linac–Magnetic Resonance Imaging System. Seminars in Radiation Oncology 2014; 24(3): 200-202.
91) Dunlop A, Mitchell A, Tree A, Barnes H, Bower L, Chick J, et al. Daily adaptive radiotherapy for patients with prostate cancer using a high field MR-linac: Initial clinical experiences and assessment of delivered doses compared to a C-arm linac. Clin Transl Radiat Oncol 2020; 23: 35-42.
92) Block KT, Chandarana H, Milla S, Bruno M, Mulholland T, Fatterpekar G, et al. Towards Routine Clinical Use of Radial Stack-of-Stars 3D Gradient-Echo Sequences for Reducing

Motion Sensitivity. J Korean Soc Magn Reson Med 2014; 18(2): 87-106.
93) Michael R. Potential of MR-imaging in the paediatric abdomen. Eur J Radiol 2008; 68(2): 235-244.
94) Lavan NA, Mandeville HC. Imaging in Pediatric Oncology Pediatric Oncology, ISSN 1613-5318. Stephan D. Voss KM, editor: Springer; 2019.
95) Darge K, Anupindi SA, Jaramillo D. MR imaging of the abdomen and pelvis in infants, children, and adolescents. Radiology 2011; 261(1): 12-29.
96) Lagendijk JJW, Raaymakers BW, Van den Berg CAT, Moerland MA, Philippens ME, van Vulpen M. MR guidance in radiotherapy. Physics in Medicine and Biology 2014; 59(21): R349-R369.
97) Chandarana H, Block KT, Winfeld MJ, Lala SV, Mazori D, Giuffrida E, et al. Free-breathing contrast-enhanced T1-weighted gradient-echo imaging with radial k-space sampling for paediatric abdominopelvic MRI. European radiology 2014; 24(2): 320-326.
98) O'Shea T, Bamber J, Fontanarosa D, van der Meer S, Verhaegen F, Harris E. Review of ultrasound image guidance in external beam radiotherapy part II: intra-fraction motion management and novel applications. Phys Med Biol 2016; 61(8): R90-R137.
99) Fontanarosa D, van der Meer S, Bamber J, Harris E, O'Shea T, Verhaegen F. Review of ultrasound image guidance in external beam radiotherapy: I. Treatment planning and inter-fraction motion management. Phys Med Biol 2015; 60(3): R77-114.
100) Grimwood A, McNair HA, O'Shea TP, Gilroy S, Thomas K, Bamber JC, et al. In Vivo Validation of Elekta's Clarity Autoscan for Ultrasound-based Intrafraction Motion Estimation of the Prostate During Radiation Therapy. Int J Radiat Oncol Biol Phys 2018.
101) Fuss M, Salter BJ, Cavanaugh SX, Fuss C, Sadeghi A, Fuller CD, et al. Daily ultrasound-based image-guided targeting for radiotherapy of upper abdominal malignancies. International Journal of Radiation Oncology*Biology*Physics 2004; 59(4): 1245-156.
102) Boda-Heggemann J, Mennemeyer P, Wertz H, Riesenacker N, Küpper B, Lohr F, et al. Accuracy of Ultrasound-Based Image Guidance for Daily Positioning of the Upper Abdomen: An Online Comparison With Cone Beam CT. International Journal of Radiation Oncology*Biology*Physics 2009; 74(3): 892-897.
103) Fuller CD, Thomas CR, Jr., Wong A, Cavanaugh SX, Salter BJ, Herman TS, et al. Image-guided intensity-modulated radiation therapy for gallbladder carcinoma. Radiotherapy and oncology : journal of the European Society for Therapeutic Radiology and Oncology 2006; 81(1): 65-72.
104) Kuban DA, Dong L, Cheung R, Strom E, De Crevoisier R. Ultrasound-Based Localization. Seminars in Radiation Oncology 2005; 15(3): 180-191.

105) Beltran C, Pai Panandiker AS, Krasin MJ, Merchant TE. Daily image-guided localization for neuroblastoma. Journal of applied clinical medical physics 2010; 11(4): 3388.
106) Cury FL, Shenouda G, Souhami L, Duclos M, Faria SL, David M, et al. Ultrasound-based image guided radiotherapy for prostate cancer: comparison of cross-modality and intramodality methods for daily localization during external beam radiotherapy. Int J Radiat Oncol Biol Phys 2006; 66(5): 1562-1567.
107) Lachaine M, Falco T. Intrafractional prostate motion management with the Clarity Autoscan system. Medical physics international. 2013; 1.
108) Wolthaus JWH, Sonke J-J, van Herk M, Belderbos JSA, Rossi MMG, Lebesque JV, et al. Comparison of Different Strategies to Use Four-Dimensional Computed Tomography in Treatment Planning for Lung Cancer Patients. International Journal of Radiation Oncology*Biology*Physics 2008; 70(4): 1229-1238.
109) Cattaneo GM, Passoni P, Sangalli G, Slim N, Longobardi B, Mancosu P, et al. Internal target volume defined by contrast-enhanced 4D-CT scan in unresectable pancreatic tumour: evaluation and reproducibility. Radiotherapy and oncology : journal of the European Society for Therapeutic Radiology and Oncology 2010; 97(3): 525-529.
110) Chen X, Lu H, Tai A, Johnstone C, Gore E, Li XA. Determination of internal target volume for radiation treatment planning of esophageal cancer by using 4-dimensional computed tomography (4DCT). Int J Radiat Oncol Biol Phys 2014; 90(1): 102-109.
111) Lens E, van der Horst A, Versteijne E, van Tienhoven G, Bel A. Dosimetric Advantages of Midventilation Compared With Internal Target Volume for Radiation Therapy of Pancreatic Cancer. Int J Radiat Oncol Biol Phys 2015; 92(3): 675-682.
112) Tai A, Liang Z, Erickson B, Li XA. Management of Respiration-Induced Motion With 4-Dimensional Computed Tomography (4DCT) for Pancreas Irradiation. International Journal of Radiation Oncology*Biology*Physics 2013; 86(5): 908-913.
113) Xi M, Liu MZ, Deng XW, Zhang L, Huang XY, Liu H, et al. Defining internal target volume (ITV) for hepatocellular carcinoma using four-dimensional CT. Radiotherapy and oncology : journal of the European Society for Therapeutic Radiology and Oncology 2007; 84(3): 272-278.
114) Liu C, Gao X. Determination of radiotherapy target volume for esophageal cancer. Precision Radiation Oncology 2018; 2(2): 52-60.
115) Hawkins MA, Aitken, K. image guided-radiotherapy-for-esophageal-cancer .pdf>. Imaging in Medicine (2012) 2012; Volume 4(Issue 5).
116) Ehrbar S, Jöhl A, Tartas A, Stark LS, Riesterer O, Klöck S, et al. ITV, mid-ventilation, gating or couch tracking – A comparison of respiratory motion-management techniques based on 4D dose calculations. Radiotherapy and Oncology 2017; 124(1): 80-88.

117) Peulen H, Belderbos J, Rossi M, Sonke J-J. Mid-ventilation based PTV margins in Stereotactic Body Radiotherapy (SBRT): A clinical evaluation. Radiotherapy and Oncology 2014; 110(3): 511-516.
118) Velec M, Moseley JL, Dawson LA, Brock KK. Dose Escalated Liver Stereotactic Body Radiation Therapy at the Mean Respiratory Position. International Journal of Radiation Oncology*Biology*Physics 2014; 89(5): 1121-1128.
119) Claude L, Malet C, Pommier P, Thiesse P, Chabaud S, Carrie C. Active breathing control for Hodgkin's disease in childhood and adolescence: feasibility, advantages, and limits. Int J Radiat Oncol Biol Phys 2007; 67(5): 1470-1475.
120) Demoor-Goldschmidt C, Chiavassa S, Josset S, Mahé MA, Supiot S. Respiratory-gated bilateral pulmonary radiotherapy for Ewing's sarcoma and nephroblastoma in children and young adults: Dosimetric and clinical feasibility studies. Cancer/Radiothérapie 2017; 21(2): 124-129.
121) Maraldo MV, Lundgaard AY, Josipovic M, Bidstrup PE, Rechner L, Hansen R, et al. The Feasibility of Deep Inspiration Breath-Hold in Children: Results of the TEDDI Pilot Study. International Journal of Radiation Oncology, Biology, Physics 2018; 102(3): e278.
122) Lundgaard AY, Hjalgrim LL, Rechner LA, Josipovic M, Joergensen M, Aznar MC, et al. TEDDI: radiotherapy delivery in deep inspiration for pediatric patients - a NOPHO feasibility study. Radiation oncology (London, England) 2018; 13(1): 56-.
123) Wolthaus JW, Sonke JJ, van Herk M, Belderbos JS, Rossi MM, Lebesque JV, et al. Comparison of different strategies to use four-dimensional computed tomography in treatment planning for lung cancer patients. Int J Radiat Oncol Biol Phys 2008; 70(4): 1229-1238.

Figure 1.1 - 15 year-old patient with a diagnosis of stage IVB classical Hodgkin's lymphoma (patient had bone involvement).

(A) Diagnostic PETCT images depicting abnormal FDG uptake within the supraclavicular, mediastinal, para-aortic and bilateral iliac nodal regions and uptake within the spleen. (B) RT target volumes (red shaded area) and the associated 95% isodose distribution (green line).

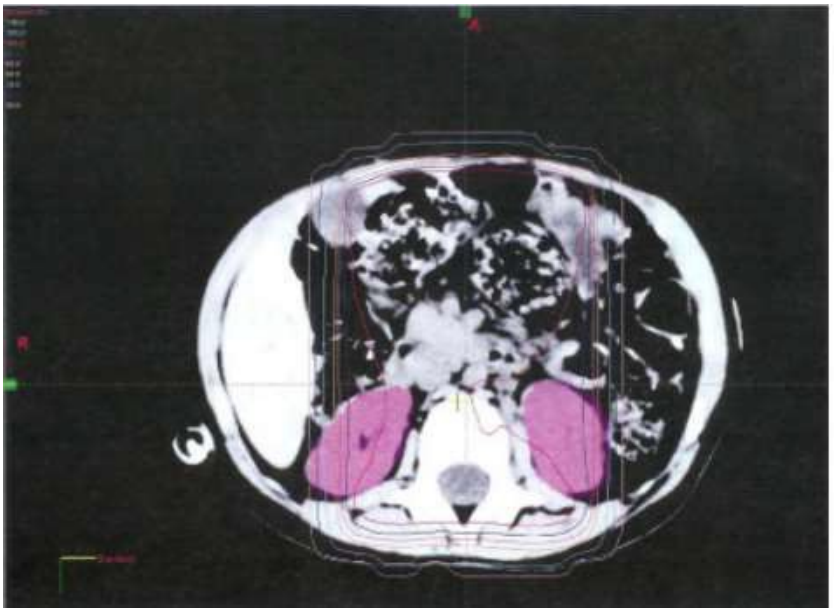

Figure 1.2 – Representation of POP beam arrangement for abdominal neuroblastoma [28].

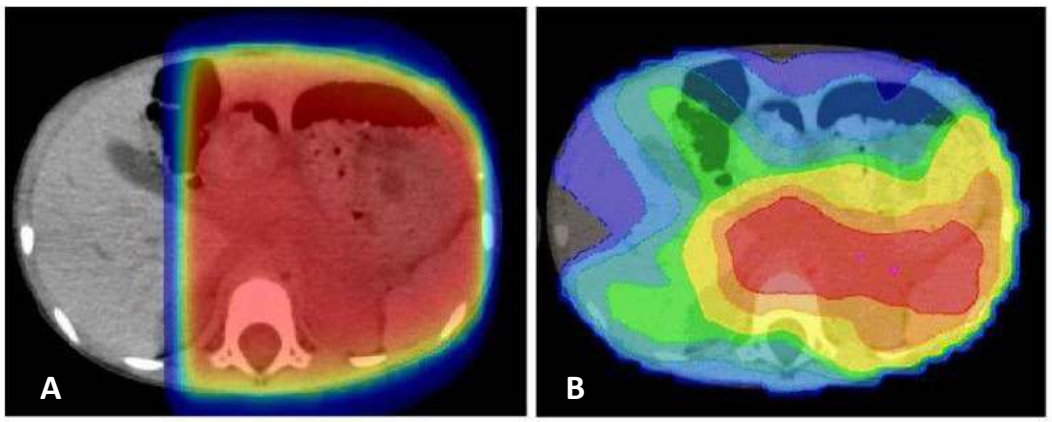

Figure 1.3 - (A) POP dose distribution, (B) VMAT dose distribution in the upper abdomen. Red colorwash: 90% isoshade. Adapted from [86].

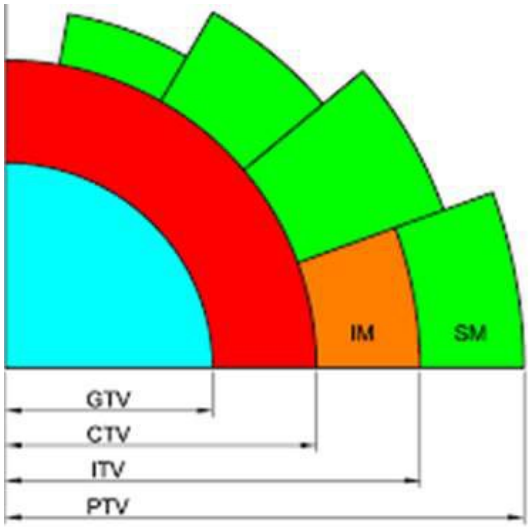

Figure 1.4 - ICRU-defined margins to account for geometric uncertainty in RT delivery. GTV: gross tumour volume. CTV: clinical target volume. ITV: internal target volume. PTV: planning target volume. IM: internal margin. SM: set-up margin. Adapted from [43, 52].

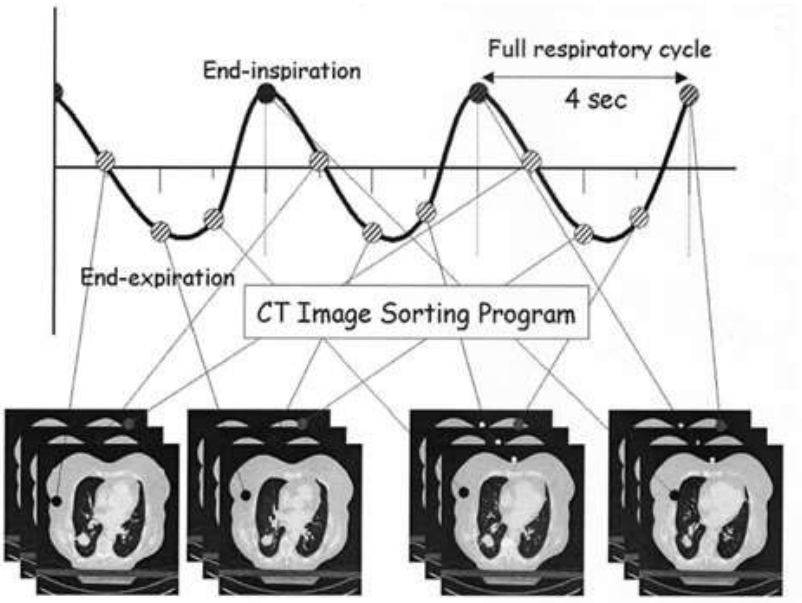

Figure 1.5 - Image acquisition process for 4DCT reconstruction.
Respiratory wave-form as registered by the respiratory surrogate, images sorted according to phase or amplitude assigned by the surrogate. Adapted from [69].

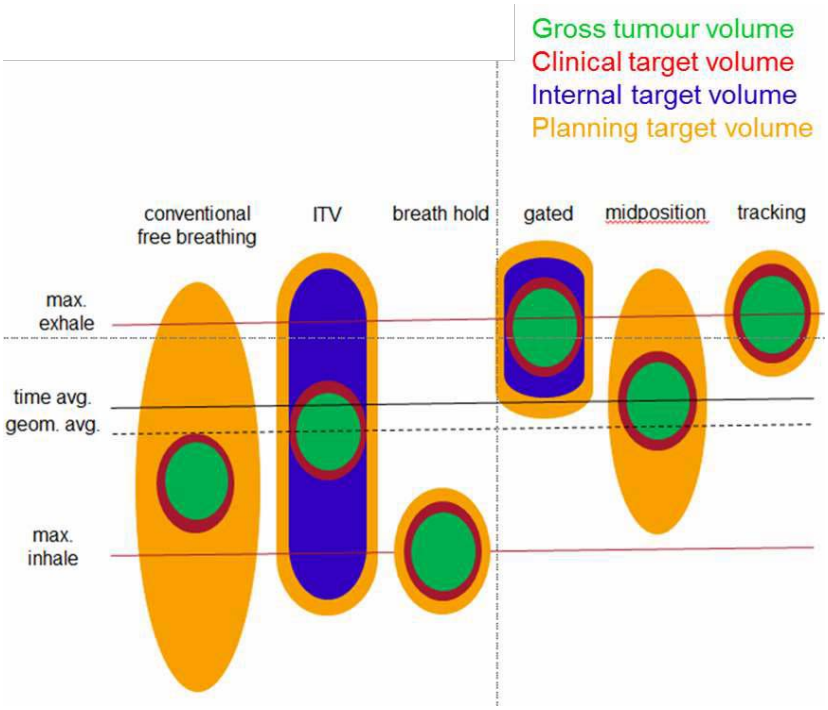

Figure 1.6 - Potential approaches to RROM management in RT pathway (courtesy of Dr. Andreas Wetscherek, adapted from (123)).

Figure 1.7 - graphical representation of the physical development between infanthood and adulthood.

Reference	Organ measured	Range (mm)	SI (mm)	AP (mm)	RL (mm)
(3)	Liver	-	9.7	4.8	-
(6)	Kidney	-	11.1 ± 4.8	3.6 +- 2.1	1.7 ± 1.4
(7)	Kidney	1.1 - 19.2 R 1.0 - 21.5 L	7.5 R 7.4 L	-	-
(8)	Kidney	11.0 R 13.0 L	-	-	-
(9)	Kidney	-	6.8 ± 2.0 R 8.6 ± 3.9 L	2.6 ± 0.5 R 1.2 ± 1.6 L	0.6 ± 0.9 R 0.6 ± 0.5 L

Table 1.1 - Mean (unless otherwise stated) kidney and liver motion (mm) in selected adult studies of RROM. R = right, L = left.

Chapter 2

Four-dimensional computed tomography for upper abdominal radiotherapy planning in children

2.1 Background

It is accepted that RROM in adults is patient-specific and individualised motion assessment is deemed necessary when using advanced RT techniques in thoracic and upper abdominal sites in adults [1, 2]. Organ motion is primarily respiratory-related. Peristalsis, gastrointestinal filling, or emptying, have all been acknowledged as potential sources of organ motion [3-5].

Four-dimensional computed tomography (4DCT) is the current standard for individualised intrafraction RROM assessment in adults. As outlined in Chapter 1, section 1.3.4.1, the increased dose associated with 4DCT has been a barrier to its routine use in paediatric RT planning in tumour sites susceptible to RROM due to concerns regarding potential second cancer induction.

In adults, early descriptions of upper abdominal organ motion were important in establishing the magnitude and variation in RROM [5-12]. Organ motion has been described in children in terms of centre of mass (COM) motion and organ edge or point of interest (POI) motion using both 4DCT and 4DMRI. Using COM displacements could underestimate organ motion as it does not take into account organ edge displacements that could occur as a result of organ deformation [13]. Deformable image registration (DIR), in the assessment of motion, quantifies the displacement of voxels between images. DIR can relate 4DCT volumes of interest at different respiratory phases to each other on a voxel by voxel basis [14]. DIR can account for motion at each point within a defined structure and may provide a more accurate representation of motion compared to COM - and POI-based estimates of organ motion.

In this chapter, I present my study of upper abdominal organ motion in children and young people. I use paediatric-specific 4DCT datasets and results are focused on deformation vector field displacements. COM displacements are presented and compared to previously published results.

2.2 Objectives of Chapter 2

My hypotheses are that it is feasible to acquire a 4DCT in children using equipment designed for acquiring 4DCT in adults, and that respiratory-related motion is child-specific.

In order to test these hypotheses, I will;

1) Determine the number of children referred for, and successfully completing, 4DCT.
2) Determine the median, standard deviation and range of respiratory-related organ displacements in children.
3) Determine the association between kidney motion and patient age, height, body surface area (BSA), and weight.
4) Compare RROM between children under GA and not under GA.

2.3 Methods

2.3.1 Patient selection

A paediatric-specific 4DCT protocol was implemented at the Royal Marsden NHS Foundation Trust in December 2015. I initiated a Committee for Clinical Research (CCR)-approved institutional service evaluation (SE508) to assess the feasibility of 4DCT in children and young people for RT planning with the secondary objectives of describing organ motion in the upper abdomen. Patients referred between December 2015 and May 2018 for RT to the thorax and/or abdomen were eligible for inclusion in this service evaluation.

2.3.2 Patient preparation and immobilisation

All patients were positioned supine, and with their arms up. If under general anaesthetic (GA), a head rest and knee fix were the only additional immobilisation used. For young children not under GA the decision to use additional vac bag immobilisation was individualised.

2.3.3 4DCT image acquisition

4DCT was acquired on a Brilliance Big Bore helical CT scanner (Philip N.V., Netherlands). Pitch is defined as the ratio of distance the table moves during a single gantry rotation to the width of the collimated beam in the longitudinal direction. The pitch is set to accommodate one breathing cycle per rotation and was altered based on the patient's breathing rate. 4DCT was not performed if a

breathing rate of less than 10 was recorded, or, if a child weighed less than 10kg. Scans were acquired at 1.5mm slice thickness.

A separate signal, related to the individual's breathing pattern, was recorded simultaneously and synchronized with image acquisition. A rubber air bellows (Philips Bellow System, Best, Netherlands) was the respiratory surrogate for scan acquisition used in this work. The bellows was connected to a pressure transducer. This transducer detected air pressure changes within the bellows as the child's chest/ abdomen rose and fell with respiration. This signal was digitised and sent to the scanner which in turn recorded a waveform trace. Each individually acquired image was tagged with a phase value (0% - 90%) linked to the respiratory trace recorded by the respiratory surrogate.

The bellows was standardly placed around the child at the level of the abdomen. If an adequate respiratory trace was not elicited with the bellows positioned as described, an attempt at recording a trace with the bellows in a different position was made. The bellows used in this work were designed for adult RT practice as a smaller paediatric-specific bellows is not commercially available. Respiratory traces of patients were observed during contrast-enhanced CT (CECT) acquisition and prior to 4DCT acquisition to allow the breathing traces to settle. Images were automatically sorted according tagged respiratory phase.

2.3.4 Organ delineation

I imported the 4DCT and CECT DICOM files for each patient from Pinnacle into RayStation™ treatment planning system (TPS) (research version 6.99,

RaySearch Laboratories AB, Stockholm). To minimise inter-observer variation and random window selection contributing to delineation error I contoured using a designated soft tissue window of Hounsfield numbers for all patients (soft tissue 40.0, 350.00). Organ contours were delineated on each phase of the 4DCT.

2.3.5 Deformable image registration

In RayStation™ DIR is performed using a hybrid intensity and structure based ANAtomically CONstrained Deformation Algorithm (ANACONDA) available within the TPS [15]. Phase 0% was designated the reference image set. Phases 10 – 90% were the target image sets. The DIR process resulted in 9 deformed image sets (0>10%, 0>20%, 0>30% …etc) for each patient.

2.3.6 Centre of mass (COM) analysis

Within the RayStation™ deformable image registration (DIR) module I extracted the x, y and z coordinates of the centre of mass (COM) position for both kidneys on each 4DCT phase relative to phase 0%. This gave me the organ COM motion pattern for each patient. From these results I calculated the maximum displacement of right and left kidney for each patient.

2.3.7 Deformation vector field (DVF) analysis

The DIR algorithm in RayStation defines a reference image set and a target image set. The DIR algorithm computes a vector field on the deformation grid; the deformation vector field (DVF). The vectors point from the individual voxels on the reference image (phase 0%) to the corresponding voxels on the target image set (phase 10%, …, 90%). In this work, individual case-specific DIR results were validated by visually reviewing the registration following DIR of the 4DCT phases, (Figure 3.1). The DVF displacements of individual voxels contained within each delineated organ (~2000 voxels per segmented structure per DIR x 9 registrations) were extracted. Organ motion assessment was achieved by calculating the maximum DVF displacement of all voxel displacements within each organ in the right/ left (RL), anterior/ posterior AP, and superior/ inferior (SI) directions. This was performed for each registration, for each patient. I selected the maximum DVF for each patient to reflect the 'worst case scenario' relevant for motion encompassing RT techniques (e.g. the generation of an internal target volume, ITV).

2.3.8 Vector analysis

Using the COM and DVF displacement results as described, I calculated vectors for the structures of interest using the following formula:

$$\sqrt{x^2 + y^2 + z^2}$$

Calculated vectors were used for comparison between metrics and patient groups.

2.3.9 Statistical analysis

As not all data followed a normal distribution (Shapiro Wilk's test for normality) descriptive statistics are used to summarise the data and non-parametric statistical tests are presented where appropriate.

The group's mean and median DVF and COM displacements and their respective standard deviations (SD) and ranges are reported.

The difference in motion magnitude between patient groups (GA versus no GA, right and left kidney combined) were compared using the Mann Whitney U test with a significance level of $p<0.05$. An average 3D vector was used for patients with two kidneys for the purpose of these group comparisons.

Correlation between motion (DVF displacement) and patient related variables (age, height, weight, BSA) used Spearman's correlation coefficients. Linear regression was performed in Microsoft Excel. Statistical analysis was performed using GraphPad Prism (version 7.00 for Windows, GraphPad Software, La Jolla California USA, www.graphpad.com).

2.4 Results

2.4.1 Feasibility

Between December 2015 and May 2018, 32 patients were eligible for 4DCT as part of RT planning. Median age of patients referred 4.7 years (SD 4.7, range 1.5 – 17.5). 4DCT was successfully acquired in 27 of the 32 patients referred (84%).

In two of the 27 patients that had a 4DCT, whole kidneys were not visualised within the imaged anatomy. The reasons for not completing a 4DCT in the 5 patients referred but not imaged are summarised in Figure 2.2.

Characteristics of patients included in the final analysis are shown in Table 2.3.

2.4.2 Organ motion results

25 of the 27 patients (with complete kidney contours visible on 4DCT) are included in my analysis of kidney motion. The reasons for patients not being included in the final analysis are outlined in Figure 2.2. Patients included in this analysis had a variety of primary diagnoses but predominantly Wilms' tumour (WT) and neuroblastoma (NBL). These two diagnoses have greatest incidence in children under the age of 5 years. For many solid tumours, surgical resection remains a key part of oncological management. Particularly for Wilms' tumour, and occasional cases of neuroblastoma, surgery includes a unilateral nephrectomy. As a result not all patients included in this analysis have two kidneys at the time of RT. Eighteen right kidneys and 19 left kidneys are included in the final analysis. Kidney motion in SI, RL and AP directions is presented.

Right and left kidney DVF displacements for all patients are presented in Table 1 and plotted according to 4DCT phase (0 - 90%) in Figure 2.3. All displacements are measured relative to the 0% phase of the 4DCT (end-inhalation). In the SI direction, DVF displacements in 4DCT phases 10 - 90% are positive relative to phase 0% (i.e. superior).

Figure 2.3 also describes the skewed distribution of my data with the majority of data points positioned to the left of the median. This is consistent with my sample of patients with ages ranging from 1.7 to 17.5 years and a median age of 4.7 year.

The greatest magnitude of kidney displacements was seen in the SI direction. In Figure 2.3, the horizontal line in the box (middle two quartiles) indicates the median of the distribution for all patients. In the SI direction; the median right kidney motion was 2.4 mm and 3.6 mm for the left, (Table 2.1). Median RL and AP displacements were 2 mm or less for right and left kidneys.

The boxplots in Figure 2.3 also demonstrate interpatient variation and a wide range of displacements in all directions. Kidney SI motion ranges from 0.3 – 12.2 mm (right kidney) and 0.4 – 13.2 mm (left kidney). SD is a measure of variation within a group. The greatest standard deviations (SD) are in the SI direction; 3.2 mm (right kidney) and 3.1 mm (left kidney).

Figure 2.4 shows COM displacements plotted according to the phase of 4DCT (0 – 90%) and relative to phase 0% (end-inhalation). COM displacements (mm) in RL, AP and SI directions are also presented in Table 1. Median right kidney SI motion was 2.8 mm and 2.7 mm for the left kidney. Median COM displacements in the RL and AP directions were ≤ 1mm for both kidneys. The range of SI kidney motion measured by COM displacement was 0.9 – 6.3 mm for the right kidney and 0.2 – 5.9 mm for the left kidney.

Vector displacements are also presented in Table 2.1. COM derived displacements were 3.1 mm and 2.9 mm for right and left kidneys compared to 4.1 mm and 4.2 mm when calculated from DVF displacements.

2.4.3 Young age, general anaesthetic (GA) and kidney motion

Median age of the 11 children in whom 4DCT was acquired under GA was 3.1 years (range 1.5 – 6.1). Six children of a similar age were not treated under GA median age 4.5 years (range 4.1 – 4.9). Median age of the 14 children not under GA was 6.0 years (range 3.9 – 17.5).

There was a statistically significant difference in vector displacements in patients under GA compared to all patients not under GA (p 0.0019, Mann Whitney U test). In children under GA; median (SD) right kidney displacement was 1.9 mm (1.5) and 2.0 mm (2.3) for the left compared to 8.5 mm (2.7) and 4.5 mm (4.5) in children not under GA, Table 2.2.

The differences in displacements were no longer significant when the two groups of similarly aged children under GA (N = 11) and not under GA (N = 6) were compared (p 0.2117, Mann Whitney U test).

Median displacements of right and left kidneys in children under GA were similar; 1.9 mm and 2.0 mm. The outlier in this group was a 2.7 year old child whose right kidney displacement measured 4.8 mm. The same patient's left kidney vector was 0.8 mm. The SD of left kidney motion (2.3 mm) suggested greater variation in left kidney displacements in this cohort of patients.

2.4.4 Correlation between magnitude of DVF 3D vector and patient related variables

I tested for associations between DVF-derived vector displacements and the following patient-related variables; age, height, weight, and BSA (body surface area). Generally, a value of r that is greater than 0.7 is considered a strong

correlation. A value of 0.5 – 0.7 is considered a moderate correlation. In Figures 2.5 and 2.6, the solid line indicates the linear trend plotted by linear regression and the dotted lines indicate the 95% confidence interval of the best fit line. The p value indicates the likelihood of the null hypothesis (that there is no relationship between the motion vector and the patient-related variable) being correct with a best fit line of this slope i.e. for all variables the chance is less than 5%.

As observed and previously discussed, SI motion is greatest and therefore most likely to influence the overall vector displacement. Rather than testing multiple associations in each cardinal direction for each kidney I tested the association between the vector displacements and the patient-related variables.

Right kidney motion was statistically significantly associated with BSA, age, height and weight (all $p < 0.01$); illustrated in Figure 5. Calculated Spearman's r values were; 0.5 for BSA, 0.6 for age, 0.6 for height, and 0.5 for weight.

Left kidney motion was again statistically significantly associated with BSA, age, height or weight (all $p < 0.01$), (Figure 2.6). Spearman r values were; 0.6 for BSA, 0.3 for age, 0.5 for height, and 0.5 for weight.

2.5 Discussion

2.5.1 4DCT

2.5.1.1 Acquisition

4DCT was successfully acquired in 82% of the study cohort referred; median age 4.7 years (range 1.5 – 17.5). This indicates that acquiring 4DCT using an adult respiratory bellows in children is feasible even in the very young and very small.

2.5.1.2 Respiratory- related organ motion modelling

A respiratory bellows designed for adult use was used for 4DCT acquisition in this work as a paediatric-specific bellows is not commercially available. The bellows must be in contact with the child's skin surface with adequate tension in order to operate effectively. Three children in this study did not have a breathing trace detected by the bellows which may have been due to the lack of adequate tension. This suggests that a respiratory bellows designed for adult use may not be the ideal respiratory surrogate, particularly in very young children whose abdominal and thoracic circumferences can be significantly smaller than adults. The Realtime Position Management (RPM) system (Varian Medical Systems, Palo Alto, CA, USA) has been used as an alternative surrogate in previously published studies of organ motion in children (16). No paper describing the use of 4DCT for organ motion assessment in children has commented on the proportion of patients referred for 4DCT in whom an adequate breathing trace was not traced by the equipment. This work

highlights a limitation in applying 4DCT in very young children using equipment designed for adults.

Lung volume is at its greatest at end-inhalation (usually 0% phase) and as a result upper abdominal organs would be expected to be at their most inferior position in this phase. As the respiratory cycle proceeds towards end-expiration (usually 50% phase) and lung volume is reduced, upper abdominal organs will move more superiorly relative to end-inspiration. This pattern is evident in the SI motion plotted relative to phase 0% in Figure 2.2 and demonstrates that the acquired 4DCT scans have modelled respiratory-related kidney motion as expected. These plots also show that peak expiratory motion does not always occur in the 50% phase. End-expiration can occur in phase 50 – 70%. These findings are similar to that found in a study examining inter- and intra-fraction motion in 15 patients with Wilms' tumours [17]. Maximum inspiration and expiration were visually confirmed for all 15 patients studied in this paper. End inspiration phase was not the 0% phase in 4 of the 15 patients and occurred in phase 10% or phase 90%. In my work, I have plotted motion data by phase relative to the 0% phase. Given the findings of Guerreiro et al, my results may misrepresent the pattern of RROM in a proportion of my patients but would not affect the overall vector magnitudes described and used for subsequent comparative analyses~~.~~ as my analyses are based on the the absolute values of measured displacements.

2.5.1.3 Dose

The dose associated with 4DCT acquisition in children is high; delivering 1.6 – 3.0 times the imaging dose of a conventional 3DCT in reported series using an adult imaging protocol [16, 18, 19]. Low dose 4DCT protocols accept a trade-

off between reduced doses delivered to the patient and reduced soft tissue contrast [16]. An initial aim of this work was to quantify liver motion on the 4DCT datasets. However, after the first three patients had been contoured it became clear that delineation of the medial liver edge was challenging on the non-contrast enhanced, paediatric – specific 4DCT and resulted in significant contouring discrepancies between phases. A decision was made to proceed with analysis of the kidney motion alone.

Conventionally, the scanning window for paediatric RT CT protocols in the thorax and upper abdomen include the lung apices down to the level of the mid-femur. This allows for the dose to whole organ at risk (OAR) volumes to be recorded i.e. lungs and heart. The dose exposure associated with 4DCT is directly proportional to the scan field of view (FOV) [19]. Reducing the scanning window for 4DCT would require a change in current practice for dose reporting in paediatric RT.

2.5.1.4 Patient – related factors

By working with highly skilled play specialist team members some young children are able to complete RT planning and treatments without the need for GA for immobilisation. GA slots require significant coordination of additional resources in a RT department. Children having GA need to fast in advance which can be incredibly challenging for infants and toddlers and their families. Treatment under GA also requires children to remain in hospital for longer periods to allow recovery post treatment. Therefore, treatment under GA can have additional impact on the children and their families. GA slots are often limited per day and if this capacity is exceeded it can even result in children being transferred to another institution for RT. One child in this study was only

able to tolerate lying still for the CECT component of the planning scans and not for the additional 4DCT acquisition; an issue that only arose at the time of simulation. Though only one patient it highlights the fine line we tread in paediatric RT. Acquiring 4DCT prolongs the simulation session and that increase in time could be the difference in completing the session with or without GA. This is perhaps the reason why 4 of 15 patients in the Guerreiro study had GA at simulation but not for treatment [17]. Contrast-enhanced 4DCT acquisition has been described in adult upper abdominal sites [20]. This approach negates the need for two scans and this approach limits the associated ionising radiation exposure risk (because the additional CECT is not acquired) and reduces the overall scan times. Adopting this approach could enable overall simulation times to be reduced and would be a favourable solution for use in paediatric RT.

2.5.1.5 Intrafraction kidney motion

In this Chapter, I demonstrated that in my cohort of 25 children with a median age of 4.5 years (range 1.5 – 17.5) kidney motion is greatest in the SI direction. Median DVF displacement for the right kidney was 2.4 mm and 3.6 mm for the left. The respective COM displacements were 2.8 mm and 2.7 mm. There was good agreement between methodologies in calculated median kidney displacements. RL, AP and, similarly, there was good agreement between overall vector displacements for both DVF and COM methodologies.

Estimating kidney motion based on COM measurements may not be accurate enough [21]. The selection of COM as a metric is often defended in publications because of its insensitivity to the effects of deformation [17]. It is recognized in adults that organs affected by respiration can display complex

non– rigid displacements i.e. deformation [22, 23]. Deformation is therefore an important source of organ motion that should be quantified [24]. Deformable image registration (DIR) may provide a better representation of geometric change and has been validated for robustness and reproducibility [25]. Deformation between 4DCT phases acquired at the same imaging session, as is the case in this work, minimises uncertainty associated with DIR as the scans share the same coordinates.

The differences between median DVF and median COM vector displacements were small and below the resolution of 4DCT slice thickness. However, DVF vector displacements ranged from 0.3 – 13.8 mm for the right kidney and 0.6 – 16.8 mm for the left. The maximum COM displacements for right and left kidneys were 6.7 mm and 7.2 mm. DVF displacements described in this Chapter suggest greater displacements between voxels in individual patients than measured by COM displacement. Greater DVF values compared to COM values is similar to results from a study of thoracic organ motion on 4DCT datasets in 5 adult patients utilizing a similar methodology [26].

Intrafraction upper abdominal organ motion was quantified in 4 previous studies, using 4DCT and 4DMR, in median 17.5 children (range 15 – 35). These publications demonstrated that intrafraction organ motion occurs, in order of decreasing magnitude, in the SI > AP > RL directions [16, 27, 28]. Mean SI right kidney displacements were 1.9 – 4.7mm and 1.4 - 4.8mm for the left kidney in three studies that considered right and left kidneys as separate structures. A single publication reported median kidney motion of 0.6 mm in 15 children with Wilms' tumour (each child had only one kidney) [17]. In all 4 studies, AP and RL kidney motion was less than 2-3mm. Median SI kidney

displacements presented in this Chapter (DVF displacements of 2.4 and 3.6 mm) compare favourably with results from these 4 publications.

Panandiker measured kidney motion on 4DCT in 20 children (median age 8 years, range 2 – 18 years). In children < 9 years of age, median right kidney SI motion was 2.0 mm (range 0.6–3.7 mm) and median left kidney SI motion was 1.6 mm (range 0.7–3.4 mm) (27). In children > 9 years of age, right kidney SI motion was 3.6 mm (range 1.5–6.3 mm) and 3.4 mm (range 0.8–4.6 mm) for the left kidney. These results suggested that intrafraction organ motion in young children is less than that seen in older children.

Guerreiro et al assessed COM motion of tumour bed (as defined by systematically placed surgical clips) and organs at risk (kidney, liver, spleen) in 15 children; average age 4 years (range 1 – 8 years). Mean SI intrafraction motion for the kidney was 0.9 mm, liver 1.1 mm and spleen 1.4 mm. SI tumour bed motion (assessed by surgical clip COM displacements) was 1.0 mm. These findings suggest that intrafraction organ motion in young children is negligible.

The difference in COM displacement published by Guerreiro et al and my results (median right kidney displacement 2.4 mm, and left kidney displacement 3.6 mm compared to 0.9 mm) could be explained by my use of absolute values of the displacements rather than considering the sign of the displacement. In this Chapter, SI kidney DVF displacements ranged from 0.3 – 12.2 mm for the right kidney, and 0.4 – 13.2 mm for the left kidney. These results indicated a wide range of kidney motion across the children in this cohort. Given that variation the difference in values could also represent patient – specific differences in intrafraction RROM.

Wilms' tumour and neuroblastoma are two common tumours that arise in the upper abdomen in children. Both pathologies most frequently present in children < 5 years i.e. the age group often requiring GA to achieve the required immobilisation for RT simulation and treatment. In the Panandiker series, all children in the younger cohort (< 9 years of age) required GA compared to just one patient in the cohort of children > 9 years of age [27]. The use of GA was therefore highly correlated with age in their series and the use of GA could affect the magnitude of intrafraction organ displacements. Median age in the younger cohort was 3 years, range 2 – 8 years and similar to the median age in my cohort of children under GA (3.1 years, range 1.5 – 6.1 years). In this Chapter I demonstrated that children under GA had statistically significantly smaller kidney displacements than children not under GA; 1.9 mm and 2.0 mm compared to 8.5 mm and 4.5 mm for right and left kidneys (p 0.2117). These results suggest that there is less organ motion in young children under GA relative to older children and adults.

When I compared kidney displacements in the 11 children under GA to those measured in the 6 children of similar young age but not under GA, the difference in median kidney displacement between the groups was no longer significant. Kannan et al similarly did not find a statistically significant difference in intra-fraction organ motion between patient subgroups based on age and use of GA [16]. Huijskens et al also did not find a statistically significant difference in the magnitude of diaphragm displacements when they compared subgroups of young children under GA and not under GA but did demonstrate that children under GA had statistically significantly smaller intrafraction variability than children not under GA [29].

In the Guerreiro paper, both right and left kidney were considered a single organ at risk. In very young children (the children often requiring GA for radiotherapy) the liver takes up a greater proportion of the abdominal cavity than in adults [30]. The relative size of the liver may influence the degree to which the right kidney moves in the SI direction in very young children. The left kidney is relatively free in anatomical space and therefore is not impeded to the same degree as the right kidney. Panandiker et al also found that motion of one kidney did not predict for motion of the other again suggesting that right and left kidneys displace to differing degrees [27].

The correlation results presented in this Chapter showed statistically significant associations between kidney vector displacements and BSA, age, height, and weight. However, Spearman correlation coefficients ranged from 0.3 – 0.6, at most. These values are indicative of poor to moderate correlations.

Published results are conflicting. Panandiker et al found a statistically significant association between right and left kidney motion and age ($p = 0.0187, 0.0323$) and height ($p = 0.017, 0.042$) for left and right kidney respectively [27]. Huijskens et al found only weak associations between intrafraction diaphragm motion and patient age, height and weight [31]. Guerreiro et al also found no statistically significant correlations between intrafraction motion and patient height and weight [17].

The patient-specific variables cannot be considered entirely independent of each other, a condition required for regression modelling; young children will be lighter and smaller than older children. However, it is reasonable to surmise that patient – related variables only explain a small proportion of the inter-patient variation in organ motion.

2.5.2 Limitations

My work describes intrafraction kidney motion. A secondary objective of the APAChe study was to quantify interfraction kidney motion. I imported cone-beam computed tomography (CBCT) scans for all children recruited to the study. At RMH, CBCT acquisition in children has been adapted to minimise the imaging dose and is optimised for bone match only (nominal CTDI dose measured in a phantom was 5mGy); a common approach adopted in paediatric RT departments internationally [32-34]. The resulting soft tissue contrast is poor compared to the planning CT quality and was not sufficient for organ at risk contouring, (Figure 2.8).

RROM can vary from day to day as well as from one breathing cycle to the next. For these reasons the reproducibility of motion as measured on a single 4DCT, such as presented in this Chapter, is potentially limited [35-37]. Huijskens et al reported on the variability of diaphragm motion in 45 children as measured on CBCT. Mean amplitude measured 10.7mm (range 4.1 - 17.4mm). Intrafraction variability was 2.4 mm and interfraction variability was 1.4 mm. Interestingly, intrafraction variability in diaphragm motion was significantly smaller in children treated under GA (1.6 mm) compared to those treated without GA (2.4 mm). This finding suggests that 4DCT may be more representative of intrafraction organ motion during the RT course in children under GA.

Intrafraction organ motion presented in the Chapter is only one component of the CTV to PTV margin. Four studies, median 35 paediatric patients (range 10 – 45), have used CBCT to quantify interfraction kidney motion [38], [31], [17,

39] ; liver motion [17], [38], and diaphragmatic motion [31], [39], [29]. These studies show that interfraction organ motion is greatest in the SI direction. One study, comparing 35 paediatric to 35 adult patients, demonstrated that median kidney motion in children was statistically significantly smaller than in adults; 2.8, 2.9mm and 5.6, 5.2mm for median vector lengths for right and left kidney respectively ($p<0.05$) [39]. As discussed in Chapter 1, interfraction motion uncertainties can be accounted for using in-room off-line (systematic component) or on-line (systematic and random components) approaches to image guided RT (IGRT). Ultrasound-based IGRT systems (discussed further in Chapter 4) are available and can be integrated with C-arm linear accelerators with potential for complementing current image-guidance strategies to enhance soft-tissue visualisation; a clear limitation of CBCT as acquired in the APAChe study and described earlier in this section.

2.6 Conclusion

4DCT acquisition in children using equipment designed for adults is feasible, even in the very young. In the context of my results, and others, the patient-specific nature of RROM in children should be accepted as it has been in adult RT planning. This supports the use of individualised motion assessment in children. However, 4DCT may not be the ideal solution due in part to the technical limitations of the equipment as described in this work but also the additional radiation dose associated with 4DCT imaging.

2.7 References

1) Keall PJ, Keall PJ, Mageras GS, Balter JM, Emery RS, Forster KM, Jiang SB, et al. The management of respiratory motion in radiation oncology report of AAPM Task Group 76a). Medical Physics 2006; 33(10): 3874-3900.
2) Benchetrit G. Breathing pattern in humans: diversity and individuality. Respiration Physiology 2000; 122(2): 123-129.
3) Korreman SS. Motion in radiotherapy: photon therapy. Phys Med Biol 2012; 57(23): R161-191.
4) Brandner ED, Chetty IJ, Giaddui TG, Xiao Y, Huq MS. Motion management strategies and technical issues associated with stereotactic body radiotherapy of thoracic and upper abdominal tumors: A review from NRG oncology. Medical physics 2017; 44(6): 2595-2612.
5) Langen KM, Jones DTL. Organ motion and its management. International Journal of Radiation Oncology*Biology*Physics 2001; 50(1): 265-278.
6) Moerland MA, van den Bergh ACM, Bhagwandien R, Janssen WM, Bakker CJG, Lagendijk JJW, et al. The influence of respiration induced motion of the kidneys on the accuracy of radiotherapy treatment planning, a magnetic resonance imaging study. Radiotherapy and Oncology 1994; 30(2): 150-154.
7) Schwartz LH, Richaud J, Buffat L, Touboul E, Schlienger M. Kidney mobility during respiration. Radiotherapy and oncology : journal of the European Society for Therapeutic Radiology and Oncology 1994; 32(1): 84-86.
8) Balter JM, Lam KL, McGinn CJ, Lawrence TS, Ten Haken RK. Improvement of CT-based treatment-planning models of abdominal targets using static exhale imaging. Int J Radiat Oncol Biol Phys 1998; 41(4): 9399-43.
9) Goitein M. Organ and tumor motion: an overview. Semin Radiat Oncol 2004; 14(1): 2-9.
10) Gierga DP, Chen GT, Kung JH, Betke M, Lombardi J, Willett CG. Quantification of respiration-induced abdominal tumor motion and its impact on IMRT dose distributions. Int J Radiat Oncol Biol Phys 2004; 58(5): 1584-1595.
11) Brandner ED, Wu A, Chen H, Heron D, Kalnicki S, Komanduri K, et al. Abdominal organ motion measured using 4D CT. International Journal of Radiation Oncology*Biology*Physics 2006; 65(2): 554-560.
12) Gwynne S, Wills L, Joseph G, John G, Staffurth J, Hurt C, et al. Respiratory Movement of Upper Abdominal Organs and its Effect on Radiotherapy Planning in Pancreatic Cancer1. Clinical Oncology 2009; 21(9): 713-719.

13) Brock KK, Hawkins M, Eccles C, Moseley JL, Moseley DJ, Jaffray DA, et al. Improving image-guided target localization through deformable registration. Acta oncologica (Stockholm, Sweden) 2008; 47(7): 1279-1285.
14) Rietzel E, Chen GTY, Choi NC, Willet CG. Four-dimensional image-based treatment planning: Target volume segmentation and dose calculation in the presence of respiratory motion. International Journal of Radiation Oncology*Biology*Physics 2005; 61(5): 1535-1550.
15) Weistrand O, Svensson S. The ANACONDA algorithm for deformable image registration in radiotherapy. Med Phys 2015; 42(1): 40-53.
16) Kannan S, Teo BK, Solberg T, Hill-Kayser C. Organ motion in pediatric high-risk neuroblastoma patients using four-dimensional computed tomography. Journal of applied clinical medical physics 2017; 18(1): 107-114.
17) Guerreiro F, Seravalli E, Janssens GO, van de Ven CP, van den Heuvel-Eibrink MM, Raaymakers BW. Intra- and inter-fraction uncertainties during IGRT for Wilms' tumor. Acta oncologica (Stockholm, Sweden) 2018; 57(7): 941-949.
18) Lavan N CE, Burland H, Mandeville HC. Development of a four-dimensional computed tomography (4DCT) imaging sequence for paediatric radiotherapy planning. International Society of Paediatric Oncology (SIOP); Dublin, Ireland. Pediatric Blood and Cancer 2016 p. S1-S321.
19) Hubbard P, Callahan J, Cramb J, Budd R, Kron T. Audit of radiation dose delivered in time-resolved four-dimensional computed tomography in a radiotherapy department. Journal of medical imaging and radiation oncology 2015; 59(3): 346-352.
20) Beddar AS, Briere TM, Balter P, Pan T, Tolani N, Ng C, et al. 4D-CT imaging with synchronized intravenous contrast injection to improve delineation of liver tumors for treatment planning. Radiotherapy and oncology : journal of the European Society for Therapeutic Radiology and Oncology 2008; 87(3): 445-448.
21) Yamashita H, Yamashita M, Futaguchi M, Takenaka R, Shibata S, Yamamoto K, et al. Individually wide range of renal motion evaluated by four-dimensional computed tomography. Springerplus 2014; 3: 131.
22) Hallman JL, Mori S, Sharp GC, Lu H-M, Hong TS, Chen GTY. A Four-Dimensional Computed Tomography Analysis of Multiorgan Abdominal Motion. International Journal of Radiation Oncology*Biology*Physics 2012; 83(1): 435-441.
23) von Siebenthal M, Szekely G, Lomax A, Cattin P. Inter-subject modelling of liver deformation during radiation therapy. Med Image Comput Comput Assist Interv 2007; 10(Pt 1): 659-666.
24) Velec M, Moseley JL, Craig T, Dawson LA, Brock KK. Accumulated dose in liver stereotactic body radiotherapy: positioning, breathing, and deformation effects. Int J Radiat Oncol Biol Phys 2012; 83(4): 1132-1140.

25) Oh S, Kim S. Deformable image registration in radiation therapy. Radiat Oncol J 2017; 35(2): 101-111.
26) Miura H, Ozawa S, Kawabata H, Doi Y, Kenjou M, Furukawa K, et al. Method of evaluating respiratory induced organ motion by vector volume histogram. Physica medica : PM : an international journal devoted to the applications of physics to medicine and biology : official journal of the Italian Association of Biomedical Physics (AIFB) 2016; 32(12): 1570-1574.
27) Pai Panandiker AS, Sharma S, Naik MH, Wu S, Hua C, Beltran C, et al. Novel Assessment of Renal Motion in Children as Measured via Four-Dimensional Computed Tomography. International Journal of Radiation Oncology*Biology*Physics 2012; 82(5): 1771-1776.
28) Uh J, Krasin MJ, Li Y, Li X, Tinkle C, Lucas JT, Jr., et al. Quantification of Pediatric Abdominal Organ Motion With a 4-Dimensional Magnetic Resonance Imaging Method. Int J Radiat Oncol Biol Phys 2017; 99(1): 227-237.
29) Huijskens SC, van Dijk IW, Visser J, Rasch CR, Alderliesten T, Bel A. Magnitude and variability of respiratory-induced diaphragm motion in children during image-guided radiotherapy. Radiotherapy and oncology : journal of the European Society for Therapeutic Radiology and Oncology 2017; 123(2): 263-269.
30) Manley L. Pediatric trauma: initial assessment and management. Journal of emergency nursing: JEN: official publication of the Emergency Department Nurses Association 1987; 13(2): 77.
31) Huijskens SC, van Dijk IWEM, de Jong R, Visser J, Fajardo RD, Ronckers CM, et al. Quantification of renal and diaphragmatic interfractional motion in pediatric image-guided radiation therapy: A multicenter study. Radiotherapy and Oncology 2015; 117(3): 425-431.
32) Bryce-Atkinson A, Whitfield G, Van Herk M. EP-1864: Design of an optimised bow-tie filter for low dose paediatric cone beam CT. Radiotherapy and Oncology 2018; 127: S1006-S7.
33) Hess CB, Thompson HM, Benedict SH, Seibert JA, Wong K, Vaughan AT, et al. Exposure Risks Among Children Undergoing Radiation Therapy: Considerations in the Era of Image Guided Radiation Therapy. International Journal of Radiation Oncology*Biology*Physics 2016; 94(5): 978-992.
34) De Jong R, Lens E, Van Herk M, Alderliesten T, Kamphuis M, Dávila Fajardo R, et al. OC-0282: Optimizing cone-beam CT presets for children to reduce imaging dose illustrated with craniospinal axis. Radiotherapy and Oncology 2014; 111: S109-S10.
35) Minn AY, Schellenberg D, Maxim P, Suh Y, McKenna S, Cox B, et al. Pancreatic tumor motion on a single planning 4D-CT does not correlate with intrafraction tumor motion during treatment. Am J Clin Oncol 2009; 32(4): 364-368.

36) Lens E, van der Horst A, Kroon PS, van Hooft JE, Davila Fajardo R, Fockens P, et al. Differences in respiratory-induced pancreatic tumor motion between 4D treatment planning CT and daily cone beam CT, measured using intratumoral fiducials. Acta oncologica (Stockholm, Sweden) 2014; 53(9): 1257-1264.
37) Huijskens SC, van Dijk I, Visser J, Balgobind BV, Rasch CRN, Alderliesten T, et al. Predictive value of pediatric respiratory-induced diaphragm motion quantified using pre-treatment 4DCT and CBCTs. Radiation oncology (London, England) 2018; 13(1): 198.
38) Nazmy MS, Khafaga Y, Mousa A, Khalil E. Cone beam CT for organs motion evaluation in pediatric abdominal neuroblastoma. Radiotherapy and Oncology 2012; 102(3): 388-92.
39) van Dijk I, Huijskens SC, de Jong R, Visser J, Fajardo RD, Rasch CRN, et al. Interfractional renal and diaphragmatic position variation during radiotherapy in children and adults: is there a difference? Acta oncologica (Stockholm, Sweden) 2017; 56(8): 1065-1071.

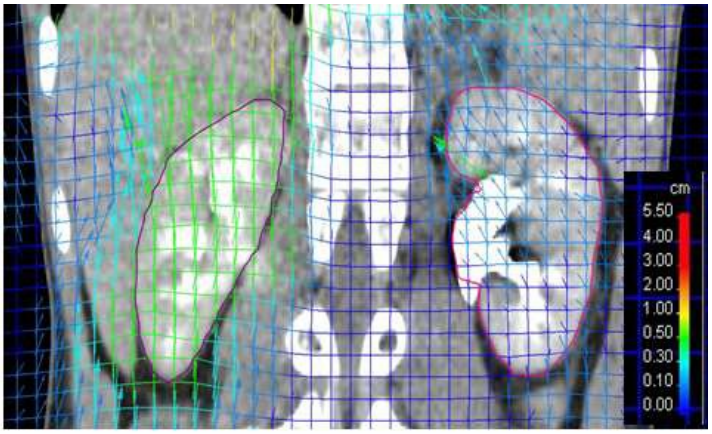

Figure 2.1 – Example deformation vector field distributions for patient 3 in a coronal reconstruction of the 0% phase (reference image) and 50 % phase (target image).The magnitude of the estimated respiratory induced organ motion between these phases is visualised in colour; scale shown in bottom right corner (cm).

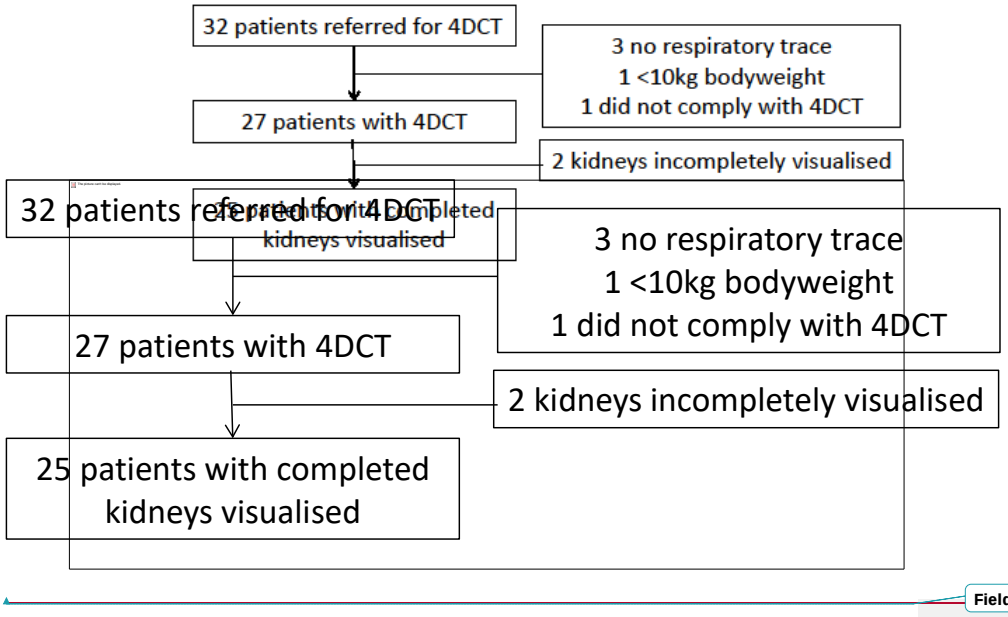

Field Code Changed

Figure 2.2 - Flowchart showing the patients referred for 4DCT and those included in the motion analysis component described in this chapter.

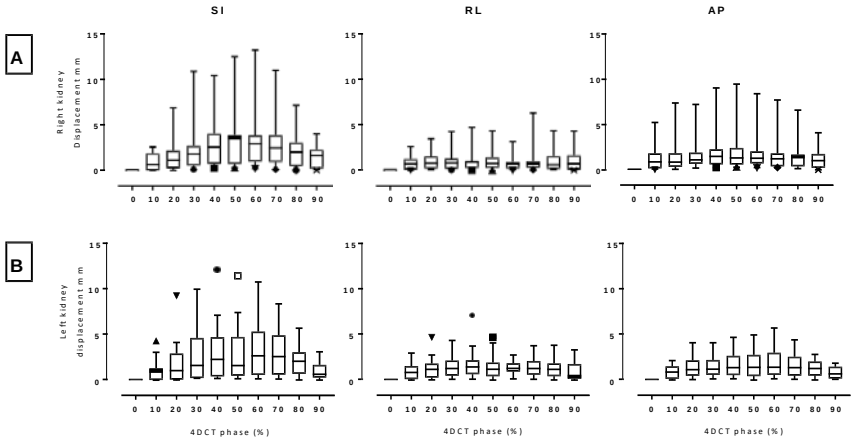

Figure 2.3 – Boxplots for right (A) and left (B) kidney DVF displacements (mm) in superior/ inferior (SI), anterior/posterior (AP) and right/ left (RL) directions according to 4DCT phase (%) for all patients.Boxes: upper and lower quartiles, whiskers: highest and lowest values excluding outliers, symbols; outliers, bar: median. Motion is relative to 0% phase (horizontal line).

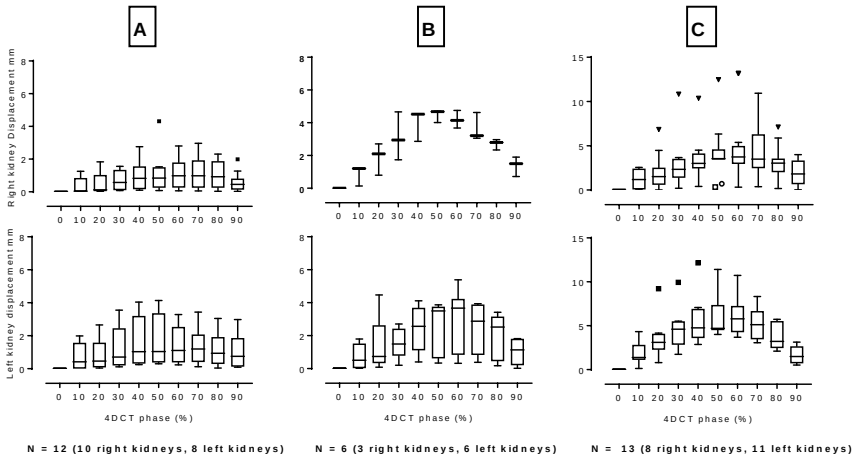

Figure 2.4 - Boxplots for right (top) and left (bottom) kidney DVF displacements (mm) in superior/ inferior (SI) direction according to 4DCT phase (%) for patients under GA (A), < 5 years not under GA (B), and all patients not under GA (C). Boxes: upper and lower quartiles, whiskers: highest and lowest values excluding outliers, symbols; outliers (same shapes = same individual patient), bar: median. Motion is relative to 0% phase (solid black line).

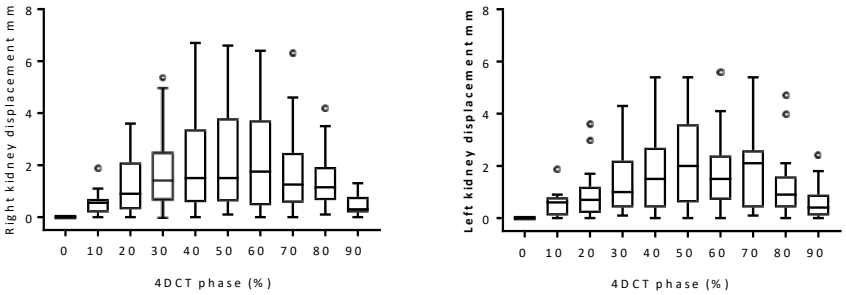

Figure 2.5 - Boxplots showing right and left kidney superior inferior (SI) centre of mass (COM) displacements (mm). Displacements are relative to the phase 0% (black line). Boxes: upper and lower quartiles, whiskers: highest and lowest values excluding outliers, symbols; outliers, bar: median. Motion is relative to 0% phase (solid black line)

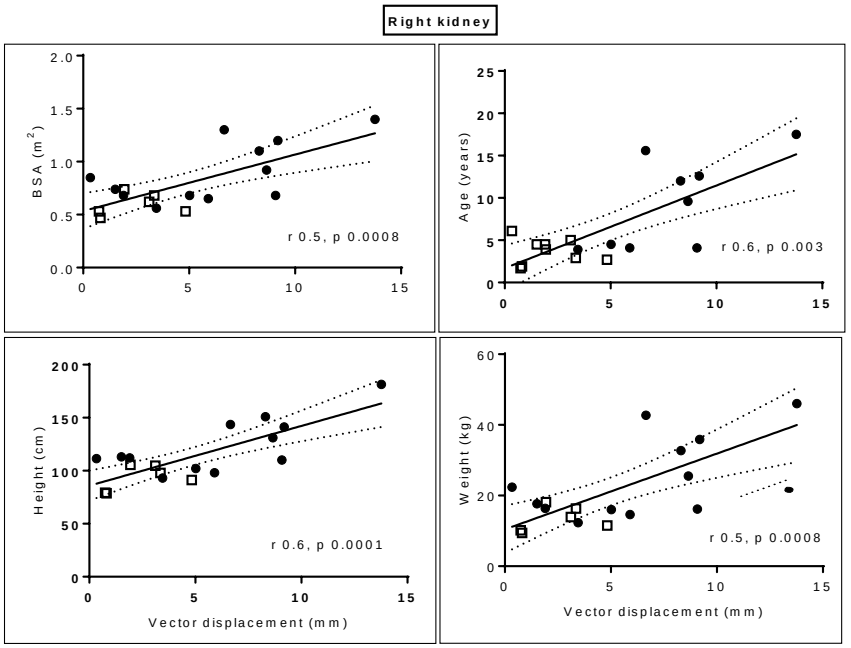

Figure 2.6 – Scatterplots with regression lines (solid) and upper, lower 95% confidence intervals (dashed line) describing the relationships between 3D vector motion (mm) right kidney and BSA, age, height and weight. Squares = patients under GA, black dots = patients not under GA.

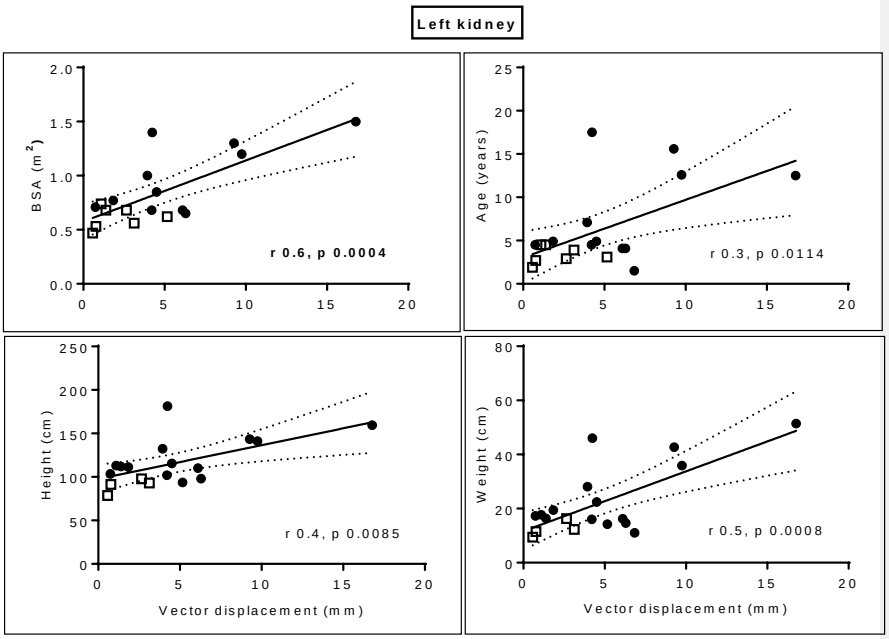

Figure 2.7 - Scatterplots with regression lines (solid) and upper, lower 95% confidence intervals (dashed line) describing the relationships between 3D vector motion (mm) left kidney and BSA, age, height and weight. Squares = patients under GA, black dots = patients not under GA.

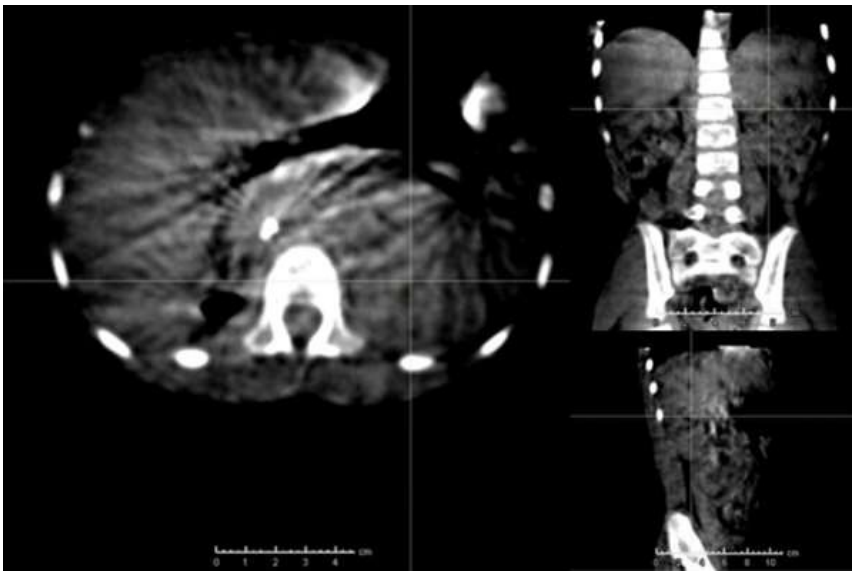

Figure 2.8 - Example CBCT acquired using low-dose protocol in a patient with abdominal neuroblastoma.

	Maximum DVF displacement (mm)				COM displacement (mm)			
	RL	AP	SI	Vector	RL	AP	SI	Vector
Right kidney	1.8 ± 1.7 (0.1 – 7.3)	1.7 ± 1.6 (0.2 – 5.8)	2.4 ± 3.2 (0.3 – 12.2)	4.1 ± 3.7 (0.3 – 13.8)	0.7 ± 0.4 (0.3 – 1.5)	1.0 ± 0.5 (0.3 – 2.0)	2.8 ± 1.7 (0.9 – 6.3)	3.1 ± 1.8 (1.2 – 6.7)
Left kidney	1.1 ± 1.8 (0.1 – 6.3)	2.0 ± 2.1 (0.3 – 9.5)	3.6 ± 3.1 (0.4 – 13.2)	4.2 ± 4.0 (0.6 – 16.8)	0.9 ± 0.5 (0.1 – 1.7)	0.9 ± 0.9 (0.1 – 4.2)	2.7 ± 1.5 (0.2 – 5.9)	2.9 ± 1.7 (0.2 – 7.2)

Table 2.1 - Median ± standard deviation and range of calculated DVF and COM displacements. Vector; displacements calculated by DVF or COM derived displacements using the formula $\sqrt{x2 + y2 + z2}$.

	GA		Young no GA		All no GA	
	Median	**SD**	**Median**	**SD**	**Median**	**SD**
Right kidney displacement (mm)	1.9	1.5	5.9	2.1	8.5	2.7
Left kidney displacement (mm)	2.0	2.3	4.4	2.2	4.5	4.5

Table 2.2 - Median and standard deviation (SD) of right and left kidney displacements (mm) in children under GA (N=12), young children < 5 years not under GA (N = 6) and all patients not under GA (N = 13).

Patient	Diagnosis	Kidney	GA	BSA (m^2)	Age (years)	Height (cm)	Weight (kg)
1	Sarcoma	Both	No	1.3	15.6	143.5	42.7
2	Neuroblastoma	Both	Yes	0.68	2.9	97.9	16.3
3	Neuroblastoma	Both	No	1.4	17.5	181.4	46
4	Neuroblastoma	Both	Yes	0.56	3.9	93	12.3
5	Sarcoma	Both	No	1.2	12.6	141.2	35.9
6	Neuroblastoma	Both	Yes	0.47	1.9	78.7	9.45
7	Neuroblastoma	Both	No	0.68	4.5	102	16
8	Neuroblastoma	Both	No	0.65	4.1	98.1	14.6
9	Neuroblastoma	Right	No	1.1	12	150.9	32.7
10	Neuroblastoma	Right	Yes	0.74	3.9	105.6	18.1
11	Neuroblastoma	Both	Yes	0.53	1.7	79.2	10.15
12	Wilms' tumour	Left	No	0.85	4.9	115.5	22.4
13	Wilms' tumour	Left	No	1.5	12.5	159.4	51.4
14	Wilms' tumour	Left	No	0.71	4.5	103.4	17.3
15	Wilms' tumour	Right	Yes	0.62	5	104.8	13.9
16	Neuroblastoma	Both	Yes	0.53	2.7	91.3	11.5
17	Wilms' tumour	Right	No	0.92	9.6	131	25.5
18	Neuroblastoma	Both	No	0.68	4.1	110	16.2
19	Wilms' tumour	Left	No	0.77	4.9	111.3	19.4
20	Wilms' tumour	Right	Yes	0.85	6.1	111.4	22.4
21	Neuroblastoma	Left	Yes	n/r	1.5	n/r	11
22	Wilms' tumour	Both	Yes	0.62	3.1	93.7	14.2
23	Neuroblastoma	Both	Yes	0.68	4.5	112	16.4
24	NBL	Both	Yes	0.74	4.5	113	17.7
25	WT	Left	No	1	7.1	132.3	28.1

Table 2.3 - Patient demographics. BSA: body surface area. n/r: not recorded.

Chapter 3

Four-dimensional magnetic resonance for individualised motion assessment in children

3.1 Background

As discussed in Chapter 2, 4DCT is the current gold standard for individualised motion assessment in adults. The increased radiation dose associated with 4DCT is a barrier to its general use in children; reflected in the relatively small numbers of publications referencing use of the technique in children [1-4]. MR does not deliver additional radiation dose to the patient [5]. MR also results in improved soft tissue contrast and organ edge detection compared to CT across a number of tumour sites, (Figure 3.5), [6-10]. Organ edge detection is important in paediatric RT as most children receive RT post-operatively when the adjacent organs at risk represent the boundaries of the tumour bed. MR can also improve intra-observer variation in RT target delineation [9]. Novel MR sampling schemes that are less sensitive to motion effects have been developed and 4DMR is emerging as a non-ionising imaging modality that can provide individualised respiratory-related organ motion (RROM) information without the need for an external respiratory surrogate [6,11,12]. I described the latter as a limitation of 4DCT acquisition in my patient cohort in Chapter 2.

The integration of diagnostic MR images in the RT treatment planning pathway to aid target delineation in paediatric RT planning is well described [13]. However, MR imaging of the abdomen in children represents unique challenges. Younger children have less abdominal fat to provide a natural contrast mechanism for MR imaging [14,15]. In adults, breath-hold is essential for upper abdominal MR imaging as respiratory induced motion can result in imaging artefacts [15]. In contrast, paediatric diagnostic abdominal MR is often performed under quiet breathing conditions. Paediatric MR imaging with breath-hold is challenging at all ages; younger children are imaged under

anaesthesia without intubation and older children may not comply reliably with breath-hold instructions [14,16]. Furthermore, MR acquisitions take longer than CT acquisitions, a 3DCT can be acquired in less than 2 minutes but an MR sequence could take 4- 5 minutes to acquire and acquiring more than one MR sequence in an imaging session is routine. As a result, patient motion can significantly degrade images in non-anaesthetised young children [11]. MR is also associated with being in an enclosed space, increased acoustic noise and potential for sensation of increased body temperature. These physical conditions could be challenging for young children to tolerate awake [17]. Children who may comply with immobilisation for a short CT scan without anaesthesia may not be able to comply for the duration of an MR scan. Therefore, MR imaging could potentially increase the use of general anaesthesia (GA) to achieve adequate immobilisation for RT planning, which in turn could have significant additional resource implications for a department.

In this Chapter, I describe the feasibility of acquiring a free-breathing 4DMR sequence in children. Kidney and liver respiratory-related motion is described. In a cohort of 6 children in whom both 4DMR and 4DCT were acquired; organ motion is compared.

3.2 Aims of Chapter 3

My hypothesis is that acquiring a 4DMR for individualised motion assessment in children is feasible and results in superior soft tissue contrast compared to 4DCT.

In order to test this hypothesis, I will;

1) Determine the number of children referred for, and successfully completing, 4DMR.
2) Determine the median, standard deviation and range of liver and kidney motion
3) Compare of 3D motion vectors in patients who have undergone both 4DMR and 4DCT imaging.

3.3 Materials and methods

3.3.1 Patient selection

Eligible patients were recruited to the APAChe study, as previously described and included in Appendix 1. Eligible patients were assessed to ensure there was no contra-indication to MR imaging. Patients were also reviewed by the specialist paediatric radiographer and play specialist to determine the requirement for GA. Parental informed consent was obtained for each patient. Patient characteristics are shown in Table 3.1.

3.3.2 4DMR acquisition

4DMR was acquired on a diagnostic 1.5T MR scanner (MAGNETOM Aera; Siemens Healthcare, Erlangen, Germany) in free breathing for all children, including those requiring GA. The 4DMR sequence used in this work consisted of the following acquisition parameters; axial T1-weighted, stack-of-stars spoiled gradient echo sequence in free-breathing, three-dimensional excitation with a radial sampling scheme [11]. Data was acquired with a spatial resolution of 1.25 x 1.25 x 3.5 mm, resulting in an acquisition time between 5-6 minutes depending on the number of slices.

Two groups of paediatric patients were studied; those referred for upper abdominal RT, and another cohort who were scheduled for routine MR imaging surveillance following previous treatment of an abdominal tumour. For those patients who were having RT, and for whom a planned comparison with 4DCT was intended, MR was acquired where possible in the treatment position. Datasets were not acquired on the same day due to logistical reasons and patient tolerability.

3.3.3 Image reconstruction

MRI raw data was sorted into 20 respiratory phases (0%, 5%, 10%….95%) based on a self-gating surrogate extracted by principal component analysis of the magnitude signal of the k-space centre [18]. Image reconstruction was performed using a prototype implementation of the joint MoCo-HDTV algorithm [19]. MR raw data processing and image reconstruction were performed by Dr. Andreas Wetscherek. For contouring purposes, 10 phases

(0%, 10% … 90%) were selected to correlate with the phase reconstruction of 4DCT.

3.3.4 Motion analysis

Motion analysis was performed on both datasets independently. 4DCT and 4DMR datasets were not fused. Kidneys and liver were contoured for all patients on all phases of the 4DMR. Deformable image registration of 4DMR datasets was performed. Phase 0 % was the reference phase and registered to target phases 10% … 90%, as described in Chapter 1, section 1.3.5.

For each patient, the maximum DVF displacement of all voxel displacements within each organ for each registered 4DMR phase was calculated in the SI, RL and AP directions. Vector displacements were calculated for each patient as a summary measure of organ motion.

3.3.5 Comparative analysis

Descriptive statistics and scatter plots are used to display motion data. For patients imaged with both 4DMR and 4DCT, differences in motion between modalities were recorded by subtracting the 4DCT measured maximum vector displacement for each organ (right and left kidney) from the 4DMR maximum vector displacement. A negative value indicated that 4DCT showed greater motion than 4DMR.

3.4 Results

3.4.1 Feasibility

The median age of patients scanned was 8.0 years (range 1.9 – 15.6). 3 patients required GA; aged 1.9 and two 4.5 year olds. One 4 year- old (patient 10) was scanned without GA. This child had a play session in the MR room prior to scanning and then watched a cartoon for the duration of the scan.

All predetermined MR sequences were acquired in all 12 patients and the addition of the 4DMR sequence did not compromise the acquisition of diagnostic MR sequences in any patient. For the 3 children scanned under GA there were no additional safety issues identified as a result of extending the time under GA by the duration of the research MR sequence. Due to logistical, and patient tolerability, reasons the 4DMR and the 4DCT were not acquired during the same session. It was not possible to extend the duration of GA to accommodate 4DMR and 4DCT acquisition in close proximity. 4DCT and 4DMR were acquired in separate departments within the hospital. Children under GA would have also had to extend the time fasting to facilitate acquiring 4DMR and 4DCT during the same imaging session. This was neither ethical nor practical. In fact, one patient screened for inclusion in this study did not proceed with the 4DMR component of the study due to the additional fasting required.

The 4DMR sequence was acquired in 5 – 6 minutes. Image reconstruction took between 7h 14 min and 15h 27 min per scan depending on the number of slices.

3.4.2 Organ motion

In 2 patients the field of view did not extend to encompass the entire upper abdomen and therefore the kidneys and liver were not completely visualised. These data were excluded from the organ motion analysis. 10 patients are included in the final analysis of organ motion on 4DMR.

Maximum DVF displacements plotted according to 4DMR phase for right, left kidneys and liver for all 10 evaluable patients are shown in Figure 3.1. The greatest organ displacements were in the superior inferior (SI) direction. For left kidney and liver, the magnitude of measured organ motion was in the order of SI > AP > RL, (Table 3.3). For the right kidney, RL motion was marginally greater than AP motion. Median liver SI displacement was 7.1mm. Median SI right and left kidney displacements were 2.8 mm and 3.2 mm respectively. Median and ranges of kidney and liver motion estimates are summarised in Table 3.2. SI range of motion was 11.0 mm for the liver, 8.4 mm for the right kidney, and 5.9 mm for the left kidney. Vector displacements as a summary of motion in all three cardinal planes are shown in Figure 3.2. The child with the smallest vector displacements was patient 7 who was aged 4.5 years and under GA.

Three children who had 4DMR under GA also had 4DCT acquired under GA (patients 5, 7 and 8). 3D motion vectors for left, right kidneys (4DMR and 4DCT) and liver (4DMR only) are summarised in Table 3.2 for the 6 patients imaged with both modalities. Pair-wise differences between 4DCT and 4DMR results for individual patients are shown in Figure 3.3, 3.4 and 3.5. The difference in motion between 4DCT and 4DMR ranged from -4.4 to +2.1 mm for the right kidney and -7.0 to + 2.3 mm for the left kidney, (Figures 3.4 and

3.5). The median difference was -1.2 mm (right kidney) and -0.2 mm (left kidney). 4DMR showed greater motion in 1 out of 5 right kidneys (patient 5) and 3 out of 6 left kidneys (patient 2, 5 and 6). Patient 8 was the youngest child included in this study, aged 1.9 years. This patient was scanned under GA for both 4DCT and 4DMR; 4DCT-derived right and left kidney motion vectors were 0.8 mm and 0.6 mm, on 4DMR the vectors were 2.9 mm for both kidneys. The greatest differences in measured displacements were seen in patient 3; right kidney displacement was 4.4 mm smaller on 4DMR compared to 4DCT, and left kidney displacement was 7.0 mm smaller on 4DMR.

3.5 Discussion

In this chapter, I demonstrated the feasibility of using 4DMR (acquired on a diagnostic scanner), with a spatial resolution of 1.25 x 1.25 x 3.5 mm, for the estimation of RROM and for radiotherapy planning in a paediatric cohort. Even the youngest patient who tolerated 4DCT awake managed to comply with immobilisation for the required duration of the MR scan awake. All predetermined sequences for all patients were acquired. MRI scans take longer than 4DCT to acquire; the 4DMR sequence alone took 6 minutes compared to 2 minutes for 4DCT. MR imaging is associated with an enclosed machine bore, additional acoustic noise and bodily sensation of warmth. These factors could have been anticipated to raise the threshold for the requirement of GA in young children but did not. Appropriate play therapy input and preparation prior to scanning is a necessary and well described component of

paediatric radiotherapy [20]. The four-year-old child who was scanned without GA had ample input from play therapy and watched a cartoon during image acquisition and complied with the immobilisation requirements for scanning.

In the 12 patients consented and referred for 4DMR as part of this work all had a 4D dataset successfully generated. The 4DMR sequence acquisition and reconstruction described in this Chapter does not rely on an external respiratory surrogate. A reliable respiratory surrogate signal is critical for retrospective respiratory phase-resolved methods as images are sorted based on the signal. Respiratory bellows have been demonstrated to be an inaccurate predictor of upper abdominal organ motion [21]. An external respiratory surrogate may also technically limit the ability to record a respiratory trace in paediatric patients. Kannan et al. used the Realtime Position Management (RPM) system (Varian Medical Systems, Palo Alto, Ca, USA) and acquired 4DCT in 15 patients with thoracic and abdominal neuroblastoma. They did not comment on patients in whom a trace was not recorded [1]. Neither do two other publications using 4DCT in children [22,23]. In Chapter 2 I demonstrated that a respiratory trace was not detectable in 3 of 32 patients referred for 4DCT and was the most common reason for not acquiring a 4DCT in my work. An assumption could be made that there is negligible RROM in patients with an undetectable respiratory trace when in fact it is as a result of the technical limitation of 4DCT in young children. This represents an advantage for 4DMR over 4DCT for individualised motion assessment in young children.

My results demonstrate that the magnitude of measured upper abdominal organ displacements varied according to the proximity of the organ to the

diaphragm, the principle muscle of respiration. Median liver displacements were greater than either kidney; liver 7.1mm, right kidney 2.8 mm and left kidney 3.2 mm. I have described median right and left kidney motion vectors of 2.8 mm and 3.2 mm on 4DMR. These results are in broad agreement with median vectors of 1.9 mm and 2.7mm as measured by 4DCT and previously presented in Chapter 2. In a previously published cohort of 6 paediatric patients (median age 3 years), 4DMR demonstrated 34% less left kidney motion and 68% less right kidney motion than that measured on 4DCT. Median SI motion of 3.8 mm and 5.3 mm for left and right kidney on 4DCT compared to 2.8 mm and 3.1 mm on 4DMR (24). My 4DMR results compare with these published 4DMR vectors. However, a subsequent larger study of abdominal organ motion in 35 paediatric patients using coronal 4DMR showed no statistically significant difference in SI motion of liver dome and kidneys (superior organ edge) between the two modalities [25].

My results and those from Uh et al. suggest that 4DMR performs similarly to 4DCT for individualised motion assessment in children. In this work, the nominal slice thickness of the 4DMR sequence was 3.5 mm, compared to a slice thickness of 2.5 mm for 4DCT. However, the 4DMR reconstruction algorithm uses the presence of motion to reconstruct at a higher- slice resolution of 1.7 mm. This spatial resolution is superior to 4DCT and that of previously reported 4DMR sequences for motion assessment in paediatric RT planning where coronal 4DMR was acquired with sequential slice thickness of 4 – 5 mm [25].

The superior resolution of MR can aid RT planning in the upper abdomen where there is less contrast between tumour/ tumour bed and adjacent organs

of similar CT-derived Hounsfield values. This is particularly relevant in children as most have RT post-operatively and the adjacent organs at risk represent the boundaries of the tumour bed. In this Chapter, I determined liver motion; this was feasible because the superior soft tissue contrast of the 4DMR sequence permitted delineation of the medial liver edge, in contrast to 4DCT where accurate delineation of the medial liver edge was challenging.

The AAPM have stipulated 5 mm as a threshold below which motion management may not be warranted, however, that recommendation is specific to photon RT in adults [26]. At present it is not known what the appropriate threshold is for much younger and smaller children. The median liver displacement in this work was 7.1 mm and as demonstrated in Figure 3.2 a proportion of children display motion of the magnitude described by AAPM as warranting consideration for motion management in RT planning.

The median differences between right and left kidney motion measurements on 4DMR and 4DCT were 1.2 mm and 0.2 mm respectively. However, the differences seen in individual patients were greater. In the case of patient 3, right kidney motion was 4.4 mm and left kidney motion was 7.0 mm less on 4DMR than on 4DCT. Contrastingly, right and left kidney motion on 4DMR was within 1.5 mm of that measured on 4DCT in the cases of patients 1, 2 and 4 indicating good agreement between the two modalities. Two of these three patients were imaged under GA (patients 2 and 4). Interpretations of the pair – wise comparisons described in this Chapter are limited as the two datasets were not acquired during the same imaging session. The differences seen may not be modality-specific but rather are as a result of differences in patient-specific breathing patterns between imaging sessions. Increased anxiety at the

time of RT preparation for children, particularly younger children, is well described [20, 27] and could contribute to intra- patient variation in breathing motion measured using two different imaging modalities. The 4DMR was reconstructed retrospectively into 20 phases. For the purposes of this work I selected 10 4DMR phases to correlate with the 10 phase reconstruction of the 4DCTs. This difference in reconstruction technique between modalities could contribute to the observed differences. Contouring variation between datasets is another possible reason for the described differences. I completed all contouring for all patients thereby minimising inter-observer variation in contouring which is greater than intra-observer variation where reported conformity indices ranged from 0.3 to 0.7 [28-31]. The longer imaging time for 4DMR acquisition, 5 – 6 minutes compared to < 2 minutes for 4DCT, is a further advantage as 4DMR may capture intra-fraction variation in breathing amplitude that is not captured during 4DCT and offer insight into potential large intrafraction amplitude variations during treatment.

My results in Figure 3.1 also demonstrate the interpatient variation, a finding consistent with previously published reports demonstrating inter-patient variation in RROM of the diaphragm, kidneys, liver and spleen in paediatric cohorts [23, 25, 32-35]. Taken together these data contribute to the evidence that an individualised approach to RROM assessment in children is necessary to optimally adopt advanced conformal RT techniques.

MRgRT treatment machines enable daily online localisation of the target and organs at risk, real-time verification of plans, and treatment adaptation [36-38]. MR-guided on board imaging also delivers superior soft tissue contrast compared to CBCT without additional imaging dose Integration of MR imaging in the RT pathway is associated with additional challenges that do

not need to be considered in a conventional CT-based RT pathway. Geometric distortion is one such consideration and arises, principally; because field gradients of an MR scanner are not perfectly linear over the entire field of view for any given scan. If uncorrected, the resulting geometric distortion would result in dosimetric uncertainties that increase in severity at increasing distance from the isocenter. Vendor-supplied distortion correction algorithms are used during the image reconstruction phase and correct, although not entirely eliminate, distortions via interpolation in image space. The potential and

feasibility of an MR-only workflow in paediatric abdominal RT has been recently presented [39. 40]. The successful treatment of a paediatric patient using MR guided RT was recently published [41].

Repeat measures of motion on 4DMR would be ideal to accurately evaluate intra-patient inter-fraction variation in organ motion. This could be achieved in a paediatric study using the MR linear accelerator system [4]. With this purpose in mind, a cohort of paediatric patients are specifically included in a prospective study on the MR Linac at the Royal Marsden Hospital, Sutton NCT02973828 [42].

3.6 Conclusion

This Chapter demonstrates feasibility and proof of concept for the use of 4DMR in children. However, as only a small number of patients are included in this work, the results should be interpreted accordingly. The advantages of improved soft tissue resolution of 4DMR without need for an external respiratory surrogate, and the absence of additional radiation dose exposure, as illustrated in this Chapter, suggest that 4DMR should be the preferred modality for individualised RROM assessment in children receiving RT for upper abdominal tumours.

3.7 References

1) Kannan S, Kannan S, Teo BK, Solberg T, Hill-Kayser C. Organ motion in pediatric high-risk neuroblastoma patients using four-dimensional computed tomography. Journal of applied clinical medical physics 2017; 18(1): 107-114.
2) Hubbard P, Callahan J, Cramb J, Budd R, Kron T. Audit of radiation dose delivered in time-resolved four-dimensional computed tomography in a radiotherapy department. Journal of medical imaging and radiation oncology 2015; 59(3): 346-352.
3) Lavan N CE, Burland H, Mandeville HC. Development of a four-dimensional computed tomography (4DCT) imaging sequence for paediatric radiotherapy planning. International Society of Paediatric Oncology (SIOP); Dublin, Ireland. Pediatric Blood and Cancer 2016 p. S1-S321.
4) Lavan NA, Saran FH, Oelfke U, Mandeville HC. Adopting Advanced Radiotherapy Techniques in the Treatment of Paediatric Extracranial Malignancies: Challenges and Future Directions. Clinical oncology (Royal College of Radiologists {Great Britain}) 2019; 31(1): 50-57.
5) Hess CB, Thompson HM, Benedict SH, Seibert JA, Wong K, Vaughan AT, et al. Exposure Risks Among Children Undergoing Radiation Therapy: Considerations in the Era of Image Guided Radiation Therapy. International Journal of Radiation Oncology*Biology*Physics 2016; 94(5): 978-992.
6) Stemkens B, Paulson ES, Tijssen RHN. Nuts and bolts of 4D-MRI for radiotherapy. Physics in Medicine & Biology 2018; 63(21): 21TR01.
7) Bainbridge H, Wetscherek A, Eccles C, Collins D, Scurr E, Leach M, et al. P2.05-042 Development of Thoracic Magnetic Resonance Imaging (MRI) for Radiotherapy Planning: Topic: RT Techniques. Journal of Thoracic Oncology 2017; 12(1): S1057.
8) Eccles C, Hunt A, McNair H, Herbert T, Tree A, Kirby A, et al. Early experience of magnetic resonance sequence evaluation using an MR-linac system. International Journal of Radiation Oncology• Biology• Physics 2018; 102(3): S130-S1.
9) Pathmanathan AU, McNair HA, Schmidt MA, Brand DH, Delacroix L, Eccles CL, et al. Comparison of prostate delineation on multimodality imaging for MR-guided radiotherapy. The British journal of radiology 2019; 92(1096): 20180948.
10) Schmidt MA, Payne GS. Radiotherapy planning using MRI. Phys Med Biol 2015; 60(22): R323-61.
11) Block KT, Chandarana H, Milla S, Bruno M, Mulholland T, Fatterpekar G, et al. Towards Routine Clinical Use of Radial Stack-of-Stars 3D Gradient-Echo Sequences for Reducing Motion Sensitivity. J Korean Soc Magn Reson Med 2014; 18(2): 87-106.
12) Chandarana H, Block KT, Winfeld MJ, Lala SV, Mazori D, Giuffrida E, et al. Free-breathing contrast-enhanced T1-weighted gradient-echo imaging with radial k-space sampling for paediatric abdominopelvic MRI. Eur Radiol 2014; 24(2): 320-326.

13) Lavan NA, Mandeville HC. Imaging in Pediatric Oncology Pediatric Oncology, ISSN 1613-5318. Stephan D. Voss KM, editor: Springer; 2019.
14) Darge K, Anupindi SA, Jaramillo D. MR imaging of the abdomen and pelvis in infants, children, and adolescents. Radiology 2011; 261(1): 12-29.
15) Lagendijk JJW, Raaymakers BW, Van den Berg CAT, Moerland MA, Philippens ME, van Vulpen M. MR guidance in radiotherapy. Physics in Medicine and Biology 2014; 59(21): R349-R69.
16) Chandarana H, Block KT, Winfeld MJ, Lala SV, Mazori D, Giuffrida E, et al. Free-breathing contrast-enhanced T1-weighted gradient-echo imaging with radial k-space sampling for paediatric abdominopelvic MRI. European radiology 2014; 24(2): 320-326.
17) Tyc VL, Fairclough D, Fletcher B, Leigh L, Mulhern RK. Children's Distress During magnetic Resonance Imaging Procedures. Children's Health Care 1995; 24(1): 5-19.
18) Paul J, Divkovic E, Wundrak S, Bernhardt P, Rottbauer W, Neumann H, et al. High-resolution respiratory self-gated golden angle cardiac MRI: Comparison of self-gating methods in combination with k-t SPARSE SENSE. Magn Reson Med 2015; 73(1): 292-298.
19) Rank CM, Heusser T, Buzan MT, Wetscherek A, Freitag MT, Dinkel J, et al. 4D respiratory motion-compensated image reconstruction of free-breathing radial MR data with very high undersampling. Magn Reson Med 2017; 77(3): 1170-1183.
20) Tyc VL, Klosky JL, Kronenberg M, de Armendi AJ, Merchant TE. Children's Distress in Anticipation of Radiation Therapy Procedures. Children's Health Care 2002; 31(1): 11-27.
21) Stemkens B, Tijssen RHN, de Senneville BD, Heerkens HD, van Vulpen M, Lagendijk JJW, et al. Optimizing 4-Dimensional Magnetic Resonance Imaging Data Sampling for Respiratory Motion Analysis of Pancreatic Tumors. International Journal of Radiation Oncology*Biology*Physics 2015; 91(3): 571-578.
22) Huijskens SC, van Dijk I, Visser J, Balgobind BV, Rasch CRN, Alderliesten T, et al. Predictive value of pediatric respiratory-induced diaphragm motion quantified using pre-treatment 4DCT and CBCTs. Radiation oncology (London, England) 2018; 13(1): 198.
23) Pai Panandiker AS, Sharma S, Naik MH, Wu S, Hua C, Beltran C, et al. Novel Assessment of Renal Motion in Children as Measured via Four-Dimensional Computed Tomography. International Journal of Radiation Oncology*Biology*Physics 2012; 82(5): 1771-1776.
24) Panandiker AS, Winchell A, Loeffler R, Song R, Rolen M, Hillenbrand C. 4DMRI Provides More Accurate Renal Motion Estimation in IMRT in Young Children. Pract Radiat Oncol 2013; 3(2 Suppl 1): S1.
25) Uh J, Krasin MJ, Li Y, Li X, Tinkle C, Lucas JT, Jr., et al. Quantification of Pediatric Abdominal Organ Motion With a 4-Dimensional Magnetic Resonance Imaging Method. Int J Radiat Oncol Biol Phys 2017; 99(1): 227-237.
26) Keall PJ, Mageras GS, Balter JM, Emery RS, Forster KM, Jiang SB, et al. The management of respiratory motion in radiation oncology report of AAPM Task Group 76a). Medical Physics 2006; 33(10): 3874-3900.

27) Filin A, Treisman S, Peles Bortz A. Radiation Therapy Preparation by a Multidisciplinary Team for Childhood Cancer Patients Aged 3½ to 6 Years. Journal of Pediatric Oncology Nursing 2009; 26(2): 81-85.
28) Kristensen I, Nilsson K, Agrup M, Belfrage K, Embring A, Haugen H, et al. A dose based approach for evaluation of inter-observer variations in target delineation. Technical innovations & patient support in radiation oncology 2017; 3: 41-47.
29) Kristensen I, Agrup M, Bergström P, Engellau J, Haugen H, Martinsson U, et al. Assessment of volume segmentation in radiotherapy of adolescents; a treatment planning study by the Swedish Workgroup for Paediatric Radiotherapy. Acta Oncologica 2014; 53(1): 126-133.
30) Muracciole X, Cuilliere J, Hoffstetter S, Alapetite C, Quetin P, Baron M, et al. Quality assurance of a French multicentric conformal radiotherapy protocol for low-stage medulloblastoma: variability in target volume delineation. International Journal of Radiation Oncology• Biology• Physics 2002; 54(2): 148-9.
31) Padovani L, Huchet A, Claude L, Bernier V, Quetin P, Mahe M, et al. Inter-clinician variability in making dosimetric decisions in pediatric treatment: a balance between efficacy and late effects. Radiotherapy and Oncology 2009; 93(2): 372-376.
32) Huijskens SC, van Dijk I, Visser J, Balgobind BV, Te Lindert D, Rasch CRN, et al. Abdominal organ position variation in children during image-guided radiotherapy. Radiation oncology (London, England) 2018; 13(1): 173.
33) Huijskens SC, van Dijk IW, Visser J, Rasch CR, Alderliesten T, Bel A. Magnitude and variability of respiratory-induced diaphragm motion in children during image-guided radiotherapy. Radiotherapy and oncology : journal of the European Society for Therapeutic Radiology and Oncology 2017; 123(2): 263-269.
34) van Dijk I, Huijskens SC, de Jong R, Visser J, Fajardo RD, Rasch CRN, et al. Interfractional renal and diaphragmatic position variation during radiotherapy in children and adults: is there a difference? Acta oncologica (Stockholm, Sweden) 2017; 56(8): 1065-1071.
35) Guerreiro F, Seravalli E, Janssens GO, van de Ven CP, van den Heuvel-Eibrink MM, Raaymakers BW. Intra- and inter-fraction uncertainties during IGRT for Wilms' tumor. Acta oncologica (Stockholm, Sweden) 2018; 57(7): 941-949.
36) Fallone BG. The Rotating Biplanar Linac–Magnetic Resonance Imaging System. Seminars in Radiation Oncology 2014; 24(3): 200-202.
37) Keall PJ, Barton M, Crozier S. The Australian Magnetic Resonance Imaging–Linac Program. Seminars in Radiation Oncology 2014; 24(3): 203-206.
38) Lagendijk JJW, Raaymakers BW, van Vulpen M. The Magnetic Resonance Imaging–Linac System. Seminars in Radiation Oncology 2014; 24(3): 207-209.
39) Guerreiro F, Koivula L, Seravalli E, Janssens GO, Maduro JH, Brouwer CL, et al. Feasibility of MRI-only photon and proton dose calculations for pediatric patients with abdominal tumors. Phys Med Biol 2019; 64(5): 055010.

40) Guerreiro F, Seravalli E, Janssens GO, van den Heuvel-Eibrink MM, Lagendijk JJW, Raaymakers BW. Potential benefit of MRI-guided IMRT for flank irradiation in pediatric patients with Wilms' tumor. Acta oncologica (Stockholm, Sweden) 2019; 58(2): 243-250.
41) Henke LE, Green OL, Schiff J, Rodriguez VL, Mutic S, Michalski J, et al. First Reported Case of Pediatric Radiation Treatment With Magnetic Resonance Image Guided Radiation Therapy. Advances in Radiation Oncology 2019; 4(2): 233-236.
42) PRIMER Available from: https://clinicaltrials.gov/ct2/show/NCT02973828?term=MR&recrs=ab&cntry=GB&draw=2&rank=16.

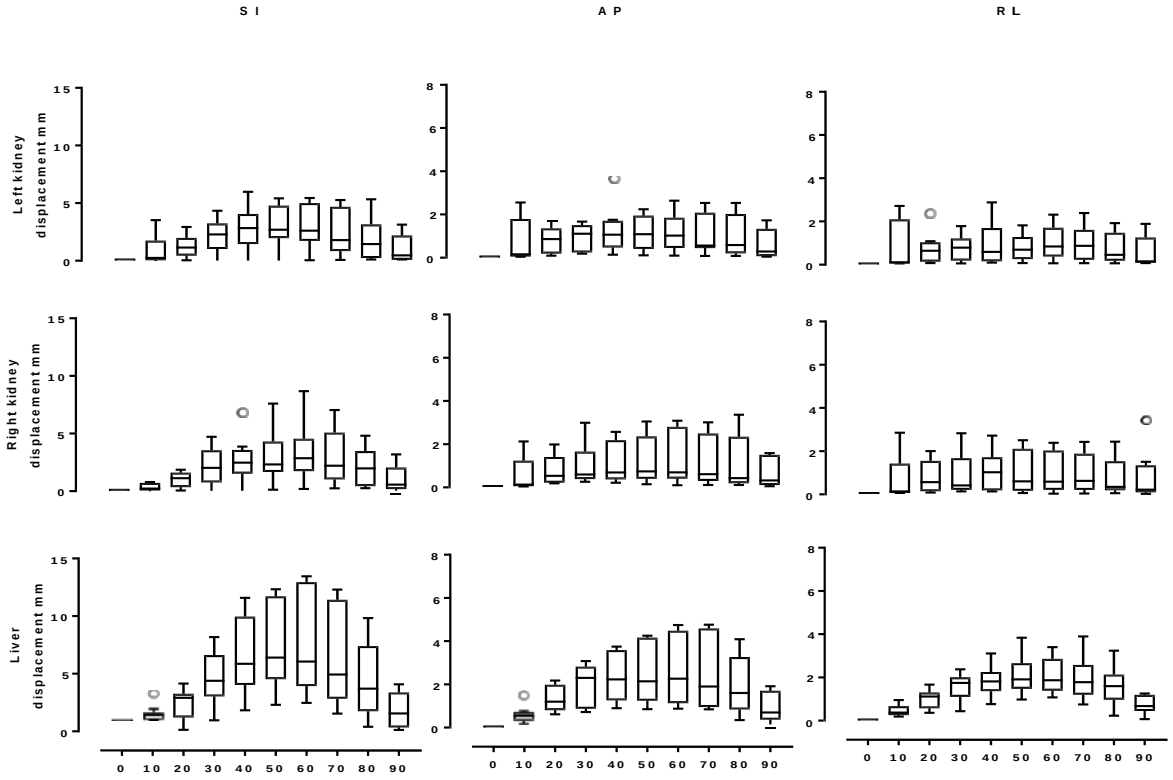

Figure 3.1 - Boxplots for left (top), right (middle) kidney and liver (bottom) DVF displacements (mm) in superior/ inferior (SI), anterior/ posterior (AP) and right/ left (RL) directions according to 4DCT phase (%) for all patients. Boxes: upper and lower quartiles, whiskers: highest and lowest values, bar: median. Motion is relative to 0% phase (solid black rectangle). Y axes differ in scales in SI and AP, RL directions.

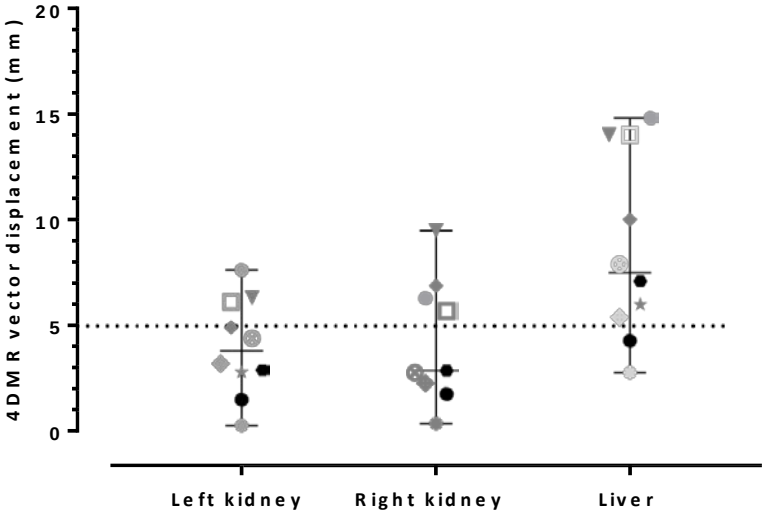

Figure 3.2 - Scatter plots describing the magnitude of vector displacements (mm) for kidneys and liver (all patients; each symbol represents a single patient). Black symbols= patients under GA, grey symbols = patients not under GA. Error bars depict medians (horizontal) and ranges (vertical). Dashed line at y axis = 5mm indicates threshold for consideration of motion management in adults as per AAPM guidelines (26).

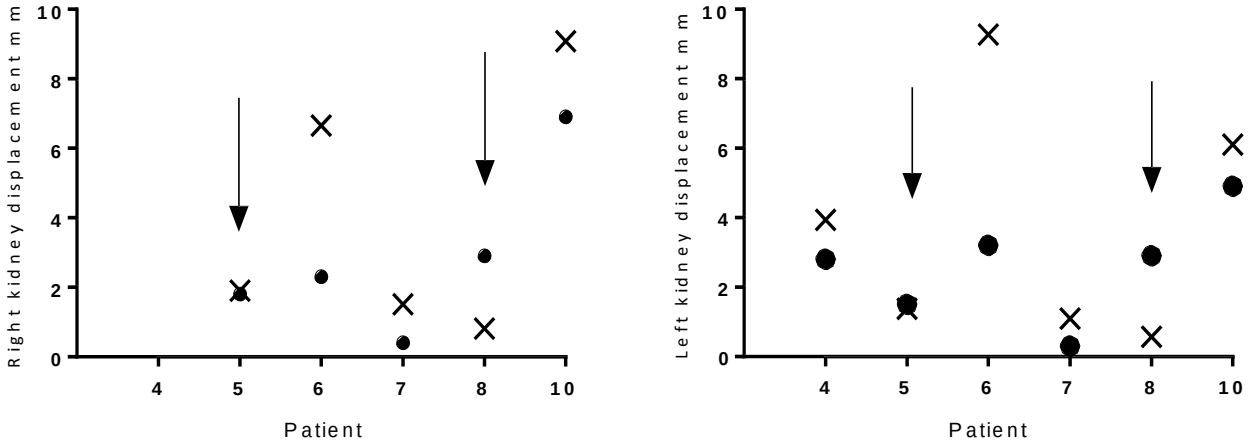

Figure 3.3 - Vector displacements in the 6 patients (patient 4, 5, 6, 7, 8, and 10) imaged with both 4DCT (crosses)

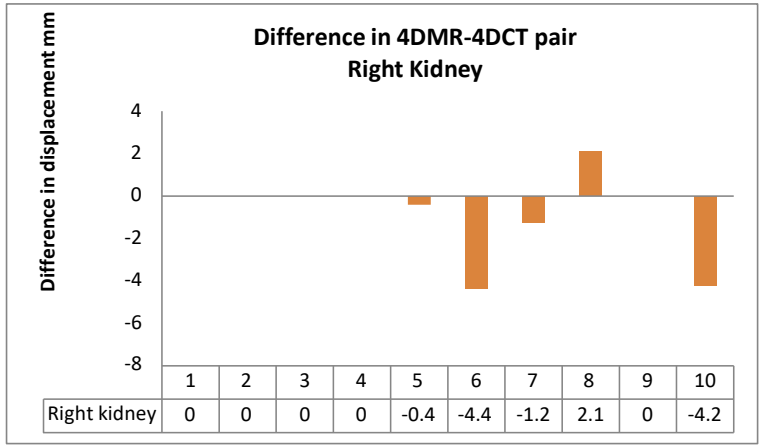

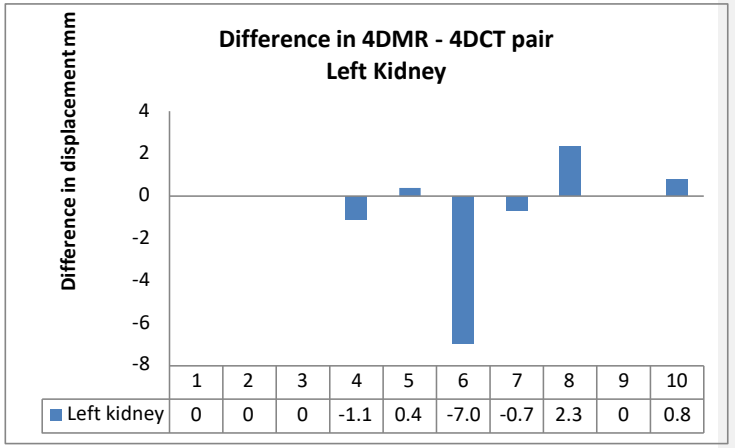

Figure 3.4 - Pairwise differences between measured right and left kidney displacements as measured by vectors Displacements (mm) on 4DMR and 4DCT. Note patient 4 had no right kidney. Negative numbers indicate 4DMR displacement is smaller than 4DCT.

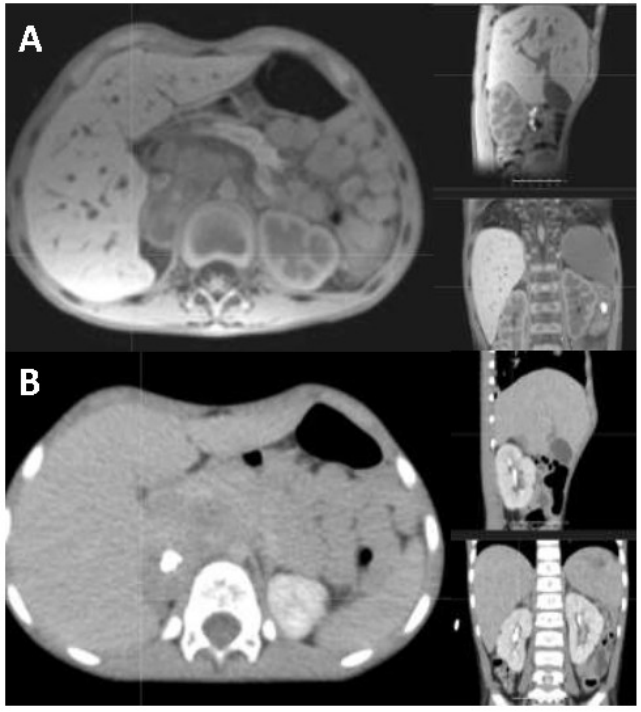

Figure 3.5 - (A) axial, sagittal and coronalMR image from a representative (patient 7),(B) axial, sagittaland coronal CT image.

Patient	Age (years)	Height (cm)	Weight (kg)	BSA (m^2)	Tumour in situ	GA	Diagnosis
1	12.3	165.5	49.6	1.5	No	No	Ganglioneuroblastoma
2	8.9	132	30.6	1.1	No	No	Ovarian teratoma
3	15.5	162.5	49.6	1.5	No	No	Neuroblastoma
4	7.1	132.3	28.1	1	No	No	Wilms' tumour
5*	4.5	112	16.4	0.68	No	Yes	Neuroblastoma
6*	15.6	143.5	42.7	1.3	No	No	Rhabdomyosarcoma
7*	4.5	113	17.7	0.74	Yes	Yes	Neuroblastoma
8*	1.9	78.7	9.45	0.47	Yes	Yes	Neuroblastoma
9*	15.2	161	47.6	1.4	No	No	Neuroblastoma
10*	4.1	110	16.2	0.68	No	No	Neuroblastoma

Table 3.1 – patient characteristics for all patients with analysable 4DMR datasets, BSA = body surface area, GA= general anaesthetic, * indicates patients imaged with 4DMR and 4DCT

	4DMR			4DCT	
	Left kidney	Right kidney	Liver	Left kidney	Right kidney
Median mm	2.9	2.3	7.5	2.7	1.9
Range mm	0.3 – 4.9	0.4 – 6.9	2.8 – 14.8	0.6 – 9.3	0.8 – 9.1

Table 3.2 - 3D motion vectors (mm) for 6 patients with 4DMR and 4DCT. Liver motion not measured on 4DCT.

	Right kidney			Left kidney			Liver		
	RL	AP	**SI**	RL	AP	**SI**	RL	AP	**SI**
Median (mm)	1.0	0.7	**2.8**	1.2	1.3	**3.2**	1.8	2.4	**7.1**
Range (mm)	0.2 - 3.5	0.3 - 3.4	**0.3 - 8.7**	0.2 - 2.9	0.2 - 3.6	**0.1 - 6.0**	1.1 - 3.9	0.9 - 4.8	**2.5 - 13.5**

Table 3.3 – Descriptive statistics of DVF 4DMR displacements (mm) in right/ left (RL), anterior/ posterior (AP) and superior/ inferior (SI) directions (all patients).

Chapter 4

Feasibility of utilising the Clarity ultrasound system for localisation of the kidney in children

4.1 Background

My results in Chapter 2 established the feasibility of acquiring 4DCT imaging in a paediatric cohort. RROM measured on a single pre-treatment 4DCT may not predict upper abdominal organ motion during the course of RT [1, 2]) and daily localisation of the target on treatment is necessary to verify target position [3]. In paediatric RT, CBCT verification is conventionally performed by way of matching bone anatomy to the planning CT [4]. Use of bone-match in paediatric image guided RT (IGRT) facilitates optimisation of CBCT acquisition parameters to reduce the additional imaging dose to the patient as additional imaging dose remains a concern in young patients due to the potential for development of a secondary malignancy [4-8]. The trade-off is often significantly reduced soft tissue contrast. Verification based on bone-match does not give adequate direct information on the location of soft tissue targets. 4D-CBCT is increasingly employed in adult lung cancer RT for the purpose of intrafraction RROM verification but 4D-CBCT delivers significant additional imaging dose to the patient over that associated with CBCT. There is scope in paediatric RT to explore alternative or adjunct non-ionising imaging modalities to enable pre- treatment soft-tissue verification where imaging dose is of concern.

US can be integrated with a standard C-arm linear accelerator to enable verification of RROM. Its use in interfraction and intrafraction motion assessment in RT has been summarised in a number of contemporaneous review articles [9-11]. US has been utilised with success in adults for interfraction and intrafraction verification of prostate location [12, 13]. US can enhance CBCT by giving additional soft tissue contrast as US, in conjunction

with CBCT, and has been shown to improve target segmentation in cervical

cancer RT [14]. US-guided RT has also been described in breast, gallbladder, pancreas and other upper abdominal tumours in adults [15-19]. US could therefore facilitate RROM assessment and treatment verification without additional imaging dose in paediatric RT. The comparative low cost of US is an important consideration from a global perspective as the majority of childhood cancers occur in low/ middle income countries [20].

The objective of this Chapter was to explore the feasibility of using the Clarity US platform (Elekta AB, Stockholm, Sweden) to localise the kidney in children in the supine radiotherapy position.

4.2 Aims of Chapter 4

My hypothesis is that acquiring ultrasound images of the kidney in the supine radiotherapy position with the Clarity US platform is feasible in children.

In order to test this hypothesis, I will;

1) Determine the feasibility and quality of ultrasound images acquired.
2) Compare kidney displacements in patients who have undergone dual imaging with US and 4DCT, and US and 4DMR.

4.3 Methods

4.3.1 Patient selection

Eligible patients were enrolled on the APACHe (**A**daptive RT **p**lanning for upper **a**bdominal tumours in **ch**ildren and t**e**enagers) study and parental consent was obtained, Appendix 1.

Two patient cohorts were eligible for US imaging in the APAChe study. **Cohort 1** included patients referred for RT to the upper abdomen. **Cohort 2** included patients referred for MR imaging for surveillance of a previously treated tumour.

4.3.2 Patient preparation and immobilisation

Considerable efforts were made in advance of acquiring US images and prior to recruiting patients to the APAChe study. The logistics were complex given the potential of five scanning locations: the pre-treatment CT simulator (Cohort 1), the RT treatment unit (Cohort 1), the preparation room in RT department (Cohort 2) and the MR department (Cohort 2).

Scanning within the MR department proved the most challenging. Dr. Sarah Mason (SM) created a prototype arm that was purpose built by clinical engineering for the purpose of this work. The Polaris camera was slotted into this arm to attach it to the MR-compatible patient couch. I needed to pay special consideration to the additional length of time that very young children would be under anaesthesia as a consequence of acquiring US images. It was

imperative that acquiring US caused the least disruption to the clinical workflow of the MR department.

4.3.2.1 Cohort 1 (patients referred for RT)

Patients in Cohort 1 were referred for RT simulation, (Figure 4.6). Patients were immobilised with standard set-up for abdominal RT planning CT and 4DCT; supine, arms at side, knee rest. US was acquired after 3DCT and 4DCT imaging were completed. If the patient was under GA for CT imaging, the child remained under GA for the duration of the US scan. Patients in this cohort also had one further US measurement, of the same kidney, following delivery of a RT fraction; the fraction of RT that this US was performed was individualised.

4.3.2.2 Cohort 2 (patients referred for surveillance MR imaging)

Patients in Cohort 2 were imaged in the MR department if under GA or in a preparation room adjacent to a Linear accelerator (Linac) bunker in the RT department if not under GA.

4.3.3 Ultrasound acquisition

The Clarity US system was used in this work and consists of the US probe and infrared detectors mounted on the probe, (Figure 4.9), [21]. The Polaris camera is fixed into the ceilings of the Linac bunker and CT simulator room. Outside of these locations the Polaris camera is mounted on a moveable tripod. The set-up in the Linac and the CT simulator room makes the system quality assurance easier and more reliable. The infrared technology of the Clarity system gives

the user spatial registration of the probe location relative to the room geometry. System calibration was performed by SM prior to each imaging session.

4.3.4 Localisation

The decision to image the right or left kidney was individualised. Some patients had a solitary kidney post nephrectomy (patients 1, 9, 10, 13, 16 and 18). In patients with residual disease at the time of imaging the contralateral kidney was imaged (patient 15). Following localisation of the kidney the US probe was orientated for optimal visualisation of the kidney in the sagittal plane. This plane was chosen to visualise in-plane motion of the kidney in the superior-inferior (SI) direction. Two-dimensional (2D US) and three-dimensional US (3D US) images were obtained. Each US acquisition took approximately 90 seconds.

In this work, I performed all probe localisations for scan acquisition and SM performed system quality assurance and adjusted acquisition parameters on the Clarity system during scanning (except for one patient; probe localisation performed by Dr. H.C. Mandeville and Clarity system operated by Dr. E. Harris).

4.3.5 Data analysis

SM visually inspected the individual 2DUS videos for quality. The following criteria were used; at least 2 breathing cycles were imaged with the kidney continuously visible, and an identifiably anatomical landmark was identified to

perform cross correlation. SM performed the cross correlation analysis of useable US images with a template-matching algorithm to track the motion of the kidney, thereby enabling quantification of the extent of motion in the SI plane, (Figure 4.8), [22]. The template was fixed, and the search region was a box contained within the kidney, (Figure 4.6). The size of the template was about 1/3 the size of the kidney, contained completely within the kidney, and centred over a region where there was little to no out-of-plane motion throughout the breathing cycle. Only 2DUS data is presented in the results of this chapter.

4.3.6 Statistical analysis

Descriptive statistics are used given the small cohort of patients included in this work. Group median amplitude, and standard deviation (SD), are presented. Mean amplitude of motion and its variability in children under GA and not under GA are presented, (Figure 4.7). 95% SI displacements measured by US are compared with 4DCT and 4DMR maximum SI deformation vector field (DVF) displacements from Chapters 2 and 3.

4.4 Results

2DUS images for 19 patients were assessed; median age 5 years (range 1.4 – 15.6 years). 8 of the 19 patients were imaged under GA. Patient characteristics are summarised in Table 4.1. In total 13 patients were recruited to Cohort 1

and were eligible for two US scans. 6 patients were recruited to Cohort 2 and were eligible for a single US image. Data for one patient assessed was acquired but not saved and was therefore not included in further analysis.

4.4.1 Feasibility

In total useable 2D US data were obtained from 12 of the 18 eligible patients (67%). Useable US images at two separate time points were available in 5 of the 13 patients recruited to Cohort 1 (38%). The reasons for 2D US data not being included in the analysis are described for each individual patient in Table 1 and discussed in further detail in subsequent sections.

4.4.2 Localisation

The left kidney was imaged in 8 out of the 19 patients assessed (patients 1, 6, 12, 13, 15, 16, 18, and 19). Only two of these eight patients had useable 2D US images (patients 13 and 15). Three out of the four patients for whom the presence of out of plane motion rendered 2D-US images unusable in the analysis were imaged on the left (patients 12, 16 and 18).

The probe was not tracked correctly by the infrared camera in patients 3, 6 and 11. Patients 6 and 11 were recruited to Cohort 2. US was performed in a preparation room in the RT department in this cohort. The dimensions of the room were smaller than the CT simulation room and so limited the position of the infrared camera and may explain why probe tracking failed in this cohort of

patients. Regardless, the finite spatial mobility of the system was a limitation in localising the best imaging planes in this study.

4.4.3 Image quality

Using the software inherent in the Clarity system, the power, gain and focus were individually adjusted for the patients in the study to account for differences in kidney depth and abdominal diameter. US image quality was rated as poor by SM at the time of data analysis in the case of patient 1 and 2. This was related to the inability to identify an anatomical structure within the imaged kidney with which to perform cross correlation. The presence of bowel gas adversely affected image quality for patient 12 (under GA). US waves do not propagate easily through air; limiting image quality in the presence of bowel gas [9].

Out of plane motion was also evident in patients 5, 12, 16 and 18 rendering the 2DUS images unusable for analysis. 3D US images were acquired but not analysed. 3DUS imaging could mitigate the adverse effect of out of plane motion on image quality required for cross correlation template matching and increase the proportion of useable US images.

4.4.4 Group assessment of kidney motion

Median amplitude for the 12 patients with usable 2D US images (at any time-point) was 3.1 mm (SD 2.1 mm), (Figure 4.1).

8 of the 19 patients were imaged under GA; median age 3.2 years, range 1.4 – 6.1 years. 2D US images were not acquired as planned in patient 7 and the reason for this is explored further in the discussion section. Using all 2DUS displacements acquired at any time-point, median displacement in children not under GA was 4.0 mm (SD 1.0) compared to 1.7 mm (SD 0.8) in children under GA.

4.4.5 US and US intra-modality comparison of motion

Five patients had useable 2D-US measurements at two time points facilitating intra-modality comparison of kidney motion, (Figure 4.2). Four of the 5 patients were imaged under GA. The mean difference between pairs was -1.6 mm (SD 1.3 mm), (Figure 4.3). The greatest difference was seen in patient 4; the second US demonstrated motion that was 3.7 mm greater than that measured on the first US.

4.4.6 US and 4DCT inter-modality comparison of motion

4DCT was acquired during the same imaging session for the same 5 patients described in the previous paragraph. The differences in measured displacements are displayed in Figure 3. Maximum kidney deformation vector displacements (DVF) were measured on 4DCT, as described in Chapter 2. In Figure 4, the displacements (mm) measured on US and the corresponding maximum kidney DVF displacements (mm) derived from 4DCT are shown for the five patients. Median difference between 4DCT and US pairs was 0.1 mm

(SD 1.3 mm) indicating that 4DCT measurement was on average 0.1 mm greater than the US measurement.

4.4.7 US and 4DMR inter-modality comparison of motion

7 patients had useable 2D US data to compare with 4DMR (patients 2, 3, 4, 10, 13, 14, and 15). Patients 10 and 13 had US and 4DMR image acquired on the same day but images were acquired in two different departments in the hospital. The remaining 5 patients had US and 4DMR images acquired on different days.

95% SI displacement measured on US and maximum SI DVF displacement measured on 4DMR was compared for each patient. The median difference between the two modalities across all 7 patients was -1.3 mm (SD 1.6 mm). The negative value indicating that motion on 4DMR was on average 1.3 mm smaller than that measured by US. Pairwise comparisons between US and 4DMR for these 7 patients are shown in Figure 5. In the case of patient 13, motion was 1.5 mm greater on 4DMR compared to that measured by US. The agreement between US and 4DMR motion was 1 mm in patients 14 and 15. Patient 3 displayed the greatest difference with motion measuring 3.4 mm less on 4DMR compared to US.

4.5 Discussion

4.5.1 Feasibility and image quality

The Clarity US probe used in this work is designed for adult patients and the system is currently in clinical use at The Royal Marsden NHS Foundation Trust for adult male patients with prostate cancer where the probe is positioned at the perineum [12]. Therefore, the probe is clearly not the desired scale for optimal use in the paediatric setting or for routine online imaging during upper abdominal radiotherapy. Despite this 2DUS images were acquired within minutes in this cohort of paediatric patients. Apart from patient 7, all US images were obtained without impacting the scheduled simulation, RT treatment, or MR imaging session. US imaging was tolerated by all children assessed in this work.

Useable 2DUS images were obtained in 63% of patients, compared to > 80% of patients referred for 4DCT, the current gold standard for motion assessment in adults; as described in Chapter 2. The reasons for 2DUS images being unusable were poor image quality (patients 1, 2); probe tracking errors (patients 3, 6, 11); out of plane motion (patients 5, 12, 16); probe motion (patient 18) and overlying bowel gas (patient 12).

Patients 1 and 2 were the first recruited to the study and therefore the first imaged. The image quality of these first US scans was rated as poor. This likely reflects a learning curve in the operation and acquisition of US images. US acquisition in this study required manual operation of the US probe. US acquired in this way is operator-dependant and inter-operator variability in US imaging in RT has been described [9]. US is also an imaging modality that is

not familiar to many clinical oncologists compared to CT and, to a lesser extent, MR. Training and experience has been shown to reduce user-dependent variability of US image acquisition [23]. An investigation of pre-treatment localisation of the kidney with the SonArray US system in children with neuroblastoma was abandoned after 4 patients because no correlation was found between the recommended cone beam CT and US pre-treatment shifts [24]. The authors commented that lack of training could have affected the results. The discrepancies could also be explained if the pre-treatment US localised the kidney at a different phase of the breathing cycle compared to the planning 3DCT scan.

Out of plane motion rendered 2DUS imaging unusable in (patients 5, 12, 16). The kidneys are located in the retroperitoneum. In the diagnostic setting, children are positioned in the lateral decubitus position for US imaging of the kidney. Such positioning was not feasible in this work as the purpose of this study was to assess the feasibility of acquiring US images in the supine RT treatment position. When I positioned the US probe at the lateral aspect of the upper abdominal wall and acquired optimal images of the kidney in the desired sagittal plane the Clarity infrared camera failed to locate the probe. When I repositioned the probe to be within range of the camera images were often suboptimal with out of plane motion evident.

My results also suggest that the left kidney is more challenging to localise successfully in the supine position. The left kidney was imaged in 8 out of the 19 patients assessed (patients 1, 6, 12, 13, 15, 16, 18, and 19). Only two of these eight patients had useable 2D US images (patients 13 and 15). Three out of the four patients for whom the presence of out of plane motion rendered

2D-US images unusable in the analysis were imaged on the left (patients 12, 16 and 18). The acquisition of 3D US images would mitigate the issue of out of plane motion.

The quality of US images in patient 12 were rated poor in part due to the presence of bowel gas obscuring visualisation of the left kidney. As US waves do not propagate easily through air this limitation has been described in adult patients when US localisation in the upper abdomen was performed [16, 17]. Patient 12 was imaged under GA and increased abdominal air is a common feature in children under GA [25]. The left kidney was imaged in this child; and would be in proximity of to the stomach – where the greatest volume of organ insufflation would be evident in children under GA.

Probe motion was evident in the analysis of images in patient 18. In this work the US probe was held by the operator (me) and the consistency of probe position during imaging is user-dependent. The Clarity Autoscan system is in clinical use at the Royal Marsden NHS Foundation Trust for prostate RT and consists of an arm and baseplate that holds the probe in contact with the patient's perineum to mitigate the effects of drift and probe placement, (Figure 4.7), [26]. The system's intra-fraction verification of prostate position has been shown to operate with millimetre precision in vivo resulting in comparable accuracy with other RT localisation techniques that are in clinical use [12].

4.5.2 Kidney motion and comparisons

The median 95% SI displacement for the group was 3.1 mm (SD 2.1 mm). This compares favourably with results presented in Chapters 2 and 3 where median

displacements for right and left kidneys measured 2.4 and 3.6 mm (4DCT), and 2.8 and 3.2 mm (4DMR). Furthermore, kidney displacement in the 5 patients imaged with US and 4DCT during the same imaging session, and in the RT treatment position, demonstrated good agreement with a median difference between US and 4DCT of 0.1 mm.

Probe drift could influence the maximum displacements measured by US. 95% SI displacement is the metric presented in this Chapter; as a measure it excludes the most extreme 5 % of data points therefore reducing the impact of probe drift on inter-modality comparisons based on maximum displacements.

This work enabled direct intra-modality comparison of inter-fraction RROM measured by US. Five patients had useable 2D-US measurements at two time points. Four of the 5 patients were imaged under GA. The mean difference in displacements between US pairs was -1.6 mm (SD 1.3 mm), (Figure 4.3). The greatest difference was seen in patient 4, aged 15.6 years, with motion 3.7 mm less on the second US measurement. In the remaining 4 patients, all under GA, differences ranged from -0.5 to -1.9 mm (negative values indicating less motion on the first ultrasound).

My results also demonstrate that children under GA display smaller intrafraction variability in RROM than those not under GA; median kidney displacement in children under GA 1.7 mm (SD 0.8) compared to 4.0 mm (SD 1.0) in children not under GA. Huijskens et al investigated intrafraction diaphragm amplitude variability in 25 patients (mean age 11, range 2 – 18 years) from 480 cone beam computed tomography (CBCT) projection images. They found that variation was statistically significantly smaller in 7 patients

aged 2 -11 years and under GA (1.6 mm) compared to 12 children aged 3 – 10 years not under GA (2.4 mm) [27].

My comparison of 2DUS and 4DMR showed that median difference in displacements was 1.3 mm (displacements were smaller on 4DMR). The agreement between US and 4DMR displacements was 1 mm in patients 14 and 15; both children were imaged under GA but on separate days. The greatest difference was -3.4 mm in patient 3, aged 15.2 years; this child was imaged on different days.

Though small numbers, these results support my results presented in Chapter 2; renal motion is smaller in young children under GA and intrafraction variation is also less in young anaesthetised children compared to older teenagers.

2DUS images were not obtained for patient 7. A multi-disciplinary decision was made prior to initiation of the APAChe study to schedule patients under GA in cohort 2 at the end of the afternoon MR list. It was imperative that the acquisition of research-related imaging did not impede or delay the scheduled MR imaging list. Patient 7 was the youngest patient in the cohort, aged 3.4 years, and had been fasting as per standard procedures. The MR list ran behind schedule and the anaesthetist was concerned about keeping the child under GA for any extended period of time. A clinical decision was made to omit the 2DUS acquisition in this patient.

The effect of US probe pressure on measured displacements and organ deformation of the prostate have been described with observed displacements of up to 10 mm [28-30]. However, given the different anatomical location, and from the available data presented in the Chapter, it ~~is impossible~~was not possible to ~~demonstrate any~~ determine the possible effect of probe pressure on the results presented in this Chapter, as the US images were

not

registered to the 4DCT. The ideal probe design for paediatric upper abdominal image guided RT, and the impact of probe pressure, need to be explored further in future studies. The presence of probe pressure in this patient cohort could be quantified by fusing the 4DCT and 3DUS image set in future analysis. The magnitude of probe pressure, if present, could be affected by the position of the probe of the child's body. Anterior abdominal imaging, as done in this Chapter, may result in greater pressure being applied to the probe on the anterior abdomen to visualize the kidney. Whereas imaging the patient in the lateral decubitus position positions the kidney in a more favourable anatomical location and may result in easier visualization of the organ without applying probe pressure.

4.6 Conclusion

It is feasible to acquire US images in the RT treatment position in children using the Clarity US system. This Chapter demonstrates that US acquisition was efficient and well tolerated and can inform the acquisition of US in future studies in children, particularly those under GA. A substantial probe redesign would be required to progress its use in paediatric RT planning or treatment verification. Enabling imaging of the kidney from the postero-lateral abdominal wall position, simulating the probe positioning used in diagnostic paediatric radiology, while still in range of the infrared camera would enhance the ability to visualise in plane kidney motion. Further analysis of the 3DUS image dataset may increase the proportion of useable images due to mitigation of out

of plane motion effect on 2D US images described in this Chapter.

4.7 References

1) Ge J, Santanam L, Noel C, Parikh PJ. Planning 4-dimensional computed tomography (4DCT) cannot adequately represent daily intrafractional motion of abdominal tumors. Int J Radiat Oncol Biol Phys 2013; 85(4): 999-10005.
2) Huijskens SC, van Dijk I, Visser J, Balgobind BV, Rasch CRN, Alderliesten T, et al. Predictive value of pediatric respiratory-induced diaphragm motion quantified using pre-treatment 4DCT and CBCTs. Radiation oncology (London, England) 2018; 13(1): 198.
3) Lens E, van der Horst A, Kroon PS, van Hooft JE, Davila Fajardo R, Fockens P, et al. Differences in respiratory-induced pancreatic tumor motion between 4D treatment planning CT and daily cone beam CT, measured using intratumoral fiducials. Acta oncologica (Stockholm, Sweden) 2014; 53(9): 1257-1264.
4) Hess CB, Thompson HM, Benedict SH, Seibert JA, Wong K, Vaughan AT, et al. Exposure Risks Among Children Undergoing Radiation Therapy: Considerations in the Era of Image Guided Radiation Therapy. International Journal of Radiation Oncology*Biology*Physics 2016; 94(5): 978-992.
5) Pearce MS, Salotti JA, Little MP, McHugh K, Lee C, Kim KP, et al. Radiation exposure from CT scans in childhood and subsequent risk of leukaemia and brain tumours: a retrospective cohort study. Lancet 2012; 380(9840): 499-505.
6) Hall EJ, Brenner DJ. Cancer risks from diagnostic radiology: the impact of new epidemiological data. The British journal of radiology 2012; 85(1020): e1316-1317.
7) Brenner DJ, Hall EJ. Cancer risks from CT scans: now we have data, what next? Radiology 2012; 265(2): 330-331.
8) Alcorn SR, Chen MJ, Claude L, Dieckmann K, Ermoian RP, Ford EC, et al. Practice patterns of photon and proton pediatric image guided radiation treatment: results from an International Pediatric Research consortium. Pract Radiat Oncol 2014; 4(5): 336-41.
9) Fontanarosa D, van der Meer S, Bamber J, Harris E, O'Shea T, Verhaegen F. Review of ultrasound image guidance in external beam radiotherapy: I. Treatment planning and inter-fraction motion management. Phys Med Biol 2015; 60(3): R77-114.
10) O'Shea T, Bamber J, Fontanarosa D, van der Meer S, Verhaegen F, Harris E. Review of ultrasound image guidance in external beam radiotherapy part II: intra-fraction motion management and novel applications. Phys Med Biol 2016; 61(8): R90-R137.
11) Western C, Hristov D, Schlosser J. Ultrasound Imaging in Radiation Therapy: From Interfractional to Intrafractional Guidance. Cureus 2015; 7(6): e280.
12) Grimwood A, McNair HA, O'Shea TP, Gilroy S, Thomas K, Bamber JC, et al. In Vivo Validation of Elekta's Clarity Autoscan for Ultrasound-based Intrafraction Motion Estimation of the Prostate During Radiation Therapy. Int J Radiat Oncol Biol Phys 2018.

13) Fargier-Voiron M, Presles B, Pommier P, Munoz A, Rit S, Sarrut D, et al. Ultrasound versus Cone-beam CT image-guided radiotherapy for prostate and post-prostatectomy pretreatment localization. Physica medica : PM : an international journal devoted to the applications of physics to medicine and biology : official journal of the Italian Association of Biomedical Physics (AIFB) 2015; 31(8): 997-1004.
14) Mason SA, White IM, O'Shea T, McNair HA, Alexander S, Kalaitzaki E, et al. Combined Ultrasound and Cone Beam CT Improves Target Segmentation for Image Guided Radiation Therapy in Uterine Cervix Cancer. Int J Radiat Oncol Biol Phys 2019; 104(3): 685-693.
15) Omari EA, Erickson B, Ehlers C, Quiroz F, Noid G, Cooper DT, et al. Preliminary results on the feasibility of using ultrasound to monitor intrafractional motion during radiation therapy for pancreatic cancer. Med Phys 2016; 43(9): 5252.
16) Boda-Heggemann J, Mennemeyer P, Wertz H, Riesenacker N, Küpper B, Lohr F, et al. Accuracy of Ultrasound-Based Image Guidance for Daily Positioning of the Upper Abdomen: An Online Comparison With Cone Beam CT. International Journal of Radiation Oncology*Biology*Physics 2009; 74(3): 892-897.
17) Fuss M, Salter BJ, Cavanaugh SX, Fuss C, Sadeghi A, Fuller CD, et al. Daily ultrasound-based image-guided targeting for radiotherapy of upper abdominal malignancies. International Journal of Radiation Oncology*Biology*Physics 2004; 59(4): 1245-1256.
18) Coles CE, Cash CJ, Treece GM, Miller FN, Hoole AC, Gee AH, et al. High definition three-dimensional ultrasound to localise the tumour bed: a breast radiotherapy planning study. Radiotherapy and oncology : journal of the European Society for Therapeutic Radiology and Oncology 2007; 84(3): 233-241.
19) Fuller CD, Thomas CR, Jr., Wong A, Cavanaugh SX, Salter BJ, Herman TS, et al. Image-guided intensity-modulated radiation therapy for gallbladder carcinoma. Radiotherapy and oncology : journal of the European Society for Therapeutic Radiology and Oncology 2006; 81(1): 65-72.
20) Kortmann R-D, Freeman C, Marcus K, Claude L, Dieckmann K, Halperin E, et al. Paediatric radiation oncology in the care of childhood cancer: A position paper by the International Paediatric Radiation Oncology Society (PROS). Radiotherapy and Oncology 2016; 119(2): 357-360.
21) Lachaine M, Falco T. Intrafractional prostate motion management with the Clarity Autoscan system. Medical physics international 2013; 1.
22) Briechle K, Hanebeck UD, editors. Template matching using fast normalized cross correlation. Optical Pattern Recognition XII; 2001: International Society for Optics and Photonics.
23) Fuss M, Cavanaugh SX, Fuss C, Cheek DA, Salter BJ. Daily stereotactic ultrasound prostate targeting: inter-user variability. Technol Cancer Res T 2003; 2(2): 161-169.
24) Beltran C, Pai Panandiker AS, Krasin MJ, Merchant TE. Daily image-guided localization for neuroblastoma. Journal of applied clinical medical physics 2010; 11(4): 3388.

25) Lim P, Rompokos V, Gillies C, Gosling A, Royle G, Chang Y, et al. Variations in bowel gas volume due to general anesthesia and its implications on dosimetric target volume coverage with Pencil Beam Scanning Proton Beam Therapy versus Intensity Modulated Radiotherapy in paediatric abdominal neuroblastoma. 2019.
26) Fargier-Voiron M, Presles B, Pommier P, Munoz A, Rit S, Sarrut D, et al. Evaluation of a new transperineal ultrasound probe for inter-fraction image-guidance for definitive and post-operative prostate cancer radiotherapy. Physica medica : PM : an international journal devoted to the applications of physics to medicine and biology : official journal of the Italian Association of Biomedical Physics (AIFB) 2016; 32(3): 499-505.
27) Huijskens SC, van Dijk IW, Visser J, Rasch CR, Alderliesten T, Bel A. Magnitude and variability of respiratory-induced diaphragm motion in children during image-guided radiotherapy. Radiotherapy and oncology : journal of the European Society for Therapeutic Radiology and Oncology 2017; 123(2): 263-269.
28) Fargier-Voiron M, Presles B, Pommier P, Rit S, Munoz A, Liebgott H, et al. Impact of probe pressure variability on prostate localization for ultrasound-based image-guided radiotherapy. Radiotherapy and oncology : journal of the European Society for Therapeutic Radiology and Oncology 2014; 111(1): 132-137.
29) van der Meer S, Seravalli E, Fontanarosa D, Bloemen-van Gurp EJ, Verhaegen F. Consequences of Intermodality Registration Errors for Intramodality 3D Ultrasound IGRT. Technol Cancer Res T 2016; 15(4): 632-638.
30) Kaar M, Figl M, Hoffmann R, Birkfellner W, Hummel J, Stock M, et al. Automatic patient alignment system using 3D ultrasound. Medical Physics 2013; 40(4): 041714.

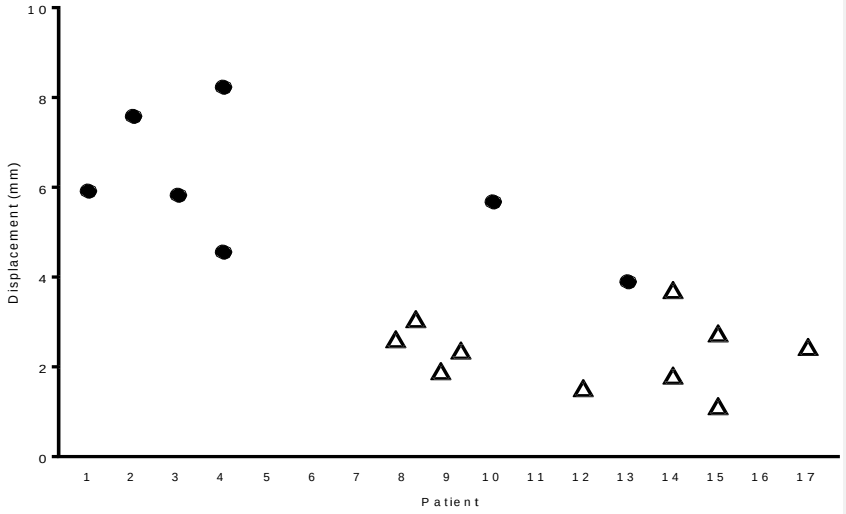

Figure 4.1 - 95% SI displacement (mm) plotted for each individual patient. Patients 4, 8, 9, 14 and 15 have two 2D US measurements. Patient 18 and 19 did not have useable 2D US images and are not included on the x axis. Triangles = patients imaged under GA. Circles = patients not under GA.

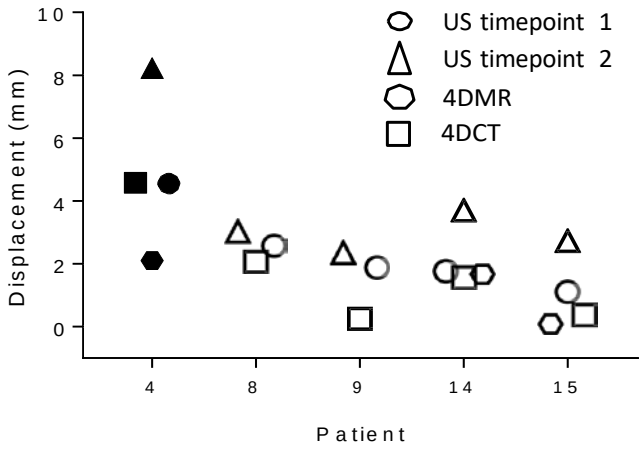

Figure 4.2 – Kidney 95% SI displacement (mm) in the 5 patients With US images acquired at two time points. Black symbols = Patient not under GA. White symbols = patients under GA.

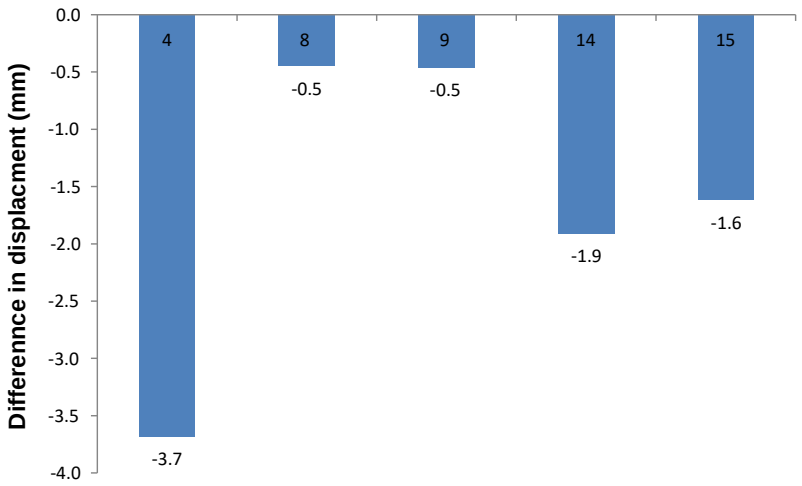

Figure 4.3 - Pairwise differences between SI displacements (mm) measured on first and second US image. Negative values indicate that motion is smaller on the first US compared to the second US.

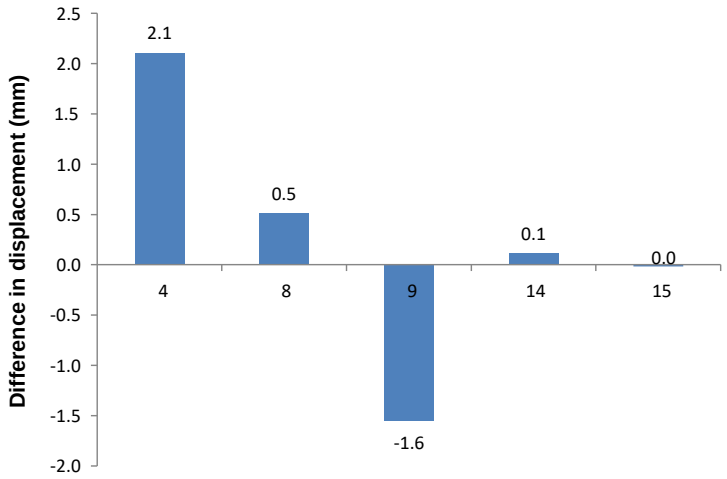

Figure 4.4 - Pairwise differences between SI displacements (mm) measured with US (95% SI displacement) and 4DCT (maximum SI DVF displacement) (acquired during the same imaging session). Negative values indicate that motion is smaller on 4DCT compared to US.

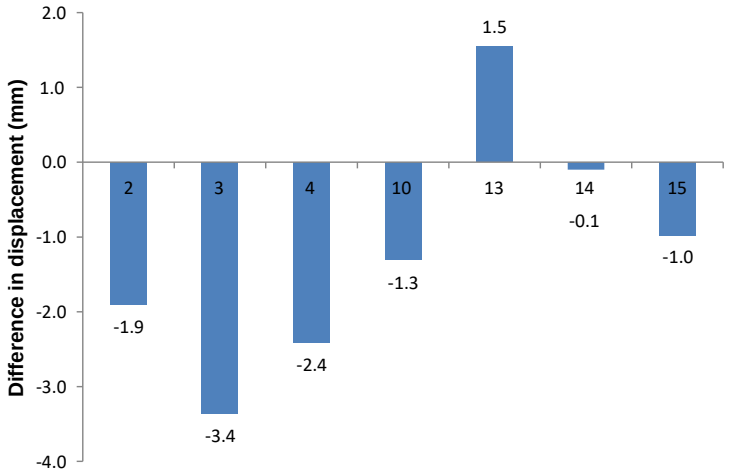

Figure 4.5 – Pairwise differences between SI displacements (mm) measured with US and 4DMR in 7 patients imaged with both modalities. Negative values indicate that motion was smaller on 4DMR compared to US.

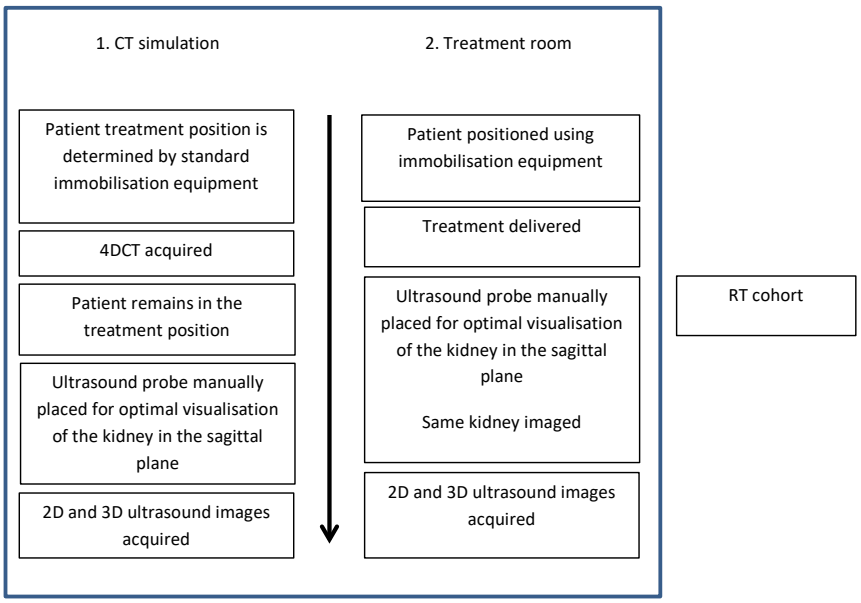

Figure 4.6 - APACHe study workflow for patients in Cohort 1 (children referred for RT).

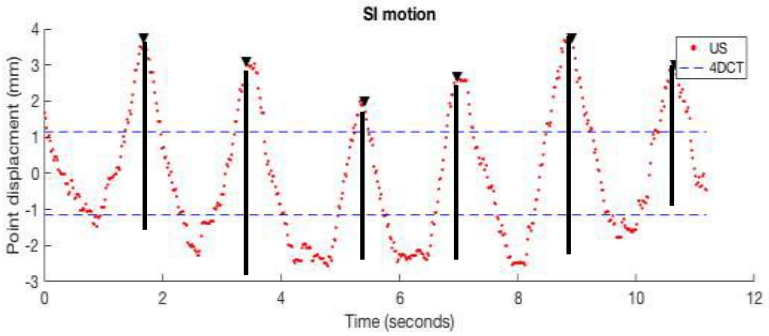

Figure 4.7 - Example of sinusoids of motion extracted from US (red dotted line). Black lines depict magnitude of displacement. Blue dashed line represents displacements derived from 4DCT.

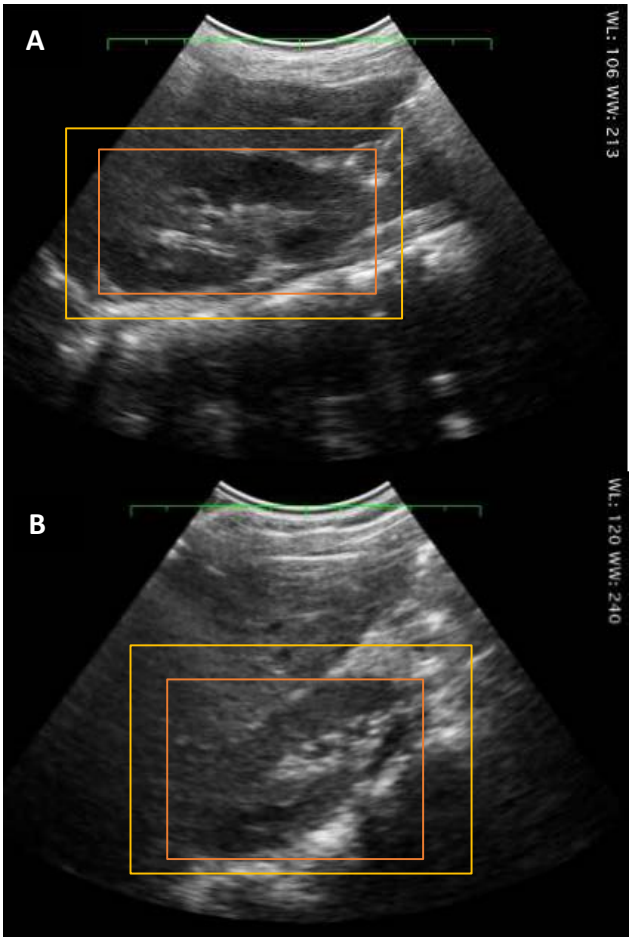

Figure 4.8 – example of useable US images (patient 2). (A) acquired after CT (patient 2) and (B) at treatment. The kidney is contained within the orange box which is used as a template for correlation tracking. The yellow box shows the tracking search region. (Image courtesy of Dr. Sarah Mason and Dr. Emma Harris).

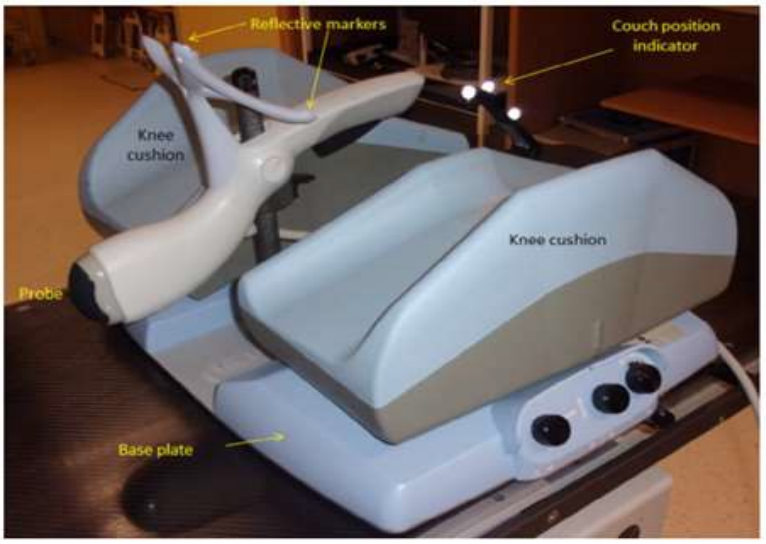

Figure 4.9 – the Clarity Autoscan system; this is the Clarity hardware and set-up used for prostate cancer IGRT (26).

Patient	Age (years)	APAChe cohort	GA	Diagnosis	Ultrasound #1	Ultrasound #2	Kidney imaged	US + 4DCT	US + 4DMR	US + US
1	4.5	1	No	Wilms tumour	Image quality poor	Useable	Left	Yes	No	No
2	4.1	1	No	Neuroblastoma	Image quality poor	Useable	Right	Yes	Yes	No
3	15.2	1	No	Neuroblastoma	Probe not tracked	Useable	Right	Yes**	Yes	No
4	15.6	1	No	Rhabdomyosarcoma	Useable	Useable	Right	Yes	Yes	Yes
5	12.3	2	No	Ganglioneuroblastoma	Out of plane motion	n/a	Left	No	Yes	No
6	9.9	2	No	Rhabdomyosarcoma	Probe not tracked	n/a	Right	No	Yes*	No
7	3.4	2	Yes	Neuroblastoma	Not acquired due to patient factors	n/a	Right	No	Yes	No
8	5	1	Yes	Wilms' tumour	Useable	Useable	Right	Yes	No	Yes
9	6.1	1	Yes	Wilms' tumour	Useable	Useable	Right	Yes	No	No
10	8.9	2	No	Ovarian teratoma	Useable	n/a	Right	No	Yes	No
11	11.5	2	No	Ovarian teratoma	Probe not tracked	n/a	Left	No	Yes*	No
12	1.4	1	Yes	Wilms tumour	Out of plane motion Bowel gas	Useable	Left	No	No	No
13	15.5	2	No	Neuroblastoma	Useable	n/a	Right	No	Yes	Yes
14	4.5	1	Yes	Neuroblastoma	Useable	Useable	Right	No***	Yes	Yes
15	4.5	1	Yes	Neuroblastoma	Useable	Useable	Left	Yes	Yes	Yes
16	1.5	1	Yes	Neuroblastoma	Out of plane motion	n/a	Left	Yes	No	No
17	3.1	1	Yes	Wilms' tumour	Not acquired	Useable	Left	Yes	No	No
18	7.1	1	No	Wilms' tumour	Probe motion	Out of plane motion	Left	Yes	No	No
19	2.4	1	No	Neuroblastoma	No data saved	No data saved	Right	No#	No	No

Table 4.1 - Patient characteristics. * 4DMR scan did not include entire kidney volume in field of view – not analysed. **4DCT did not visualise entire kidney volume. ***Clarity US machine in clinical use. # No detectable respiratory trace recorded at the time of CT – no 4DCT.

Chapter 5

A four-dimensional computed tomography generated internal target volume approach to paediatric high risk neuroblastoma to reduce organ at risk and normal tissue irradiation

5.1 Publications and Presentations

Results in this Chapter were presented in poster format at the International Society of Paediatric Oncology (SIOP) Paediatric Radiation Oncology Society (PROS) Meeting, Kyoto Japan November 2018.

Paper submitted to Radiotherapy and Oncology for consideration May 2020.

5.2 Background

NBL commonly arises in the suprarenal region and is in close proximity to the diaphragm. Chapter 2 demonstrated that the magnitude of upper abdominal respiratory-related organ motion (RROM) is influenced by proximity of organs and tumour bed to the diaphragm. The internal margin (IM) accounts for variation in position of the target due to physiological organ motion [1]. As described in Chapters 1 – 3 there is evidence that RROM is child-specific and that RROM is smaller in magnitude in younger children than in older children and adults. Therefore there is scope to rationalise the IM as a component of the PTV in paediatric RT planning. Individualised motion information from four dimensional CT (4DCT) can define an internal target volume (ITV), a volume that encompasses the full extent of target motion derived from 4DCT. This approach is commonly used in adult tumour sites susceptible to RROM such as the lung and upper abdomen.

The aim of this chapter is to describe an individualised ~~paediatric~~ child-specific ITV technique and evaluate the dosimetric consequences of applying such an approach to rotational IMRT planning, compared to conventional PTV margins, for children and young people with HR-NBL.

5.3 Aims of Chapter 5

My hypothesis is that incorporating a child-specific internal target volume is feasible and will offer improved normal tissue sparing compared to conventional PTV margins.

In order to test this hypothesis, I will;

1) Determine the volume difference of planning target volumes (PTV) generated with different approaches.
2) Determine the differences in organ at risk doses between approaches.

5.4 Materials and Methods

5.4.1 Patient selection

4DCT scans were acquired as part of the previously described APACHe study, a prospective study approved by the RMH research ethics committee, Appendix 1. We selected patients < 19 years of age and with upper abdominal NBL for the purpose of this planning study. Children receiving RT for abdominal neuroblastoma who had a 4DCT at RT simulation at University College London Hospital were included in the APAChe Study and the analysis contained in this Chapter.

5.4.2 Radiotherapy simulation

Patients were simulated supine using a head-rest and knee-fix and with their arms positioned above their heads. All patients had contrast-enhanced three-dimensional computed tomography (3DCT) followed by 4DCT. The helical 4DCT was acquired on a multi-detector, 16-slice CT scanner (Philips Healthcare, Cleveland, OH) using an integrated respiratory surrogate (Philips

respiratory bellows). Pitch was varied according to the patient's breathing rate allowing a complete breathing cycle to occur at each couch position. Images were retrospectively sorted into ten 3D volumes according to the breathing phase assigned by the surrogate. 4DCT acquisition is described in detail in Chapter 2.

5.4.3 Target volume delineation

4DCT datasets were imported into a treatment planning system; (RayStation, v6.99, RaySearch, Stockholm, Sweden). The post-chemotherapy, pre-operative tumour volume, including macroscopic disease if present, (virtual GTV), was defined with reference to diagnostic CT and according to the recent SIOPEN HR-NBL (EudraCT Number 2006-001489-17) and IMAT (International Standard Randomised Controlled Trial Number 10746820) study protocols [2] [3]. The average intensity projection phase of the 4DCT was selected for delineation and planning. This methodology was preferred over delineating the ITV volumes on the 4DCT phases and the standard PTV volumes on the 3D contrast-enhanced planning CT ~~This was done to avoid~~ as doing this was considered to introduc~~ing~~e potential bias in the position of the adjacent OARs as the contrast-enhanced CT is acquired at an arbitrary respiratory phase relative to the 4DCT. Differences in dosimetric outcomes could then have been a result of differences in OAR position relative to the PTV and confounded the results presented. I performed target volume and organ at risk (OAR) delineation in all cases.

5.4.4 ITV definition

The virtual GTV (and residual macroscopic disease if present) was defined on the average phase and copied to INH and EXH to create virtual GTV_INH and virtual GTV_EXH. These structures were then expanded by 5mm to create anatomically constrained CTV_INH and CTV_EXH. Liver and kidneys are commonly positioned adjacent to the virtual GTV. For the purpose of this work

they were considered to be surrogates for motion of the post-operative tumour bed. Liver, kidneys and vertebral bodies were contoured on three phases; the average, peak-inhalation (INH) and peak-exhalation (EXH) 4DCT phase (usually 0% and 50%). CTV_INH and CTV_EXH were edited at boundaries of uninvolved liver, kidney and vertebral bodies. The ITV was the combination of CTV_INH and CTV_EXH. Contours were visually inspected in cine mode to ensure that maximum excursions of the organ were included in the contour. An isotropic 5mm expansion of the ITV was used to create the planning target volume (PTV_itv).

5.4.5 Standard PTV definition

The standard PTV was also defined on the average phase of the 4DCT. A 5mm margin was added to the virtual GTV to create an anatomically constrained CTV (CTV_standard). A 10mm margin was added to CTV_standard to create a PTV (PTV_standard) as described in the recent SIOPEN HR-NBL 1 study (EudraCT Number 2006-001489-17) [3]. This 10mm CTV – PTV margin would be comprised of a 5 mm set-up margin and a further 5 mm internal margin to account for inter- and intra-fraction organ motion.

5.4.6 Treatment planning technique

All treatment plans were designed using RayStation. In addition to the PTV, vertebral bodies adjacent to the PTV were designated as a target structure and assigned a minimum objective of D95% ≥ 18Gy (95% of the volume covered by the 18Gy isodose). This dose constraint for the adjacent vertebral body organ at risk volume was chosen according to departmental practice in the

Royal Marsden Hospital. The vertebral bodies situated immediately superior and inferior to the PTV were given a dose constraint of V10Gy < 5% (where V10 is the volume receiving doses above 10 Gy). If this constraint was not physically achievable due to a short distance between superior and inferior vertebral

bodies and the adjacent vertebral body structure, the dose was as low as reasonably achievable. The clinical dose objectives for kidney differed according to the position of the PTV; lateralised versus midline. For midline targets, the clinical objective was for less than 40% of the bilateral (combined) kidney volume to receive a dose of 14 Gy (V14 Gy, the relative volume receiving 14 Gy, < 40%). For lateralised targets, the clinical objective was for less than 10% of the contralateral kidney to receive a dose of 14 Gy (V14Gy < 10%). For both geometries, the respective V14 Gy kidney objective was considered a mandatory constraint and prioritised over PTV coverage, if necessary. Clinical dose objectives from the IMAT study (International Standard Randomised Controlled Trial Number 10746820 [2] were used with the exception of the dose objective for adjacent vertebral body, (Table 5.2). The dose objective used for vertebral body coverage was in line with recently published The European Society for Paediatric Oncology (SIOPE) recommendations for the management of vertebral body dose [4].

Two dual arc volumetric modulated arc therapy (VMAT) plans were created for each patient; ITV plan and standard plan, (Figure 5.6). Plans were optimised using bespoke dose constraints for each patient to generate optimal plans and to satisfy the clinical dose objectives. The full list of clinical dose objectives used is outlined in Table 2. The dose, 21Gy, was prescribed to the PTV median dose. RT plans were produced for a 6MV Elekta Synergy linear accelerator (Elekta AB, Stockholm, Sweden) with Agility multi-leaf collimator [5]. Dose distributions were calculated using a collapsed cone algorithm on a 0.25 x 0.25 x 0.25 cm dose grid.

5.4.7 Plan evaluation

D98%, D95%, D5% and D2% were used for comparative dosimetric analysis of PTV coverage where Dn% is the minimal dose to n% of that structure. Mean dose and V14 Gy to combined or contralateral kidney according to tumour location were also compared. Additional dose statistics for liver, lung, heart and non-PTV integral dose (NPID) are reported. NPID was calculated as mean dose (Gy) x [external – PTV] (cc).

5.4.8 Statistical analysis

Bland-Altman plots were created to visualise the differences in dose to OAR between the two approaches. For both plans, the means over the patient group for each parameter were calculated. Differences and relative differences between the two approaches were determined and tested using a Wilcoxon matched–pairs signed rank test with a significance level of $p<0.05$. Statistical analysis was performed using GraphPad prism (version 7.00 for Windows, GraphPad Software, La Jolla California USA, www.graphpad.com).

5.5 Results

5.5.1 Patients

14 patients, median age 4.1 years (range: 1.5 – 18.9 years), were included in this study. Nine patients required general anaesthetic (GA). Five patients had lateralised target volumes, 9 had midline target volumes. Three patients had macroscopic tumour visible on the planning CT; two did not undergo surgical

resection prior to high dose chemotherapy with stem cell rescue (patient 6, 11). One patient had a complete response to induction chemotherapy and did not proceed to surgical resection (patient 1). Patient characteristics are summarised in Table 5.1.

5.5.2 Plan comparison

PTV volumes generated using an ITV approach were statistically significantly smaller; median 215.3 cc (range 58.2 – 1030.2cc) compared to 350.0 cc (range 107.3 – 1339.5cc), P = 0.0001.

There was a statistically significant difference in mean D98 between ITV (mean 20.4 Gy) and standard plans (19.9 Gy), p = 0.02. For patient 6 and 14 the achieved D98 coverage was less than the desired objective of ≥ 18.9 Gy (90% prescribed dose) in the standard plan. Acceptable D95 coverage was achieved in patient 14. However, in patient 6 it was necessary to compromise even the D95 objective, in addition to D98. For both plans PTV coverage was compromised to meet mandatory dose objectives for kidney.

All 14 ITV plans met all dose objectives and were clinically acceptable. There was no difference in mean near maximum dose (D5, D2) between the two approaches. PTV D98 and D95 for all patients and according to location of target, GA and resection status are shown in Figure 5.2.

Differences in OAR dose parameters are shown in Bland Altman plots in Figures 5.3 and 5.4. Differences in dose statistics are outlined in Table 5.3. The ITV approach resulted, in general, in lower OAR doses. There was a marginal increase (0.2 Gy) in contralateral kidney mean dose in patients with lateralised targets planned with an ITV approach, Table 5.2. This difference

was not statistically significant. There were statistically significant reductions in mean heart dose of 1.0 Gy and in mean lung dose of 1.1 Gy ($p < 0.001$, $p = 0.001$). Generation of an ITV resulted in fewer vertebral bodies being irradiated to ≥18Gy in 6/13 patients. Median non- PTV integral dose (NPID) was statistically significantly lower for ITV plans; 27.8 (~~Gy~~ Gy*L) compared to 30.4 ($p < 0.001$).

5.6 Discussion

5.6.1 Comparison of target volumes

The dosimetric advantages and potential benefit of using an ITV approach in HR-NBL RT planning were investigated in this Chapter. I demonstrated that image-guided IMRT can be refined through the integration of individualised motion assessment using 4DCT and an ITV approach. This strategy resulted in greater than 30% reduction in absolute PTV volumes compared to the use of a standard margin (as recommended in the RT guidance for the recent SIOPEN HRNBL international study).

It could be argued that the reported difference in PTV volumes is due to the different CTV to PTV expansions used between the two approaches (5mm for the ITV approach and 10 mm for the standard PTV approach). As estimates of organ motion for paediatric RT planning have been extrapolated pragmatically from adult data, paediatric trials have historically applied isotropic expansions of the reconstructed virtual GTV of up to 1 cm to create a clinical target volume CTV, also including the adjacent vertebrae. In the UK, the IMAT-neuroblastoma study (ISRCTN10746820), a contemporary phase two trial, is

currently investigating the role of rotational IMRT, and escalation of RT dose from 21Gy to 36Gy [2]. In the IMAT- neuroblastoma trial, the CTV is extended into adjacent organs at risk by 5 mm even if uninvolved by tumour [2]. Both of these practices account for an IM of 5 – 10 mm at CTV and uninvolved organ interfaces and is comparable to the PTV margin of 10mm used for standard plans in this study.

In my work, PTV coverage was achieved for most patients using VMAT regardless of the CTV to PTV margin used, (Figure 5.1 and 5.2). Two standard plans did not achieve objectives for target coverage. Patient 6 was 1.9 years of age, treated under GA with a midline target volume. The patient's target volumes were close to the median values for the group despite the patient not undergoing surgical resection of the primary prior to RT; standard PTV 392.6 cc and PTV_ITV 257.5 cc. Patient 14 was 1.5 years of age and treated under GA. This patient had a gross total resection prior to RT and a lateralised target volume with a standard PTV volume of 220.3 cc and a PTV_ITV 130.8 cc. These findings suggest that VMAT/ IMRT alone is not sufficient to improve target coverage in all patients. Reassessment of the components of the CTV to PTV margin, such as the IM as demonstrated in this Chapter, is necessary for optimal use of highly conformal RT techniques in anatomical sites susceptible to RROM.

5.6.2 Comparison of normal tissue dosimetry

A large CTV to PTV margin limits the potential for dose escalation and increases the volume of normal tissue irradiated to moderate and high dose. Children treated with RT are at risk of late effects and second malignancies [6,

7]. High dose regions surrounding normal tissues have been implicated in the

development of RT-related toxicities [8]. Results in Chapter 2 – 4 and other published reports on RROM demonstrate that motion is smaller in children compared to adults; the greatest motion observed in the superior/inferior directions and minimal, <2mm, right/ left and anterior/ posteriorly [9-11]. Anisotropic internal margins generated by individualised motion assessment likely produced the additional dosimetric gains in this work by reducing the volume of irradiated kidney, particularly for midline targets. This is demonstrated by the statistically significant difference in combined kidney dose statistics between ITV and standard plans.

Children demonstrating minimal RROM on 4DCT still had a relative reduction in CTV to PTV expansions superiorly thereby reducing the volume of heart irradiated. We demonstrate a statistically significant reduction in mean heart dose of 1 Gy with an ITV approach. Individual patients showed reductions of up to 2.5 Gy mean heart dose, (Figure 5.2a). Heart dose is increasingly reported as an adverse risk in adult breast and lung RT [12, 13]. It has been shown that the risk of major coronary events increased in women receiving radiation for breast cancer by 7.4% per Gy mean heart dose [12]. Individualised ITV generation and reduced PTV volume in the cranial-caudal direction resulted in fewer vertebral bodies being irradiated to ≥18Gy in 6/13 patients. This has the potential to reduce musculoskeletal late effects such as reduced sitting height [14].

One prior retrospective study described the use of an ITV approach in eight patients aged 20 months – 5 years with HR-NBL [15]. All patients were treated under GA. The authors applied an ITV margin of 1mm radially and inferiorly and 4mm superiorly in all patients instead of generating individual ITVs for

each patient as I did in this work. This class solution was derived from an estimation of renal motion using 4DCT in 10 patients under the age of 9 and under GA [9]. Studies have demonstrated significant inter-patient variation in RROM in children and such studies have failed to consistently demonstrate associations between RROM and patient-related variables such as the use of GA [9, 10, 16-18]. This approach could underestimate organ motion, particularly in older children or younger children not under GA as included in this chapter. The authors used a 2mm PTV margin. Such a margin is arguably at the technical limits of treatment delivery and not reflective of PTV margins used in routine practice in North America or in Europe [19-21]. Furthermore, reported normal tissue doses were limited to kidneys and liver.

Modelling studies have suggested that the increased integral dose associated with IMRT techniques may increase the risk of secondary malignancy by almost a factor of 2 [22]. The bath of low dose radiation leading to an increase in integral dose characteristic of multiple beam/ arc delivery was postulated to contribute to the increased risk of secondary malignancy. However, it is increasingly acknowledged that many RT-induced second malignancies arise in regions of high dose outside of the target, thereby challenging these original estimates [23, 24]. Results presented in this Chapter show that reductions in absolute PTV volumes will reduce integral doses as demonstrated by a statistically significantly smaller NPID for ITV plans compared to standard PTV plans, 27.8 versus 30.4 ($p \leq 0.001$).

5.6.3 The ITV approach

An ITV approach takes respiratory motion into account by a linear addition of the amplitude to the CTV. If this amplitude is not representative of the amplitude during treatment this results in a suboptimal volume or, if correct, could be overly conservative. Alternatively, the mid-ventilation (MidV) concept extracts a time-averaged target position and its standard deviation from a 4DCT and motion is then considered a random positioning error in a probabilistic safety margin calculation [35]. Using a MidV with daily on-line imaging in adult lung RT has demonstrably achieved similar local control and a 30% reduction in PTV volume compared to ITV-generated PTV [36] [37]. MidV has been described in planning studies for pancreatic cancer but requires daily soft tissue verification of target position prior to treatment [25]. Daily soft tissue verification imaging is not routine in paediatric RT practice given the additional dose delivered to the child. Placement of fiducials in the operative bed is also not routine. This limits the ability to perform soft-tissue matching in these patients who often have no macroscopic tumour present at the time of RT. Chapter 2 demonstrated that the differences in the magnitude of RROM between children and adults is greatest in very young children. NBL typically arises in children under the age of 5 years. A MidV approach was therefore unlikely to result in volumetric reductions of the same magnitude as seen in adult studies where patients display greater magnitude of RROM. In my results, I demonstrated that the relative difference between median CTV and ITV volumes was only 1.2%. Taking the ITV as a surrogate for limited organ displacements in this cohort of patients, as represented on 4DCT, supports the decision to adopt an ITV approach.

5.6.4 Limitations

Under and over-representation of RROM motion from a single pre-treatment 4DCT has been described in the adult upper abdomen [26, 27]. This limitation with a single measurement of motion prior to RT delivery is addressed in adults by using daily online soft tissue verification of target position prior to treatment. Huijsken's et al determined that respiratory-related diaphragm motion on 4DCT did not accurately predict diaphragm motion determined on subsequent cone beam CT in 9 out of 12 children analysed [28]. However, it has not yet been determined whether the diaphragm can be considered a reliable surrogate for upper abdominal organ motion in this age group and so this finding cannot be extrapolated to other organs in the upper abdomen [9, 29]. Furthermore, the cohort of children studied were older (mean age 14.5, range 8.6 – 17.9 years) than those included in my work median age 4.1 years (range: 1.5 – 18.9 years). Young children under GA have been shown to have less intrafraction variation in diaphragm motion compared to adults; suggesting that in a cohort of anaesthetised children measurement of motion on 4DCT may be more representative of daily motion than it is in older children or adults [29].

Paediatric abdominal RT is often delivered following chemotherapy and/ or surgery. Accurate target definition is compounded by the challenge of reconstructing a pre-operative tumour volume while respecting often significant post-operative changes in anatomy [19]. Significant inter-observer delineation variation has been demonstrated in RT planning for Wilms tumour, another common upper abdominal paediatric malignancy [30]. I performed the delineation in all cases to minimise inter-observer variation for the purpose of this work. In contemporary clinical practice, peer review of target volume

delineation is recommended [31], and QUARTET, a platform for prospective radiotherapy quality assurance in paediatric clinical trials, is being implemented in Europe [32].

5.7 Conclusion

In this chapter I demonstrated the feasibility of individualised motion assessment to generate clinically acceptable RT plans. It is not possible to determine a priori which children will demonstrate clinically significant RROM. 4DCT and an ITV approach will therefore rationalise the IM in patients with less motion but equally capture those in whom the IM could be underestimated by population-based margins. Whether the normal tissue sparing achieved using an ITV-based approach translates into reduced late toxicity for patients will require testing in prospective clinical studies. The findings presented in this Chapter are applicable to other paediatric tumours in the upper abdomen requiring RT where intrafraction RROM is present.

5.8 References

1) Landberg T, Chavaudra J, Dobbs J, Gerard JP, Hanks G, Horiot JC, et al. Report 62. Journal of the International Commission on Radiation Units and Measurements 1999; os32(1): NP-NP.
2) CRCTU B. IMAT Neuroblastoma [Available from: https://www.birmingham.ac.uk/research/activity/mds/trials/crctu/trials/IMAT-Neuroblastoma/index.aspx.
3) Ladenstein R, Valteau-Couanet D, Brock P, Yaniv I, Castel V, Laureys G, et al. Randomized Trial of prophylactic granulocyte colony-stimulating factor during rapid COJEC induction in pediatric patients with high-risk neuroblastoma: the European HR-NBL1/SIOPEN study. J Clin Oncol 2010; 28(21): 3516-3524.
4) Hoeben BA, Carrie C, Timmermann B, Mandeville HC, Gandola L, Dieckmann K, et al. Management of vertebral radiotherapy dose in paediatric patients with cancer: consensus recommendations from the SIOPE radiotherapy working group. Lancet Oncol 2019; 20(3): e155-e166.
5) Bedford JL, Thomas MD, Smyth G. Beam modeling and VMAT performance with the Agility 160-leaf multileaf collimator. Journal of applied clinical medical physics 2013; 14(2): 4136.
6) Perwein T, Lackner H, Sovinz P, Benesch M, Schmidt S, Schwinger W, et al. Survival and late effects in children with stage 4 neuroblastoma. Pediatr Blood Cancer 2011; 57(4): 629-635.
7) Cohen LE, Gordon JH, Popovsky EY, Gunawardene S, Duffey-Lind E, Lehmann LE, et al. Late effects in children treated with intensive multimodal therapy for high-risk neuroblastoma: high incidence of endocrine and growth problems. Bone Marrow Transplant 2014; 49(4): 502-508.
8) Paulino AC. The promise of intensity modulated radiation therapy. Pediatr Blood Cancer 2016; 63(9): 1513-1514.
9) Pai Panandiker AS, Sharma S, Naik MH, Wu S, Hua C, Beltran C, et al. Novel Assessment of Renal Motion in Children as Measured via Four-Dimensional Computed Tomography. International Journal of Radiation Oncology*Biology*Physics 2012; 82(5): 1771-1776.
10) Huijskens SC, van Dijk IWEM, de Jong R, Visser J, Fajardo RD, Ronckers CM, et al. Quantification of renal and diaphragmatic interfractional motion in pediatric image-guided radiation therapy: A multicenter study. Radiotherapy and Oncology 2015; 117(3): 425-31.
11) van Dijk I, Huijskens SC, de Jong R, Visser J, Fajardo RD, Rasch CRN, et al. Interfractional renal and diaphragmatic position variation during radiotherapy in children and adults: is there a difference? Acta oncologica (Stockholm, Sweden) 2017; 56(8): 1065-1071.
12) Darby SC, Ewertz M, McGale P, Bennet AM, Blom-Goldman U, Bronnum D, et al. Risk of ischemic heart disease in women after radiotherapy for breast cancer. N Engl J Med 2013; 368(11): 987-998.

13) Bradley JD, Paulus R, Komaki R, Masters G, Blumenschein G, Schild S, et al. Standard-dose versus high-dose conformal radiotherapy with concurrent and consolidation carboplatin plus paclitaxel with or without cetuximab for patients with stage IIIA or IIIB non-small-cell lung cancer (RTOG 0617): a randomised, two-by-two factorial phase 3 study. The Lancet Oncology 2015; 16(2): 187-199.
14) Bolling T, Willich N, Ernst I. Late effects of abdominal irradiation in children: a review of the literature. Anticancer Res 2010; 30(1):227-231.
15) Pai Panandiker AS, Beltran C, Gray J, Hua C. Methods for image guided and intensity modulated radiation therapy in high-risk abdominal neuroblastoma. Pract Radiat Oncol 2013; 3(2): 107-114.
16) Uh J, Krasin MJ, Li Y, Li X, Tinkle C, Lucas JT, Jr., et al. Quantification of Pediatric Abdominal Organ Motion With a 4-Dimensional Magnetic Resonance Imaging Method. Int J Radiat Oncol Biol Phys 2017; 99(1): 227-237.
17) Kannan S, Teo BK, Solberg T, Hill-Kayser C. Organ motion in pediatric high-risk neuroblastoma patients using four-dimensional computed tomography. Journal of applied clinical medical physics 2017; 18(1): 107-114.
18) Huijskens SC, van Dijk I, Visser J, Balgobind BV, Te Lindert D, Rasch CRN, et al. Abdominal organ position variation in children during image-guided radiotherapy. Radiation oncology (London, England) 2018; 13(1): 173.
19) Alcorn SR, Chen MJ, Claude L, Dieckmann K, Ermoian RP, Ford EC, et al. Practice patterns of photon and proton pediatric image guided radiation treatment: results from an International Pediatric Research consortium. Pract Radiat Oncol 2014; 4(5): 336-341.
20) Nazmy M, O'Shea E, McCrickard E, O'Sullivan C. OC-0079: CTV-to-PTV margin for treatment setup errors: paediatric vs adult. Radiotherapy and Oncology 2015; 115: S40.
21) ElBeltagi MN, Wall V, Marignol L. Planning target volume (PTV) margin practice patterns in adults and paediatrics among the Paediatric Radiation Oncology Society (PROS) members: an international survey. Journal of Radiotherapy in Practice 2018; 17(4): 368-372.
22) Hall EJ, Wuu C-S. Radiation-induced second cancers: the impact of 3D-CRT and IMRT. International Journal of Radiation Oncology*Biology*Physics 2003; 56(1): 83-88.
23) Olch AJ. Pediatric Radiotherapy Planning and Treatment. London, UNITED STATES: CRC Press; 2013.
24) Olch AJ, Hua C-H. Basic Principles and Advances in Technology Used for Pediatric Radiotherapy. In: Merchant TE, Kortmann R-D, editors. Pediatric Radiation Oncology. Cham: Springer International Publishing; 2018. p. 343-362.
25) Lens E, van der Horst A, Versteijne E, van Tienhoven G, Bel A. Dosimetric Advantages of Midventilation Compared With Internal Target Volume for Radiation Therapy of Pancreatic Cancer. Int J Radiat Oncol Biol Phys 2015; 92(3): 675-682.

26) Minn AY, Schellenberg D, Maxim P, Suh Y, McKenna S, Cox B, et al. Pancreatic tumor motion on a single planning 4D-CT does not correlate with intrafraction tumor motion during treatment. Am J Clin Oncol 2009; 32(4): 364-368.
27) Lens E, van der Horst A, Kroon PS, van Hooft JE, Davila Fajardo R, Fockens P, et al. Differences in respiratory-induced pancreatic tumor motion between 4D treatment planning CT and daily cone beam CT, measured using intratumoral fiducials. Acta oncologica (Stockholm, Sweden) 2014; 53(9): 1257-1264.
28) Huijskens SC, van Dijk I, Visser J, Balgobind BV, Rasch CRN, Alderliesten T, et al. Predictive value of pediatric respiratory-induced diaphragm motion quantified using pre-treatment 4DCT and CBCTs. Radiation oncology (London, England) 2018; 13(1): 198.
29) Huijskens SC, van Dijk IW, Visser J, Rasch CR, Alderliesten T, Bel A. Magnitude and variability of respiratory-induced diaphragm motion in children during image-guided radiotherapy. Radiotherapy and oncology : Journal of the European Society for Therapeutic Radiology and Oncology 2017; 123(2): 263-269.
30) Padovani L, Huchet A, Claude L, Bernier V, Quetin P, Mahe M, et al. Inter-clinician variability in making dosimetric decisions in pediatric treatment: A balance between efficacy and late effects. Radiotherapy and Oncology 2009; 93(2): 372-376.
31) (London) RCoR. Radiotherapy target volume definition and peer review – RCR guidance. In: RCR, editor.
32) SIOP. [Available from: https://www.siope.eu/2016/05/25/quartet-project/.

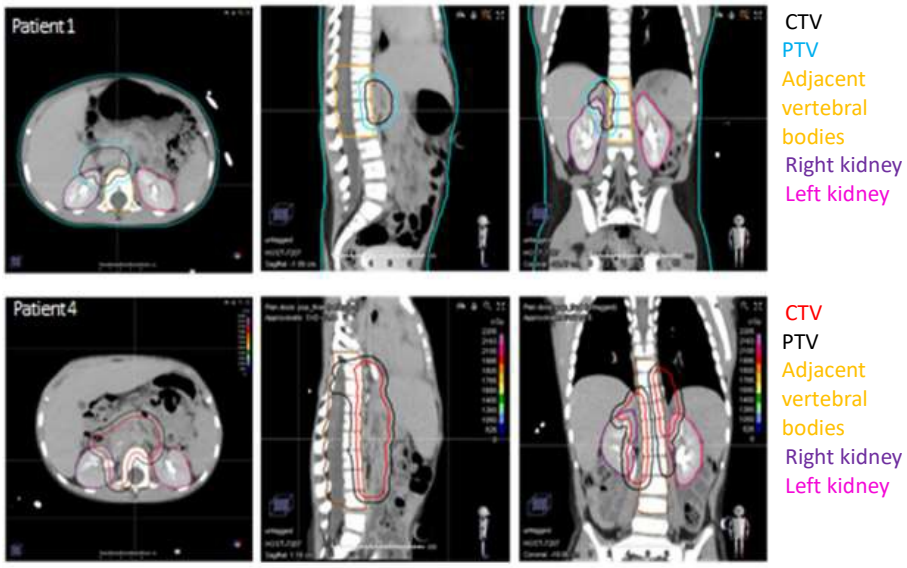

Figure 5.1 – Target volumes for two example patients demonstrating the Significant variation in target volume and position between cases.

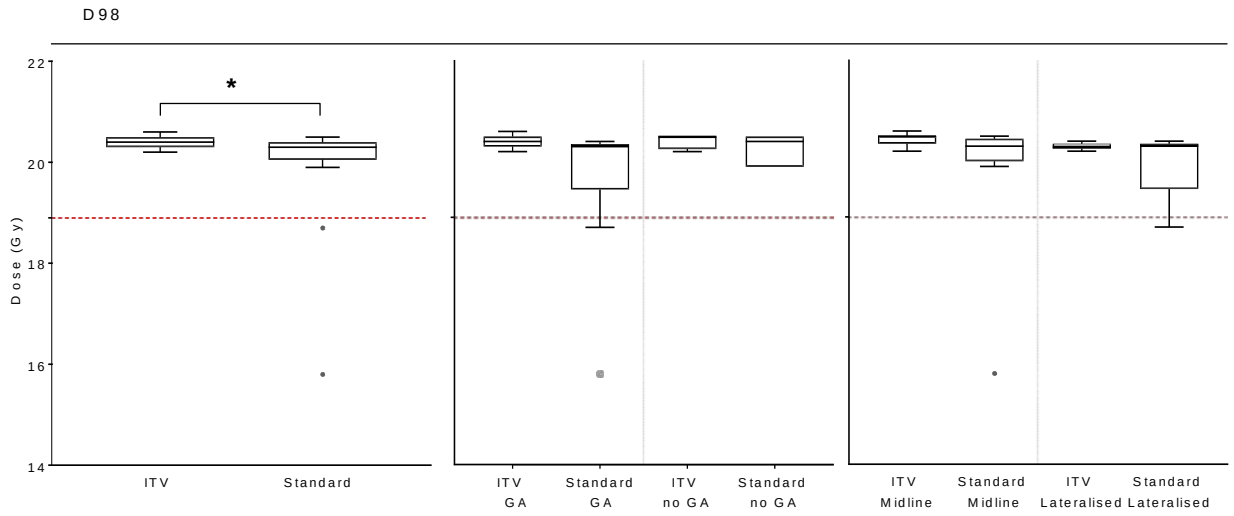

Figure 5.2 - Boxplot indicating the D98 for ITV and standard plans, all patient (left), according to GA (middle) and according to position of target volume (right). Horizontal bars, boxes and whiskers represent median, interquartile range and range, circles denote outliers. Dashed red line indicates the dose objective for D98 (18.9 Gy). *Significant differences ($p<0.05$). GA = general anaesthetic.

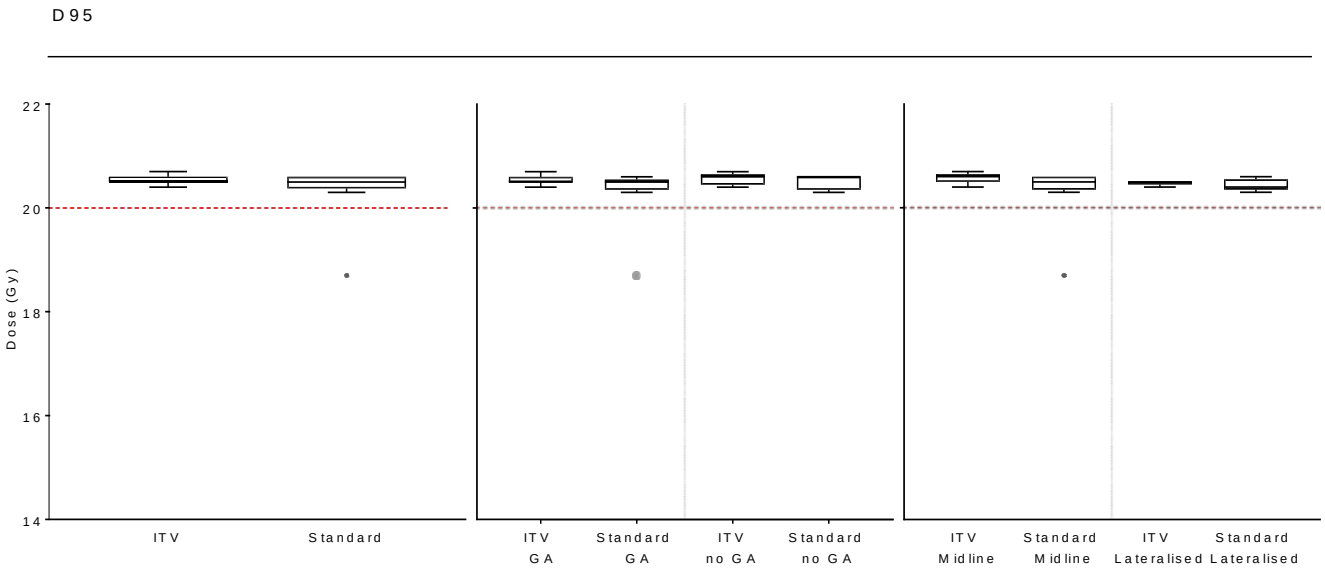

Figure 5.3 - Boxplot indicating the D95 for ITV and standard plans, all patient (left), according to GA (middle) and according to position of target volume (right). Horizontal bars, boxes and whiskers represent median, interquartile range and range, circles denote outliers Dashed red line indicates the dose objective for D95 (20.0 Gy).

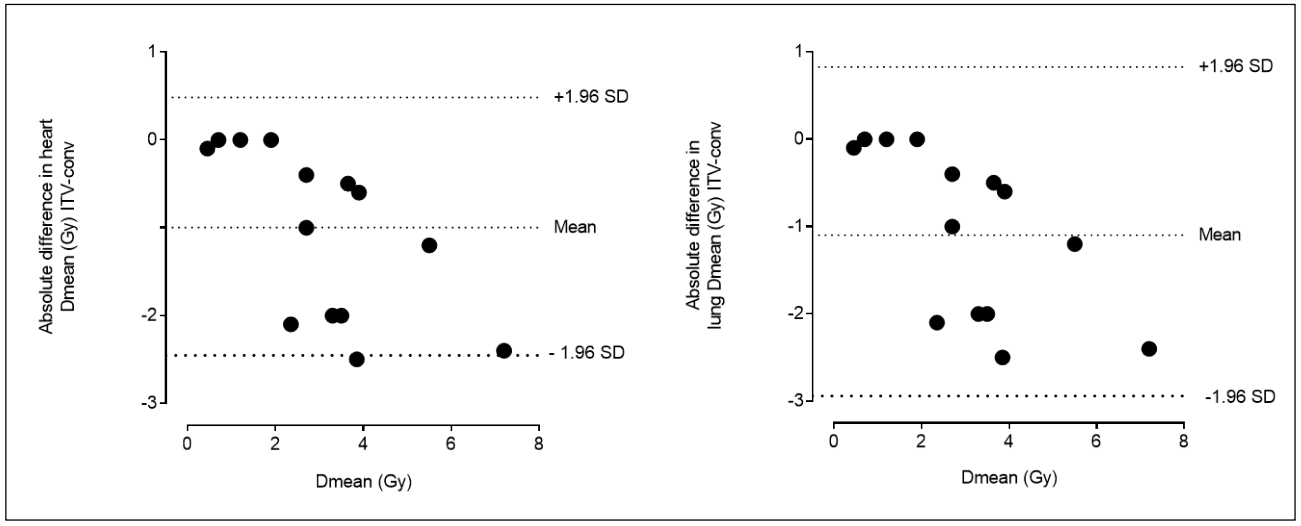

Figure 5.4 - Bland-Aitman plots for heart and lung (Dmean), showing the difference (i.e. lTV- PTV_ standard) for all patients.

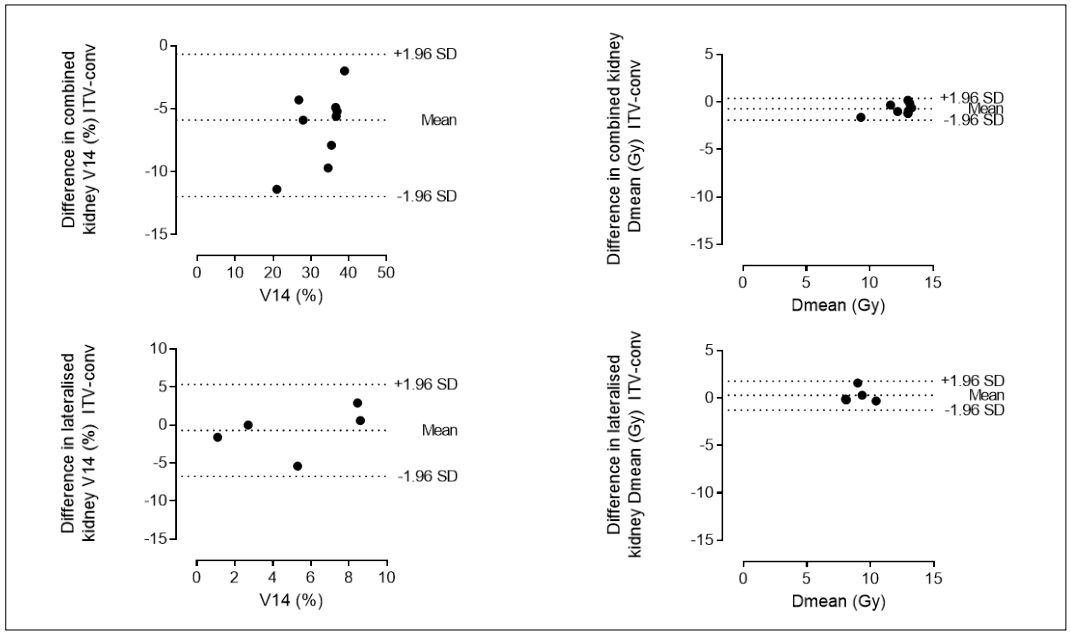

Figure 5.5 - Bland-Aitman plots for combined kidney (top left and right) and contralateral kidney (bottom left and right) showing for each dosimetric parameter the difference (i.e. ITV- PTV_standard) for patients with midline targets (top) and patients with lateralised targets (bottom).

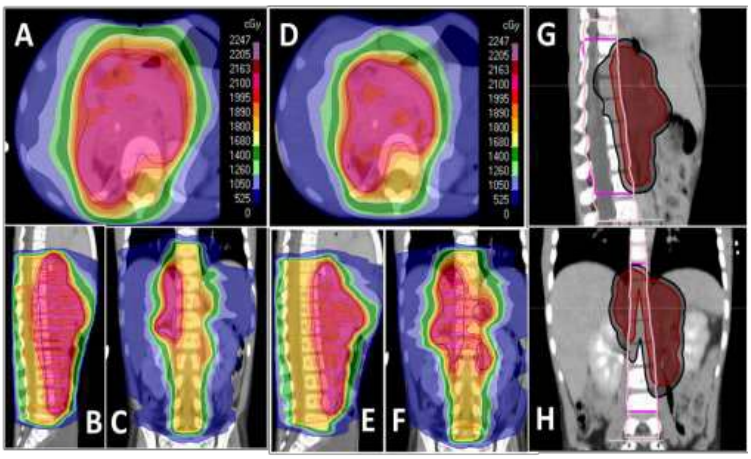

Figure 5.6 – Representative patient plan dosimetry ITV (A, B, C) and Standard (D, E, F). Representative patient volume delineation (G, H), black: PTV_standard; red: PTV_ITV; light pink: vertebral bodies adjacent to PTV_standard to be irradiated to prescription dose; dark pink: vertebral bodies adjacent to PTV_itv to be irradiated to prescription dose.

Patient	Sex	Age	GA	Target position	Status of primary tumour at time of RT	standard PTV volume (cc)	ITV_PTV volume (cc)
1	M	4.5	no	midline	No surgery (CR to pre-operative chemotherapy)	107.3	58.2
2	M	4.1	no	midline	GTR	339.9	215.9
3	M	17.5	no	midline	STR	573.3	391.0
4	M	4.1	yes	midline	GTR	373.1	225.4
5	F	1.7	yes	midline	GTR	311.3	202.2
6	F	1.9	yes	midline	No surgery (surgical risk factors)	392.6	257.5
7	F	3.9	yes	midline	GTR	230.9	136.0
8	F	2.7	yes	lateralised	GTR	405.3	254.1
9	M	2.9	yes	lateralised	GTR	300.6	176.0
10	F	4.5	yes	lateralised	GTR	257.9	163.9
11	M	4.5	yes	midline	No surgery (surgical risk factors)	708.5	483.0
12	M	5.4	no	midline	GTR	360.0	214.7
13	F	18.9	no	lateralised	GTR	1339.5	1030.2
14	F	1.5	yes	lateralised	GTR	220.3	130.8

Table 5.1 - Patient characteristics.

Structure	Index	Dose/ volume required (%)	Dose required (Gy)
PTV	D98 %	≥90 %	≥18.9
PTV	D95 %	≥95 %	≥20
PTV	D50 %	= 100 %	21
PTV	D5 %	≤105 %	≤22.1
PTV	D2 %	≤107 %	≤22.5
Combined kidneys (midline target)	V14 Gy	≤40 %	
Contralateral kidney (lateral target)	V14 Gy	≤10%	
Vertebrae in field	V18 Gy	≥95%	

Table 5.2 - Clinical dose objectives.

Structure	Dose statistic	PTV standard	PTV itv	Difference ITV - standard	Relative difference (%)	P value
CTV/ITV volume, cc	-	109.1	111.7	2.7	1.2	ns
PTV volume, cc	-	350.0	215.3	-134.7	-38.5	≤0.001
PTV	D98 (Gy)	19.9	20.4	0.5	2.5	0.02
	D95 (Gy)	20.4	20.5	0.1	0.5	0.05
	D5 (Gy)	21.4	21.4	0	0	ns
	D2 (Gy)	21.6	21.6	0	0	ns
Combined kidneys (midline target)	mean (Gy)	12.8	12	-0.8	-6.3	0.01
	V14 (%)	35.7	29.8	-5.9	-16.5	0.04
Contralateral kidney (lateral target)	mean (Gy)	8.9	9.1	0.2	2.2	ns
	V14 (%)	5.5	4.9	-0.6	-10.9	ns
NPID	Mean (Gy L)	30.4	27.8	-2.6	-9.2	≤0.001
Heart	Mean (Gy)	3.0	2.0	-1.0	-32.9	≤0.001
Lung	Mean (Gy)	3.6	2.5	-1.1	-29.4	≤0.001
	V15 (%)	4.3	2.4	-1.9	-45.0	≤0.001
	V12 (%)	6.8	3.8	-2.9	-43.4	0.02
Liver	V21 (%)	3.4	1.4	-2.0	-60.0	≤0.001
	V19 (%)	8.7	4.9	-3.8	-43.9	≤0.001

Table 5.3 - Comparison of dose statistics for PTV_standard and PTV_ITV plans; median target volumes (cc) and mean OAR dosimetric parameters. CTV: clinical target volume; ITV: internal target volume; PTV: planning target volume; NPID: non PTV integral dose.

Chapter 6

Concluding discussion

6.1 Adopting advanced photon techniques in paediatric radiotherapy

In the era of modern oncology, more than 80% of children with a diagnosis of cancer will be long-term survivors [1]. Survival comes with the very real risk of developing significant treatment-related morbidity. For children in whom RT ~~cannot be avoided~~is needed, reducing the volume of normal tissue receiving moderate to high doses has the potential to translate into less late RT-related morbidity for these young patients.

Technological advances in the field of radiation oncology are enabling us to deliver increasingly accurate and precise treatments and reduce the volume of normal tissue irradiated to moderate / high dose. Using highly conformal photon techniques necessitates an understanding of geometric uncertainties in treatment planning and delivery in order to maintain treatment efficacy while optimising normal tissue effects. Quantifying intra-fraction organ motion specifically in children, as examined in this thesis, forms an important part of this process.

6.2 Optimising paediatric RT

6.2.1 Individualised motion assessment

4DCT is the current gold standard in adult RT treatment planning for assessment of RROM. The unique aspects of paediatric RT relative to adult RT, as outlined in Chapter 1, mean that it is necessary to investigate the feasibility of introducing techniques commonplace in adult RT. This was

addressed in Chapter 2, where it was demonstrated that acquiring 4DCT in children using equipment designed for adults is feasible, even in the very young. 4DCT was successfully acquired in 82% of children referred.

Chapter 2 described a paediatric-specific 4DCT imaging protocol that was optimised, compared to standard adult 4DCT imaging protocols, balancing the lowest possible imaging dose with reduced image quality [2]. Reduced image quality is a practical solution when treatment fields are defined by bone anatomy alone, as was the case in the era of two-dimensional and early 3D-conformal RT paediatric RT. As discussed in Chapter 2, liver contouring was challenging, and ultimately abandoned, due to the lack of soft tissue contrast for accurate organ edge detection. It is arguably counter-intuitive to accept reduced image quality if the purpose of volumetric, contrast-enhanced imaging with individualised motion assessment is to improve accuracy and precision in paediatric RT delivery. Further efforts should be made when implementing 4DCT in children to achieve adequate soft tissue contrast without unacceptably high dose to allow accurate target delineation.

Chapter 2 also outlined the limitations of acquiring 4DCT in very young and small children. A respiratory trace was not captured by the Philip's respiratory bellows system in 3 children referred for 4DCT. Median age 2.4 years (range 1.9 – 2.9 years); all 3 children were under GA.

The respiratory surrogate used for 4DMR retrospective reconstruction is derived from the child's internal anatomy. As described in Chapter 3, all children referred for 4DMR had 4D image sets successfully reconstructed; in contrast to 4DCT.

In Chapter 3, section 3.4.2, I determined that 4DMR- derived median SI right and left kidney displacements were 2.8 mm and 3.2 mm. These results compared favourably with the median SI displacements of 2.4 mm and 3.6 mm as measured by 4DCT and were previously presented in Chapter 2, section 1.4.2. These results suggest that 4DMR performs at least as well as 4DCT for individualised motion assessment in children without the inherent disadvantage of radiation dose exposure and without the limitations of using a respiratory surrogate designed for adults.

Delineation of liver, in addition to the kidneys, was also possible on 4DMR due to the better soft tissue contrast compared to 4DCT. The improved organ edge detection is important in paediatric RT when RT is often delivered post-operatively and the edges of adjacent OARs represent the clinical target volume boundary. The 4DMR sequence described in Chapter 3 has superior resolution (1.7 mm) compared to the 2.5 mm slice thickness 4DCT. This enhanced spatial resolution has the potential to improve accuracy in target delineation and motion assessment compared to 4DCT.

6.2.2 Organ motion observations in children

Organ motion studies (3-10) in children are summarised, and compared to my results from Chapter 2, in Tables 2.1 (intra-fraction motion) and 2.2 (inter-fraction motion). In summary, abdominal organ motion is consistently greatest in the SI direction, with displacements of no more than 2.0 mm in the RL and AP directions.

Attempts, including mine as described in Chapter 2, section 2.4.2, to correlate organ motion with patient variables have been made in the pursuit of a variable

predictive of ‘significant’ organ motion in paediatric patients. Such a variable would negate the need for pre-treatment 4DCT in all children with abdominal or thoracic tumours thereby minimising additional radiation exposure for the child. Unfortunately no significant correlations between organ motion and patient-related variables (age, height, weight, BMI, BSA) have been established. Others have suggested that pooling larger datasets could increase the statistical power to detect meaningful associations and inform population-based planning margins [5]. I would suggest that as the evidence presented and summarised in this thesis indicates that RROM is child-specific that and an individualised approach to assessment and motion management, similar to our approach in adult tumour sites susceptible to RROM, is warranted when highly conformal RT techniques are used. In the setting of improved geometrical certainty in treatment delivery with more favourable dose distributions compared to conventional POP techniques, the additional dose delivered with 4DCT and image-guidance is justified.

Although patient-related variables have not correlated with RROM, some technical factors appear to influence motion. Median intrafraction organ displacements are < 2 mm in young children under GA. Whilst this might suggest that 4DCT may not be required in this group of children, I demonstrated maximum displacements in children under GA of up to 4 mm. Without acquisition of 4DCT for all children the magnitude of intrafraction RROM will be underestimated in this cohort and may impact on the accuracy of radiotherapy delivery.

The pair-wise differences in kidney motion between the two US measurements, presented in Chapter 4 section 4.4.5, were <2 mm in the 4

children under GA compared to 3.7 mm a 15 year old not under GA. These results suggest that children under GA have less variation in intrafraction RROM and this was also demonstrated by Huijskens et al [11]. These findings suggest that 4DCT, or 4DMR, assessment of RROM in children under GA has the potential to be more predictive of RROM throughout the course of RT. This is in contrast to the known limitation of the reproducibility RROM measured on a single 4DCT in adults.

6.2.3 Verification of moving targets

As outlined in Chapter 2, section 2.5.3, an initial aim of the APAChe study was to determine interfraction organ motion using CBCT datasets. At the Royal Marsden NHS Foundation Trust the paediatric CBCT protocol used has nominal computed tomography dose index (CTDI) dose as measured in a phantom of 5mGy. This CBCT protocol has been adapted to facilitate bone match for registration of the planning CT and the soft tissue resolution of CBCT is further reduced compared to adult pre-sets. As discussed in Chapter 2, it was not possible to delineate the kidneys on CBCTs acquired using this pre-set. Similarly, Guerreiro et al. described a CBCT pre-set which was optimised to deliver four times less imaging dose compared to a standard adult CBCT pre-set. The authors also commented on the reduced visibility of organ boundaries as a result of the poor soft-tissue contrast on CBCT [10].

The Clarity US system imaging has the potential to augment CBCT in soft tissue matching for in-room IGRT, and without any additional radiation exposure [12]. In Chapter 4, I present the preliminary results from the use of the Clarity US system, designed and clinically implemented for adult prostate

cancer, for imaging the kidney in children. In Chapter 4, section 4.4.6, I demonstrated that the median difference in assessment of SI kidney motion between 4DCT and US pairs (acquired within the same imaging session) was 0.1 mm; indicating good agreement between the two modalities. Useable 2D US images for the assessment of kidney motion were acquired in 67% of patients. Though less than the 82% success rate of 4DCT acquisition, it is better than the described inability to delineate the kidney using CBCT as acquired in this work. It is anticipated that the 3DUS images obtained but not analysed would increase the proportion of useable images.

6.2.4 Internal target volume approach to upper abdominal RT planning in children

My findings in Chapter 2, supported by other studies, demonstrate that motion is greatest SI and the magnitude of motion RL and AP is less; this suggests that anisotropic PTV expansions are warranted. The benefit of 4DCT and the individual assessment of RROM, for radiotherapy planning of paediatric upper abdominal tumours were investigated in this thesis. A 4DCT – generated internal target volume approach to RT planning for abdominal neuroblastoma was described in Chapter 5. This approach has not yet been routinely adopted in the European SIOPEN high risk neuroblastoma studies. A statistically significantly lower mean kidney dose for midline targets was achieved with the ITV approach; V14 29.8 % versus 35.7 %, $p < 0.04$. This relative reduction in this dose objective is likely the result of the resultant anisotropic internal margin reducing the volume of PTV overlapping the adjacent kidneys. The data from

Chapter 5 also demonstrated that using an ITV approach led to reductions in mean heart and lung doses of up to 2.5 Gy in individual patients.

6.3 Limitations

In order to reduce the CTV to PTV margin, a comprehensive assessment of all uncertainties considered in that margin is required. Intra-fraction RROM is just one of the relevant uncertainties and that is a limitation in the broader application of the work that I have presented here. Other components of the CTV to PTV margin that were not addressed in this thesis are discussed in the following sections.

6.3.1 Delineation uncertainty

Target contouring and its variability remains the most significant source of uncertainty that will challenge strategies aimed at reducing the CTV to PTV margin, as delineation error is considered in the generation of population-based margins [13]. In paediatric RT, manual delineation of targets and organs at risk is still standard practice internationally. Both intra- and inter-observer variability in adult upper abdominal RT is well described [14-19]. The magnitude of delineation uncertainty in paediatric RT is not reported to the same extent as it has been for adults. A small number of studies have described inter-observer variability in contouring in medulloblastoma, thoracic, and abdominal targets in children [19-21]. Inter-observer variation in target volume delineation has been shown to unsurprisingly affect the RT dose delivered to adjacent OARs in children [22]. Paediatric clinical/ radiation

oncologists may also adapt target volume delineation in light of patient-related factors in attempts to balance RT dose and potential toxicities [23]. Variation in delineation in 3 thoracic/ abdominal paediatric cases was assessed in a single study [24], and was quantified using a generalised conformity index generated for the volume of overlap between individual contours and the gold standard; CI was as low as 0.40– 0.59. As results in this study were limited to conformity indices it is not possible to determine a magnitude of delineation error in order to apply it to a population-based margin recipe.

Consensus contouring statements and atlases together with quality assurance of RT contours and plans in clinical trials are all aimed at minimising the uncertainty from delineation error [25, 26]. QUARTET, a platform for prospective radiotherapy quality assurance in paediatric clinical trials, is being implemented in Europe; this is an international platform to ensure all trial patients have access to RT quality assurance [27]. These efforts, in addition to routine peer review of volumes, will be important in reducing delineation uncertainty in paediatric RT.

6.3.2 Set-up error in paediatric Radiotherapy

As discussed in Chapter 1, the use of image-guided RT (IGRT) strategies can reduce systematic and random patient set-up uncertainties and lead to a reduction in the SM component of the PTV margin [28-30]. The SM will be specific to each RT department as it is influenced by the type of immobilisation, and imaging modality and frequency used [31]. Appropriate use of patient immobilization devices (e.g. vacuum bag) can attain set-up reproducibility in the region of 3-5 mm for children in abdominal sites [32, 33]. Implementation of

a daily IGRT strategy in children with abdominal NBL reduced the interfraction set-up uncertainty (bone match) from 5.6, 5.2, 5.2 mm with weekly imaging to 1.7, 2.1, 1.5 mm (SI, AP and RL) [34, 35]. Another study reported the use of daily CBCT (bone match) in 15 children receiving abdominal RT for Wilms' tumours [10]. Calculated inter-fraction set-up errors were less than 0.2 mm in all orthogonal directions. Intra-fraction set-up errors, quantified using post-treatment CBCT acquired on the first 3 – 5 fractions in the same 15 patients, were less than 0.8 mm in all orthogonal directions. The strategies described have used daily image guidance. The contribution of IGRT imaging dose in children was highlighted recently [36]. Similar to the use of 4DCT, the additional imaging dose is justified if it facilitates increased accuracy and precision in RT delivery. However, as previously discussed the poor soft tissue resolution of modified CBCT protocols (Chapter 2, Figure 2.8) limits their use to IGRT based on bone match.

6.4 Future directions

6.4.1 Proton therapy

The characteristic dose deposition of protons (the Bragg Peak) results in negligible exit dose and the ability to deliver conformal dose distributions with fewer beams (equivalent arc) compared to advanced photon techniques. This equates to less non-target tissue in the irradiated volume receiving medium to low dose which in turn is anticipated to reduce late normal tissue toxicities. This reduction in normal tissue irradiation has already made it the preferred modality in other paediatric tumour sites, especially the brain, spine and pelvis.

High energy proton RT became clinically available in the UK in 2018, with the opening of the facility in University College London Hospital, scheduled for 2021, will see the service expand further in the very near future.

With increased availability, the indications for proton RT in children are likely to expand. Tumours arising in thoracic and abdominal sites, such as Hodgkin lymphoma, Wilms' tumour and abdominal neuroblastoma, have not yet been routinely referred for proton RT. Proton beam quality is influenced by range uncertainty. Changes in the volume and density of tissue in the beam path during treatment can result in range over- or under-calculation of dose. RROM is a significant contributor to these range uncertainties. These errors have the potential to overdose normal tissue or under-dose the target. The more modern pencil beam scanning PT (PBS-PT) techniques, delivering complex intensity modulated proton RT, are even more sensitive to such changes compared to passive scattering techniques [37]. This further emphasises the importance of quantifying organ and target displacements in anatomical sites susceptible to RROM in children for accurate dose placement in PBT.

6.4.2 MR-guided Radiotherapy

As discussed in Chapter 1, section 1.3.5.1, MR-guided RT systems are now in clinical use in the UK and a recently reported first in man treatment has been published [38]. Because of the inherent advantages of MR in children, as discussed in Chapter 3, MR-guided RT is an attractive system for use in children. In 15 patients with Wilms' tumours an MR-guided RT approach to treatment enabled the theoretical reduction of the ITV to PTV margin from 5mm to 3 mm, compared to VMAT photon planning. This reduction was

facilitated by the theoretical ability to perform daily on-line imaging and the assumption that the inter-fraction uncertainties were null. This paper suggests that MR-guided RT could facilitate further improvements in the therapeutic ratio for paediatric RT by reducing the PTV margin [39].

My results in Chapter 3 have demonstrated the feasibility of acquiring 4DMR in children. In the Royal Marsden NHS Foundation Trust, children are being recruited to two prospective studies using the Elekta Unity MR Linac; the PRIMER [40] and PERMIT (Integrated Research Application System number (IRAS): 236188) studies to further investigate the clinical feasibility and utility of the MRL in children.

6.4.3 Conclusion

When I began developing the protocol for the APAChe study to generate data for this thesis, a search of the terms “radiotherapy AND (respiratory OR breathing) AND (4D OR organ motion OR 4DCT or 4DMR OR 4D Cone Beam CT OR cine-MRI)); yielded hundreds of publications for adults, but only 4 publications specific to children (for paediatric added AND (children OR paediatric). As I complete my thesis, the same search yields 12 publications. Research focussed on RROM in children, and its management, is still young with scope for further development just like the children we treat and study. We have the ability and technology to further refine paediatric RT, improving target definition, conformity of dose delivered to the target, and sparing greater volumes of normal tissue. I hope the bright future of highly conformal, high precision adaptive paediatric RT can contribute to the realisation of bright futures for our young cancer survivors.

6.5 References

1. Pritchard-Jones K, Dixon-Woods M, Naafs-Wilstra M, Valsecchi MG. Improving recruitment to clinical trials for cancer in childhood. The Lancet Oncology 2008; 9(4): 392-399.
2. Lavan N CE, Burland H, Mandeville HC. Development of a four-dimensional computed tomography (4DCT) imaging sequence for paediatric radiotherapy planning. International Society of Paediatric Oncology (SIOP); Dublin, Ireland. Pediatric Blood and Cancer 2016 p. S1-S321.
3. van Dijk I, Huijskens SC, de Jong R, Visser J, Fajardo RD, Rasch CRN, et al. Interfractional renal and diaphragmatic position variation during radiotherapy in children and adults: is there a difference? Acta oncologica (Stockholm, Sweden) 2017; 56(8): 1065-1071.
4. Huijskens SC, van Dijk IW, Visser J, Rasch CR, Alderliesten T, Bel A. Magnitude and variability of respiratory-induced diaphragm motion in children during image-guided radiotherapy. Radiotherapy and oncology : journal of the European Society for Therapeutic Radiology and Oncology 2017; 123(2): 263-269.
5. Huijskens SC, van Dijk IWEM, de Jong R, Visser J, Fajardo RD, Ronckers CM, et al. Quantification of renal and diaphragmatic interfractional motion in pediatric image-guided radiation therapy: A multicenter study. Radiotherapy and Oncology 2015; 117(3): 425-431.
6. Uh J, Krasin MJ, Li Y, Li X, Tinkle C, Lucas JT, Jr., et al. Quantification of Pediatric Abdominal Organ Motion With a 4-Dimensional Magnetic Resonance Imaging Method. Int J Radiat Oncol Biol Phys 2017; 99(1): 227-237.
7. Pai Panandiker AS, Sharma S, Naik MH, Wu S, Hua C, Beltran C, et al. Novel Assessment of Renal Motion in Children as Measured via Four-Dimensional Computed Tomography. International Journal of Radiation Oncology*Biology*Physics 2012; 82(5): 1771-1776.
8. Nazmy MS, Khafaga Y, Mousa A, Khalil E. Cone beam CT for organs motion evaluation in pediatric abdominal neuroblastoma. Radiotherapy and Oncology 2012; 102(3): 388-392.
9. Kannan S, Teo BK, Solberg T, Hill-Kayser C. Organ motion in pediatric high-risk neuroblastoma patients using four-dimensional computed tomography. Journal of applied clinical medical physics 2017; 18(1): 107-114.
10. Guerreiro F, Seravalli E, Janssens GO, van de Ven CP, van den Heuvel-Eibrink MM, Raaymakers BW. Intra- and inter-fraction uncertainties during IGRT for Wilms' tumor. Acta oncologica (Stockholm, Sweden) 2018; 57(7): 941-949.
11. Huijskens SC, van Dijk I, Visser J, Balgobind BV, Rasch CRN, Alderliesten T, et al. The effectiveness of 4DCT in children and adults: A pooled analysis. Journal of applied clinical medical physics 2018.
12. Mason SA, White IM, O'Shea T, McNair HA, Alexander S, Kalaitzaki E, et al. Combined Ultrasound and Cone Beam CT Improves Target

Segmentation for Image Guided Radiation Therapy in Uterine Cervix Cancer. Int J Radiat Oncol Biol Phys 2019; 104(3): 685-693.
13. Royal College of R, Institute of P, Engineering in M, College of R. On target: ensuring geometric accuracy in radiotherapy. London: Royal College of Radiologists; 2008.
14. Jansen EP, Nijkamp J, Gubanski M, Lind PA, Verheij M. Interobserver variation of clinical target volume delineation in gastric cancer. Int J Radiat Oncol Biol Phys 2010; 77(4): 1166-1170.
15. Versteijne E, Gurney-Champion OJ, van der Horst A, Lens E, Kolff MW, Buijsen J, et al. Considerable interobserver variation in delineation of pancreatic cancer on 3DCT and 4DCT: a multi-institutional study. Radiation oncology (London, England) 2017; 12(1): 58.
16. Vinod SK, Jameson MG, Min M, Holloway LC. Uncertainties in volume delineation in radiation oncology: A systematic review and recommendations for future studies. Radiotherapy and oncology : journal of the European Society for Therapeutic Radiology and Oncology 2016; 121(2): 169-179.
17. Wu DH, Mayr NA, Karatas Y, Karatas R, Adli M, Edwards SM, et al. Interobserver variation in cervical cancer tumor delineation for image-based radiotherapy planning among and within different specialties. Journal of applied clinical medical physics 2005; 6(4): 106-110.
18. Loo SW, Martin WM, Smith P, Cherian S, Roques TW. Interobserver variation in parotid gland delineation: a study of its impact on intensity-modulated radiotherapy solutions with a systematic review of the literature. The British journal of radiology 2012; 85(1016): 1070-1077.
19. Coles CE, Hoole ACF, Harden SV, Burnet NG, Twyman N, Taylor RE, et al. Quantitative assessment of inter-clinician variability of target volume delineation for medulloblastoma: quality assurance for the SIOP PNET 4 trial protocol. Radiotherapy and Oncology 2003; 69(2): 189-194.
20. Muracciole X, Cuilliere J, Hoffstetter S, Alapetite C, Quetin P, Baron M, et al. Quality assurance of a French multicentric conformal radiotherapy protocol for low-stage medulloblastoma: variability in target volume delineation. International Journal of Radiation Oncology• Biology• Physics 2002; 54(2): 148-149.
21. Kristensen I, Agrup M, Bergström P, Engellau J, Haugen H, Martinsson U, et al. Assessment of volume segmentation in radiotherapy of adolescents; a treatment planning study by the Swedish Workgroup for Paediatric Radiotherapy. Acta Oncologica 2014; 53(1): 126-133.
22. Padovani L, Huchet A, Claude L, Bernier V, Quetin P, Mahe M, et al. Inter-clinician variability in making dosimetric decisions in pediatric treatment: a balance between efficacy and late effects. Radiotherapy and Oncology 2009; 93(2): 372-376.
23. Padovani L, Huchet A, Claude L, Bernier V, Quetin P, Mahe M, et al. Inter-clinician variability in making dosimetric decisions in pediatric treatment: a balance between efficacy and late effects. Radiotherapy and oncology : journal of the European Society for Therapeutic Radiology and Oncology 2009; 93(2): 372-376.

24. Kristensen I, Nilsson K, Agrup M, Belfrage K, Embring A, Haugen H, et al. A dose based approach for evaluation of inter-observer variations in target delineation. Technical innovations & patient support in radiation oncology 2017; 3: 41-47.
25. Hoeben BA, Carrie C, Timmermann B, Mandeville HC, Gandola L, Dieckmann K, et al. Management of vertebral radiotherapy dose in paediatric patients with cancer: consensus recommendations from the SIOPE radiotherapy working group. Lancet Oncol 2019; 20(3): e155-e66.
26. Ajithkumar T, Horan G, Padovani L, Thorp N, Timmermann B, Alapetite C, et al. SIOPE – Brain tumor group consensus guideline on craniospinal target volume delineation for high-precision radiotherapy. Radiotherapy and Oncology 2018; 128(2): 192-197.
27. SIOP. [Available from: https://www.siope.eu/2016/05/25/quartet-project/.
28. De Los Santos J, Popple R, Agazaryan N, Bayouth JE, Bissonnette JP, Bucci MK, et al. Image guided radiation therapy (IGRT) technologies for radiation therapy localization and delivery. Int J Radiat Oncol Biol Phys 2013; 87(1): 33-45.
29. Bujold A, Craig T, Jaffray D, Dawson LA. Image-Guided Radiotherapy: Has It Influenced Patient Outcomes? Seminars in Radiation Oncology 22(1): 50-61.
30. ICRU. Report 83. Journal of the International Commission on Radiation Units and Measurements 2010; 10(1): NP-NP.
31. ElBeltagi MN, Wall V, Marignol L. Planning target volume (PTV) margin practice patterns in adults and paediatrics among the Paediatric Radiation Oncology Society (PROS) members: an international survey. Journal of Radiotherapy in Practice 2018; 17(4): 368-372.
32. Olch AJ. Pediatric Radiotherapy Planning and Treatment. London, UNITED STATES: CRC Press; 2013.
33. Pai Panandiker AS, Beltran C, Gray J, Hua C. Methods for image guided and intensity modulated radiation therapy in high-risk abdominal neuroblastoma. Pract Radiat Oncol 2013; 3(2): 107-114.
34. Beltran C, Pai Panandiker AS, Krasin MJ, Merchant TE. Daily image-guided localization for neuroblastoma. Journal of applied clinical medical physics 2010; 11(4): 3388.
35. Beltran C, Lukose R, Gangadharan B, Bani-Hashemi A, Faddegon BA. Image quality & dosimetric property of an investigational imaging beam line MV-CBCT. Journal of applied clinical medical physics 2009; 10(3): 3023.
36. Hess CB, Thompson HM, Benedict SH, Seibert JA, Wong K, Vaughan AT, et al. Exposure Risks Among Children Undergoing Radiation Therapy: Considerations in the Era of Image Guided Radiation Therapy. International Journal of Radiation Oncology*Biology*Physics 2016; 94(5): 978-992.
37. Mohan R, Das IJ, Ling CC. Empowering Intensity Modulated Proton Therapy Through Physics and Technology: An Overview. Int J Radiat Oncol Biol Phys 2017; 99(2): 304-316.

38. Pathmanathan A, Bower L, Creasey H, Dunlop A, Hall E, Hanson I, et al. The PRISM Trial- First UK Experience of MRI-Guided Adaptive Radiotherapy. International Journal of Radiation Oncology*Biology*Physics 2019; 105: E301.
39. Guerreiro F, Seravalli E, Janssens GO, van den Heuvel-Eibrink MM, Lagendijk JJW, Raaymakers BW. Potential benefit of MRI-guided IMRT for flank irradiation in pediatric patients with Wilms' tumor. Acta oncologica (Stockholm, Sweden) 2019; 58(2): 243-250.
40. PRIMER [Available from: https://clinicaltrials.gov/ct2/show/NCT02973828?term=MR&recrs=ab&cntry=GB&draw=2&rank=16.

Reference	Mean age (years) (range)	Patient number	Number of patients under GA	Right kidney			Left kidney			Diaphragm	Liver	Spleen	GTV
				RL	SI	AP	RL	SI	AP	SI	SI	SI	SI
(7)	4.1 (2-8)	11	11	0.7	**1.9**	0.7	0.7	**1.7**	0.9	5.1	**n/r**	**n/r**	**n/r**
	12.3 (9-18)	9	1	1.1	**3.9**	1.4	0.9	**3.1**	0.9	9.5	**n/r**	**n/r**	**n/r**
(9)	nr (1.5–10)	15	10	0.3	**-1.9**	0.4	0.4	**-1.4**	0.4	-3.6L* -4.4R*	-2.5	-3.1	**n/r**
LAVAN	**4.5 (1.5–17.5)**	**25**	**12**	**0.8**	**3.1**	**1.0**	**0.9**	**2.7**	**1.0**	**n/r**	**n/r**	**n/r**	**n/r**
(6)	nr (1- 8)	17	17	0.5	**2.3**	0.8	0.5	**1.6**	0.6	**n/r**	3.2	3.0	1.6
	nr (9- 20)	18	1	1.0	**4.7**	1.5	0.9	**4.8**	1.0	**n/r**	6.8	6.9	4.7
(10)	4 (1– 8)	15	10	0.0	0.6**	**0.1**	-	**-**	-	-	3.0	3.2	0.8 ^

Table 6.1 - Selected published mean intrafraction COM motion mm) parameters. N/R; not recorded. Negative integers indicates exhale motion was more extreme than inhale.* L/R; left and right dome of diaphragm. GTV; gross tumour volume. ** displacements for right and left kidneys as combined structure given. ^ Superior tumour bed clips as surrogate.

Reference	Mean age (SD/ range)	Patient number (number under GA)	Measure of displacement	Right kidney			Left kidney			Diaphragm	Liver	Target (calcification)		
				RL	SI	AP	RL	SI	AP	SI	SI	RL	AP	SI
(8)	4.1 (1.6)	9	max upper pole	1	10.0	1	1	8	1	nr	11	2	5	3
		(9)	max lower edge	nr	nr	nr	nr	nr	nr	nr	13	nr	nr	nr
(5)	8 (1.6 - 17.8)	39 (2)	mean COM	0.6	0.5	0	-0.6	1.5	0	1.1	nr	nr	nr	nr
(3)	10.3 (3.1 - 17.8)	35 (5)	mean COM	-0.1	0.7	-0.4	-0.4	1.0	-0.9	-0.8	nr	nr	nr	nr
(10)	4.0 (1 – 8)	15 (10)	mean COM*	0.1	-0.2	0.4					-0.2			1.0^

Table 6.2 - Published results on interfraction organ motion in mm. SD; standard deviation. NR; not recorded. RL, SI, AP; right/left, superior/inferior, anterior/posterior. Negative integers reflect motion in left, superior and anterior directions. * displacements for right and left kidneys as combined structure given. ^ Superior tumour bed clips as surrogate.

Appendix 1: Adaptive Radiotherapy Planning for Upper Abdominal Tumours in Children and Teenagers; the APACHe study protocol

Adaptive Radiotherapy Planning for Upper Abdominal Tumours in Children and Teenagers.

Title: Adaptive radiotherapy planning for upper abdominal tumours in children and teenagers

Short Title: *APAChe*

Chief Investigator:	Dr. Henry Mandeville
Principal Investigator:	Dr. Henry Mandeville
Co-investigators:	Prof. Uwe Oelfke
	Dr. Simeon Nill
	Dr. Andreas Wetscherek
	Dr. Emma Harris
	Ms Sarah Mason
	Dr. Helen McNair
	Ms. Naomi Hopkins
	Dr. Naomi Lavan
	Dr. Cynthia Eccles
	Prof. Doh Mu Koh
Trial Manager	Ms Beverley Wharram
Statistician:	Ms. Komel Khabra

Sponsor:

The Royal Marsden Hospital NHS Foundation Trust

Downs Road, Sutton, Surrey SM2 5TP

Protocol Reference:	CCR4556
Version Number & Date:	Version 1.1, 23.05.16
Effective Date:	
Superseded Version Number & Date (If applicable)	n/a

PROTOCOL SIGNATURE PAGE

Study title: Adaptive radiotherapy planning for upper abdominal tumours in children and teenagers

Protocol version: CCR4556 v1.1 23.05.2016

Version date: 10.05.2016

Approved by the Chief Investigator:

Signature

Dr Henry Mandeville _____

Name of CI Date (DD-MM-YYYY)

Investigator's Agreement

I have read the attached protocol entitled "Adaptive radiotherapy planning for upper abdominal tumours in children and teenagers" dated 23rd May 2016 and agree to abide by all provisions set forth therein. I agree to comply with the principals of Good Clinical Practice (GCP) and with the ethical principles laid down in the revision of the Declaration of Helsinki (October 1996). I agree to ensure that the confidential information contained in this document will not be used for any purpose other than the evaluation or conduct of the clinical investigation without the prior written of the Paediatric Trials Unit of the Royal Marsden NHS Foundation Trust.

Signature

Dr Henry Mandeville _____

Name of PI Date (DD-MMM-YYYY)

Table of Contents

1. Background

1.1 Advanced radiotherapy planning and adaptive radiotherapy

The development of high-precision adaptive radiotherapy and its importance in the delivery of a quality radiation oncology service has been outlined in a 2012 National Radiotherapy Advisory Group (NRAG) report [1]. Advanced planning techniques such as volumetric and intensity modulated radiotherapy (VMAT and IMRT) can enable increased normal tissue sparing compared to 3D conformal radiotherapy (3DCRT) and have enhanced the therapeutic ratio in the treatment of many tumour sites [2]. The beam characteristics of proton beam therapy (PBT) further spares normal tissue primarily due to an absence of exit dose compared to photons. PBT is the treatment modality of choice for many paediatric tumours. Geometric certainty in radiotherapy treatment is crucial when such high- precision treatments are employed.

1.2 Motion and the implications for radiotherapy treatment delivery

A radiotherapy target is rarely a static structure. Internal motion in radiotherapy is divided into inter-fraction motion (changes in anatomy occurring between radiotherapy treatments) and intra-fraction motion (changes in anatomy occurring during a single radiotherapy treatment fraction). Changes in tumour and organ position occur due to a number of physiological processes inclusive of but not limited to respiration, peristalsis, rectal and bladder filling. For upper abdominal tumours the dominant process affecting intra-fraction motion is respiratory-related motion [3]. Notably motion is not confined to cardinal x, y and z directions but can be the result of complex changes such as deformation and rotation. The true magnitude of intra-fraction displacement that may occur is not visualised on conventional 3D radiotherapy planning imaging. This uncertainty is in addition to the potential inter-fraction changes that may occur between treatments and intrafraction variability. These uncertainties introduce potential random and systematic errors into the treatment delivery process. In the absence of a reliable method to quantify motion generic planning margins are used to ensure adequate coverage of the target. In an anatomical location susceptible to significant positional change such as the upper abdomen these margins need to be more generous than in other sites and result in a greater amount of normal tissue being irradiated.

The International Commission on Radiation Units and Measurements (ICRU) – 62 guidelines were published in relation to conformal photon radiotherapy reporting and planning [4]. These guidelines introduce the concept of an internal treatment volume (ITV) inclusive of a clinical target volume (CTV) and an internal margin (IM). The latter explicitly accounts for physiological

motion affecting the target volume. An equivalent volume applies to organs at risk (OAR); the planning risk volume (PRV). Inherent to these concepts is the ability to take organ motion into account. It is recommended that respiratory management techniques be considered in the following scenarios:

(i) If greater than 5 mm motion is observed in any direction
(ii) If significant normal tissue sparing can be gained through the use of a respiration management technique [5].

Motion can change the radiological depth from beam entry to the target volume. The resultant effect on a photon dose distribution may be small but the potential effect on the dose distribution of a proton plan can be significant. This is especially important in the setting of dynamic dose delivery such as intensity modulated proton beam treatment [6].

1.3 Current methods for motion assessment

Four- dimensional computed tomography (4DCT) is the current gold standard for motion assessment. 4DCT image acquisition is synchronized with the patient's respiratory cycle thereby capturing the positional change of anatomy relative to inspiration and expiration. These anatomical changes are representative of intra-fraction (occurring during a single radiotherapy treatment) motion. This is in contrast to the 'snapshot in time image' acquired with 3DCT. Patients' breathing patterns can vary in both magnitude and regularity during the course of a radiotherapy treatment [5]. A limitation of 4DCT is that it does not capture the variability that may occur in an individual's breathing pattern. This is because scan acquisition occurs over the timescale of a finite number of breathing cycles [6]. Longer imaging sequences using MR and ultrasound potentially capture motion over the course of a greater number of respiratory cycles and may provide an advantage over 4DCT. Respiratory-correlated 4DMR can be reconstructed from 2DMR images enabling volumetric processing and analysis. Image acquisition occurs over minutes and therefore simulates a timeline similar to that of a radiotherapy treatment better than 4DCT. Ultrasound can also image over the course of a number of breathing cycles. The known limitations of ultrasound imaging have been discussed in section 1.2.

1.4 Current evidence of organ motion in the upper abdomen

Results for upper abdominal organ motion as quantified by 4DCT and MR have been published in adult patients [7-10]. A number of methodologies to quantify this motion have been employed in these studies. Significant variation in measured displacement has been

recorded though it is well established that cranio-caudal displacement is the dominant motion trajectory for organs in the upper abdomen. Published series in the paediatric population echo results from adult series but report smaller overall mean displacements [11-13]. Inter- and intra-patient variability as a feature of organ motion persists in young patients. The result is that no clear guidelines exist to aid definition of appropriate margins for paediatric/ young adult abdominal irradiation. The most recent European High Risk (HR) Neuroblastoma Study recommends a CTV to PTV margin of 5mm to 10 mm to take into account the uncertainties of positioning and possible organ motion [14]. Published results show a range of cranio-caudal renal motion from 5mm- 52mm [11-13]. A PTV margin of either magnitude would be compromised in the setting of organ motion at the upper limit of what is reported in the literature.

1.5 Image guided radiotherapy (IGRT)

IGRT is the term ascribed to the concept of evaluating and reducing geometric uncertainty during a radiotherapy treatment course. Both random and systematic errors contribute to geometric uncertainty. The current IGRT technology employed for patients applicable to this work consists of a kilovoltage cone beam CT (kvCBCT). Systematic error is calculated by taking the average value of the isocentre displacement as measured by CBCT taken before each of the first three fractions of treatment. The systematic error is corrected to zero by adjusting the isocentre position before the fourth fraction is delivered. A further CBCT is taken prior to fraction four to confirm the process. Thereafter CBCTs are performed weekly if measured displacement remains within the predefined tumour site-specific tolerance. This approach addresses inter-fraction motion. Inter-fraction motion includes both setup variations and translational changes in organ position. Therefore though patient set-up may be addressed by an off-line IGRT strategy the issue of internal organ motion as a potential source of error persists. Magnetic resonance (MR) and ultrasound-based IGRT are attractive potential alternatives to CBCT as neither modality is associated with additional radiation dose, an important consideration in young patients. MR provides better soft tissue contrast compared to CBCT. On-line MR-based IGRT will provide the possibility real-time image guidance (further detail in section 1.6) but remains a relatively novel application. Ultrasound is inherently real-time, relatively inexpensive, and also provides better soft tissue contrast when compared to CBCT. Ultrasound- based IGRT has been described in the context of prostate radiotherapy [15-17]. However unresolved limitations exist including image distortion in the presence of bone or air cavities and significant inter- user variability [18]. Ultrasound is a commonly used diagnostic technique for liver and renal pathology hence its attraction as a potential alternative for image guidance in the upper abdomen. 3D ultrasound-based IGRT in the treatment of upper abdominal tumour sites has been explored [19-20]. Further studies are required to

ascertain its full potential as an IGRT tool in this anatomical location.

1.6 The MR Linac and MR-guided radiotherapy

MR provides superior soft tissue definition compared to CT. This is achieved without additional radiation dose to the patient. Replacement of current x-ray-based IGRT with MR-guided radiotherapy (MRgRT) may improve radiotherapy delivery by providing more accurate visualisation of the target. MRgRT will also make real-time, on-line imaging during radiotherapy treatment possible and will facilitate on-line adaptive radiotherapy treatment delivery. Online adaptive treatment delivery can enable further reductions in treatment planning margins with the potential benefit of reducing normal tissue toxicity [21]. The MR Linac integrates high-definition imaging based on 1.5 Tesla MR technology with state-of-of-the-art therapy delivery through a linear accelerator [22]. The ICR/RMH has been awarded Programme Grant funding from MRC (Grant Number MR/M009068/1) to procure and install a prototype ELEKTA MR Linac. It will be installed, commissioned and ready to treat the first patient in the third quarter of 2017. Prior to this, work is needed to develop a CT-MR and MR-MR workflow. This will begin with the acquisition of radiotherapy planning MR scans. MR planning scans are performed in the treatment position, often involving the use of immobilisation devices. Specific sequences and volumetric-based image acquisition is needed for radiotherapy target definition and treatment planning. Diagnostic MR scans are therefore not appropriate. APAChe will contribute to the acquisition of MR images for the purpose of exploratory and developmental work in anticipation of a clinical throughput on the MR Linac. A BRC-funded, CCR-approved protocol (CCR Trial No. 4477) has been developed for the acquisition and development of radiotherapy planning scans in adult tumour sites. Paediatric upper abdominal tumour sites differ in that a gross tumour volume is not present for the majority of cases. Furthermore, the physical differences between children and adults preclude the use of these MR planning scans in the development of an adult MR library of scans to facilitate an online adaptive workflow. We are extending the BRC-funded adult work to develop a paediatric and teenager specific library and to include the assessment of tumour and organ motion.

1.7 Current methods of motion management

Motion management techniques inclusive of breath hold and gating methods are best described for hypofractionated lung and upper abdominal radiotherapy treatments [23-25]. Description of these techniques in children and young adults is less well defined. Successful use of active breathing coordinator (ABC) in patients aged 13 – 18 years has been described [26]. Young children requiring anaesthesia for radiotherapy and imaging at the Royal Marsden Hospital are under deep sedation without respiratory muscle paralysis and intubation. This is

one limitation in the use of respiratory management techniques in this patient cohort as simulation of a breath hold technique is not feasible under deep sedation. However, given the AAPM recommendations, avenues towards motion management need to be explored. We will explore a voluntary inspiration breath hold in patients aged 5 -12 years as a feasibility and reproducibility study.

2. Rationale

The observed inter-patient variability in organ motion makes the potential application of an ITV class solution to this population challenging [27]. Coupled with the range in published recommendations for margin definition a strong argument exists to adopt an individual approach to margin definition and respiratory management techniques in this cohort of patients.

In this study we will evaluate respiratory-related upper abdominal organ and tumour bed/tumour motion quantitatively using 4D-derived imaging. We will compare conventional population-derived PTV-based photon planning to photon planning using an individualised ITV approach. Further comparisons with planning techniques employing an ITV-approach (proton and MR-guided planning) will be made. The feasibility and tolerability of voluntary inspiration breath hold motion management technique will be explored. MR planning sequence acquisition and development will be in line with CCR Protocol No. 4477 and referenced in detail in Appendix 1.

3. Aims

3.1 Primary Aims

Quantify upper abdominal respiratory-related intrafraction organ motion using 4DCT, 4DMR and US.

3.2 Secondary Aims

3.2.1. Modality-specific objectives:

Measure agreement between intrafraction organ motion as measured by 4DCT, MR and US (primary endpoint) including intra-modality comparison to assess variability in intrafraction motion at different time-points (US only).

Quantify deformation (organ, tumour and/or tumour bed) during respiration.

Quantify interfraction organ motion on kilovoltage cone beam CT (kvCBCT).

Compare organ motion measured by 2D ultrasound with organ motion measured with 3D ultrasound.

Measure agreement between motion and biometric variables: age, height, weight and the use of general anaesthetic.

Feasibility of voluntary inspiratory breath-hold procedure and reproducibility of breath hold during radiotherapy in patients aged 5-12 years of age.

3.2.2. Planning objectives for paediatric upper abdominal tumours:

Compare conventional photon planning using population-derived PTV approach to photon planning using ITV approach.

Compare proton beam planning to conventional photon radiotherapy planning (ITV approach).

Compare MR-guided radiotherapy planning (ITV approach) to conventional photon radiotherapy planning (ITV approach).

Evaluate dosimetric effects of 4D-derived respiratory-related organ motion.

3.2.3 MR planning sequence acquisition and development in the free breathing paediatric upper abdomen (Appendix 1, section 18.2)

Creation of library of atlases for each tumour site to facilitate automated image segmentation for delineation of tumour volumes and organs-at-risk.

Determine automated methods for real-time registration and segmentation of MRI data obtained during treatment with the images employed for treatment planning.

Establish rapid and automatic calibration techniques to obtain the electron density values required for radiotherapy planning from MRI data.

Creation of library of treatment plans based on specific anatomy to facilitate rapid automated daily online planning for adaptive RT.

Assessment of the impact of specific features of the integrated MR Linac technology on treatment-planning strategies and plan quality.

4. Endpoints

4.1 Primary endpoint

Position of centre of mass (COM) of each target organ for each patient on each respiratory phase for each imaging modality (4DCT, 4DMR and US).

4.2 Secondary endpoints

4.2.1 Modality-specific objectives:

Check level of agreement between the COM positions measured as primary endpoint on 4DCT, 4DMR and US.

Measure relative distance between points of interest (POI) for target organs for each patient on each respiratory phase of imaging (4DCT, 4DMR and US). Measure difference in volume for target organs for each patient on each respiratory phase of imaging (4DCT, 4DMR and US). Measurement of DICE similarity coefficient (DSC) for tumour bed/ tumour for each patient on each respiratory phase of imaging (4DCT and 4DMR only).

Measure relative position of COM for each target organ on each CBCT compared to planning CT.

Check level of agreement between peak-to-peak motion measured on 2D and peak-to-peak motion measured on 3D US.

Check the correlation between measured motion (COM) and variables: age, height and weight. Compare the median of measured motion (COM) for each modality in anaesthetised and non-anaesthetised patients.

Proportion of patients achieving a 20 second breath hold (feasibility) and proportion of patients achieving the same breath hold procedure week one and at the end of radiotherapy (reproducibility).

4.2.2. Planning objectives: (I-IV)

Integral dose, irradiated volume, GTV coverage, PTV coverage including conformality indices for PTV coverage (when applicable) and dose constraint metrics (Table 1) for each phase of the respiratory cycle for each patient for conventional radiotherapy, proton beam planning and MR-guided radiotherapy.

KIDNEY	
CONSTRAINT	TARGET
Mean dose (Gy)	15Gy
V12 contralateral †	10% (lateralised target)
combined¶	≤55% (midline target)
V20 combined¶	<32%
V23 combined¶	<30%
V28 combined¶	<20%
LIVER	
CONSTRAINT	TARGET
V19†	≤100%
V21†	50%

TABLE 1. Dose volume constraints for organs at risk: ¶ QUANTEC [28], † HR-NBL-1/SIOPEN trial protocol [14].

4.2.3 Exploratory endpoints (MR planning scans)

Refer to Appendix 1, section 18.3.

5. Study Design

This will be a prospective study comprised of two patient cohorts:

- Patients with an indication for upper abdominal radiotherapy.
- Patients undergoing MR surveillance imaging for a known malignancy in the upper abdomen.

See sections 6 and 7 for details of study procedures.

6. Inclusion/Exclusion Criteria

6.1 Inclusion criteria

1. Patients with an indication for radiotherapy to the abdomen.
2. Patients with an indication for radiotherapy to the thorax (these patients are only eligible for inclusion in the breath hold feasibility and reproducibility part of the study)
3. Patients requiring surveillance MR imaging of the abdomen.
4. <19 years of age.
5. Signed written informed consent.

6.2 Exclusion criteria

1. For the Radiotherapy Cohort: exclusion criteria for 4DCT acquisition will be demonstration of an unsuitable respiratory trace as defined in the 4DCT imaging protocol (standard of care)
2. **NB. Patients will still have ultrasound measurements as described in section 8.4** For patients in both Radiotherapy Cohort (eligible for planning MR) and Non-Radiotherapy Cohort: a contraindication to MR scanning as defined in the respective standard operating procedures.
3. For patients in the Radiotherapy Cohort eligible for 4DCT and planning MR: patients with inadequate renal function precluding intravenous (IV) contrast as defined in the respective standard operating procedures [J-3-ONC-2-001] (measured or estimated GFR < 60ml/min/1.73m^2).
4. Pregnant or lactating females of reproductive age.

6.3 Subject Withdrawal Criteria

Patients will be free to withdraw and to not proceed with additional scan sequences at any point. Exclusion criteria are routinely screened as standard of care prior to imaging of the patient.

7. Methodology

7.1 Recruitment

Eligible patients will be identified at multidisciplinary team (MDT) meetings, audit or outpatient clinics. There are three groups of patients that will be enrolled in the study.

1) Patients with an indication for radiotherapy suitable for an additional MR radiotherapy planning scan.
2) Patients with an indication for radiotherapy suitable for 4DCT radiotherapy planning scan.
3) Patients without an indication for radiotherapy but undergoing surveillance MR imaging of the upper abdomen.

1 and 2 will be referred to as the 'Radiotherapy Cohort'. 3 will be referred to as the 'Non-Radiotherapy Cohort'.

Group 1 and 2: Radiotherapy cohort (Figure 1)

Patients will be recruited during clinician-led radiotherapy clinics. If the patient and/or guardian agree to participate, written consent will be obtained. Consent will include trans-abdominal ultrasound measurement during the planning process and at a minimum of 1 time-point during treatment for all patients. Consent will also include planning MR, 4DMR sequence and breath hold when applicable.

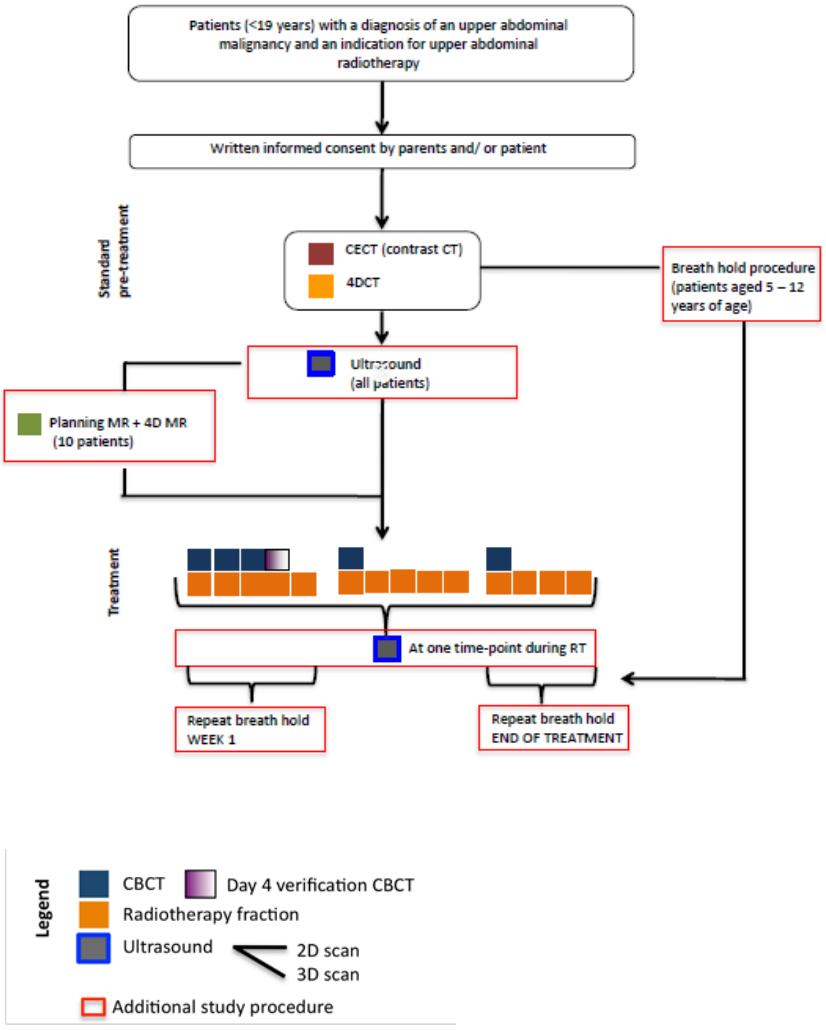

Figure 1: Timeline for RT-Cohort recruitment and treatment. Fractionation depicts the standard high-risk neuroblastoma treatment schedule (the expected majority of patients recruited to the Radiotherapy Cohort).

Group 3: Non-Radiotherapy Cohort (Figure 2)

Patients will be identified at MDT and/or clinic. The patient and/or guardian will consent to trans-abdominal ultrasound measurement before or after their scheduled MR scan. Consent will cover additional 4DMR sequence acquisition.

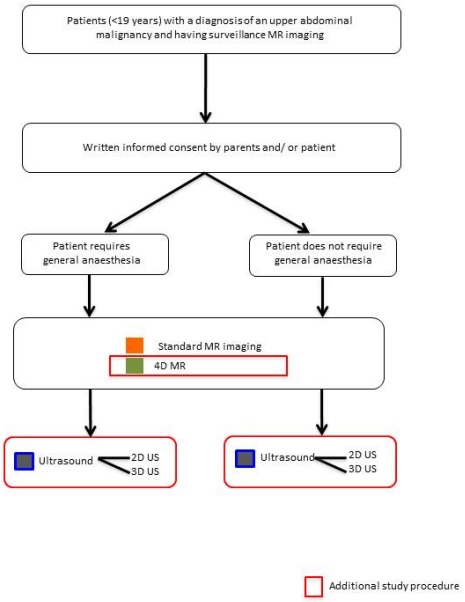

Figure 2: Timeline for Non-Radiotherapy-Cohort recruitment.

7.2 Radiotherapy Cohort methodology

All patients have an indication for radiotherapy to the upper abdomen and will undergo a CT planning scan and additional ultrasound measurement. A proportion (N=10) of these patients will be suitable for an MR planning scan. The MR planning scan will be performed in the radiotherapy treatment position. MR is non-invasive and not associated with any additional radiation dose. Patients unsuitable for MR can be easily identified by screening questionnaire and not recruited. In suitable patients there are no known side effects or complications.

Trans-abdominal ultrasound is non-invasive, not uncomfortable and is not associated with any

additional radiation dose. There are no known side effects or complications. Ultrasound measurement will be performed pre-treatment coincident with the planning CT, and if tolerated, at a minimum of one time-point during treatment. Each of the ultrasound sessions will include the acquisition of a time series of both 2D and 3D images. 2D and 3D measurements are acquired using the same ultrasound probe; see section 7.4 for further details. Acquisition will take 90 seconds for each measurement.

CBCT images will also be captured for this cohort of patients. CBCT frequency will be dictated by the relevant tumour site protocol and no additional CBCTs will be performed as a result of this study. CBCT frequency as per standard departmental off-line IGRT approach is depicted in Figure 1 and described in section 1.3.

Additional support for performing a breath hold technique will be provided in the pre-simulation play session (standard of care for paediatric patients referred for RT) carried out by Play Specialists. Voluntary inspiration breath hold is non-invasive and does not require additional skin tattoos. Breath hold will not be utilised for radiotherapy treatment. We will enrol patients aged 8-12 initially and if 8 year olds tolerate the method we will include patients aged 5-7 years.

7.3 Rationale for 'Radiotherapy Cohort' methodology

- All 4DCT and US images acquired will address the primary endpoint of quantifying respiratory-related motion.
- The inclusion of both 2D and 3D ultrasound images within a single scanning session will address the secondary endpoint of comparing 2D and 3D ultrasound imaging.
- Ultrasound measurement at more than one time-point will garner data for addressing the primary endpoint of quantifying kidney motion. Additionally, acquiring ultrasound measurements on more than one occasion in individual patients will allow limited assessment of intra-patient intrafraction variability of respiratory-related organ motion: this will inform whether or not kidney motion is constant, or variable on a day-to-day basis.
- All CBCT images acquired will address the secondary endpoint of quantifying interfraction organ motion.

- Ultrasound measurement is acquired after the delivery of anaesthesia (if required) to address a secondary endpoint of comparing kidney motion in anesthetised and un-anaesthetised patients.
- Acquisition of 4DMR sequences will contribute to the primary endpoint of quantifying organ and tumour/ tumour bed motion and to the secondary endpoints of quantifying deformation.
- Acquisition of planning MR scans will contribute to appropriate endpoints as defined in CCR Protocol Number 4477. See Appendix 1, section 1.2 for further detail.
- Performance of voluntary inspiratory breath hold contributes to secondary endpoint of determining the proportion of patients aged 5- 12 years in whom this technique is feasible and reproducible.

7.4 Non-Radiotherapy Cohort methodology

All patients will be receiving routine follow-up diagnostic MR. Patients attending for MR attend the Oak Centre for Children and Young People for cannulation if required. Ultrasound measurements will be carried out in a designated room outside of the MR department for non-anaesthetised patients and in the MR department procedure room for anaesthetised patients. The ultrasound scanning session is comprised of both 2D and 3D measurements. As this cohort is not receiving radiotherapy patients are not immobilised in a treatment position.

7.5 Rationale for 'Non-Radiotherapy Cohort' methodology

- 4DMR images will be used to address the primary endpoint of quantifying motion. These patients are scheduled for imaging hence no additional hospital attendances result from this study.
- The 4DMR sequences will contribute to optimising acquisition for radiotherapy planning purposes.
- The ultrasound measurements will be used to answer the primary endpoint of quantifying kidney motion.
- The ultrasound equipment is not MR compatible therefore ultrasound scanning cannot be performed when the patient is lying on the MR couch. This necessitates transporting the patient to a separate US scanning room; the location will be determined by the need for general anaesthesia..

- Ultrasound measurement is acquired after the delivery of anaesthesia (if required) to address a primary endpoint of comparing kidney motion in anesthetised and un-anaesthetised patients.
- The inclusion of both 2D and 3D ultrasound measurements within a single session will address the secondary endpoint of comparing 2D and 3D ultrasound measurements.

7.6 Rationale for including 2 patient cohorts

The overall incidence of paediatric cancers is low. We have therefore included all patients with an upper abdominal malignancy (regardless of the type of treatment received) in order to obtain sufficient data.

8. Data Acquisition

All images will be transferred to the appropriate treatment planning system for data analysis purposes. Contrast-enhanced CT and 4DCT will be transferred to Pinnacle treatment planning system for radiotherapy delineation and planning as standard. A proportion of 4DCT datasets acquired in a national phase II study; the IMAT study; will be included in APAChe in addition to 4DCT and CBCT datasets obtained as part of a prospective in house service evaluation.

8.1 Radiotherapy planning CT (contrast- enhanced and 4D CT)

Radiotherapy planning CT data will be acquired and stored as part of the radiotherapy treatment process as per departmental protocol (Radiotherapy Cohort only).

8.2 CBCT

CBCT data will be acquired as per departmental protocol as part of the radiotherapy treatment process (Radiotherapy Cohort only). CBCT data will be exported to appropriate treatment planning software for data analysis.

8.3 MR

MR data will be acquired in the Non-Radiotherapy Cohort and for a proportion of patients in the Radiotherapy Cohort (MR planning scans). An MR physicist will develop the 4D imaging sequences. MR scanning will be performed by MR radiographers as standard and overseen

by the MR Head of Department. 4DMR images of the upper abdomen will be acquired in the free breathing state. MR planning scans will be performed in the treatment position. See Appendix 1, section 18.1 for further detail.

8.4 Ultrasound

The patient will be positioned on either the Linac treatment couch (Radiotherapy Cohort), or a wheeled hospital cot (Non-Radiotherapy Cohort). The ultrasound operator will apply a layer of ultrasound gel, and hold the probe directly on top of the rib cage (on the distal side of the patient) with a slight amount of pressure adjusting the angle and position of the probe until a satisfactory view of the kidney is achieved. A dedicated tool will be used to hold the ultrasound probe in place such that the desired pressure and angle of the probe is maintained throughout the measurements. Two 90-second measurements will be acquired for the kidney: one in 3D mode and one in 2D mode, giving two time-series of 3DUS volumetric images and 2DUS images respectively. Ultrasound measurements will be performed by a nominated co-investigator of the study with support from the physics US team and therapy radiographers.

8.5 Target Delineation and Contouring

Contouring of tumour/tumour bed and organs at risk (liver and kidneys) will be completed as per the relevant individual tumour site protocol. The 4DCT ITV will be defined as the volume between the maximal and minimal excursion of the adjacent OAR (liver, kidneys) relative to the tumour bed CTV. The degree of excursion will be assessed on each respiratory phase. PTV expansion will be per departmental protocol.

8.6 Breath-hold procedure

At the time of the pre treatment play session (standard of care for patients referred for RT) patients will be introduced to the concept of voluntary breath hold and a trial of the technique will be carried out. On the day of CT simulation, breath hold simulation will take place in a designated room. The patient will be positioned and reference anatomical marks placed in free-breathing as standard. Breath hold manoeuvre will be carried out as per standard operating procedure J-3-EXB-5-031. An attempt will be made at 10, 15 and 20 second breath holds (feasibility endpoint). The patient will be asked to repeat the breath hold manoeuvre at week 1 and final week of treatment and measurements checked to ensure the degree of

abdominal excursion is consistent with pre treatment with an accepted tolerance of 5mm [5] (reproducibility endpoint).

9. Image Analysis

9.1 Motion analysis

I. Organ motion

- Centre of mass (COM) trajectory will be calculated from the COM for each organ in each patient at each respiratory phase along three axes; superior- inferior (SI); right- left (RL), anterior- posterior (AP). COM will be measured for 4DCT, 4DMR and 3DUS. Centroid (the 2D equivalent of COM) will be measured for 2DUS.

9.2 Deformation analysis

I. Organ deformation

- For POI analysis three points and three dimensions will be identified for each individual kidney and the corresponding slice in millimetres and distance respectively recorded.
    - The location of the three POI points [superior, middle and inferior third of the organ] will be delineated consistently on all respiratory phases of the 4DCT for each patient.
    - The dimensions measured will include superior/inferior (SI), anterior/posterior (AP), right/left (RL) as demonstrated on the axial/sagittal and coronal reconstructions respectively.
- For each patient the right and left kidney relative mean, absolute median and standard deviation for the three dimensions and the three POI [superior, middle and inferior third of the organ] will be measured on each respiratory phase for each imaging modality.
- For POI analysis of the liver six points will be consistently identified on each phase as the most superior/inferior/medial/lateral/anterior and posterior point on the relevant axial/coronal and sagittal planes respectively.
- For each patient the liver relative mean, absolute median and standard deviation for each direction (SI, AP, RL) will be determined for each respiratory phase for each imaging modality.

- The volume of each organ will be calculated for each patient from manually drawn contours on each respiratory phase for each imaging modality.
    - The relative mean, absolute median and standard deviation for organ volume for each modality will be reported.

- These metrics are applicable to 4DCT, 4DMR and 3DUS.
- For the 2DUS images, the geometric parameters quantified for the kidneys are the 2-dimensional versions of the parameters described in 9.2; points of interest (POI) and area.

I. Tumour bed deformation.

- This will be calculated for 4DCT and 4DMR. The DICE similarity coefficient (DSC) will be the metric used to assess the spatial overlap between the tumour bed contour as delineated on each phase of the 4D-derived imaging dataset. For 4DCT the end-expiration phase will be taken as the reference image to which the other phase contours are compared. For 4DMR an arbitrary but consistent respiratory time point equating to end-expiration will be selected to function as the reference image.

$$DSC(A,B) = 2(A \cap B)/(A+B)$$

(Where ∩ is the intersection, where A and B contain the same image pixels)

The lower the DSC of the two volumes between different time points, the greater the motion/deformation of the tumour bed. A DSC of 1 will indicate no positional or shape change of the tumour bed between the time points assessed.

II. *CBCT*

Interfraction motion will be assessed by comparing organ (kidney, liver) volume, shape and COM as contoured on the CBCT images to those contoured on the reference CT planning scan.

- Rigid registration of the CBCT to the reference planning CT scan will be performed using bone match with placement of clipbox as per tumour site protocol. The bone match will resolve patient positioning (setup) error.

- Soft tissue alignment of right, left kidney and liver on each registered CBCT for each patient will be done following bone match. This will quantify organ motion in three dimensions (x, y and z directions).

IV Breath hold procedure

- Proportion of patients achieving 20 second inspiratory breath hold at CT simulation.
- Proportion of patients reproducing 20 second inspiratory breath hold week one and at the end of radiotherapy.

V. MR planning images

- Refer to Appendix 1, section 1.3.

9.3 Planning objectives

Details of planning objectives are outlined in sections 3.2.2 and 11.2.

- Integral dose (Gy) will be calculated as the product of the mean dose (Gy) delivered to the Boolean structure 'external minus PTV' by its volume (cc), where external represents volume encompassed by the body contour.
- The irradiated volume will be calculated as the volume of the structure 'external' receiving ≥ 5Gy (V5Gy reported in cc).
- GTV and PTV coverage will be reported as the dose to 2% of the volume PTV (D2%) and the dose to 98% of the volume PTV (D98%).
- Conformity indices for PTV coverage (when applicable) as a surrogate for plan quality will be recorded for individual plans defined as the ratio between the target volume (PTV) and the irradiated volume at specified prescription dose (PTV V95/PTV vol).
- Dose constraints for kidney and liver are displayed in Table 1. Median dose (Gy) and respective ranges will be reported.

10. Study Organisation/Trial Monitoring and Management Strategy

10.1 Responsibilities

The overall responsibility for the study will lie with the Chief Investigator (CI), who will comply with the clinical trials regulations and principles of Good Clinical Practice (GCP). The designation for responsibility for the day-to-day clinical running of the study including patient accrual and consent will be made by the CI. The CI will identify responsible individuals for the management of case report forms, data collection, data processing, data storage and protection of intellectual property.

Risk assessment for the radiological studies will be made by the CI, together with staff directly involved in the radiological procedures, to ensure that procedures are GCP compliant and that only eligible patients, according with the inclusion/exclusion criteria, will be included in the study.

The study will not be run by the RM CTU but within the paediatric unit as it is a single centre imaging study without therapeutic consequence. As such, and after discussion with the GCP Compliance team, it has been agreed that the study represents little, if any, risk and therefore does not require formal monitoring.

Patients will be recruited at the paediatric oncology clinics of the Royal Marsden NHS Foundation Trust. All study investigations and the delivery of all trial treatment will be carried out within the Trust. The paediatric oncology trials team will have day to day operational responsibility for the study, as appropriately delegated by the CI.

10.2 Start Date Definition

The study will not commence until written approval has been received from the HRA, Research Ethics Committee and the RM Committee for Clinical Research.

10.3 Patient Screening

Patients who fulfil the inclusion criteria are eligible to take part in the study. Patient screening will take place at MDT, audit and outpatient clinic as discussed in section 6.

10.4 Study Completion

For the purposes of REC Approval the trial end date will be the final participant's last visit. The CI will notify the Ethics committee of the end of the trial appropriately and an End of Study Report will be provided within 12 months of the end of the trial according to the definition above.

10.5 Follow Up

Patient follow up will be as standard practice for individual tumour sites. No follow up is required for study purposes.

11. Adverse Events

11.1 Definitions of adverse events:

Adverse Event (AE): Any untoward medical occurrence or experience in a patient that occurs after the administration of a medicinal product, regardless of the dose, including occurrences which are not necessarily caused by or related to that product.

Adverse Reaction (AR): Any untoward and unintended response to an investigational medicinal product related to any dose administered.

Unexpected Adverse Reaction (UAR): An adverse reaction, the nature or severity of which is not consistent with the information about the medicinal product in question.

Serious Adverse Event (SAE),

An AE that results in death, is life-threatening, or leads to hospitalisation, prolongation of hospitalisation, persistent or significant disability or incapacity, congenital anomaly or birth defect.

As this is not a trial of an Investigational Medicinal Product it is not anticipated that Serious

Adverse Reactions (SARs) or Suspected Unexpected Serious Adverse Reactions (SUSARs) will occur and are therefore not defined in this document.

11.2 Adverse event reporting

The contrast agents used in CT and MR are iodine and gadolinium respectively. Clinical standard operating procedure (SOP) involves a patient questionnaire prior to scanning that elucidates possible contraindications to the use of contrast. Additionally, prior to MR scanning a questionnaire is completed to identify contraindications to magnetic field exposure. .

As this is an observational study it is not anticipated that participants will experience AE's/SAE's, however all participants will be monitored for any events which may occur due to their participation in the study and these will be reported as per national and local guidelines (Trust's SOP for Adverse Events Reporting for Non-CTIMP Trials sponsored by RMH/ICR) .

12. Statistical Considerations

12.1 Sample size and duration of the study

A review was conducted of the number of patients treated in the radiotherapy department over the preceding 12 months. This captured 10 patients that would fulfil our inclusion criteria. A similar review was conducted of patients attending the MR department for upper abdominal MR imaging in the preceding 12 months. This captured 41 patients scanned that would fulfill our inclusion criteria. As a result of the relatively small number of patients eligible for recruitment during the timeframe of this study a formal sample size calculation is not required.

A minimum of 10, maximum of 20, patients will be recruited in the timeframe of this study to each cohort. For the primary endpoint:

- 4DCT will be performed in the Radiotherapy Group only.
- 4DMR will be performed in both the Radiotherapy and Non-Radiotherapy Groups.
- 2DUS will be performed in Radiotherapy and Non-Radiotherapy Groups.

- 3DUS will be performed in Radiotherapy and Non-Radiotherapy Groups.

From the study [11], the mean direction ranged from -0.6 to 1.mm and the standard deviation ranged from 1.1 to 3.1mm for all directions.

Since the number of patients will vary for each imaging method below is a table of 95% CI of the mean direction for different numbers of patients and different standard deviations ranging from 1.0 to 3.0.

Standard Deviation (SD)	Width 95% CI of the mean (mm)			
	N=10	N=20	N=30	N=40
1.0	+/-0.62	+/- 0.44	+/- 0.36	+/- 0.31
2.0	+/-1.24	+/- 0.88	+/- 0.72	+/- 0.62
3.0	+/-1.86	+/- 1.32	+/- 1.07	+/- 0.93

Notably for the pooled analysis for 4DCT, 10 patients are involved in the service evaluation "Evaluation of 4DCT simulation in the paediatric and teenage/ young adult (TYA) cohort and the impact of assessment of tumour and organ motion on treatment". The analysis will pool patients in the service evaluation together with patients included in this study. Furthermore a Cancer Research UK funded phase II trial called the IMAT Study aims to recruit 50 paediatric/TYA patients. These patients will undergo 4DCT. We aim to include 4DCT data from a proportion of patients in our pooled analysis.

12.2 Statistical Analysis

Primary endpoints

I. For each imaging method (4DCT, 4DMR, 3DUS) as described in 8.1, the mean, median, range and standard deviation for the kidney and liver COM will be presented. For 2DUS method the mean, median, range and standard deviation of centroid will be presented for both kidney and liver.

Secondary endpoints

I. Bland Altman plots will be used to check the level of agreement of kidney and liver motion measured by 4DCT, 4DMR and US.
II. The mean, median, standard deviation and ranges of DSC used to check tumour/ tumour bed deformation for 4DCT and 4DMR will be presented. The mean, median, standard deviation and ranges of POI measurements and organ volume for kidney and liver will be presented.
III. Bland Altman plots will be used to check the level of agreement of the kidney and liver COM coordinates between CBCT and contrast-enhanced CT scan.
IV. The level of agreement of kidney motion between 2DUS data 3DUS data will be checked using Bland Altman plots.
V. Correlation between measured motion for each modality and age, height, weight and use of general anaesthetic. Spearman's or Pearson's correlation coefficient will be calculated between motion and age, height and weight. The mean, standard deviation, median and range motion will be presented between those you use general anaesthetic and those who do not.
VI. Proportion of patient cohort to comply with breath-hold technique as outlined in section 8.6 will be presented with a 95% CI.

Planning endpoints

I. The mean, median, standard deviation and ranges for dose to structures as outlined in section 3.2.2 and 9.3 will be presented.

MR planning sequence acquisition and development in the free breathing paediatric upper abdomen endpoints

Refer to Appendix 1, section 18.3

13. Regulatory & Ethics Committee Approval

13.1 Ethical Considerations

This study has been designed, shall be implemented and reported in accordance with the ICH Harmonized Tripartite Guidelines for Good Clinical Practice, with applicable local regulations and with the ethical principles laid down in the revision of the Declaration of Helsinki (October

1996).

The protocol will be approved by the Health Research Authority (HRA), a Research Ethics Committee (REC) and the Committee for Clinical Research (CCR) of the Royal Marsden NHS Foundation Trust before patients are entered.

13.2 Informed Consent

Patients may only be included in this study after providing written (witnessed where required by law or regulation), informed consent or, if incapable of doing so, after such consent has been provided by a legally acceptable representative of the patient. In cases where the patient's representative gives consent, the patient should be informed about the study to the extent possible given his/her understanding. If the patient is capable of doing so, he/she should indicate assent by personally signing and dating the written consent form or separate assent form. Participants that reach the age of 16 during the trial will be approached to personally consent to the trial. Informed consent must be obtained before conducting any study specific procedures. The process of obtaining informed consent should be documented in the patient source documents.

13.3 Patient Confidentiality

Personal data recorded on all documents will be regarded as strictly confidential and will be handled and stored in accordance with the Data Protection Act 1998. Patients will be identified using only their unique trial number and initials on the Case Report Forms (CRF). All such information which is designated as confidential information shall not be used for any purpose other than participation in the clinical trials and performance of obligations under this trial.

Any confidential information will not be copied or disclosed to a third party with the exception of employees and healthcare professionals that require access to this information to perform their transferred obligations. No individual will be identifiable in any analysis, report or published study results.

14. Data Handling and Record Keeping

14.1 Storage & Recording of data

The Investigator(s)/institution(s) will permit trial related monitoring, audits, IRB/IEC reviews providing direct access to source data/documents.

The data will be recorded on a validated database using CRSWeb. The database file will be stored on password protected hospital computers. No names will be recorded. Patients will be identified by their study code.

14.2 Data collection

The study Clinical Trial Administrator will maintain the electronic database. CRFs and SAE forms must be completed by the Investigator or an authorised member of the research team. The SAE form must be co-signed by the Investigator (see section 11.1 for further details).

Data reported on each form should be consistent with the source data. If information is not known, this much be clearly indicated on the form. All missing and ambiguous data will be clarified. All sections are to be completed before being submitted (with the exception of the SAE form). CRFs and SAE forms may be amended, as appropriate, throughout the duration of the trial. This will not constitute a protocol amendment.

In all cases it remains the responsibility of the Investigator to ensure that the CRF has been completed correctly and that the data are accurate.

14.3 Archiving

It is the responsibility of the Chief Investigator to ensure that all essential trial documentation and source records (e.g. correspondence with ethical committees, the protocol and its amendments, the patient identification list, the CRFs) will be stored according the NHS policy on the retention of research records for a minimum of 5 years following the end of the study.

15. Financing, Indemnity & Insurance

The following funding bodies will contribute for the conduct of the trial;

- NIHR RM Biomedical Research Centre

This is a single centre study which will be open at the Royal Marsden. No specific compensation arrangement exists for harmful events which might arise from participation in the study. However, the study is covered for negligent claims occurring within the NHS by Crown Indemnity. There is no pre-existing arrangement for non-negligent claims arising from the conduct of the study.

16. Publication Policy

Results of this trial will be submitted for publication in peer reviewed journals. Manuscripts will be prepared by the Chief Investigator, the statistician and other members of the research team at the Royal Marsden NHS Foundation Trust and the Institute of Cancer Research and authorship will be determined by mutual agreement, taking account the contribution made by each team member. Any publications and presentations prepared by Investigators must be reviewed and authorized by the Chief Investigator. Manuscripts must be submitted in a timely fashion and in advance of being submitted for publication, to allow time for review and resolution of any outstanding issues. Authors must acknowledge that the trial was performed with the support of the ICR/RMH.

17. Abbreviations

NRAG	National Radiotherapy Advisory Group
VMAT	volumetric modulated arc therapy
IMRT	intensity modulated radiotherapy
3DCRT	three- dimensional conformal radiotherapy
PBT	proton beam therapy
IGRT	image guided radiotherapy
ICRU	International Commission on Radiation Units and Measurements
kvCBCT	kilovoltage cone beam computed tomography
4DCT	four-dimensional computed tomography
4DMR	four-dimensional magnetic resonance
US	ultrasound
2DUS	two-dimensional ultrasound
3DUS	three-dimensional ultrasound
OAR	organs at risk
ITV	internal target volume
CTV	clinical target volume
IM	internal margin
PRV	planning risk volume
3DCT	three-dimensional computed tomography
MR	magnetic resonance
ABC	active breathing coordinator
AAPM	American Association of Physicists in Medicine
NIHR	National Institute for Health Research

CRF	case report form
RMH/ RM	Royal Marsden Hospital
ABC	active breathing co-ordinator
SAE	serious adverse event
IRB	institutional review board
ICH	International Council for Harmonisation of Technical Requirements for Registration of Pharmaceuticals for Human Use
COM	centre of mass
POI	point of interest
Gy	Gray
IV	intravenous

18. References

1. National Radiotherapy Implementation Group Report. Image Guided Radiotherapy (IGRT). Guidance for implementation and use. 2012
2. De Neve W, De Gersem W, Madani I. Rational use of intensity-modulated radiation therapy: the importance of clinical outcome. InSeminars in radiation oncology 2012 Jan 31 (Vol. 22, No. 1, pp. 40-49). WB Saunders.
3. Brandner ED, Wu A, Chen H, Heron D, Kalnicki S, Komanduri K, Gerszten K, Burton S, Ahmed I, Shou Z. Abdominal organ motion measured using 4D CT. International Journal of Radiation Oncology* Biology* Physics. 2006 Jun 1;65(2):554-60.
4. Wambersie, A., and T. Landgerg. "ICRU Report 62: Prescribing, Recording and Reporting Photon Beam Therapy." *ICRU Publ Bethesda MD* (1999).
5. Keall PJ, Mageras GS, Balter JM, Emery RS, Forster KM, Jiang SB, Kapatoes JM, Low DA, Murphy MJ, Murray BR, Ramsey CR. The management of respiratory motion in radiation oncology report of AAPM Task Group 76a). Medical physics. 2006 Oct 1;33(10):3874-900.
6. Korreman SS. Motion in radiotherapy: photon therapy. Physics in medicine and biology. 2012 Nov 20;57(23):R161.
7. Shankar S, Pham D, Gill S, Bressel M, Dng K et al. An analysis of respiratory kidney motion on four-dimensional computed tomography and its implications for stereotactic kidney radiotherapy. Radiotherapy Oncology 8 (2013): 248
8. Hallman JL, Mori S, Sharp GC, Lu HM, Hong TS, Chen GT. A four-dimensional computed tomography analysis of multiorgan abdominal motion. International Journal of Radiation Oncolgy*Biology*Physics. 2012 May 1:83(1):435-41
9. Bussels B, Goethals L, Feron M, Bielen D, Dymarkowski S, Suetens P et al. Respiration-induced movement of the upper abdominal organs: a pitfall for the three-dimensional conformal radiation of pancreatic cancer. Radiotherapy and Oncology. 2003 Jul 31;68(1):69-74
10. Moerland MA, Van den Bergh AC, Bhagwandien R, Janssen WM, Bakker CJ, Lagendijk JJ et al. The influence of respiration induced motion of the kidneys on the accuracy of radiotherapy treatment planning, a magnetic resonance imaging study. Radiotherapy and Oncology. 1994 Feb 28;30(2):150-4
11. Panandiker AS, Sharma S, Naik MH, Wu S, Hua C, Beltran C, Krasin MJ, Merchant TE. Novel assessment of renal motion in children as measured via four-dimensional computed tomography. International Journal of Radiation Oncology* Biology* Physics. 2012 Apr 1;82(5):1771-6.
12. Nazmy MS, Khafaga Y, Mousa A, Khalil E. Cone beam CT for organs motion evaluation in pediatric abdominal neuroblastoma. Radiotherapy and oncology. 2012 Mar 31;102(3):388-92.
13. Huijskens SC, van Dijk IW, de Jong R, Visser J, Fajardo RD, Ronckers CM, Janssens GO, Maduro JH, Rasch CR, Alderliesten T, Bel A. Quantification of renal and diaphragmatic interfractional motion in pediatric image-guided radiation therapy: A multicenter study. Radiotherapy and Oncology. 2015 Dec 31;117(3):425-31.
14. HR-NBL-1/SIOPEN protocol.
15. Fargier-Voiron M, Bolsa-Ferruz M, Presles B, Pommier P, Munoz A, Rit S, Sarrut D, Biston MC. Feasibility of image guided radiotherapy based on ultrasound modality for prostate inter and intra fraction motion. Physica Medica: European Journal of Medical Physics. 2014 Jan 12;30:e123.
16. Yu Y, Molloy JA, Acton ST. Segmentation of the prostate from suprapubic ultrasound images. Medical physics. 2004 Dec 1;31(12):3474-84.
17. Scarbrough TJ, Golden NM, Ting JY, Fuller CD, Wong A, Kupelian PA, Thomas CR. Comparison of ultrasound and implanted seed marker prostate localization methods: Implications for image-guided radiotherapy. International Journal of Radiation Oncology* Biology* Physics. 2006 Jun 1;65(2):378-87.

18. Brock KK, Dawson LA. Adaptive management of liver cancer radiotherapy. In Seminars in radiation oncology 2010 Apr 30 (Vol. 20, No. 2, pp. 107-115). WB Saunders.
19. Boda-Heggemann J, Mennemeyer P, Wertz H, Riesenacker N, Küpper B, Lohr F, Wenz F. Accuracy of ultrasound-based image guidance for daily positioning of the upper abdomen: an online comparison with cone beam CT. International Journal of Radiation Oncology* Biology* Physics. 2009 Jul 1;74(3):892-7.
20. Fuss M, Salter BJ, Cavanaugh SX, Fuss C, Sadeghi A, Fuller CD et al. Daily ultrasound-based image-guided targeting for upper abdominal malignancies. International Journal of Radiation Oncoloyg*Biology*Physics 2004 59(4):1245-1256
21. Kupelian, Patrick et al. Magnetic Resonance–Guided Adaptive Radiotherapy: A Solution to the Future. Seminars in Radiation Oncology 24(3), 227 – 232.
22. Lagendijk, Jan J.W. et al. The Magnetic Resonance Imaging–Linac System. Seminars in Radiation Oncology 24 (3) 207 2014.
23. Brock J, McNair HA, Panakis N, Symonds-Tayler R, Evans PM, Brada M. The Use of the Active Breathing Coordinator Throughout Radical Non–Small-Cell Lung Cancer (NSCLC) Radiotherapy. International Journal of Radiation Oncology* Biology* Physics. 2011 Oct 1;81(2):369-75.
24. McNair HA, Brock J, Symonds-Tayler JR, Ashley S, Eagle S, Evans PM, Kavanagh A, Panakis N, Brada M. Feasibility of the use of the Active Breathing Co ordinator™(ABC) in patients receiving radical radiotherapy for non-small cell lung cancer (NSCLC). Radiotherapy and Oncology. 2009 Dec 31;93(3):424-9.
25. Eccles C., Brock KK, Bissonnette JP, Hawkins M, Dawson LA. Reproducibility of liver position ising active breathing coordinator for liver cancer radiotherapy. International Journal Radiation Oncology Biology Physics 64(3) 751-759.
26. Claude L, Malet C, Pommier P, Thiesse P, Chabaud S, Carrie C. Active breathing control for Hodgkin's disease in childhood and adolescence: feasibility, advantages, and limits. International Journal of Radiation Oncology* Biology* Physics. 2007 Apr 1;67(5):1470-5.
27. Wysocka B, Kassam Z, Lockwood G, Brierley J, Dawson LA, Buckley CA, Jaffray D, Cummings B, Kim J, Wong R, Ringash J. Interfraction and respiratory organ motion during conformal radiotherapy in gastric cancer. International Journal of Radiation Oncology* Biology* Physics. 2010 May 1;77(1):53-9.
28. Marks, L.B., Yorke, E.D., Jackson, A., Ten Haken, R.K., Constine, L.S., Eisbruch, A., Bentzen, S.M., Nam, J. and Deasy, J.O., 2010. Use of normal tissue complication probability models in the clinic. International Journal of Radiation Oncology* Biology* Physics, 76(3), pp.S10-S19.

18. Appendix 1

18.1 MRI acquisition procedure

Planning MR scans will be acquired for 10 patients in the Radiotherapy Cohort. These scans will be performed at 1.5T. Patients will be assessed for contraindications to MRI and intravenous contrast. A standard safety check for entry into the magnet will be performed as per hospital policy and intravenous access, if required, will be secured. Standard MRI exclusion criteria apply (section 6.2).

Following positioning on the scanner couch the relevant sequences will be obtained (Table 2). The superior-inferior extent of the region of interest (ROI) will be identified using the anatomical T1-weighted (T1W) and T2-weighted (T2W) images. A 3D volume will be positioned at the centre of the ROI.

The scans will be transferred to the treatment planning system Raystation® (RaySearch laboratories).

Table 2: MR sequence acquisition

	Sequence
Paediatric abdomen	T1+C, T2W and motion sequence

18.2 Exploratory Endpoints

Secondary Endpoints CCR Trial No. 4477

1. Creation of library of atlases for each tumour site to facilitate automated image segmentation for delineation of tumour volumes and organs-at-risk.
2. Determine automated methods for real-time registration and segmentation of MRI data obtained during treatment with the images employed for treatment planning.
3. Establish rapid and automatic calibration techniques to obtain the electron density values required for radiotherapy planning from MRI data.
4. Creation of library of treatment plans based on specific anatomy to facilitate rapid automated daily online planning for adaptive RT.
5. Assessment of the impact of specific features of the integrated MR Linac technology on treatment-planning strategies and plan quality.

18.3 Develop and validate MR protocols across the radiotherapy treatment pathway

The MRI scans acquired in the study will be used to create a library of GTV (when applicable), CTV and OAR structures sets and treatment plans. This will be used to validate software for automated CT-MR image fusion/segmentation, including automated methods for real-time registration and segmentation from MR data obtained during treatment with the images employed for treatment planning. This will be used to facilitate rapid automated daily online planning for adaptive radiotherapy.

The MR library acquired will be used to validate algorithms for rapid and automatic calibration for the tissue electron density values required for radiotherapy planning. It will be used to assess the impact of specific features of the integrated MR Linac technology on treatment-planning strategies and plan quality. This information will be used to develop clinically applicable dosimetry protocols and methods for patient-specific verification of delivered doses in a CT-MR and MR only workflow.

The image and plan library will be securely stored in password protected computers in the department of radiotherapy and medical physics at RMH.

Clinical Oncology 31 (2019) 50e57

Contents lists available at ScienceDirect

Clinical Oncology

journal homepage: www.clinicaloncolo g yon line.net

Overview

Adopting Advanced Radiotherapy Techniques in the Treatment of Paediatric Extracranial Malignancies: Challenges and Future Directions

N.A. Lavan *, F.H. Saran y, U. Oelfke z, H.C. Mandeville y

* The Institute of Cancer Research, Sutton, UK
y The Royal Marsden NHS Foundation Trust, Sutton, UK
z Joint Department of Physics at the Institute of Cancer Research and the Royal Marsden NHS Foundation Trust, Sutton, UK

Received 25 May 2018; accepted 1 August 2018

Abstract

Geometric uncertainties in radiotherapy are conventionally addressed by defining a safety margin around the radiotherapy target. Misappropriation of such margins could result in disease recurrence from geometric miss or unnecessary irradiation of normal tissue. Numerous quantitative organ motion studies in adults have been published, but the first paediatric-specific studies were only published in recent years. In the very near future, intensity-modulated proton beam therapy and magnetic resonance-guided radiotherapy will be clinically implemented in the UK. Such techniques offer the ability to deliver radiotherapy to the pinnacle of precision and accuracy, if geometric uncertainty relating to internal organ motion and deformation can be optimally managed. The optimal margin to account for internal organ motion in children remains largely undefined. Continuing efforts to characterise motion in children and young people is necessary to optimally define safety margins and to realise the full potential of intensity-modulated radiotherapy, magnetic resonance-guided radiotherapy and intensity-modulated proton beam therapy. This overview offers a timely review of published reports on paediatric organ motion, in anticipation of the increasing application of advanced radiotherapy techniques in paediatric radiotherapy.

Key words: IMRT; motion; MR-guided radiotherapy; paediatric; radiotherapy; respiratory

Statement of Search Strategies Used and Sources of Information

References for this review were identified by conducting a search, using PubMed and Medline, with the following words: paediatric/pediatric, radiotherapy, motion, respira- tory, proton, 4DCT, MR-guided, magnetic resonance image, ultrasound. The search included meeting abstracts and was restricted to papers available in English. Further references were identified following a manual search of the reference list of included articles. Identified studies were first screened by title and/or abstract with a further full-paper screening to generate the final list of publications relevant to the scope of this review.

Author for correspondence: N.A. Lavan, The Institute of Cancer Research, 15 Cotswold Road, Sutton SM2 5NG, UK.
E-mail address: naomi.lavan@icr.ac.uk (N.A. Lavan).

Introduction

A diagnosis of cancer in infants and children under 18 years of age is rare; representing <1% of all cancer cases in the UK from 2013 to 2015, although a 13% overall increase in incidence since the early 1990s has been reported [1]. About
40e50% of children diagnosed with cancer will receive radiotherapy as part of their first-line treatment [2].
The prognosis is excellent for most, with childhood cancer survival in the UK doubling over the last 40 years. Today, 80% of patients survive 5 years or more and 50% survive 10 years or more [1]. For those patients who have an excellent prognosis and in whom radiotherapy is indicated, such as Hodgkin lymphoma, radiotherapy treatment vol- umes need to include involved sites either in the thorax, abdomen or pelvis; in some cases, radiotherapy volumes encompass all three anatomical regions. Conversely, for patients with diagnoses of metastatic neuroblastoma and

https://doi.org/10.1016/j.clon.2018.08.020

atively poor.
All survivors of childhood cancer live with a real risk of treatment-related morbidity and mortality. The use of radiotherapy as part of the multimodal

treatment of child- hood cancer is risk stratified and/or response-adapted wherever possible in order to minimise the exposure of patients to irradiation and its potential late effects. Con- siderations for those responsible for delivering paediatric radiotherapy revolve around how best to minimise radio- therapy late effects for long-term survivors while max- imising disease control and the chance of cure in those for whom prognosis remains poor.

The ability to deliver highly conformal radiotherapy on available treatment platforms is approaching the technical limits of precision. Reduced volumes of normal tissue irra- diated as a result of intensity-modulated radiotherapy (IMRT) have translated into clinical benefits in several adult tumour sites [3]. For children and young people in whom radiotherapy is deemed essential, it is highly recommend- able that advanced treatment delivery techniques are made available where appropriate [4]. According to the ICRU62 report, the planning treatment volume (PTV) for photon treatment techniques comprises a set-up margin and an internal margin [5], designed to take into account potential sources of geometric uncertainty in treatment delivery [6]. The conventional approach to planning for much of paedi- atric radiotherapy was to use parallel opposed beam ar- rangements. Such beam arrangements offer a buffer to changes in internal organ position during treatment that is lost when techniques with highly conformal, complex dose distributions and steep dose gradients are introduced. As a consequence, inadequate safety margins in the latter setting could result in relapse due to geographical misses. Conversely, overly generous margins could negate the po- tential benefits of enhanced normal tissue sparing.

In this era of ever-increasing dose conformality in radiotherapy it is of the upmost importance to develop greater understanding of the components of geometric uncertainty that are particular to children and young peo- ple. Pragmatically adopting margins derived from adult organ motion studies for all patients under 18 years is predictably suboptimal. As we look towards the establish- ment of intensity-modulated proton beam therapy (IMPT) and magnetic resonance-guided radiotherapy (MRGRT) services within the UK, there is a need to quantify internal organ motion for extracranial tumour sites in children and young people, and evaluate its potential impact on radio- therapy delivery to ensure delivery of the best possible dose distributions with the steepest dose gradients at normal tissue/target interfaces.

Organ Motion and its Potential Impact on Radiotherapy

The American Association of Physicists in Medicine (AAPM) Task Group 76 reports on the management of res- piratory motion in radiotherapy and identifies paediatrics

knowledge on respiratory motion patterns and treatment implications is absent or scarce [7]. Assessments of geo- metric uncertainty in children and young people for intra- cranial/head and neck [8e14] and extracranial [15e21] tumour sites have been reported. Extracranial sites are predominantly upper abdominal, reflecting the anatomical site of the two common paediatric extracranial malig- nancies requiring radiotherapy: neuroblastoma and Wilms'

tumour.

Interfraction set-up uncertainties for the paediatric abdomen have been demonstrably reduced with the inte- gration of daily low-dose (1 cGy) megavoltage cone-beam computed tomography (CBCT); reducing set-up uncer- tainty from 5.6, 5.2 and 5.2 mm to 1.7, 2.1 and 1.5 mm in the superior/inferior, anterior/posterior and right/left di- rections, respectively, compared with weekly imaging [15]. As patient set-up uncertainties reduce, it is important to adequately account for motion uncertainties, as they will represent the limiting factors in treatment accuracy [7].

Target position in the thorax and upper abdomen is affected primarily by respiratory-related organ motion (RROM), with contribution from cardiac pulsation, peri- stalsis and gastrointestinal filling or emptying depending on anatomical location [22e24]. In adults, intrafraction motion (organ motion and set-up error combined) has been shown to have a negative effect on photon dose distribu- tions due to dose 'blurring' and interplay effects [7,25]. The potential degradation of the planned dosimetry will be influenced by factors such as the magnitude of motion, fractionation schedule, beam delivery (static versus dy- namic) and beam-on time. Mitigating RROM is challenging due to breathing cycle and amplitude irregularities, target drift and interfraction reproducibility of organ motion that is measured days to weeks before treatment starts [7]. The interplay effect is potentially greater for IMPT and, impor- tantly, it is not only target motion that can perturb proton therapy dose distributions, but rather motion of any tissue present in the beam path that can impact range uncertainty in proton therapy delivery [26].

As part of the multimodal treatment of childhood cancer, radiotherapy is often delivered after surgery; organ motion is measured as a surrogate for tumour bed motion in the absence of macroscopic tumour. Four studies, median 35 paediatric patients (range 10e45), have used CBCT to quantify interfraction motion of the kidneys [16,18,20]; liver [20] and diaphragm [16e18] (Table 1). These studies show that motion is greatest in the superior/inferior direction; confirming adult organ motion findings. One study, comparing 35 paediatric with 35 adult patients, showed that median kidney motion in children was statistically significantly smaller than in adults; 2.8, 2.9 mm and 5.6, 5.2 mm for median vector lengths for right and left kidney, respectively ($P < 0.05$) [16].

Intrafraction organ motion in the abdomen has been quantified using four-dimensional computed tomography and magnetic resonance imaging (4DCT and 4DMR) in a median of 20 patients (range 15e35) [19,21,27]. These studies show that intrafraction displacement occurs, in

order of decreasing magnitude, superior/inferior > anterior/ posterior > right/left with mean superior/inferior dis- placements reported for the right and left kidney, liver, spleen and diaphragm; 1.9e4.7 mm, 1.4e4.8 mm, 3.2e6.8 mm, 3.0e6.9 mm and 3.6e9.6 mm, respectively, and no more than 2e3 mm anterior/posterior and right/left (Table 2).

Young children having radiotherapy often require gen- eral anaesthesia for treatment. Van Dijk et al. [16] reported no difference in interfraction kidney motion between five children under general anaesthesia and seven similarly aged children not under general anaesthesia (3.1e7.6 years; 3.3e7.9 years, respectively), adjusted $P > 0.007$. 4DCT and

4DMR measures of intrafraction motion are numerically smaller in patients categorised according to general anaesthesia (age ranges <9 versus 9e18 years) [19,21] (Table 2). Huijsken et al. [17] showed that intrafraction variation in diaphragm displacement was statistically significantly smaller for a subset of anaesthetised children compared with non-anaesthetised children of similar ages (n ¼ 7; 2e11 years, n ¼ 12; 3e10 years); 1.6 mm versus 2.4 mm, respectively, P < 0.05, but the mean amplitude and interfractional variation of diaphragm motion did not differ between the groups [17].
Attempts to correlate organ motion with patient vari- ables have been made in the pursuit of a variable predictive of 'significant' organ motion in paediatric patients to avoid acquiring pretreatment 4DCT on all patients. Estimates of a population-based paediatric-specific margin would also aid radiotherapy departments without access to four- dimensional imaging, noting that a significant proportion of childhood cancers occur in low-to middle-income countries [4]. No consistently significant correlations be- tween organ motion and patient-related variables (age, height, weight, body mass index) have been established so far [9e31]. Huijskens et al. showed a significant but weak correlation between age, height, weight and mean dia- phragm amplitude (Spearman's P ¼ 0.40, 0.45, 0.33, P value
0.007, 0.03, 0.002, respectively), suggesting that patient- related factors explain only a small proportion of the dif- ferences between patients. Interpatient variation is a persistent finding in all studies of both intra- and inter-fraction organ motion, suggesting that motion is patient specific, even under general anaesthesia and an individu- alised approach to motion assessment is required.

Individualised Motion Assessment for Paediatric Radiotherapy

Techniques to address RROM require individualised motion assessment before treatment and 4DCT is the cur- rent gold standard in adult radiotherapy planning. Methods for image acquisition and sorting, using phase- or amplitude-based binning techniques, have been previously described in detail for adults [28e30]. 4DCT still has accepted limitations, with artefacts occurring despite 4DCT image reconstruction techniques, due to variability in amplitude and frequency of breathing cycles within

characterise respiratory-related motion is potentially limited [32,33]. The stability of respiratory motion as measured on a single 4DCT in children is yet to be estab- lished. A major factor limiting adoption of 4DCT for paedi- atric radiotherapy planning is the associated radiation dose;
4DCT protocols are often acquired at twice the dose of standard computed tomography and dose exposure in children and young people is a prime consideration due to the risk of secondary malignancy induction. The adaptation of paediatric-specific imaging protocols has in the past been optimised for 3DCT-based planning and accepted a trade- off between lower dose and slightly reduced image qual- ity. Following this rationale, published low-dose protocols can acquire 4DCT at 1.6 times the dose of 3DCT [27]. Although the clinical benefit of incorporating individualised motion

information into paediatric radiotherapy planning has yet to be defined, we would argue that accepting reduced image quality, although practical when treatment portals were defined by bone anatomy alone, is contradic- tory if the purpose of volumetric, contrast-enhanced im- aging with individualised motion assessment is to improve accuracy and precision in paediatric treatment delivery.

Individualised ICRU62 Appropriate Planning Volumes for Paediatric Radiotherapy

In adults, a common approach to motion management is to encompass the entire magnitude of motion for a partic- ular patient within the PTV; a 'motion encompassing technique' [7]. 4DCT is used to determine the target position during the entire breathing cycle, which in turn defines a volume that encompasses the full extent of target excur- sion; the internal target volume (ITV) [5]. Including the entire magnitude of motion can be seen as a conservative approach [34]. Alternatively, the mid-ventilation (MidV) concept extracts the target's time-averaged position and its standard deviation from 4DCT and motion is then consid- ered a random positioning error in a probabilistic safety margin calculation [35]. MidV, with an online set-up correction strategy, has been shown to reduce PTV size by up to 30% compared with an ITV approach in adult lung radiotherapy with a reported 98% local control rate at a median follow-up of 21.9 months [36,37]. MidV has been described in planning studies in the upper abdomen despite the different tissue composition resulting in a narrower beam penumbra than is the case in lung [38,39]. Given the relatively small motion trajectory of paediatric upper abdominal organs, adopting an ITV approach is a reasonable initial step, but further work investigating MidV planning for paediatric radiotherapy should be undertaken.

Daily verification of target positioning is necessary to avoid geometric misses in treatment delivery [39]. Bone anatomy is recognised to be a poor surrogate for tumour position in the lung, abdomen and pelvis [40]. Interfraction variation in target position in many adult tumour sites is addressed using online or offline soft tissue verification protocols. Paediatric radiotherapy in-room image guidance uses low-dose imaging protocols based on bone anatomy. Such protocols have comparatively poor soft tissue contrast limiting the ability to perform a soft tissue match and making interfraction changes in target shape challenging to address. In the absence of non-ionising image guidance, a soft tissue match will be necessary to implement motion management techniques and the associated increased im- aging dose would be offset if improved localisation and reduction in irradiation of adjacent normal tissues enhances local control and reduces normal tissue toxicity. It is clear from previous reports that centres are already looking to adopt such an image-guided radiotherapy (IGRT) approach and efforts to harmonise IGRT use in paediatric radio- therapy and collate prospective data to inform protocols and evaluate outcomes should be a priority [41].

Motion management strategies are not limited to motion-encompassing

approaches [7]. Advanced photon planning techniques, using non-coplanar beam arrange- ments have been described that reduce dose delivered to lung and breast tissue in Hodgkin lymphoma [42]. The excellent prognosis associated with Hodgkin lymphoma at all stages makes the risk reduction for radiotherapy- induced second malignancy and cardiovascular disease in survivors important [43]. Motion management strategies using inspiratory breath holding have been described in patients with mediastinal Hodgkin lymphoma. Such studies rarely include patients under the age of 18 years, although a single planning study has described the dosimetric advan- tage of active breathing coordinator and deep inspiration breath hold in patients aged 13e18 years with mediastinal Hodgkin lymphoma [44].

Current Status of Advanced Radiotherapy Techniques and Associated Challenges in Children and Young People

Evidence for paediatric IMRT is largely limited to non- randomised and dosimetric planning studies predomi- nantly in intracranial and head and neck sites [45]. The use of more beams (or arc in the case of rotational IMRT), compared with conformal photon and proton therapy treatments, achieves dose distributions that conform to irregularly shaped targets and is implemented in paediatric cases where greater conformity gives target coverage that, if delivered using a conventional approach, would have exceeded normal tissue tolerance [46]. IMRT reduces the volume of normal tissue receiving a high dose, the dose region implicated in the development of many normal tis- sue toxicities, but comes at the price of a low-dose bath. An increased integral dose has been postulated to increase the risk of second malignancy induction, although there is a realisation that second cancers often arise in the high-dose region [46,47]. In cases where the improved high-dose conformity achieved with IMRT is substantial, the compromise of increased integral dose is considered acceptable and IMRT has demonstrably reduced grade 3 and

4 ototoxicity in medulloblastoma survivors and reduced mucositis in the treatment of childhood nasopharyngeal carcinoma [48]. In the UK, an open phase II study is inves- tigating the role of rotational IMRT, and dose escalation from 21 to 36 Gy, in high-risk abdominal neuroblastoma, highlighting the potential role for advanced photon tech- niques in the abdomen for a cohort of patients where renal tolerance can be dose-limiting [49].

Stereotactic body radiotherapy (SBRT) and stereotactic radiosurgery (SRS) techniques incorporate precise immo- bilisation and localisation imaging allowing the use of small or minimal PTV margins. Highly conformal dose distribu- tions with relative sparing of adjacent normal tissues en- ables delivery of higher biologically effective ablative doses of radiotherapy in a single or few fractions that, for some adult tumours, result in local control rates comparable with surgery. Historically, studies in children exploited the ste- reotactic set-up in order to apply smaller PTV margins while maintaining the benefits of fractionation on normal tissue recovery. This paradigm has been used without detriment in local control in low-grade glioma, medulloblastoma,

craniopharyngioma and intracranial germ cell tumours [50e52]. Ablative strategies in children whose growing tissues are inherently more radio- sensitive to radiotherapy are evolving. The largest case series of extracranial SBRT in
14 patients with metastatic and recurrent Ewing and oste- osarcoma reports its feasibility as a treatment paradigm although not without risk of grade 2 and 3 toxicity [53]. Prospective studies will be required to define treatment standards and aid patient selection for use of SBRT/SRS in children and young people.
Current estimates suggest that about 250 paediatric pa- tients per year in the UK will receive proton therapy [54]. Proton therapy (passively scattered and intensity modu- lated) reduces integral dose by a factor of 2e3 compared with IMRT and IMPT has the potential to equal the dose conformity achieved by IMRT [55]. This dosimetric advan- tage is expected to translate into less treatment-related morbidity and second malignancy induction. Proton ther- apy delivery is currently associated with a number of technical and physical limitations, such as the magnitude of the lateral penumbra, uncertainties in particle range esti- mates and relative biological effectiveness [55]. A range uncertainty of 2.5e3.5% of depth of penetration, with an additional margin of 1e3 mm for delivery system, biological and geometric uncertainties translating into a distal and proximal CTV margin of 8 mm at a depth of 20 cm, is representative of current passive scattering proton therapy techniques [26]. The consequent dosimetric effect on skin dose and permanent alopecia in patients receiving cranio- spinal proton therapy for medulloblastoma has been described [56]. Such a margin exceeds, depending on anatomical location, safety margins commonly applied in photon radiotherapy. Despite the greater vulnerability of proton therapy to geometric uncertainties, kilovoltage planar imaging was up until recently the only available in- room image guidance, although kilovoltage CBCT capabil- ities are now commercially available on new systems. Following the opening of high energy proton therapy

expand beyond what is currently approved for funding [54]. Realising the maximal benefits of IMPT treatments in the presence of inter- and intrafraction organ motion in the abdomen and thorax will be challenging.

Future Directions

There is potential for magnetic resonance to positively impact the radiotherapy delivery pathway from target delineation and planning through to treatment delivery. Magnetic resonance sequences have been used to assess organ motion in adults and, more recently, in children [21] and could be substituted in place of 4DCT for individualised motion assessment without additional imaging dose. Hybrid MRGRT platforms, integrating clinical quality mag- netic resonance imaging with a modern linear accelerator, are in active development [57e60]. The MRIdian system (ViewRay Inc., Oakwood Village, OH, USA) has been clini- cally operational since 2014 and prototype Elekta magnetic resonance linac machines, installed in two centres in the UK, will be clinically implemented this year. The delivery of real-time MRGRT is a reality and offers the opportunity to expand the integration of in-room IGRT for children and

young people without additional ionising exposure risk and enable the reduction of PTV margins. To date, limited published data are available to describe MRGRT in children and initial clinical use of the Elekta MRLinac in the UK will be within the setting of a research study that specifically includes a paediatric and young patient treatment cohort (NCT02973828) [61].

Ultrasound imaging systems offer non-ionising, real-time volumetric imaging with excellent soft-tissue contrast. Platforms are in development that offer two-, three- and four-dimensional anatomical and functional imaging capa- bilities for inter- and intrafraction imaging [62]. Integration of ultrasound into IGRT for upper abdominal sites, primarily liver, has been described [63e65], including one paediatric paper reporting its use in a cohort of patients with neuro-blastoma comparing ultrasound quantified set-up couch shifts to that of CBCT-based shifts [15]. Finding that ultra- sound localisation did not correlate with CBCT shifts, the authors cited user-dependency and user-experience as po-tential barriers to implementing ultrasound. However, as a non-ionising imaging modality it should be a research pri- ority for paediatric radiotherapy and proof of principle two- and three-dimensional ultrasound measurement of kidney motion is currently being investigated in a non-randomised phase II study exploring four-dimensional imaging platforms in children and young people (IRAS project ID 195329).

Conclusion

The highest incidence of cancer occurs in children younger than 5 years, falls among 5e14 year olds, but rises again in young people over the age of 15 years. Children and

tive rarity of a cancer diagnosis in childhood, represents a challenge in the development of robust research strategies. Multinational clinical trials, with centralised radiotherapy quality assurance, are necessary for sufficient power to detect clinically significant results from therapeutic strate- gies in children and young people. Recruitment over extended periods of time is necessary such that radio- therapy guidance may no longer be deemed current when patient accrual is completed. This challenges valid inter-pretation of results in light of rapidly changing radiotherapy practices. This will be the greatest challenge in evaluating the exciting opportunities for additional clinical benefit to young patients made possible with emerging competing platforms and radiotherapy techniques. The impetus to develop proton beam therapy, MRGRT and stereotactic ablative body radiotherapy in the UK in a co-ordinated manner through the implementation of Cancer Research UK Advanced Radiotherapy Technologies Network (ART- NET) has been recently outlined in this journal [66]. Pae- diatric radiotherapy is uniquely placed, given its present centralisation, to contribute to parallel advances in children and young people. Future national and multinational studies will be important in maximising their benefits without compromising current patient outcomes. The potentially increasing complexity of treatment delivery arguably warrants further concentration of services in order to consolidate expertise in the application of these techniques.

Conflict of interest

The authors declare no conflict of interest.

Acknowledgement

The ICR and RMH work in partnership as a National Institute of Health Research (UK) Biomedical Research Centre. We acknowledge Cancer Research UK (CRUK) Network Accelerator Award A21993 (ARTNET), CRUK pro- gramme grant C33589/A19727 and MRC programme grant MR/M009068/1. NL's position is jointly funded by the Children's and Neuro-oncology Unit funds at the RMH NHS Foundation Trust.

References

[1] Cancer Research UK. Children's cancer statistics. Available at: http://www.cancerresearchuk.org/health-professional/ cancer-statistics/childrens-cancers#heading-Zero.
[2] Royal College of Radiologists. Radiotherapy dose fractionation e paediatric radiotherapy 2016. Available at: https://www.rcr. ac.uk/system/files/publication/field_publication_files/ bfco163_9_paediatric.pdf.
[3] Veldeman L, Madani I, Hulstaert F, De Meerleer G, Mareel M, De Neve W. Evidence behind use of intensity-modulated radiotherapy: a systematic review of comparative clinical studies. Lancet Oncol 2008;9:367e375.

[4] Kortmann R-D, Freeman C, Marcus K, Claude L, Dieckmann K, Halperin E, et al. Paediatric radiation oncology in the care of childhood cancer: a position paper by the International Pae- diatric Radiation Oncology Society (PROS). Radiother Oncol 2016;119(2):357e360.
[5] Landberg T, Chavaudra J, Dobbs J, Gerard JP, Hanks G, Horiot JC, et al. Report 62. J ICRU 1999;32(1).
[6] British Institute of Radiology. Geometric uncertainties in radiotherapy: defining the planning target volume. London: British Institute of Radiology; 2003.
[7] Keall PJ, Mageras GS, Balter JM, Emery RS, Forster KM, Jiang SB, et al. The management of respiratory motion in ra- diation oncology report of AAPM Task Group 76a). Med Phys 2006;33(10):3874e3900.
[8] Beltran C, Pegram A, Merchant TE. Dosimetric consequences of rotational errors in radiation therapy of pediatric brain tumor patients. Radiother Oncol 2012;102(2):206e209.
[9] Beltran C, Krasin MJ, Merchant TE. Inter- and intrafractional positional uncertainties in pediatric radiotherapy patients with brain and head and neck tumors. Int J Radiat Oncol Biol Phys 2011;79(4):1266e1274.
[10] Beltran C, Merchant TE. Dependence of intrafraction motion on fraction duration for pediatric patients with brain tumors. J Appl Clin Med Phys

2011;12(4):3609.
[11] Beltran C, Naik M, Merchant TE. Dosimetric effect of target expansion and setup uncertainty during radiation therapy in pediatric craniopharyngioma. Radiother Oncol 2010;97(3):
399e403.
[12] Beltran C, Naik M, Merchant TE. Dosimetric effect of setup motion and target volume margin reduction in pediatric ependymoma. Radiother Oncol 2010;96(2):216e222.
[13] Beltran C, Trussell J, Merchant TE. Dosimetric impact of intrafractional patient motion in pediatric brain tumor pa- tients. Med Dosim 2010;35(1):43e48.
[14] Altunbas C, Hankinson TC, Miften M, Tello T, Plimpton SR, Stuhr K, et al. Rotational setup errors in pediatric stereotactic radiation therapy. Pract Radiat Oncol 2013;3(3):194e198.
[15] Beltran C, Pai Panandiker AS, Krasin MJ, Merchant TE. Daily image-guided localization for neuroblastoma. J Appl Clin Med Phys 2010;11(4):3388.
[16] van Dijk IW, Huijskens SC, de Jong R, Visser J, Fajardo RD, Rasch CR, et al. Interfractional renal and diaphragmatic posi- tion variation during radiotherapy in children and adults: is there a difference? Acta Oncol 2017;56:1065e1071.
[17] Huijskens SC, van Dijk IW, Visser J, Rasch CR, Alderliesten T, Bel A. Magnitude and variability of respiratory-induced dia- phragm motion in children during image-guided radio- therapy. Radiother Oncol 2017;123(2):263e269.
[18] Huijskens SC, van Dijk IWEM, de Jong R, Visser J, Fajardo RD, Ronckers CM, et al. Quantification of renal and diaphragmatic interfractional motion in pediatric image-guided radiation ther- apy: a multicenter study. Radiother Oncol 2015;117(3):425e431.
[19] Pai Panandiker AS, Sharma S, Naik MH, Wu S, Hua C, Beltran C, et al. Novel assessment of renal motion in children as measured via four-dimensional computed tomography. Int J Radiat Oncol Biol Phys 2012;82(5):1771e1776.
[20] Nazmy MS, Khafaga Y, Mousa A, Khalil E. Cone beam CT for organs motion evaluation in pediatric abdominal neuroblas- toma. Radiother Oncol 2012;102(3):388e392.
[21] Uh J, Krasin MJ, Li Y, Li X, Tinkle C, Lucas Jr JT, et al. Quanti- fication of pediatric abdominal organ motion with a 4- dimensional magnetic resonance imaging method. Int J Radiat Oncol Biol Phys 2017;99(1):227e237.
[22] Langen KM, Jones DTL. Organ motion and its management. Int
J Radiat Oncol Biol Phys 2001;50(1):265e278.

[23] Suh Y, Dieterich S, Cho B, Keall PJ. An analysis of thoracic and abdominal tumour motion for stereotactic body radiotherapy patients. Phys Med Biol 2008;53(13):3623e3640.
[24] van Herk M. Different styles of image-guided radiotherapy.
Semin Radiat Oncol 2007;17(4):258e267.
[25] Bortfeld T, Jiang SB, Rietzel E. Effects of motion on the total dose distribution. Semin Radiat Oncol 2004;14(1):41e51.
[26] Mohan R, Das IJ, Ling CC. Empowering intensity modulated proton therapy through physics and technology: an overview. Int J Radiat Oncol Biol

Phys 2017;99(2):304e316.
[27] Kannan S, Teo BK, Solberg T, Hill-Kayser C. Organ motion in pediatric high-risk neuroblastoma patients using four- dimensional computed tomography. J Appl Clin Med Phys
2017;18(1):107e114.
[28] Vedam SS, Keall PJ, Kini VR, Mostafavi H, Shukla HP, Mohan R.
Acquiring a four-dimensional computed tomography dataset using an external respiratory signal. Phys Med Biol 2003;
48(1):45e62.
[29] Rietzel E, Pan T, Chen GT. Four-dimensional computed to- mography: image formation and clinical protocol. Med Phys
2005;32(4):874e889.
[30] Keall P. 4-dimensional computed tomography imaging and treatment planning. Semin Radiat Oncol 2004;14(1):81e90.
[31] Korreman SS. Motion in radiotherapy: photon therapy. Phys
Med Biol 2012;57(23):R161eR191.
[32] Ge J, Santanam L, Noel C, Parikh PJ. Planning 4-dimensional computed tomography (4DCT) cannot adequately represent daily intrafractional motion of abdominal tumors. Int J Radiat Oncol Biol Phys 2013;85(4):999e1005.
[33] Lens E, van der Horst A, Kroon PS, van Hooft JE, Davila Fajardo R, Fockens P, et al. Differences in respiratory-induced pancreatic tumor motion between 4D treatment planning CT and daily cone beam CT, measured using intratumoral fidu- cials. Acta Oncol 2014;53(9):1257e1264.
[34] Mutaf YD, Brinkmann DH. Optimization of internal margin to account for dosimetric effects of respiratory motion. Int J Radiat Oncol Biol Phys 2008;70(5):1561e1570.
[35] Ehrbar S, Jo€hl A, Tartas A, Stark LS, Riesterer O, Klo€ck S, et al.
ITV, mid-ventilation, gating or couch tracking e a comparison of respiratory motion-management techniques based on 4D dose calculations. Radiother Oncol 2017;124(1):80e88.
[36] Wolthaus JWH, Sonke JJ, van Herk M, Damen EMF. Recon- struction of a time-averaged midposition CT scan for radio- therapy planning of lung cancer patients using deformable registration. Med Phys 2008;35(9):3998e4011.
[37] Peulen H, Belderbos J, Rossi M, Sonke J-J. Mid-ventilation based PTV margins in stereotactic body radiotherapy (SBRT): a clinical evaluation. Radiother Oncol 2014;110(3):511e516.
[38] Velec M, Moseley JL, Dawson LA, Brock KK. Dose escalated liver stereotactic body radiation therapy at the mean respiratory position. Int J Radiat Oncol Biol Phys 2014;89(5):1121e1128.
[39] Lens E, van der Horst A, Versteijne E, van Tienhoven G, Bel A.
Dosimetric advantages of midventilation compared with in- ternal target volume for radiation therapy of pancreatic can- cer. Int J Radiat Oncol Biol Phys 2015;92(3):675e682.
[40] Brandner ED, Wu A, Chen H, Heron D, Kalnicki S, Komanduri K, et al. Abdominal organ motion measured using
4D CT. Int J Radiat Oncol Biol Phys 2006;65(2):554e560.
[41] Alcorn SR, Chen MJ, Claude L, Dieckmann K, Ermoian RP, Ford EC, et al. Practice patterns of photon and proton pediatric image guided radiation treatment: results from an Interna- tional Pediatric Research consortium. Pract

Radiat Oncol 2014;
4(5):336e341.
[42] Voong KR, McSpadden K, Pinnix CC, Shihadeh F, Reed V, Salehpour MR, et al. Dosimetric advantages of a 'butterfly'

phoma. Radiat Oncol 2014;9:94.
[43] Castellino SM, Geiger AM, Mertens AC, Leisenring WM, Tooze JA, Goodman P, et al. Morbidity and mortality in long- term survivors of Hodgkin lymphoma: a report from the Childhood Cancer Survivor Study. Blood 2011;117(6):
1806e1816.
[44] Claude L, Malet C, Pommier P, Thiesse P, Chabaud S, Carrie C.
Active breathing control for Hodgkin's disease in childhood and adolescence: feasibility, advantages, and limits. Int J Radiat Oncol Biol Phys 2007;67(5):1470e1475.
[45] Paulino AC. The promise of intensity modulated radiation therapy. Pediatr Blood Cancer 2016;63(9):1513e1514.
[46] Royal College of Radiologists. Good practice guide paediatric radiotherapy 2012. Available at: https://www.rcr.ac.uk/ publication/good-practice-guide-paediatric-radiotherapy; 2012.
[47] Hall EJ. Intensity-modulated radiation therapy, protons, and the risk of second cancers. Int J Radiat Oncol Biol Phys 2006;
65(1):1e7.
[48] Paulino AC, Lobo M, Teh BS, Okcu MF, South M, Butler EB, et al.
Ototoxicity after intensity-modulated radiation therapy and cisplatin-based chemotherapy in children with medulloblas- toma. Int J Radiat Oncol Biol Phys 2010;78(5):1445e1450.
[49] Gains JE, Stacey C, Rosenberg I, Mandeville HC, Chang YC, D'Souza D, et al. Intensity-modulated arc therapy to improve radiation dose delivery in the treatment of abdominal neu- roblastoma. Future Oncol 2013;9(3):439e449.
[50] Marcus KJ, Goumnerova L, Billett AL, Lavally B, Scott RM, Bishop K, et al. Stereotactic radiotherapy for localized low- grade gliomas in children: final results of a prospective trial. Int J Radiat Oncol Biol Phys 2005;61(2):374e379.
[51] Saran F, Baumert BG, Creak AL, Warrington AP, Ashley S, Traish D, et al. Hypofractionated stereotactic radiotherapy in the management of recurrent or residual medulloblastoma/ PNET. Pediatr Blood Cancer 2008;50(3):554e560.
[52] Minniti G, Saran F, Traish D, Soomal R, Sardell S, Gonsalves A, et al. Fractionated stereotactic conformal radiotherapy following conservative surgery in the control of craniophar- yngiomas. Radiother Oncol 2007;82(1):90e95.
[53] Brown LC, Lester RA, Grams MP, Haddock MG, Olivier KR, Arndt CA, et al. Stereotactic body radiotherapy for metastatic and recurrent Ewing sarcoma and osteosarcoma. Sarcoma
2014;2014:418270.
[54] Department of Health. National Proton Beam Therapy Service Development Programme - Strategic Outline Case 2012 [1/10/
2017]. Available at: https://www.gov.uk/government/uploads/

strategic-outline-case-16102012.pdf; 2012.
[55] Leroy R, Benahmed N, Hulstaert F, Van Damme N, De Ruysscher D. Proton therapy in children: a systematic review of clinical effectiveness in 15 pediatric cancers. Int J Radiat Oncol Biol Phys 2016;95(1):267e278.
[56] Min CH, Paganetti H, Winey BA, Adams J, MacDonald SM, Tarbell NJ, et al. Evaluation of permanent alopecia in pediatric medulloblastoma patients treated with proton radiation. Radiat Oncol 2014;9:220.
[57] Mutic S, Dempsey JF. The ViewRay System: magnetic resonance-guided and controlled radiotherapy. Semin Radiat Oncol 2014;24(3):196e199.
[58] Lagendijk JJW, Raaymakers BW, van Vulpen M. The magnetic resonance imagingelinac system. Semin Radiat Oncol 2014;
24(3):207e209.
[59] Keall PJ, Barton M, Crozier S. The Australian magnetic reso- nance imagingelinac program. Semin Radiat Oncol 2014;
24(3):203e206.
[60] Fallone BG. The rotating biplanar linacemagnetic resonance imaging system. Semin Radiat Oncol 2014;24(3):200e202.
[61] PRIMER. Available at: https://clinicaltrials.gov/ct2/show/NCT02973828?term¼MR&recrs¼ab&cntry¼GB&draw¼
2&rank¼16.
[62] Fontanarosa D, van der Meer S, Bamber J, Harris E, O'Shea T, Verhaegen F. Review of ultrasound image guidance in external beam radiotherapy: I. Treatment planning and inter-fraction motion management. Phys Med Biol 2015;60(3):R77eR114.
[63] Boda-Heggemann J, Mennemeyer P, Wertz H, Riesenacker N, Ku€pper B, Lohr F, et al. Accuracy of ultrasound-based image guidance for daily positioning of the upper abdomen: an online comparison with cone beam CT. Int J Radiat Oncol Biol Phys 2009;74(3):892e897.
[64] Bloemen-van Gurp E, van der Meer S, Hendry J, Buijsen J, Visser P, Fontanarosa D, et al. Active breathing control in combination with ultrasound imaging: a feasibility study of image guidance in stereotactic body radiation therapy of liver lesions. Int J Radiat Oncol Biol Phys 2013;85(4):1096e1102.
[65] Fuss M, Salter BJ, Cavanaugh SX, Fuss C, Sadeghi A, Fuller CD, et al. Daily ultrasound-based image-guided targeting for radiotherapy of upper abdominal malignancies. Int J Radiat Oncol Biol Phys 2004;59(4):1245e1256.
[66] Harrington K, Hall E, Hawkins M, Henry A, MacKay R, Maughan T, et al. Introducing the Cancer Research UK Advanced Radiotherapy Technologies Network (ART-NET). Clin Oncol 2017;29(11):707e710.

Appendix 2: Publications arising from this thesis

RADIATION TREATMENT PLANNING IN PEDIATRIC ONCOLOGY

Authors

Naomi A Lavan, Henry C Mandeville

Affiliation

Institute of Cancer Research and Royal Marsden Hospital NHS Foundation Trust, Sutton, United Kingdom

Keywords: Pediatrics
Radiation therapy
Radiotherapy treatment planning
Radiotherapy imaging
Pediatric stereotactic radiotherapy
Molecular radiotherapy
Brachytherapy

Abstract

Radiotherapy (RT) plays an important role in the multimodality treatment of a number of pediatric tumors, both in the curative and palliative settings. In general, treatment paradigms in pediatric oncology look to risk-stratify and response-adapt treatment for patients, with the overarching tenet of delivering the minimum treatment required for cure. This paradigm looks to minimize long-term sequelae in those treated at young ages; the majority of whom will be long-term survivors. The late consequences of radiotherapy, dependent on the treated site, can include cognitive, endocrine, growth, vascular, fertility effects and the induction of second malignancy.

In recent decades, RT treatment delivery techniques have become increasingly sophisticated. It is now possible to deliver complex treatments where the prescribed dose is sculpted to the target, and normal tissues are maximally spared moderate to high doses. This is achieved through increased accuracy and precision in target definition and the ability to better visualize the target during the course of treatment thereby reducing geometric uncertainties in treatment delivery. Imaging plays an integral role in the ability to deliver such accurate and precise RT treat- ment.

Introduction

In the discipline of radiation oncology the primary aim of treatment is to deli v- er ionizing radiation to the target while simultaneously minimizing dose delivered to adjacent normal tissues. The biological basis of RT includes cell and tissue- specific inherent radiation-sensitivity and the exploitation of the differences in tu- mor and normal tissue responses to ionizing RT. The balance between tumor con- trol probability (TCP) and normal tissue complication probability (NTCP) is often referred to as the therapeutic ratio.

The interaction of ionizing radiation within the cells of the body produce direct effects and, more commonly, indirect effects on DNA mediated by free hydroxyl radicals produced through the ionization of water. DNA damage can be lethal (double strand DNA breaks) or sub-lethal (single strand DNA breaks, DNA cross- links or base damage). Repair of sub-lethal damage in normal cells typically oc- curs within 6 hours and this forms the basis of fractionated delivery of RT. Nor- mal cells are able to repair such damage correctly whereas dysfunctional repair pathways are more likely to occur in tumor cells. Cells with cumulative chromo- somal aberrations from poorly repaired DNA damage usually undergo cell death either soon after exposure or during subsequent cell divisions.

In pediatric radiation oncology conventionally fractionated RT is delivered in five daily fractions of 1.5- 1.8Gy. The total prescribed dose is determined by the tumor type with doses ranging from as low as 10.5Gy for Wilms' tumor up to ~60Gy for some sarcomas and brain tumors. Prescribed dose and fractionation varies according to tumor type, tumor burden i.e. microscopic versus macroscopic disease and treatment intent (radical versus palliative). The need for RT in chil- dren and young people is always carefully balanced between therapeutic effect and the risk of treatment-related morbidity. The vast majority of pediatric RT treatments are prescribed according to national or international trial protocols or guidelines.

RT can be delivered by external beam RT (EBRT) using photons, electrons, protons or other particles, and internally; using brachytherapy and molecular RT . The following discussion will give an overview of these modalities with a primary focus on EBRT photon treatment as this is, at present, the most common mode of RT delivery for children and young people.

The radiotherapy planning process

The process of delivering a RT treatment course can be divided into three main parts; target definition, treatment planning and treatment delivery. Cross-sectional imaging is integral to all stages.

There are particular elements in pediatric RT planning that make the pathway

quite distinct from the treatment of adults. For example, very young children often require general anesthesia for simulation image acquisition and treatment. This generally applies to patients under the age of three, and for a significant proportion of patients aged between three and five years. This age range can vary significant- ly between centers depending on their equipment, treatment times and support staff; older children, or even teenagers and young adults, who are unable to com- ply with lying still for treatment due to learning or behavioral issues may also re- quire anesthesia. Play specialists play an important role in the preparation and support of children and young people for RT and their involvement can allow a child to proceed with treatment without the need for general anesthesia; this can have significant resource implications for a RT department.

Children are assumed to be inherently more radiation sensitive compared to adults and this is reflected in the use of lower doses per fraction and lower overall total doses compared to fractionation schedules used for adult cancers (1). Muscu- loskeletal late effects from RT can result in significant deformity so care is taken to irradiate vertebrae adjacent to a target volume homogenously to avoid future kyphosis or scoliosis. Radiation sensitivity also needs to be considered in the se- lection and modification of imaging parameters in order to minimize dose expo- sure from all imaging procedures as much as possible.

Common terms in RT treatment planning

Internationally accepted terminology in RT treatment planning and additional commonly used terms that are referred to in this chapter are summarized in the Table 1.

TABLE 1. GLOSSARY OF TERMS

EBRT	External beam RT
RTP	Radiotherapy planning scan
GTV	Gross tumor volume
CTV	Clinical target volume
ITV	Internal target volume
PTV	Planning target volume
PRV	Planning at risk volume
IM	Internal margin
SM	Setup margin
IGRT	Image guided radiotherapy
OAR	Organ at risk
Linac	Linear accelerator
MV	Megavoltage
KV	Kilovoltage
EPID	Electronic portal image dosimetry
CBCT	Cone beam computed tomography
MLC	Multileaf collimator

Guidance on conformal RT treatment planning and reporting is supplied by the

International Commission on Radiation Units and Measurements (ICRU). ICRU –
50, 62 and 83 were published in relation to conformal photon radiotherapy report- ing and planning (2-4).

The GTV is the macroscopic visible tumor mass as defined on clinical examination and/ or imaging. For many pediatric tumors, RT is given following surgery meaning that a GTV, according to the ICRU definition, may not be visible. In this instance, a 'virtual' GTV is reconstructed with reference to pre-operative imaging to define the areas of contact between tumor and surrounding normal tissues or- gans. The CTV represents the area of microscopic disease involvement; this is an anatomical expansion that can be confined by natural barriers of spread e.g. unin- volved bone and muscle. The PTV is a geometric expansion of the CTV and con- stitutes a safety margin to account for systematic and random uncertainties in pa- tient set-up relative to the treatment beam geometry (set-up margin) and in target position relative to the patient's bony anatomy (internal margin) (5). Convention- ally, large, population-based PTV margins are used to address such geometric uncertainty so that the clinical target volume (CTV) is positioned within the PTV with suitably high probability. The PTV can be defined by using mathematical 'margin recipes' that take such errors, for a representative patient population, into
account (6).

Imaging requirements for target definition

Once a multidisciplinary decision to treat a patient is made, and the patient has given written informed consent, the first step in the process is for the patient to have a RT planning (RTP) scan. This dataset is used to determine the target vol- ume for RT and to calculate treatment dosimetry. In pediatrics this step requires intensive coordination and communication between members of the multi- disciplinary team including radiographers, play specialists and anesthetists.

Computed tomography (CT) is the most common primary imaging modality used for this purpose. CT serves 2 important purposes, providing a three-dimensional (3D) representation of the tumor and patient's anatomy, and also al- lows direct computation of RT dose through the conversion of Hounsfield units to electron densities within treatment planning software (TPS) systems. The integra- tion of volumetric CT images into RT treatment planning pathways allows dose delivery to be conformed to the patient's anatomy; so called 3D conformal RT (3DCRT or CRT).

Despite significant technological developments within the field of radiation oncology, target delineation is well recognized as the weakest link in the precision and accuracy of the RT pathway (7, 8). The challenge of accurate target definition is further compounded in pediatric RT where it is common to deliver RT after sur- gical resection of gross disease. The clinician is then tasked with

the reconstruc- tion of the pre-operative tumor volume while respecting, often significant, changes in anatomy following surgery (9). In pediatrics, RT guidelines within trial proto- cols along with the provision of central review aids standardized target delineation for this challenging treatment group (8). International RT quality assurance pro- grams for pediatric RT are well established in U.S and more recently implement- ed in Europe following the important recognition that protocol compliance is im- portant in the prospective evaluation of patient outcomes in the setting of clinical trials (8).

Efforts to standardize treatment volumes, particularly for common adult tumor types such as lung cancer, have been made through the development of consensus contouring guidelines and atlases e.g. Radiation Therapy Oncology Group (RTOG), training platforms provided by collaborative bodies such as American Society for Radiation Oncology (ASTRO) and European Society for Radiotherapy and Oncology (ESTRO), and the integration of complimentary imaging modalities in addition to CT. To determine the GTV, or 'virtual' GTV, reference diagnostic imaging is consulted together with the RTP scan. Common modalities in pediatric RT planning include magnetic resonance imaging (MRI), positron emission to- mography computed tomography (PET CT) and metaiodobenzylguanidine (MIBG) scintigraphy. Most TPS platforms enable image registration, allowing clinicians to utilize rigid fusion of multi-modality imaging to further enhance GTV definition. The use of image fusion requires careful consideration to immo-

bilization and positioning in both sets of images to minimize the introduction of significant geometric error because of differences in patient positioning between the fused image sets.

Given the fundamental importance that the treatment target is correctly identi- fied collaboration between radiation oncologist and diagnostic imaging specialists is essential for accurate interpretation of imaging when determining the treatment target.

CT, though the mainstay of RT at present, offers only limited soft tissue con- trast. The superior soft tissue contrast on MR makes it an attractive modality for use in RT. Many departments have the ability to perform MR RTP scans. These scans are performed with the same patient immobilization and setup relative to skin marks as RTP CT scan acquisition; enabling confident fusion of the two im- aging modalities. At the present time, it is not yet possible to plan directly on MR but with the availability of hybrid MR/ RT treatment platforms (10-13) the devel- opment of MR-only workflows is an active area of research. Greater integration of MR into the RT pathway is expected to have significant benefits for young pa- tients as additional imaging will not result in additional radiation dose to the pa- tient.

An overview of imaging modalities incorporated into RT planning of common- ly occurring pediatric tumors is given in the table below (Table 3) as reflected in our institutional guidelines. The use of imaging modalities auxiliary to CT in RT

planning can vary between institutions depending on available resources.

Figure 1a Figure 1b
15 year-old patient with a diagnosis of stage IVB classical Hodgkin's lymphoma (patient had bone involvement). Figure 1a; Diagnostic PETCT images depicting abnormal FDG uptake within the supraclavicular, mediastinal, para-aortic and bi- lateral iliac nodal regions and uptake within the spleen. Figure 1b; RT treatment volumes (red shaded area) with associated dose distribution (green line). Note dif- ferent arm position in diagnostic PETCT compared to RT treatment position.

Figure 2: Example T2-weighted MRI (left); contrast-enhanced RTP CT (middle) and fused MR/ RTP CT (right)

RADIATION TREATMENT PLANNING IN PEDIATRIC ONCOLOGY

TUMOUR TYPE TARGET DEFINITION OF GTV/CTV ON CONTRAST-

ENHANCED CT AND ADJUNCTIVE IMAGING* FOR ADDITIONAL ANATOMICAL INFORMATION *may be fused with RTP CT scan
CNS (high grade) Surgical cavity and any residual enhancement visible on gadolinium-enhanced T1-weighted MRI. (Figure 2)
CNS (low grade) High signal intensity on T2-weighted or fluid-attenuated inversion recovery (FLAIR) MRI
CNS (cranio-spinal) T1-weighted MRI is used to identify the thecal sac
Hodgkin lymphoma All areas of disease according to PET-CT at the time of diagnosis. (Figure 1a and 1b) Boost is indicated to areas of persistent FDG avidity on late response assessment PET-CT
Neuroblastoma 'virtual GTV' reconstructed with reference to preoperative CT or MR 123 I mIBG, 68Gallium DOTATOC/ DOTATATE PETCT may be used to give additional anatomical in- formation
Wilms' tumor 'virtual GTV' reconstructed with reference to preoperative CT or MR
Soft tissue sarcoma 'virtual GTV' reconstructed with reference to diagnostic and preoperative CT or MR
Ewing sarcoma 'virtual GTV' reconstructed with reference to diagnostic and preoperative CT or MR

Table 2 Royal Marsden Hospital, London, U.K. guidelines for target definition is given as an illustrative example of the integration of imaging into the RT planning pathway.

Motion assessment

Internal organ motion can cause imaged structures to move in or out of the CT slice window during scan acquisition. This motion results in artefacts which are commonly seen in the thorax and upper abdomen, as these sites are susceptible to respiratory-related motion (14). Such artefacts can distort the appearance of both target structures and organs at risk thereby introducing systematic delineation er- rors into the RT planning process. 4DCT was developed as a means to reduce mo- tion-related image artefact seen on 3DCT (15, 16).

Internal motion also represents a significant source of residual error in treat- ment delivery. Motion of tumor and OAR in the thorax and abdomen of children and young people is increasingly described in the literature (17-23). Though of smaller magnitude than observed in adults (21), 4DCT, the current gold standard for motion assessment in adults, is increasingly used to generate individualized margins in pediatric patients (17, 23). 4DCT imaging results in increased dose de- livered to the patient but the use of low-dose protocols looks to maintain the ALARA principle of dose exposure (23).

Despite the time-resolved nature of 4DCT there are accepted limitations in its application; such as in the setting of irregular breathing patterns. The ability of a single 4DCT to fully characterize respiratory-related motion is potentially limited

as irregular breathing can result in improper ‘binning’ in retrospective sorting methods.
Alternative imaging modalities with potential to derive motion information include ultrasound (US) and magnetic resonance imaging (MRI) but, as yet, there are limited published results relating to their use in children (18) (24).

Treatment planning

With treatment targets defined the next step is treatment dosimetry; the iterative process of determining appropriate beam arrangements for treatment delivery. Each beam delivers a proportion of the prescribed dose and the trajectory of each beam is depicted on the RTP scan. For many pediatric tumor sites conformal RT using anterior and posterior directions suffice but in some cases more sophisticated beam arrangements and delivery techniques might be preferential; for example complex target shapes adjacent to critical normal tissue. In recent decades, developments within the field of RT have enabled increasingly conformal dose distributions to be generated; called intensity-modulated RT (IMRT). IMRT is now readily available in the clinic.
The output of the dosimetry process is the combined dose distribution of all beams presented as a plan on the RTP scan and its associated dose volume histogram (DVH). A DVH is a graphical representation of the radiation dose received by segmented tissues, normal and tumor, within the beam trajectories. Known tolerance doses for OAR are reflected in RT guidelines within clinical trials. Data for

normal tissue tolerances in RT are frequently extrapolated from laboratory or animal studies and normal tissue tolerance is often multifactorial but guidance is taken from the quantitative analysis of normal tissue effects in the clinic (QUANTEC) reports in adults (25-40). Given the accepted physiological differences between children and adults, pediatric-specific guidance is warranted and awaited (41).

Treatment delivery

The reference RTP CT on which the treatment plan is generated is the geometric representation of the patient’s anatomy at an arbitrary snapshot in time. The TPS-generated RT plan and its dose distribution are defined relative to a treatment machine reference point (usually the isocentre). A plan can become suboptimal if the location of the target relative to the planned dose distribution changes during treatment. As previously mentioned, such changes can result from variation in patient set up relative to the beam isocentre (setup errors), and variation in the target position relative to the patient’s bone anatomy (target volume changes). These changes have systematic or random components that can occur during or between treatment fractions (intra- and inter-fraction respectively) and represent the geometric uncertainties involved in RT delivery.

The ability to confidently deliver increasingly conformal dose distributions depends on accurate and precise knowledge of the target position. This process of harnessing image guidance to manage geometric uncertainty in RT treatment de- livery is called IGRT and the clinical benefit derived from normal tissue sparing and/ or dose escalation as a result of increasing accuracy has been demonstrated in a number of adult tumor sites (42).

Patient position at the time of treatment is verified relative to the reference CT dataset (i.e. the planned position) using skin marks/ tattoos and lasers aligned to an external coordinate system. Setup error can be reduced through the use of patient positioning systems and rigid immobilization devices. Appropriate use of current patient immobilization devices (vacuum bag, alpha cradle) can now attain patient set-up reproducibility in the region of 3-5mm (1). However, it is well recognized that internal anatomy may not be well correlated to external skin marks.

Modern linear accelerators are integrated with in-room IGRT systems, such as planar imaging, cone beam CT and more recently MRI, together with automated couch correction; summarized in Table 2 (adapted from (43)). IGRT imaging al- lows the quantification of some geometric uncertainties and the assessment of in- ter and intra-fraction error in pediatric RT delivery is well described (44-51). IGRT imaging protocols require adaptation to deliver the minimal additional dose to the pediatric patient (52).

Motion information extracted from 4DCT can be verified at the time of treatment delivery by imaging of the tumor itself via, e.g., fluoroscopy or respiratory-correlated 4D-CBCT (53); imaging of fiducial markers implanted in the tumor; in- ferring tumor position from a surrogate breathing motion signal; and non-radiographic tracking of a marker implanted in the tumor (7). Treatment delivery can be gated; where treatment delivery is interrupted when the anatomy is out of position, or tracked where motion is compensated by the machine using dynamic multileaf collimators (MLC), or moving the treatment couch and machine e.g. Cyberknife (Accuray Inc., Sunnyvale, CA, USA) (54).

In addition to identifying target position, IGRT imaging can identify anatomi- cal changes that could adversely affect the delivered dose. Re-planning prompted by observed anatomical changes is referred to as adaptive RT (ART). This has been described in the setting of pediatric craniopharyngioma where changes in cyst volume during a treatment course and the potential adverse dosimetric impact of not re-planning based on changes in target size has been described (48).

Imaging modality Dose per image Geometric accuracy
Type of tissue match used for treatment localization
EPID
MV / KV 1-3 mGy 1-2mm Bone match
2D planar imaging
CBCT
KV / MV 30-50mGy ≤1mm Soft tissue match
Tomographic reconstruction from a series of planar images obtained in one rotation of the gantry around the patient providing volumetric anatomical information
Time-resolved CBCT reconstruction possible
'CT-on-rails' 10-50 mGy ≤1mm Soft tissue match
Diagnostic quality volumetric images
Fanbeam
MV CT 10-30 mGy ≤1mm Soft tissue match
Volumetric
Stereoscopic
KV 0.10-200
mGy

0.33-0.55 mGy <1 mm 2-D
Match based on implanted fiducial markers or bone anatomy

Match based on bone anatomy, six degree of freedom correction of translational and rotational set-up corrections
Imaging
modality Dose per
image Geometric
accuracy Type of tissue match used for treatment localization
Ultrasound No dose 3-5mm Soft tissue match
Clinically available for prostate (Clarity ™)
MR No dose 1-2mm Soft tissue match

14

Table 3: radiation-based in-room IGRT systems and non-ionising modalities.Legend: EPID: electronic portal image dosimetry,
2D; two-dimensional, MV: megavoltage, KV: kilovoltage, CBCT: cone-beam CT

Other therapeutic RT delivery techniques

Stereotactic ablative radiotherapy

Stereotaxis is the use of an external, three-dimensional frame of reference for localization. This ability has been incorporated into photon-based EBRT in the form of stereotactic radiosurgery (SRS) stereotactic ablative radiotherapy (SABR). SRS and SABR involve the delivery of large doses of radiation over one or few treatment fractions. Large doses of RT are delivered with the aim of ablating the target tissue. The delivery of single fraction SRS relies on the induction of cell death and necrosis in the target tissue without biologic sparing of normal tissues contained within the treatment target. A number of clinically available platforms are capable of delivering SRS and SABR. Some require a frame-based localization system, others do not. With the delivery of such high doses and such treatment ef- fect, IGRT is a prerequisite for delivering these treatments where applied safety margins may be negligible.

The use of SABR/ SRS has been reported for select pediatric tumors; primarily CNS tumors (55). Due to the ability to treat using small safety margins, SABR is an attractive option for use in the re-irradiation setting; and its application has been described in this setting for ependymoma and other CNS tumors (55-57). There is also increasing interest in the use of ablative RT in extra-cranial sites e.g. spine, lung and also in the management of oligometastatic disease (58).

Proton beam therapy

The physical characteristics of the charged proton beam result in negligible exit dose as the particles have a finite range. It is also possible to deliver conformal dose distributions with fewer beams (equivalent arc) using PBT compared to con- formal photon RT. PBT delivers increased conformity of treatment delivery and exposes smaller volumes of normal tissue to moderate or low dose radiation (59). These advantages are likely to translate into less long-term morbidity from normal tissue late effects and second malignancy induction and so, even in the absence of randomized evidence, many pediatric tumors, particularly in the CNS, are treated with PBT.

The body of evidence for PBT use in children comes from dosimetric studies and case series with now increasing follow up. Dosimetric studies have demonstrated favorable sparing of normal tissue, primarily in CNS tumors but also for cranio-spinal delivery. From published case series, disease control is equivalent to photon EBRT and late toxicity, when reported, is favorable.

The geometric uncertainties in treatment delivery already described could have

greater impact on PBT delivery as the dose deposition is affected by particle range

and radiological depth of the target. Until recently, PBT in room IGRT equipment lagged behind parallel developments of photon IGRT platforms (60). Planar imag- ing was, and still is, frequently used for PBT image guidance. Intensity-modulated treatments are deliverable with current PBT technology. With this, advances in IGRT platforms for PBT will likely follow those seen for photon delivery.

Furthermore, it is clear the biological effects of PBT are distinctly different from photon EBRT. The relative biological effectiveness (RBE) of PBT is taken to be 1.1 relative to photon beam therapy. It is now increasingly apparent that the RBE changes along the beam trajectory and in fact increases towards the end of the particle range (61).

Though PBT is now preferentially chosen for many pediatric tumors it will be important to confirm the advantages with an evidence base of mature survivorship data (62).

Brachytherapy

Brachytherapy (BT) is a RT modality than involves the placement of radioactive sources within a body cavity (intracavity), within tissue (interstitial) or surface moulds that can be sculpted to a tumor bed. BT is characterized by the ability to deliver high biologically effective doses, relative to EBRT, with very steep dose gradients. The latter is a result of both the low energy radiation of BT and the in- verse square law that dictates that dose at a distance from a radioactive source is inversely proportional to the square of that distance.

The dose profiles of BT can achieve local control with better organ and function preservation than could be achievable with EBRT for certain tumor sites. Pe- diatric tumor sites, in which the use of BT is best described include rhabdomysocarcoma (extremity, genitourinary, and head and neck sites), other soft tissue sarcoma subtypes arising along trunk or extremities, and retinoblastoma. BT can be delivered as the sole local therapy or as a boost following EBRT. BT can be de- livered using pulse dose rate (PDR) techniques or remote high dose rate (HDR); either fractionated or intra-operative.

Due to the highly skilled nature of BT it is delivered within specialized centers and only for a select proportion of pediatric patients. The principles of BT are sim- ilar for both adult and pediatric indications.

Cross sectional imaging has revolutionized BT and is now routinely incorporated in BT and CT, MR, ultrasound and fluoroscopy all play a role in BT for var- ious anatomical sites. Sectional imaging aids the placement of radioactive sources/ applicators thereby improving treatment dosimetry and aid the definition of target volumes and OAR.

Molecular radiotherapy

Molecular RT (MRT) is a modality of treatment whereby unsealed radioactive sources are delivered systemically to the patient. MRT can be used in the treatment of malignant e.g. neuroendocrine cancer and benign disease e.g. hyperthy- roidism. Molecular RT requires collaboration between nuclear medicine clini- cians, diagnostic imaging specialists and oncologists. In the setting of neuroendocrine tumors the rate of treatment success can be predicted by pre- therapy imaging and new tracers offer potential to improve the sensitivity and specificity for uptake in cancer cells (63).

The interdependence of diagnostic imaging and molecular RT delivery is illustrated in two contemporary studies in the field recruiting with in the United Kingdom. In pediatric patients with metastatic neuroblastoma a novel imaging practice using I-124 as a PET tracer instead of the standard I-123 tracer is being investigat- ed. The study's hypothesis is that the superior spatial resolution of PET imaging will allow greater precision in localizing small foci of metastatic disease and allow reliable and reproducible quantitative assessment of the extent of disease. If suc- cessful, I-124 imaging will offer improved disease evaluation and could be uti- lized for treatment planning with 131-I MIBG (64). 177Lu- DOTATATE is being investigated in a phase IIA study in children with primary refractory or relapsed high risk neuroblastoma. Eligible patients for therapy undergo diagnostic imaging using radiolabeled 68Ga-DOTATATE PETCT which allows higher sensitivity and improved spatial resolution for disease assessment. Pre- and post-therapy quantita- tive imaging is used to provide patient-specific absorbed dose (65).

The potential benefit of therapeutic 131-I MIBG therapy in high risk neuroblastoma, for patients with a poor response to induction therapy, will be explored in the SIOPEN VERITAS study (66). If positive, this would expand the indication for MRT in high risk neuroblastoma.

Future directions

Adaptive RT (ART) and the introduction of MR-guided RT will see further development in the integration of imaging and RT. For a discipline conventionally reliant on CT imaging, adopting an MR-only workflow will necessitate even greater communication between diagnostic imaging specialists and radiation on- cologists to ensure correct interpretation of imaging for planning and treatment purposes. There may even be a need to incorporate a broader scope of formal di- agnostic imaging education modules into post graduate training for

radiation on- cology as our reliance on MR and other auxiliary imaging modalities intensifies. As an example, ultrasound has real untapped potential for RT image guidance (67,
68) but it is widely acknowledged that its success as an image guidance tool is op- erator dependent; to integrate this modality training of both clinicians and thera-

peutic radiographers will be necessary. Both MR and ultrasound are of particular relevance for young patients given the absence of additional radiation dose and their development should be made a focus of pediatric RT research and develop- ment.

References

1. Olch AJ. Pediatric Radiotherapy Planning and Treatment. London, UNITED STATES: CRC Press; 2013.
2. Jones D. ICRU Report 50—Prescribing, Recording and Reporting Photon
Beam Therapy. Medical Physics. 1994;21(6):833-4.
3. Landberg T, Chavaudra J, Dobbs J, Gerard JP, Hanks G, Horiot JC, et al. Report 62. Journal of the International Commission on Radiation Units and Measurements. 1999;os32(1):NP-NP.
4. Report 83. Journal of the International Commission on Radiation Units and Measurements. 2010;10(1):NP-NP.
5. International Commission on Radiation Units and Measurements (ICRU). Report 62. Prescribing,
Recording and Reporting Photon Beam Therapy (Supplement to ICRU Report 50). Bethesda, MD: ICRU, 1999.
6. van Herk M, Remeijer P, Rasch C, Lebesque JV. The probability of correct target dosage: dose-population histograms for deriving treatment margins in radiotherapy. International Journal of Radiation Oncology*Biology*Physics.
2000;47(4):1121-35.
7. Keall PJ, Mageras GS, Balter JM, Emery RS, Forster KM, Jiang SB, et al. The management of respiratory motion in radiation oncology report of AAPM Task Group 76a). Medical Physics. 2006;33(10):3874-900.
8. Gaze MN, Boterberg T, Dieckmann K, Hormann M, Gains JE, Sullivan KP, et al. Results of a quality assurance review of external beam radiation therapy in the International Society of Paediatric Oncology (Europe)

Neuroblastoma Group's High-risk Neuroblastoma Trial: a SIOPEN study. Int J Radiat Oncol Biol Phys. 2013;85(1):170-4.
9. Chen AB, Killoran J, Kim H, Mamon H. Treatment planning for resected abdominal tumors: differences in organ position between diagnostic and radiation- planning computed tomography scans. Int J Radiat Oncol Biol Phys.
2005;63(5):1613-20.
10. Keall PJ, Barton M, Crozier S. The Australian Magnetic Resonance Imaging–Linac Program. Seminars in Radiation Oncology. 2014;24(3):203-6.
11. Mutic S, Dempsey JF. The ViewRay System: Magnetic Resonance–
Guided and Controlled Radiotherapy. Seminars in Radiation Oncology. 2014;24(3):196-9.
12. Lagendijk JJW, Raaymakers BW, van Vulpen M. The Magnetic Resonance Imaging–Linac System. Seminars in Radiation Oncology.
2014;24(3):207-9.
13. Fallone BG. The Rotating Biplanar Linac–Magnetic Resonance Imaging
System. Seminars in Radiation Oncology. 2014;24(3):200-2.

14. Chen GT, Kung JH, Beaudette KP. Artifacts in computed tomography scanning of moving objects. Semin Radiat Oncol. 2004;14(1):19-26.
15. Vedam SS, Keall PJ, Kini VR, Mostafavi H, Shukla HP, Mohan R. Acquiring a four-dimensional computed tomography dataset using an external respiratory signal. Phys Med Biol. 2003;48(1):45-62.
16. Rietzel E, Pan T, Chen GT. Four-dimensional computed tomography: image formation and clinical protocol. Med Phys. 2005;32(4):874-89.
17. Pai Panandiker AS, Sharma S, Naik MH, Wu S, Hua C, Beltran C, et al. Novel Assessment of Renal Motion in Children as Measured via Four-Dimensional Computed Tomography. International Journal of Radiation Oncology*Biology*Physics. 2012;82(5):1771-6.
18. Uh J, Krasin MJ, Li Y, Li X, Tinkle C, Lucas JT, Jr., et al. Quantification of Pediatric Abdominal Organ Motion With a 4-Dimensional Magnetic Resonance Imaging Method. Int J Radiat Oncol Biol Phys. 2017;99(1):227-37.
19. Huijskens SC, van Dijk IW, Visser J, Rasch CR, Alderliesten T, Bel A. Magnitude and variability of respiratory-induced diaphragm motion in children during image-guided radiotherapy. Radiotherapy and oncology : journal of the European Society for Therapeutic Radiology and Oncology. 2017.
20. Huijskens SC, van Dijk IWEM, de Jong R, Visser J, Fajardo RD, Ronckers CM, et al. Quantification of renal and diaphragmatic interfractional motion in pediatric image-guided radiation therapy: A multicenter study. Radiotherapy and Oncology. 2015;117(3):425-31.
21. van Dijk IW, Huijskens SC, de Jong R, Visser J, Fajardo RD, Rasch CR, et al. Interfractional renal and diaphragmatic position variation during radiotherapy in children and adults: is there a difference? Acta oncologica (Stockholm, Sweden). 2017:1-7.
22. Nazmy MS, Khafaga Y, Mousa A, Khalil E. Cone beam CT for organs

motion evaluation in pediatric abdominal neuroblastoma. Radiotherapy and Oncology. 2012;102(3):388-92.
23. Kannan S, Teo BK, Solberg T, Hill-Kayser C. Organ motion in pediatric high-risk neuroblastoma patients using four-dimensional computed tomography. Journal of applied clinical medical physics. 2017;18(1):107-14.
24. Beltran C, Pai Panandiker AS, Krasin MJ, Merchant TE. Daily image-guided localization for neuroblastoma. Journal of applied clinical medical physics.
2010;11(4):3388.
25. Bhandare N, Jackson A, Eisbruch A, Pan CC, Flickinger JC, Antonelli P, et al. Radiation Therapy and Hearing Loss. International Journal of Radiation Oncology • Biology • Physics.76(3):S50-S7.
26. Dawson LA, Kavanagh BD, Paulino AC, Das SK, Miften M, Li XA, et al. Radiation-Associated Kidney Injury. International Journal of Radiation Oncology • Biology • Physics.76(3):S108-S15.
27. Deasy JO, Moiseenko V, Marks L, Chao KSC, Nam J, Eisbruch A. Radiotherapy Dose–Volume Effects on Salivary Gland Function. International Journal of Radiation Oncology • Biology • Physics.76(3):S58-S63.

28. Gagliardi G, Constine LS, Moiseenko V, Correa C, Pierce LJ, Allen AM, et al. Radiation Dose–Volume Effects in the Heart. International Journal of Radiation Oncology • Biology • Physics.76(3):S77-S85.
29. Kavanagh BD, Pan CC, Dawson LA, Das SK, Li XA, Ten Haken RK, et al. Radiation Dose–Volume Effects in the Stomach and Small Bowel. International Journal of Radiation Oncology • Biology • Physics.76(3):S101-S7.
30. Kirkpatrick JP, van der Kogel AJ, Schultheiss TE. Radiation Dose–Volume Effects in the Spinal Cord. International Journal of Radiation Oncology • Biology • Physics.76(3):S42-S9.
31. Lawrence YR, Li XA, el Naqa I, Hahn CA, Marks LB, Merchant TE, et al. Radiation Dose–Volume Effects in the Brain. International Journal of Radiation Oncology • Biology • Physics.76(3):S20-S7.
32. Marks LB, Bentzen SM, Deasy JO, Kong F-M, Bradley JD, Vogelius IS, et al. Radiation Dose–Volume Effects in the Lung. International Journal of Radiation Oncology • Biology • Physics.76(3):S70-S6.
33. Mayo C, Martel MK, Marks LB, Flickinger J, Nam J, Kirkpatrick J. Radiation Dose–Volume Effects of Optic Nerves and Chiasm. International Journal of Radiation Oncology • Biology • Physics.76(3):S28-S35.
34. Mayo C, Yorke E, Merchant TE. Radiation Associated Brainstem Injury. International Journal of Radiation Oncology • Biology • Physics.76(3):S36-S41.
35. Michalski JM, Gay H, Jackson A, Tucker SL, Deasy JO. Radiation Dose–Volume Effects in Radiation-Induced Rectal Injury. International Journal of Radiation Oncology • Biology • Physics.76(3):S123-S9.
36. Pan CC, Kavanagh BD, Dawson LA, Li XA, Das SK, Miften M, et al. Radiation-Associated Liver Injury. International Journal of Radiation Oncology • Biology • Physics.76(3):S94-S100.
37. Rancati T, Schwarz M, Allen AM, Feng F, Popovtzer A, Mittal B, et al. Radiation Dose–Volume Effects in the Larynx and Pharynx.

International Journal of Radiation Oncology • Biology • Physics.76(3):S64-S9.
38. Roach M, III, Nam J, Gagliardi G, El Naqa I, Deasy JO, Marks LB. Radiation Dose–Volume Effects and the Penile Bulb. International Journal of Radiation Oncology • Biology • Physics.76(3):S130-S4.
39. Viswanathan AN, Yorke ED, Marks LB, Eifel PJ, Shipley WU. Radiation Dose–Volume Effects of the Urinary Bladder. International Journal of Radiation Oncology • Biology • Physics.76(3):S116-S22.
40. Werner-Wasik M, Yorke E, Deasy J, Nam J, Marks LB. Radiation Dose- Volume Effects in the Esophagus. International Journal of Radiation Oncology • Biology • Physics.76(3):S86-S93.
41. PENTEC. [Available from: https://www.pentecradiation.org/.
42. Dawson LA, Jaffray DA. Advances in image-guided radiation therapy. J Clin Oncol. 2007;25(8):938-46.
43. De Los Santos J, Popple R, Agazaryan N, Bayouth JE, Bissonnette JP, Bucci MK, et al. Image guided radiation therapy (IGRT) technologies for

radiation therapy localization and delivery. Int J Radiat Oncol Biol Phys. 2013;87(1):33-45.
44. Beltran C, Pegram A, Merchant TE. Dosimetric consequences of rotational errors in radiation therapy of pediatric brain tumor patients. Radiotherapy and oncology : journal of the European Society for Therapeutic Radiology and Oncology. 2012;102(2):206-9.
45. Beltran C, Krasin MJ, Merchant TE. Inter- and intrafractional positional uncertainties in pediatric radiotherapy patients with brain and head and neck tumors. Int J Radiat Oncol Biol Phys. 2011;79(4):1266-74.
46. Beltran C, Merchant TE. Dependence of intrafraction motion on fraction duration for pediatric patients with brain tumors. Journal of applied clinical medical physics. 2011;12(4):3609.
47. Beltran C, Sharma S, Merchant TE. Role of adaptive radiation therapy for pediatric patients with diffuse pontine glioma. Journal of applied clinical medical physics. 2011;12(2):3421.
48. Beltran C, Naik M, Merchant TE. Dosimetric effect of target expansion and setup uncertainty during radiation therapy in pediatric craniopharyngioma. Radiotherapy and oncology : journal of the European Society for Therapeutic Radiology and Oncology. 2010;97(3):399-403.
49. Beltran C, Naik M, Merchant TE. Dosimetric effect of setup motion and target volume margin reduction in pediatric ependymoma. Radiotherapy and oncology : journal of the European Society for Therapeutic Radiology and Oncology. 2010;96(2):216-22.
50. Beltran C, Trussell J, Merchant TE. Dosimetric impact of intrafractional patient motion in pediatric brain tumor patients. Medical dosimetry : official journal of the American Association of Medical Dosimetrists. 2010;35(1):43-8.
51. Altunbas C, Hankinson TC, Miften M, Tello T, Plimpton SR, Stuhr K, et al. Rotational setup errors in pediatric stereotactic radiation therapy. Pract Radiat Oncol. 2013;3(3):194-8.
52. Beltran C, Lukose R, Gangadharan B, Bani-Hashemi A, Faddegon BA. Image quality & dosimetric property of an investigational imaging beam line MV-

CBCT. Journal of applied clinical medical physics. 2009;10(3):3023.
53. Sonke JJ, Zijp L, Remeijer P, van Herk M. Respiratory correlated cone beam CT. Med Phys. 2005;32(4):1176-86.
54. Jaffray DA. Image-guided radiotherapy: from current concept to future perspectives. Nat Rev Clin Oncol. 2012;9(12):688-99.
55. Murphy ES, Chao ST, Angelov L, Vogelbaum MA, Barnett G, Jung E, et al. Radiosurgery for Pediatric Brain Tumors. Pediatric Blood & Cancer. 2016;63(3):398-405.
56. Hoffman LM, Plimpton SR, Foreman NK, Stence NV, Hankinson TC, Handler MH, et al. Fractionated stereotactic radiosurgery for recurrent ependymoma in children. J Neurooncol. 2014;116(1):107-11.

57. Saran F, Baumert BG, Creak AL, Warrington AP, Ashley S, Traish D, et al. Hypofractionated stereotactic radiotherapy in the management of recurrent or residual medulloblastoma/PNET. Pediatr Blood Cancer. 2008;50(3):554-60.
58. Brown LC, Lester RA, Grams MP, Haddock MG, Olivier KR, Arndt CA, et al. Stereotactic body radiotherapy for metastatic and recurrent ewing sarcoma and osteosarcoma. Sarcoma. 2014;2014:418270.
59. Yock TI, Tarbell NJ. Technology insight: Proton beam radiotherapy for treatment in pediatric brain tumors. Nat Clin Pract Oncol. 2004;1(2):97-103; quiz
1 p following 11.
60. Alcorn SR, Chen MJ, Claude L, Dieckmann K, Ermoian RP, Ford EC, et al. Practice patterns of photon and proton pediatric image guided radiation treatment: results from an International Pediatric Research consortium. Pract Radiat Oncol. 2014;4(5):336-41.
61. Peeler CR, Mirkovic D, Titt U, Blanchard P, Gunther JR, Mahajan A, et al. Clinical evidence of variable proton biological effectiveness in pediatric patients treated for ependymoma. Radiotherapy and oncology : journal of the European Society for Therapeutic Radiology and Oncology. 2016;121(3):395-401.
62. Merchant TE. Clinical Controversies: Proton Therapy for Pediatric Tumors. Seminars in Radiation Oncology. 2013;23(2):97-108.
63. National Cancer Research Institute (NCRI). CTRad: identifying opportunities to promote progress in molecular radiotherapy research in the UK. 2016. 2016.
64. Phase I/II study of [124I]mIBG PET/CT in neuroblastoma [Available from: https://www.hra.nhs.uk/planning-and-improving-research/application- summaries/research-summaries/phase-iii-study-of-124imibg-petct-in- neuroblastoma/.
65. LuDo [Available from: http://www.cancerresearchuk.org/about-cancer/find-a-clinical-trial/a-trial-looking-177-lutetium-dotatate-neuroblastoma-children-young-people-ludo.
66. Trial Evaluating and Comparing Two Intensification Treatment Strategies for Metastatic Neuroblastoma Patients With a Poor Response to Induction Chemotherapy (VERITAS) 2017 [cited 1/10/2017. Available from: https://clinicaltrials.gov/ct2/show/NCT03165292.

67. O'Shea T, Bamber J, Fontanarosa D, van der Meer S, Verhaegen F, Harris E. Review of ultrasound image guidance in external beam radiotherapy part II: intra-fraction motion management and novel applications. Phys Med Biol.
2016;61(8):R90-R137.
68. Fontanarosa D, van der Meer S, Bamber J, Harris E, O'Shea T, Verhaegen F. Review of ultrasound image guidance in external beam radiotherapy: I. Treatment planning and inter-fraction motion management. Phys Med Biol. 2015;60(3):R77-114.